



A thesis submitted in fulfilment of the
requirements for the degree of
Doctorate of Philosophy in Surgery,
The University of Auckland, 2015.

Tissue Oxygenation and Wound Healing in Vascular Surgery

Nathaniel Chiang (1027950)

Abstract

Are there simple adjuncts that can be applied in patients with peripheral vascular disease that could enhance wound healing and tissue oxygenation? Two large-scale clinical studies were conducted with the aims of targeting two stages of care, namely (i) perioperative treatments to enhance peripheral oxygenation by influencing oxygen delivery via chemical and thermal vasodilation (high-dose oxygen, a prostacyclin analogue, and extended active warming) during bypass surgery to the lower limbs, and (ii) topical negative therapy (TNP) dressings for high-risk foot wounds, such as following debridement or minor amputations in the diabetic foot. These therapies have been shown to be of benefit in other clinical settings, such as abdominal surgery and to treat abdominal wounds. How these adjuncts would help in patients with vascular disease is unknown.

Mechanisms underlying the potential effects of these treatments on wound healing were assessed biochemically by quantifying hydroxyproline (a surrogate marker of collagen), growth factors, cytokines, and their respective mRNAs. Healing rates were determined by changes in wound volume over time using an innovative stereophotographic device (FastScan™). Tissue oxygenation was measured using hyperspectral technology (OxyVu™). The reliability and feasibility of using these devices was tested in clinical studies.

Measurements obtained using these innovative instruments yielded excellent inter-operator and intra-operator reliability and correlated well with other methods of measurement, thus showing promise for assessment of tissue oxygenation and wound healing in clinical settings. No benefits were demonstrated in 71 patients with regard to surgical wound healing or tissue oxygenation in bypass surgery by perioperative adjunctive treatment. OxyVu identified increased tissue oxygenation in the foot in the acute phase following bypass surgery, validating its clinical use. In acute foot wounds treated with TNP, there was no significant difference in wound volume reduction at 2 weeks when compared with traditional dressings (44.2% for TNP versus 20.9% for the control; $p=0.15$). However, there was a trend towards an enhanced healing rate, and maximum wound depth was significantly less than that achieved using traditional dressings (36.0% for TNP versus 17.6% for the control; $p=0.03$). Given that no differences were found in hydroxyproline levels, growth factors, or tissue oxygenation, the benefits of TNP might involve more than merely enhanced production of granulation tissue, possibly involving mechanical (macrostrain) effects.

Preface

This thesis was a seven-year project, including two years of full-time research and 5 years part-time. For three of the five part-time years, I was working full-time as a trainee in vascular surgery, completing professional examinations and furthering my knowledge in areas outside of the thesis. This project was based in the vascular surgery unit at Waikato Hospital (Hamilton, New Zealand) where there was a strong emphasis on research but without an established department or academic support. In fact, this was the first PhD thesis undertaken in that unit. This in itself had its merits but also a number of challenges that contributed to some setbacks during this research.

Mr Thodur Vasudevan was my co-supervisor in the unit, with whom I had most of the discussions relating to establishing the project. He did not meet the requirements of the university to be the main supervisor and nor did the other members of the surgical unit. The main supervisor was Professor Jamie Sleight, a member of the Waikato Medical Research Foundation and a widely respected Professor of Anaesthesiology with a consistent research output and experience in supervision of students undertaking higher degrees. I was always drawn to the well-established surgical research unit at Auckland Hospital, University of Auckland, headed by Professor John Windsor and Associate Professor Lindsay Plank. I wanted guidance and a point of contact at such a unit, and it was an honour that Associate Professor Plank agreed to provide such support as a co-supervisor.

One of my personal highlights were supervising six summer studentship projects over three years, one of which saw the student win a number of accolades and secure scholarships to fund her elective. I also took pride in securing the various grants and scholarships that funded the first hyperspectral transcutaneous oxygenation measurement system (OxyVu™) to be used outside the US where it was developed. The most notable setbacks in this thesis were the inability to complete patient recruitment and the failure to complete analyses of mRNA for growth factors and cytokines. Despite spending 6 months in the laboratory purifying the tissue samples, meaningful results could not be obtained due to inadequate sampling.

My utmost gratitude is extended to all who supported and funded the study, in particular the University of Auckland, Waikato Medical Research Foundation, Health Research Council, and Royal Australasian College of Surgeons.

Project ownership and contributions

Apart from the initial concept provided by Mr Thodur Vasudevan to study tissue oxygenation and wound healing following perioperative supplemental oxygen during infra-inguinal bypass, the design and completion of the project were my own work. Assistance was required in the validation studies, whereby medical students were employed as part of their summer studentships to determine the inter-operator reliability of the devices. I conducted the laboratory work, including the biochemical analyses of hydroxyproline and growth factors, under supervision. Statistical analysis of the data and the thesis writing were completed by myself. The thesis was professionally edited by Susan Albrecht prior to submission.

Achievements

DATE	TITLE OF PRESENTATION	MEETINGS	PRIZE
Oct '09	Validation of OxyVu (preliminary data)	ANZSVS 2009	
Feb '10	Validation of Silhouette and FastScan	NZVS 2010	Best presentation
Sep '10	Validation of Silhouette and FastScan	ANZSVS 2010	
Aug '13	WOIOW study	RACS Surgery 2013	Finalists for Louis Barnett Prize
Oct '13	WOIOW study	ANZSVS 2013	
Oct '13	Validation of OxyVu	ANZSVS 2013	Best poster
Oct '13	Setting standards for TCOM	ANZSVS 2013	
Oct '15	TNP study	ANZSVS 2015	

Time frame

	PHD PROGRESS	MILESTONE
2008: Year 1 (part-time) Lecturer in Surgery (UoA)	<p>Concept and research design</p> <p>Literature search</p> <p>Seek funding for full-time PhD and consumables (OxyVu™ and TCOM)</p>	<p>PhD Registration</p> <p>Faculty Research Development Fund (\$45,000)</p> <p>Braemar Charitable Trust Research Grant (\$5,000)</p> <p>Bayer Health Care Fund (\$5,000)</p> <p>Purchased OxyVu and TCOM</p>
2009: Year 2 (part-time) Clinical research training fellowship (HRC)	<p>Start validation of OxyVu</p> <p>Start WOLOW Study</p> <p>Seek funding for FASTScan™ and Silhouette™</p>	<p>Waikato Medical Research Foundation Grant (\$10,000)</p> <p>Department Grant-in-Aid (\$12,000)</p> <p>PBRF Fund Allocation (\$5220.80)</p> <p>Postgraduate Student Fund (\$1,000)</p> <p>PReSS Fund (\$2,750)</p> <p>Purchased FASTScan and Silhouette</p>
2010: Year 3 (full-time) clinical research training fellowship (HRC)	<p>Start validation of FASTScan and Silhouette</p> <p>Start TNP study</p>	<p>PBRF Fund Allocation (\$5004)</p> <p>Waikato Medical Research Foundation Grant (\$4996)</p> <p>PReSS Fund (\$2,750)</p>
2011: Year 4 (full-time)	<p>Complete patient recruitment</p>	

RACS Eric Bishop Scholarship	Biochemical analysis	
	(hydroxyproline, growth factors and mRNA)	PBRF Fund Allocation (\$5004) Waikato Medical Research Foundation Grant (\$4996)
	Data analysis	PreSS Fund (\$2,750) Postgraduate Student Fund (\$1,500)
	Thesis writing	
2012-2016: Years 5–8 (part-time), 5% research/95% full-time employment	Presentations in continental and national conferences (e.g., RACS: surgery, ANZSVS, NZVS). First thesis submission Thesis resubmission	PreSS Fund (\$2,750)

Other supports

ORGANISATION	TYPE OF SUPPORT
Waikato District Health Board	Full support from Anaesthetic and Surgical Departments Access to Ilomedin®, Bair Hugger™, VAC®, traditional dressings, sutures and surgical instruments.
University of Auckland	Support in laboratory work with hydroxyproline and growth factor analyses.
University of Waikato	Support in laboratory work with mRNA analyses at the Department of Molecular Genetics.
Atrium™	Free supply of ePTFE tubes

Declaration of interests

This research project was sponsored by independent organisations. There were no conflicts of interest with HyperMed Inc (developer of the OxyVu™), Intermed® (manufacturer of VAC®) or ARANZ (manufacturer of the FastScan™ and Silhouette Mobile™). The devices were purchased or leased using independent research funds.

Acknowledgements

Supervisor:

Prof Jamie Sleigh

Co-Supervisors:

Mr. Thodur Vasudevan

Associate Professor Lindsay Plank

Advisors:

Dr. Christina Buchanan (Department of Molecular Medicine and Pathology, University of Auckland)

Dr. Ray Cursons (Department of Molecular Genetics, University of Waikato)

Dr. Sofian Tijono (Department of Medical Sciences, University of Auckland)

Susan Albrecht (Professional editing)

Others:

Waikato District Health Board

Health Research Council

Royal Australasian College of Surgery

Faculty of Health and Medical Sciences,
University of Auckland

ARANZ Medical Sciences

Braemar Charitable Trust

Atrium®

Prof John Windsor

Mr. Scott Aitken

Dr. Isabel Wright

Dr. Melanie Hwang

Dr. Anna Kang

Dr. Tim Hill

Dr. Ashwini Pondicherry

Dr. Simone Oldham

Table of contents

Abstract.....	ii
Preface.....	iii
Project ownership and contributions.....	iv
Achievements.....	iv
Time frame.....	v
Other supports.....	vi
Declaration of interests.....	vi
Acknowledgements.....	vii
Table of contents.....	viii
List of Tables and Figures.....	xiv
Tables.....	xiv
Figures.....	xvii
Glossary.....	xxii
1. Background.....	1
1.1 Wound healing process.....	1
1.2 Evaluation of wound healing.....	7
Collagen.....	7
Hydroxyproline.....	8
Growth factors and cytokines.....	10
1.3 Factors influencing wound healing.....	13
1.4 Role of oxygen in wound healing.....	15
1.5 Perioperative adjunctive treatments.....	19
Perioperative supplemental oxygen.....	19
Extended perioperative warming.....	19

Perioperative Ilomedin®.....	20
1.6 Infra-inguinal bypass surgery.....	25
1.7 Peripheral vascular disease.....	26
1.8 Management of infra-inguinal occlusive disease.....	29
1.9 Peripheral vascular disease in New Zealand	32
1.10 Tissue perfusion	34
1.11 Assessment of tissue oxygenation.....	35
Measurement of toe pressure	35
Laser Doppler flowmetry	35
Laser angiography	35
Transcutaneous oximetry measurement	36
OxyVu™	41
1.12 Diabetic foot	49
Pathophysiology of DFU	50
1.13 Local wound management.....	54
1.14 Topical negative pressure therapy.....	56
Clinical evidence for TNP.....	60
1.15 Assessment of wound dimensions.....	64
2 Objectives.....	67
2.1 Aims	67
2.2 Summary of studies.....	68
3 Methods.....	70
3.1 Validation of OxyVu™.....	70
3.2 Wound healing and oxygenation in IIB surgery.....	73
3.3 Validation of FastScan™ and Silhouette Mobile™	80
3.4 Wound healing and tissue oxygenation in TNP therapy.....	81

3.5	Statistical methods	84
3.6	Laboratory investigations.....	86
3.6.1	Hydroxyproline assays.....	86
3.6.2	Analysis of growth factors and cytokines	90
3.6.3	Analysis of growth factor mRNA	92
3.7	Operating devices.....	97
3.7.1	OxyVu™	97
3.7.2	Transcutaneous oxygenation measurement	99
3.7.3	Ankle-brachial pressure index.....	101
3.7.4	FastSCAN™	103
3.7.5	Silhouette Mobile™	104
3.7.6	Three-dimensional CT reconstruction	105
4	Results: Validation of OxyVu™	106
	Evaluating inter-operator reliability.....	106
	Evaluating intra-operator reliability.....	110
	Comparing HTCOT to TCOM, skin temperature, ABI and severity of PVD	112
	Estimation of kurtosis and skewness for the variables	113
	OxyVu™ measurements in diseased limb and contralateral limb.....	115
	Comparing OxyVu™ measurements of lower limb to the chest	117
	Correlation between OxyVu™ readings and severity of PVD.....	119
	Correlation between hyperspectral measurements and skin temperature.....	122
	Correlation between hyperspectral measurements and Doppler ABI.....	123
	Correlation between hyperspectral and TCOM measurements.....	124
	Correlation between hyperspectral oxygenation and demographics	127
	Correlation between HT-Sat and TcPO ₂	128
5	Results: WOLOW study.....	130

Patient recruitment and demographics	130
Systemic effects of perioperative adjuncts.....	134
Accumulation of hydroxyproline.....	135
Balance between growth factors and cytokines	136
Analyses of mRNA	136
Assessments of tissue oxygenation.....	137
Long-term follow-up.....	145
6 Results: Validation of FastScan™ and Silhouette Mobile™	147
Patient recruitment	147
Evaluation of intra-operator and inter-operator reliability.....	149
Correlation between SM and FS versus CT reconstruction.....	149
7 Results: Wound healing and tissue oxygenation in TNP therapy.....	155
Patient recruitment and demographics	155
Changes in wound dimensions.....	157
Changes in collagen content of granulation tissue.....	160
Changes in growth factor and cytokine levels.....	160
Changes in skin perfusion	161
Clinical outcome	162
8. Discussion.....	164
8.1 Key findings.....	164
8.2 Validation of OxyVu™.....	166
8.3 WOIOW study	171
8.4 Validation of FastScan™ and Silhouette Mobile™	175
8.5 Wound healing and tissue oxygenation in TNP therapy.....	181
8.6 The future.....	184
8.7 Conclusions.....	187

9. Appendices.....	188
A.1 Definitions	188
A.1.1 Risk factors.....	188
A.1.2 Rutherford and Fontaine classifications	189
A.1.3 V-POSSUM	190
A.2 Consent forms	Error! Bookmark not defined.
A.2.1 Validation of OxyVu™	Error! Bookmark not defined.
A.2.2 WOIOW study.....	Error! Bookmark not defined.
A.2.3 Validation of FastScan™ and Silhouette Mobile™	Error! Bookmark not defined.
A.2.4 Wound healing and tissue oxygenation in TNP therapy	Error! Bookmark not defined.
A.3 Study information sample (from WOIOW study)	Error! Bookmark not defined.
A.3.1 Patient information sheet	Error! Bookmark not defined.
A.3.2 For the control group	Error! Bookmark not defined.
A.3.3 For the oxygen group.....	Error! Bookmark not defined.
A.3.4 For the Ilomedin® group	Error! Bookmark not defined.
A.3.5 For the temperature group.....	Error! Bookmark not defined.
A.4 Data collection sheet sample (from WOIOW study)	Error! Bookmark not defined.
A.5 Post-operative Ilomedin® protocol.....	191
A.6 Additional tables from results: Validation of OxyVu™	193
A.6.1 Correlation between OxyVu and TCOM of the diseased limb.....	193
A.6.2 Correlation between OxyVu and TCOM of the contralateral limb and chest...	194
A.6.3 ANOVA to determine confounding factors that affect OxyVu™.....	195
A.6.4 Correlation between hyperspectral oxygenation and haemoglobin	196
A.7 Additional results from the WOIOW study.....	200

A.7.1. P-values for hydroxyproline and growth factors in treatment arms versus the control group	200
A.8 Additional results: Wound healing and tissue oxygenation in TNP therapy	201
A.8.1. Summary of kurtosis and skewness values on variables.....	201
10 Determining time duration for TCOM electrodes to reach equilibrium.	202
Background.....	202
Aim.....	202
Methods	202
Results	203
Changes in measurements over time.....	204
Discussion.....	207
Conclusion	208
References	209

List of Tables and Figures

Tables

Table 1. 1. Summary of clinical studies on topical negative pressure therapy and wound dimension assessment.....	60
Table 3. 1. Interventions received in each study arm.	73
Table 3. 2. Code for relevant primers.	95
Table 4. 1. Summary of ICC values and 95% CIs for OxyVu™ measurements.....	108
Table 4. 2. Summary of mean differences in OxyVu™ measurements between two operators.	109
Table 4. 3. Summary of mean differences of OxyVu™ measurements in each comparison.	110
Table 4. 4. Summary of CV and 95% CI for OxyVu™ measurements.....	111
Table 4. 5. Basic demographics of participants.....	112
Table 4. 6. Summary of skewness and kurtosis for all continuous variables.....	114
Table 4. 7. Summary of OxyVu™ findings in vascular patients.	115
Table 4. 8 Summary of OxyVu™ findings in terms of BPI in vascular patients.	115
Table 4. 9. Summary of OxyVu™ findings in volunteers.....	116
Table 4. 10. Summary of OxyVu™ findings in terms of BPI in volunteers.....	116
Table 4. 11. Hyperspectral readings at the chest.	117
Table 4. 12. Summary of OxyVu™ findings with regard to RPI in vascular patients.....	118
Table 4. 13. Correlation between RPI and BPI describing correlation coefficients and p-values.	118
Table 4. 14. Spearman's rank correlation coefficients and p-values comparing OxyVu™ readings for the diseased limb with severity of peripheral vascular disease.	121
Table 4. 15. Spearman's rank correlation coefficients and p-values comparing OxyVu™ readings of the contralateral limb with severity of peripheral vascular disease.	122
Table 4. 16. Summary of Pearson's correlation coefficients and p-values comparing skin temperature with OxyVu™ measurements of the diseased limb.	122
Table 4. 17. Descriptive summary of ABI in the diseased and contralateral limb according to severity of vascular disease using the Simplified Severity Score.....	123

Table 4. 18. Summary of Spearman’s rank correlation coefficients and p-values when comparing ABI with severity of peripheral vascular disease.	124
Table 4. 19. Summary of Pearson’s correlation coefficients and p-values when comparing the ABI of the diseased limb with OxyVu™ readings.....	124
Table 4. 20. Descriptive summary of TCOM readings of the diseased limb according to severity of peripheral vascular disease using the Simplified Severity Score.	125
Table 4. 21. Summary of Spearman’s rank correlation coefficients and p-values when comparing transcutaneous oxygenation measurement readings for the diseased limb with the severity of peripheral vascular disease using the Simplified Severity Score.	125
Table 4. 22. Summary of transcutaneous oxygenation measurement findings for reference points according to severity of peripheral vascular disease using the SSS.....	126
Table 4. 23. Summary of Pearson’s correlation coefficients and p-values when comparing transcutaneous oxygenation measurement readings for the diseased limb with OxyVu™ readings.....	126
Table 4. 24. Summary of p-values from linear regression investigating how race, gender, and age affected OxyVu™ findings.....	127
Table 5. 1. Basic demographics of study participants.....	132
Table 5. 2. Operative findings in the participants.....	133
Table 5. 3. Influence of supplemental oxygen and active warming on arterial oxygenation and core temperature.....	134
Table 5. 4. Mean (SD) hydroxyproline and growth factor levels in tissue samples from each group.	136
Table 5. 5. Summary of statistically significant changes in OxyVu™ readings at the foot in the treatment arms versus the control group.	144
Table 5. 6. Summary of postoperative complications.	144
Table 5. 7. Patency, limb salvage, and mortality rates in the four groups.	145
Table 6. 1. Intra-operator and inter-operator reliability of Silhouette Mobile™	149
Table 6. 2. Intra-operator and inter-operator reliability of FastScan™.	149
Table 6. 3. Depth and volume measurements using Silhouette Mobile™ compared with those from computed tomography.	150

Table 6. 4. Summary of Pearson’s correlation coefficients when comparing measurements for Silhouette Mobile™, FastScan™, and computed tomography.....	154
Table 7. 1. Basic patient demographic and clinical characteristics.	156
Table 7. 2. Summary of wound dimensions at day 0.	157
Table 7. 3. Summary of absolute and relative reduction in wound dimensions between the two treatment groups.....	158
Table 7. 4. Wound dimensions at day 0 for wounds at the toe and those at forefoot/heel.	159
Table 7. 5. Absolute and relative reductions in wound dimension between wounds at the toes and those at the forefoot and heel.....	159
Table 7. 6. Summary of mean OHP findings at baseline and percentage increase at 14 days for the TNP group and the control group.	160
Table 7. 7. Mean TGF-β findings at baseline and mean percentage increase at 14 days for the TNP group and the control group.	161
Table 7. 8. OxyVu™ findings at baseline and mean percentage increase at 14 days in the TNP group and the control group.	162
Table 7. 9. Comparison of OxyVu™ findings at baseline and day 14, showing mean differences and their p-values.....	162
Table 7. 10. Comparison of survival analysis outcome between TNP group and control group..	163
Table 9. 1. Descriptive summary for HT-Sum and haemoglobin.....	196
Table 9. 2. Summary of unstandardised coefficients and p-values using linear regression to identify confounding factors for Hb and HT-Sum.....	197
Table 10. 1. Basic demographics of the three groups of patients	203

Figures

Figure 1. 1. Initial stages of the wound healing process.....	1
Figure 1. 2. Role of neutrophils in the inflammatory phase.....	3
Figure 1. 3. Role of macrophages in the inflammatory phase.....	3
Figure 1. 4. Later stages of the wound healing process.	6
Figure 1. 5. Accumulation of hydroxyproline in polytetrafluoroethylene tubing in normal human subjects.	9
Figure 1. 6. Oxygen, the substrate for collagen synthesis.	17
Figure 1. 7. Structural comparison of iloprost and prostacyclin.....	20
Figure 1. 8. Effects of critical limb ischaemia on the microcirculation.	21
Figure 1. 9. Effects of iloprost on the microcirculation.	21
Figure 1. 10. Effect of prostaglandin I ₂ (iloprost) on vascular smooth muscle.....	23
Figure 1. 11. Prognosis of patients with peripheral vascular disease.....	27
Figure 1. 12. Two-year prognosis following below-knee amputation.....	28
Figure 1. 13. Trans-Atlantic Inter-Society Consensus classification of femoral-popliteal lesions.	29
Figure 1. 14. Proposed electrode behaviour during equilibrium.....	38
Figure 1. 15. A schematic diagram demonstrating how a transcutaneous oximetry measurement electrode works.	39
Figure 1. 16. Photograph of the OxyVu-2™ system.	41
Figure 1. 17. Diagram illustrating how the OxyVu™ works.....	42
Figure 1. 18. OxyVu™ using different wavelengths to detect specific chromophores.	44
Figure 1. 19. Graph demonstrating the chromophores of oxyhaemoglobin and deoxyhaemoglobin.	44
Figure 1. 20. Example of an OxyVu™ reading.	45
Figure 1. 21. Application of VAC® foam.....	56
Figure 1. 22. Effects of topical negative pressure therapy.....	57
Figure 1. 23. Image of the Silhouette Mobile™	66
Figure 1. 24. Image of the FastScan™	66
Figure 3. 1. Illustration of implanting and explanting the PTFE tubing from the surgical wound	77

Figure 3. 2. Location of the ePTFE implant and sites where oxygenation was measured using OxyVu™	79
Figure 3. 3. ePTFE tube hydrolysed in 6 M HCl, OHP solute in microtube, and ePTFE tube following hydrolysis.	87
Figure 3. 4. Photograph of the SpeedVac®.	87
Figure 3. 5. Example of the 96-microwell plate containing standards and samples prior to spectrometry.	89
Figure 3. 6. An example of a Nanodrop® report for an RNA sample from one of the study participants.	93
Figure 3. 7. An example of gel electrophoresis following reverse transcriptase polymerase chain reaction of a sample from four study participants.	96
Figure 3. 8. Example of an OxyVu™ reading.	98
Figure 3. 9. Operating the OxyVu™	98
Figure 3. 10. Image of transcutaneous oxygenation measurement monitor.	100
Figure 3. 11. Measurement of ankle-brachial pressure index.	102
Figure 3. 12. Image explaining measurement of the ankle-brachial pressure index.	102
Figure 3. 13. Example of wound dimension analysis using the FastScan Volumator.	103
Figure 3. 14. Image of Silhouette Mobile™	104
Figure 4. 1 Scatter plot showing the variation in HT-Oxy measurements between two operators.	106
Figure 4. 2. Scatter plot showing the variation in HT-Deoxy measurements between two operators.	107
Figure 4. 3. Scatter plot showing the variation in HT-Sat measurements between two operators.	107
Figure 4. 4. Scatter plot showing the variation in skin temperature measurements between two operators.	108
Figure 4. 5. Bland-Altman (scatter) plot for HT-Oxy measured by two operators.	109
Figure 4. 6. Error bar graph showing the mean ± 95% CI of HTCOT readings in the lower limb of individual A and B.	110
Figure 4. 7. Error bar graph showing the mean ± 95% CI for skin temperature in the lower limb of individual A and B	111

Figure 4. 8. Bar chart showing the distribution of the study population according to severity of peripheral vascular disease.	113
Figure 4. 9. Boxplot of T _{cp} CO ₂ of the diseased limb of all patients including the outlier.	113
Figure 4. 10. Bar chart showing the number of patients who had chest OxyVu™ measurements according to Rutherford classification.	117
Figure 4. 11. Bar chart showing how OxyVu™ measurements for the diseased limb varied according to Rutherford classification.....	119
Figure 4. 12. Bar chart showing how the bilateral perfusion index of the diseased limb varied according to Rutherford classification.....	120
Figure 4. 13. Bar chart showing how OxyVu™ readings in the diseased limb vary according to severity of peripheral vascular disease.	120
Figure 4. 14. Bar chart showing how the bilateral perfusion index of the diseased limb varied according to the severity of peripheral vascular disease.	121
Figure 4. 15. Scatter plot of the ankle-brachial pressure index in the diseased and contralateral limb according to the Simplified Severity Score.....	123
Figure 4. 16. Oxygen-haemoglobin dissociation curve.	128
Figure 4. 17. Scatter plot with an S-curve showing the association between HT-Sat and T _{cp} O ₂	129
Figure 5. 1. Flow diagram showing patient recruitment.	130
Figure 5. 2. Change in core temperature over time with active warming in the preoperative period.....	134
Figure 5. 3. Changes in HT-Sat at the surgical wound site over time.	137
Figure 5. 4. Changes in HT-Sum at the surgical wound site over time..	138
Figure 5. 5. Changes in HT-Sum BPI of the diseased foot over time.....	139
Figure 5. 6. Changes in HT-Sat BPI of the diseased foot over time.....	140
Figure 5. 7. Changes in ABI of the diseased limb over time.	141
Figure 5. 8. Changes in T _{cp} O ₂ BPI of the diseased foot over time.	142
Figure 5. 9. Changes in T _{cp} CO ₂ BPI of the diseased foot over time.	142
Figure 5. 10. Changed in ABI of the contralateral limb over time.....	143
Figure 6. 1. Image from Silhouette Mobile™ of several lower limb diabetic ulcers.....	147

Figure 6. 2. Image from Silhouette Mobile™ of an infected surgical wound on a lower limb. 147

Figure 6. 3. Image from FastScan™ of an infected surgical wound on a lower limb. Blue stylus points outline the wound boundary..... 148

Figure 6. 4. Image from Silhouette Mobile™ of an open foot wound following digital amputation..... 148

Figure 6. 5. Image from FastScan™ of an open foot wound following digital amputation.. 148

Figure 6. 6. Bland-Altman plot showing the difference in volume measurements between Silhouette Mobile™ and computed tomography..... 151

Figure 6. 7. Bland-Altman plot showing the difference in depth measurements between Silhouette Mobile™ and computed tomography..... 152

Figure 6. 8. Bland-Altman plot showing the difference in volume measurements between FastScan™ and computed tomography..... 152

Figure 6. 9. Bland-Altman plot show the difference in depth measurements between FastScan™ and computed tomography..... 153

Figure 7. 1. Flow diagram detailing the recruitment process..... 155

Figure 7. 2. Error bar graph showing the mean ± 95% CI of the relative reduction of various wound dimensions between the two groups..... 157

Figure 7. 3. Kaplan-Meier curve showing wound failure-free survival between the two groups. 163

Figure 8. 1. Error bar graph showing the mean ± 95% CI of T_{cp}O₂ and T_{cp}CO₂ of the diseased limb subdivided according to the severity of peripheral vascular disease.. 167

Figure 8. 2. Image from Silhouette Mobile™ showing a small ulcer on the dorsal surface of the toe..... 176

Figure 8. 3. Image from Silhouette Mobile™ showing a small ulcer on the lateral dorsal surface of the foot..... 176

Figure 8. 4. Image from Silhouette Mobile™ showing an open wound on an above-knee amputation stump. 177

Figure 8. 5. Wound report using SM from one of the participants showing variation in volume over time..... 180

Figure 9. 1. Rutherford and Fontaine classifications for peripheral vascular disease.....	189
Figure 9. 2. Physiological score for V-POSSUM.....	190
Figure 9. 3. Operative score for V-POSSUM.....	190
Figure 9. 4. Bar chart showing the variation in HT-Sum and haemoglobin according to severity of peripheral vascular disease using the Simplified Severity Score.	196
Figure 9. 5. ROC curve to determine if HT-Sum of the contralateral limb would be an accurate tool to diagnose haemoglobin.	199
Figure 10. 1. Bar chart showing the total number of measurements per set of readings....	203
Figure 10. 2. Line graph showing mean variation in T _{cp} O ₂ and T _{cp} CO ₂ over time.	204
Figure 10. 3. Line graph showing proportional change in T _{cp} O ₂ over time.....	205
Figure 10. 4. Line graph showing proportional change in T _{cp} CO ₂ over time.	205
Figure 10. 5. Line graph showing the proportional change in T _{cp} O ₂ in subgroups over time.	206
Figure 10. 6. Line graph showing the proportional change in T _{cp} CO ₂ in subgroups over time.	206
Figure 10. 7. Line graph showing the proportional change in T _{cp} O ₂ and T _{cp} CO ₂ over time in the 16 diseased limbs of patients with PVD.....	207

Glossary

<	Less than
>	More than
°C	Degrees Celsius
3D	Three-dimensional
μ	Micron (10 ⁻⁶)

A

AAA	Abdominal aortic aneurysm
ABI	Ankle-brachial index
ACS	Acute coronary syndrome
AK	Above knee
AKA	Above-knee amputation
ANOVA	Analysis of variance
ANZSVS	Australia and New Zealand Society of Vascular Surgery
ASVS	Asian Society of Vascular Surgery
AT	Anterior Tibial
ATM	Atmospheric pressure
AU	Artificial unit
AUC	Area under the curve
AV	Arteriovenous

B

B	Unstandardised coefficient
BK	Below knee
BKA	Below-knee amputation
BMI	Body mass index
BP	Blood pressure
BPG	Bypass graft

BPI	Bilateral perfusion index
-----	---------------------------

C

cAMP	Cyclic adenosine monophosphate
CABG	Coronary artery bypass graft
CBF	Cutaneous blood flow
cDNA	Complementary DNA
CEA	Carotid endarterectomy
CFA	Common femoral artery
CI	Confidence interval
CLI	Critical limb ischaemia
cm	Centimetre
COPD	Chronic obstructive pulmonary disease
CO ₂	Carbon dioxide
CT	Computed tomography
CTA	Computed tomography angiogram
CTGF	Connective tissue growth factor
CTO	Chronic total occlusion
CV	Coefficient of variation
CVA	Cerebrovascular accident

D

Deoxy	Deoxyhaemoglobin
DFU	Diabetic foot ulcers
DM	Diabetes mellitus
DNA	Deoxyribonucleic acid
DSA	Digital subtraction angiogram
DTT	Dithiothreitol

E

ECM	Extracellular matrix
EDCF	Endothelium-derived constricting factor
EDHF	Endothelium-derived hyperpolarising factor
EDRF	Endothelium-derived relaxing factor
EGF	Epidermal growth factor
eGFR	Estimated glomerular filtration rate
ELISA	Enzyme-linked immunosorbent assay
eNOS	Endothelial nitric oxide synthase
ERK	Extracellular signal-regulated kinase
ESRF	End-stage renal failure
ESVS	European Society for Vascular Surgery

F

Fe ²⁺	Iron
FGF	Fibroblast growth factor
FiO ₂	Inspired oxygen concentration
FS	FastScan™

G

g	gram
---	------

GITC	Guanidine thiocyanate
GSV	Great saphenous vein

H

Hb	Haemoglobin
HbA _{1c}	Glycated haemoglobin
HBOT	Hyperbaric oxygen therapy
HCl	Hydrochloric acid
HIF-1	Hypoxia-inducible factor 1
HR	Heart rate
HTcOM™	Hyperspectral transcutaneous oxygenation measurement
HT-Deoxy	Deoxyhaemoglobin concentration measured by OxyVu™
HTML	HyperText Markup Language
HT-Oxy	Oxyhaemoglobin concentration measured by OxyVu™
HT-Sat	Oxyhaemoglobin saturation measured by OxyVu™
HT-Sum	Sum of Oxy- and deoxy-haemoglobin

I

IC	Intermittent claudication
ICAM-1	Intercellular adhesion molecule-1

ICC	Intraclass correlation coefficient
ICG	Indocyanine green
IGF-1	Insulin-like growth factor 1
IHD	Ischaemic heart disease
IIB	Infra-inguinal bypass
IL	Interleukin
iNOS	Inducible NO synthase
IP-10	Interferon-inducible protein
IPA	Isopropanol (isopropyl-alcohol)

J-L

KGF	Keratinocyte growth factor
kPa	Kilopascals (pressure)
LDF	Laser Doppler flowmetry
LEDs	Light-emitting diodes
LRTI	Lower respiratory tract infection

M

M	Molar
MCP-1	Monocyte chemotactic protein-1
mg	milligram
ml	millilitre
mm	millimetre
mmHg	mm of mercury (pressure)
MMP	Matrix metalloproteinase

MQ	Milli-Q™ (water)
MRA	Magnetic resonance angiogram
MRSA	Methicillin-resistant <i>Staphylococcus aureus</i>
mRNA	Messenger RNA
MW	Molecular weight

N

NADPH	Nicotinamide adenine dinucleotide phosphate-oxidase
NaOH	Sodium hydroxide
NICE	National Institute of Health and Clinical Excellence guidelines
nm	Nanometre
NO	Nitric oxide
NSAIDS	Non-steroidal anti-inflammatory drugs
NZ	New Zealand

O

OHP	Hydroxyproline
OR	Odds ratio
OS	Operative score
Oxy	Oxyhaemoglobin

P-Q

PAI	Plasminogen activator inhibitor
PAOD	Peripheral arterial occlusive disease
PDA	Personal digital assistant
PDGF	Platelet-derived growth factors
PFA	Profunda artery
PGI ₂	Prostacyclin I ₂
pH	Measurement of acidity and basicity
P _i O ₂	Partial pressure of inspired oxygen
Pop	Popliteal
PS	Physiological score
PT	Posterior tibial
PTA	Percutaneous transluminal angioplasty
PTFE	Polytetrafluoroethylene
PU	Polyurethane
PVA	Polyvinyl alcohol foam
PVD	Peripheral vascular disease

R

R	Correlation coefficient
RCT	Randomised controlled study
ROI	Region of interests
ROC	Receiver operating characteristic

ROS	Reactive oxygen species
RPI	Regional perfusion index
RT	Reverse transcriptase

S

SA	Surface area
Sat	Saturation
SBP	Systolic blood pressure
SD	Standard deviation
SE	Standard error
SFA	Superficial femoral artery
SM	Silhouette Mobile™
SSI	Surgical site infection
SSS	Simplified severity score
SVS	Society of Vascular Surgery

T

TASC	Trans-Atlantic Inter-Society Consensus Document on Management of Peripheral Arterial Disease
TCOM	Transcutaneous oxygenation measurement
TcpO ₂	Transcutaneous partial pressure of oxygen
TcpCO ₂	Transcutaneous partial pressure of carbon dioxide
TGF-α	Transforming growth factor-α
TGF-β	Transforming growth factor- β

TIA	Transient ischaemic attack
TIMP	Tissue inhibitors of metalloproteinase
TNF- α	Tumor necrosis factor- α
TNP	Topical negative pressure
t-PA	Tissue plasminogen activator
TPT	Tibial peroneal trunk

	Healing in infra-inguinal bypass surgery
--	------------------------------------------

U

USS	Ultrasound
UV	Ultraviolet

V-Z

VAC®	Vacuum Assisted Closure
VEGF	Vascular endothelial growth factor
Vol	Volume
V-POSSUM	Vascular-physiological and operative severity score for the enumeration of mortality and morbidity
VSGBI	Vascular Society of Great Britain and Ireland
Wifi	Wound, Ischemia, and foot Infection (classification)
WOIOW	Effects of perioperative Warming, Oxygen and Ilomedin (PGI ₂) on Oxygenation and Wound

1. Background

1.1 Wound healing process

Wound healing is an intricate cascade that includes collagen formation, angiogenesis, and production of epithelial tissue, and is dependent on both physiology and the environment. It is commonly described in four stages that overlap in time. The key phase of wound healing in terms of collagen deposition is the first 3 days, where accumulation of growth factors and cell proliferation dictate the potential for wound healing.^{1,2}

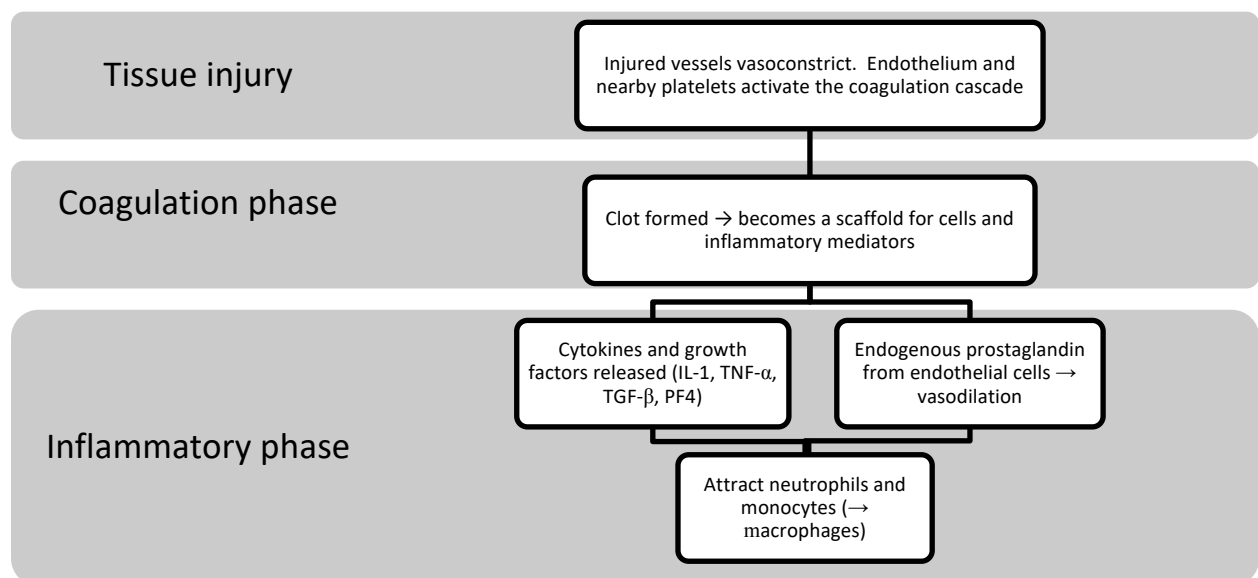


Figure 1. 1. Initial stages of the wound healing process. **Abbreviations:** IL-1, interleukin-1; TNF, tumor necrosis factor; TGF, transforming growth factor; PF4, platelet factor 4.

Coagulation phase

Immediately following acute tissue injury, the surrounding platelets aggregate, resulting in haemostasis. A thrombus is formed, composed of cross-linked fibrin and extracellular matrix (ECM) proteins such as fibronectin³⁻⁵ (Figure 1.1). This clot acts as a scaffold for inflammatory cells and mediators, and provides a barrier against micro-organisms.⁶ Cytokines and growth factors, such as platelet-derived growth factor (PDGF), transforming growth factor-beta (TGF- β), and fibroblast growth factor (FGF), are released from degranulated platelets, surrounding monocytes, and macrophages.⁷ These factors have chemotactic effects on proliferation and migration of endothelial cells.⁸⁻¹⁰

Inflammatory phase

The inflammatory phase typically commences 6 hours following injury and is characterised by chemotactic migration of neutrophils, macrophages, monocytes, lymphocytes, and fibroblasts stimulated by growth factors and cytokines, such as PDGF, tumor necrosis factor (TNF)- α , interleukin (IL)-1, and TGF- β released into the exposed wound.^{11 12} Synthesis of these cytokines by the above cells further enhances chemotaxis in an autocrine manner.¹³ Endogenous prostaglandins released from endothelial cells cause vasodilation and intensify the chemotactic process.⁸

The wound is initially dominated by neutrophils, with lymphocytes appearing after 24 hours (Figure 1.2). By 48 hours, there is a high concentration of lymphocytes, monocytes, macrophages, and a few fibroblasts. While macrophages and monocytes are usually attracted by cytokines, migration can also be stimulated by hypoxia, lactate, fibronectin, collagen, elastin, foreign body reaction, and endothelial integrins.¹⁴ Monocytes at the wound site differentiate into macrophages at around 48–96 hours, when fibronectin binds to the surface.¹⁵

Activation of macrophages is an important step in transition into the proliferative phase (Figure 1.3). Macrophages mediate:

- angiogenesis by synthesising VEGF, FGF, and TNF- α
- fibroplasia by synthesising TGF- β , EGF, PDGF, IL-1, and TNF- α
- epithelial regeneration by synthesising PDGF
- synthesis of nitric oxide (NO) via activation of inducible NO synthase by IL-1 and TNF- α .¹⁶

Neutrophils clear invading bacteria and cleanse the wound of cellular debris by releasing proteases to break down the damaged ECM, thus laying the foundation for wound healing.¹⁷ Proteases are grouped by their preferred target, i.e., proteins, amino acids, or metal ions. Serine proteases, such as elastase, have broad activity, whereas metalloproteinase specifically digests collagen. The matrix in non-wounded tissue is protected by protease inhibitors.¹⁸ Neutrophils also generate reactive oxygen free radicals through the myeloperoxidase pathway. These products combine with chlorine to sterilize the wound.¹⁸

Neutrophils eventually undergo apoptosis and are replaced by macrophages, which phagocytose the dead neutrophils. Macrophages, like neutrophils, digest pathogenic organisms and debris by phagocytosis. They also kill pathogens by generating NO. Inducible NO synthase from macrophages is stimulated by TNF- α and IL-1 to synthesise NO, which reacts with peroxide ion oxygen radicals to yield toxic peroxynitrite and hydroxyl radicals.¹⁹

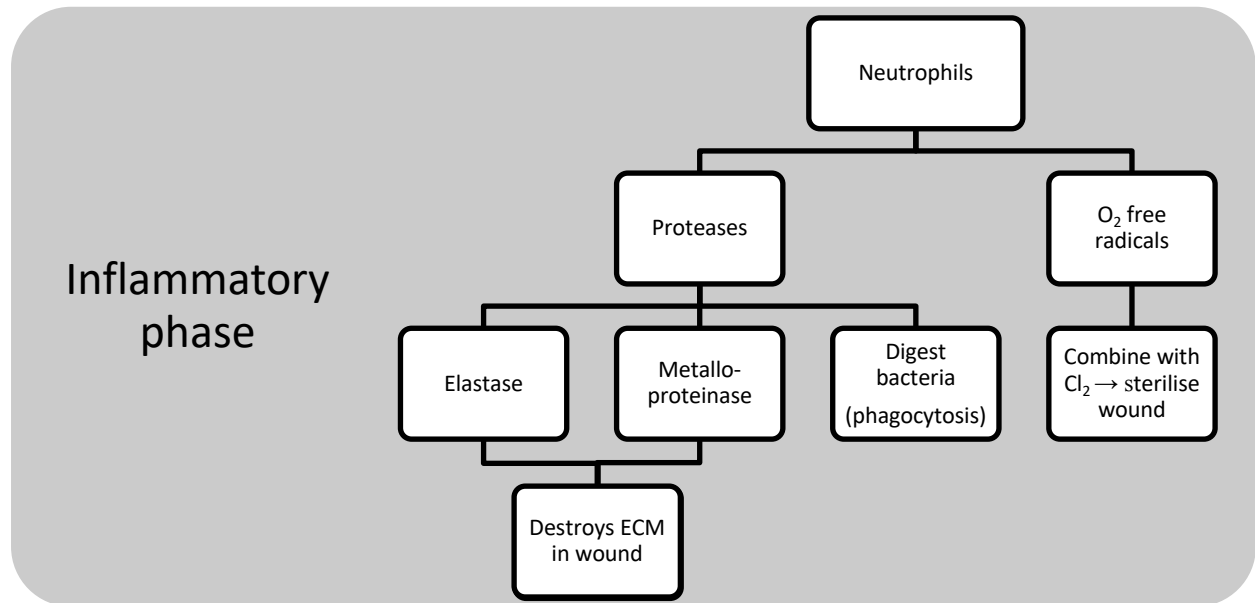


Figure 1. 2. Role of neutrophils in the inflammatory phase. **Abbreviation:** ECM, extracellular matrix

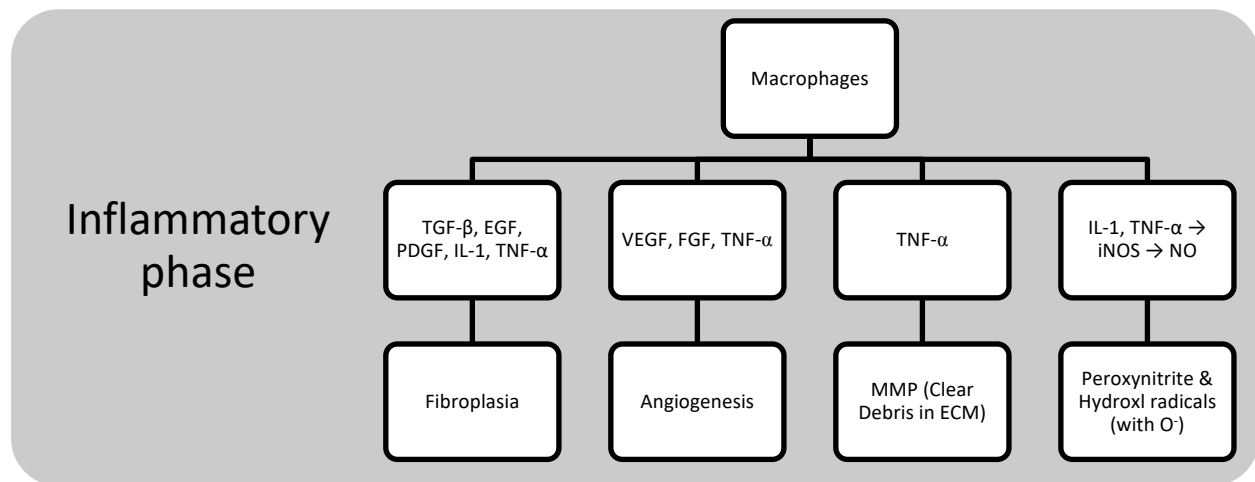


Figure 1. 3. Role of macrophages in the inflammatory phase. **Abbreviations:** ECM, extracellular matrix; EGF, epidermal growth factor; IL-1, interleukin-1; MMP, matrix metalloproteinase; PDGF, platelet-derived growth factor; TGF- β , transforming growth factor-beta; TNF- α , tumor necrosis factor-alpha; VEGF, vascular endothelial growth factor

At the end of the inflammatory phase, neutrophils, platelets, and leucocytes trigger lipoygenases to synthesise lipid mediators, i.e., lipoxins (LXA4 and LXB4). Lipoxins are the stop signal for inflammation and neutrophil infiltration.²⁰

Proliferative phase

Accumulation of growth factors and cytokines leads to the proliferative phase occurring between days 4 and 14. This is characterised by deposition of granulation tissue composed of macrophages, myofibroblasts, and fibroblasts in the ECM.¹⁴

Initially, epithelial cells at the skin edges are stimulated by EGF and TGF- α to start proliferating and re-establish a protective barrier against fluid loss and further bacterial invasion.^{21 22} Migration, proliferation, and eventual differentiation of keratinocytes in the epidermis is triggered by keratinocyte growth factor-1, keratinocyte growth factor-2, and IL-6 produced by fibroblasts, which in turn are upregulated by IL-1 and TNF- α .^{23 24}

Fibroblasts and endothelial cells are the key proliferating cells in this phase. Fibroblasts around the wound are known as wound fibroblasts. Their main actions are stimulated by PDGF and EGF (Figure 1.4). These actions include:^{8 9 14}

- Amplification of PDGF expression by autocrine and paracrine signalling
- Formation of a provisional matrix as early as day 3, comprising mainly type III collagen, which is a temporary and weaker collagen. Hyaluronic acid, glycosaminoglycans, and fibronectin provide low impedance for cell motility and serve as the scaffold.²⁵
- Synthesis of type I collagen after day 5, stimulated by TGF- β 1, a permanent and stronger collagen providing tensile strength.
- Attracting fibroblasts with a contractile phenotype from the periphery and transforming them into myofibroblasts (smooth muscle cells) in the presence of TGF- β 1. These elongate and increase wound contraction. Fibroblasts also release chemokines that result in synthesis, migration, and proliferation of ECM proteins.

- Decreasing the release of proteases, increasing tissue inhibitors of metalloproteinase, and increasing production of cell adhesion proteins, which in turn increases production of ECM.¹⁹

Angiogenesis and nerve sprouting occur simultaneously around the wound edge. Angiogenic cytokines, namely VEGF, FGF, and TGF- β , interact with endothelial cells, angiopoietin, and the ECM. This starts the process of angiogenesis, typically on day 2.^{26 27} VEGF is secreted predominantly by keratinocytes at the wound edge, but also by macrophages, fibroblasts, platelets, and endothelial cells.²⁸ NO produced by endothelial NO synthase in response to hypoxia stimulates further production of VEGF. The increased concentrations of NO also protect the tissue from the toxic effects of ischaemia and reperfusion injury and cause vasodilation.²⁹

Granulation tissue matures with ongoing synthesis and catabolism of collagen. While wound hypoxia stimulates certain aspects of the complex wound healing process, oxygen is important for migration and replication of cells, such as macrophages and fibroblasts, and their synthesis of growth factors. The role of oxygen in wound healing is discussed later.

Interferon-inducible protein is the stop signal for this phase, inhibiting fibroblast motility and thereby limiting recruitment of fibroblasts. It also has a negative mitogenic effect on fibroblasts.³⁰

Remodelling phase

The remodelling phase continues for up to 2 years, during which the cellular composition of the wound bed and the ECM undergoes continuous change. The thinner type III collagen is replaced by thicker type I collagen. The new collagen is aligned in a more orderly pattern with the fibrils orientating parallel to the lines of tension, giving optimum isometric tensile strength.³¹ This is controlled by matrix metalloproteinase (MMP) induced by IL-1, TNF- α , FGF-2, EGF, and PDGF. Fibronectin is also removed from the ECM. Fibroblasts continue to convert to myofibroblasts. Collagen bundles grow in size and numbers, and proteoglycans are deposited, making the tissue resilient to tension.

An increased rate of collagen synthesis may be observed as early as 24 hours, and increases exponentially after day 5, reaching a maximum at approximately 6–14 days.^{4 32} The rate of collagen synthesis remains elevated for more than 10 weeks. The tensile strength, in contrast, increases sharply after 7–14 days, reaches 40% of the strength of intact tissue after one month, and plateaus after 13 weeks. Tensile strength rarely exceeds 80% a year after injury.³³

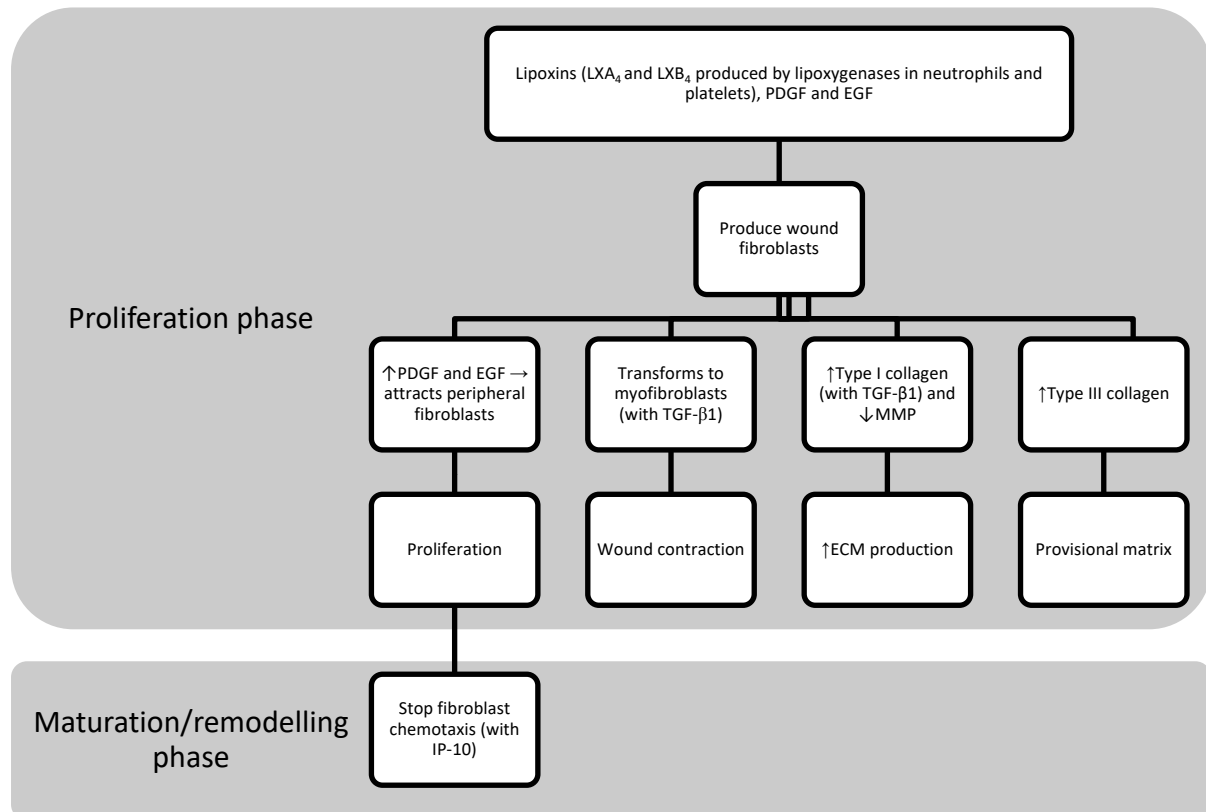


Figure 1. 4. Later stages of the wound healing process. **Abbreviations:** ECM, extracellular matrix; EGF, epidermal growth factor; IP-10, interferon-inducible protein; MMP, matrix metalloproteinase; PDGF, platelet-derived growth factor; TGF-β1, transforming growth factor-beta1

1.2 Evaluation of wound healing

Measuring the tensile strength of a human wound would be unjustifiable and unethical, so *in vitro* and *in vivo* tissue models, such as organ cultures of human skin and a rabbit model of ear chamber wounds, respectively, have been used to assess wound tensile strength, even though they are not a genuine reflection of human biological activity.

1. Collagen is a key ingredient of wound granulation tissue, and wound tensile strength is directly proportional to the amount of collagen deposition in primary closed wounds.¹³ Quantifying collagen deposition is hence a surrogate marker of wound healing.
2. Studying concentrations of growth factors and cytokines in the wound would also provide an indirect insight into the wound maturation profile.

Collagen

Collagen is the most abundant protein in the body, and comprises more than a third of the total amount of protein therein. It is present in the skin, bones, tendons, and other connective tissues. Collagen fibrils are arranged in different ways depending on the biological function of specific tissues. In tendons, fibres are arranged in parallel to yield strength without stretch, whereas in skin the interlacing network laid out in sheets provides multiple dimensions of strength. Most collagen contains about 35% glycine and 11% alanine. Collagen is distinctive in containing about 12% proline and 9% hydroxyproline (OHP). Hydroxyproline is more prominent in types III and IV collagen than in types I and II collagen. Type I collagen is highly prevalent in normal uninjured skin (80%–90%) when compared with type III collagen (20%), which is typically found in acute wounds. Type III collagen runs in reticular fibres and provides no significant increase in wound tensile strength. It is produced by mesenchymal cells and can be detected in an acute wound within 1–2 days, during which time there is no type I collagen.

The secondary structure of the polypeptide chains of collagen is a triple helix. Collagen molecules comprise more than nine different α -chains when pro-collagen is synthesised. The pre-peptides are proteolytically cleaved from pro- α -chains. The proline and lysine residues of the molecule are hydroxylated in the cisternae of the rough endoplasmic reticulum by three different enzymes (prolyl 4-hydroxylase, prolyl 3-hydroxylase, and lysyl hydroxylase), all of

which require oxygen, iron (Fe^{2+}), α -ketoglutarate, and ascorbate. The products, hydroxylysine and hydroxyproline, are nearly 100% specific to collagen.

The hydroxylysine residues undergo glycosylation catalysed by two specific transferases and Mn^{2+} . The pro- α -chains then fold into a triple helix. This requires 4-hydroxylation of the proline and interchain disulfide bonding between the C-terminal propeptides. The helix is stabilised by the hydroxyl group of the 4-hydroxyproline, whereas hydroxylysine is essential for formation of crosslinks later in the process. The helical structure prevents further interaction with enzymes.

Soluble tropocollagen is transported out of the rough endoplasmic reticulum through the Golgi apparatus before secretion from the cell. The quantity of proline synthesised determines the rate of collagen synthesis. The production of proline is enhanced by its precursors ornithine, glutamate, glutamine, and arginine.

The N-terminal and C-terminal propeptides are cleaved extracellularly by proteases. This process leads to assembly of the chains and formation of fibrils. Lysine and hydroxylysine residues undergo oxidative deamination by lysyl oxidase, which requires oxygen and copper. This leads to formation of aldehydes, which form the crosslinks within collagen fibrils, providing stability. Lysyl hydroxylase and lysyl oxidase regulate collagen cross-linking.^{34 35}

Hydroxyproline

Hydroxyproline ($\text{C}_5\text{H}_9\text{O}_3\text{N}$) is a non-essential amino acid confined exclusively to collagen, connective tissue selenoproteins, and elastin. It is therefore the most reliable surrogate marker of wound healing.^{36 37} The hydroxyproline content in granulation tissue can be quantified using spectrophotometry or high performance liquid chromatography.³⁸

Laboratory analysis of hydroxyproline

Various artificial *in vivo* models have been developed for implantation in subcutaneous tissue to harvest wound fluid and granulation tissue containing collagen. The Schilling-Hunt mesh chamber was the earliest model. However, its size limits its use in humans. The Cellstick® model constructed by Viljanto is a miniature silicon wound drain housing a small viscose cellulose sponge to entrap inflammatory cells and wound fluid.³⁷ A modification of this model

by Diegelmann used a 1 mm wide and 2.5 cm long polyvinyl alcohol implant (PVA) surrounded by a perforated silicone tube.²²

The expanded polytetrafluoroethylene (ePTFE) model introduced by Goodson and Hunt in 1982 used a 1 mm thin Gore-Tex® tube model (30 µm pore size).³⁹ It was easy to insert and remove at specific intervals, such as 5 to 14 days, and had a lumen allowing topical application of drugs or sampling of wound fluid. It was also soft enough to allow sectioning for analyses. Implantation was minimally invasive, with less of a foreign body reaction. Tissue deposition was similar to that of normally organised granulation tissue and findings were reproducible.

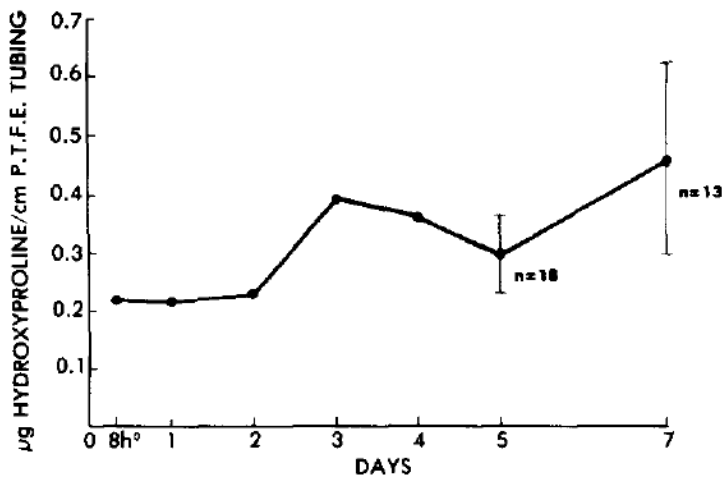


Figure 1. 5. Accumulation of hydroxyproline in polytetrafluoroethylene tubing in normal human subjects. (Source Goodson et al, 1982³⁹)

More than 60 published wound healing studies have successfully used larger ePTFE tubes (diameter 2.4 mm; pore size 90–120 µm) with hydrophilic properties to maximize permeability and harvest more of the collagen deposited de novo for histological assessment of granulation tissues and study of collagen synthesis.⁴⁰

The median rate of hydroxyproline deposition on ePTFE in humans was 88% higher on day 10 when compared with day 5. (Figure 1.5) Matrix deposition and cellularity were higher on the outer part of the tube than inside the lumen and were lowest within the wall of the tube. The median quantity of hydroxyproline was 12% higher in the middle of the implant than at the ends.⁴⁰ Healthy tissue wounds have less collagen and wound breaking strength than localised tissue trauma wounds, which are characterised by more inflammation and local ischaemia.

Inter-ePTFE variability was 1.25, such that the amount of hydroxyproline was typically 25% higher in one of the two ePTFEs evaluated. Intra-ePTFE variability in repeated measurements of the same tube was 88% ($\rho=0.88$). The content of hydroxyproline in the ePTFE model and that in the modified PVA model designed by Diegelmann correlated significantly, although the former accumulated 2.5 times more hydroxyproline.⁴⁰ The ePTFE model was found to be safe, with only one wound infection reported as a result of the implant in a study of 85 patients.⁴⁰

Growth factors and cytokines

These are small secreted proteins that exert effects on immune and other cells. Key growth factors and cytokines are discussed.

Platelet-derived growth factors

Upon injury, degranulated platelets release PDGF via a paracrine mechanism. PDGF is a major player in wound healing and was the first growth factor shown to be chemotactic. Moreover, PDGF enhances proliferation of fibroblasts and production of ECM. It stimulates fibroblasts to contract collagen and induces a myofibroblast phenotype. Non-healing skin ulcers, a history of diabetes, ageing skin, and glucocorticoid administration (in a rodent model) are associated with reduced PDGF levels.^{9 41 42} PDGF is the first growth factor approved for the treatment of human ulcers.

Transforming growth factor- β

TGF- β regulates cell proliferation, cell differentiation, and other cellular functions. The TGF- β superfamily plays an integral part in development and in the repair process. It also plays a role in immunity, cancer, heart disease, diabetes, and Marfan syndrome.⁴³ The three TGF- β isoforms (TGF- β 1, TGF- β 2, and TGF- β 3) are amongst the most studied molecules in wound healing.

TGF- β isoforms stimulate formation of granulation tissue and re-epithelialisation by enhancing angiogenesis, proliferation of fibroblasts, differentiation of myofibroblasts, and matrix deposition.⁴⁴⁻⁴⁶ Exogenous TGF- β increases both the rate of healing and the strength of the healed wound.⁴⁵ Paradoxically, TGF- β also has an inhibitory role, acting as a negative regulator of re-epithelialisation and inducing expression of integrins for migration of keratinocytes.^{47 48}

The three TGF- β isoforms have distinct and overlapping functions. TGF- β 1 and TGF- β 2 are detected early in wound repair, whereas expression of TGF- β 3 is seen at later stages. Following injury, platelets release a large quantity of TGF- β 1 for chemotaxis, which stimulates their infiltration into inflammatory cells.⁴⁹ As well as active TGF- β s, latent forms are also produced and delivered within the wound matrix, allowing their sustained and continued release.⁹ It is not clear whether the effect of TGF- β 3 is to increase the dermal matrix or to antagonise the effect of other TGF- β isoforms and inhibit scarring.⁵⁰ TGF- β 1 plays a crucial role in inhibition of scarring, and acts in a paracrine fashion to increase expression of mRNA for type I collagen and hydroxyproline.⁵¹ Deficiency of TGF- β 1 results in a severe inflammatory wound response, decreased re-epithelialisation, and less deposition of collagen. Overexpression of TGF- β 1 and TGF- β 2 is found in keloid tissue and keloid-derived fibroblasts.^{52 53}

Fibroblast growth factors

Fibroblast growth factors comprise more than 22 structurally related polypeptides. They stimulate proliferation of various cells of mesodermal, ectoderm, and endoderm origin. They also regulate migration and differentiation of target cells, and some FGFs are cytoprotective and support cell survival.⁵⁴ FGF1, FGF2, and FGF7 affect wound healing.

FGF2, like FGF1, stimulates angiogenesis and the mitogenic effects of fibroblasts and keratinocytes. Reduced FGF2 at the wound site causes reduction in cellularity and vascularisation, along with a 25%–35% reduction in collagen by day 7 of wound healing, causing slowing of the rate of re-epithelialisation and reduced deposition of collagen.^{9 55} FGF receptor signalling is critical in wound repair; its absence or malfunction can cause epidermal atrophy, dermal thickening, and a 90% reduction in keratinocytes.⁹

Vascular endothelial growth factor

The VEGF family includes six members, namely VEGF-A, VEGF-B, VEGF-C, VEGF-D, VEGF-E, and placental growth factor (PLGF). These bind to three different transmembrane tyrosine kinase receptors.

VEGF-A is a major regulator of vasculogenesis and angiogenesis during development and is also a regulator of wound healing.⁵⁶ Expression of the VEGF-A gene is upregulated by

keratinocytes and macrophages following injury to the dermis.^{57 58} Its receptors, VEGFR-1 and VEGFR-2, are found on blood vessels in granulation tissue, so VEGF-A induces wound angiogenesis in a paracrine manner.^{59 60}

Reduced functioning of VEGF-A is associated with wound healing defects, reduction in wound angiogenesis, fluid accumulation, and formation of granulation tissue.^{61 62} Furthermore, application of VEGF-A or VEGF-A-overexpressing fibroblasts accelerates healing of ischaemic wounds.^{63 64}

VEGF-C, VEGF-D, and VEGFR-3 are responsible for lymphangiogenesis, including formation of lymphatic vessels in skin wounds.⁶⁵ PLGF is a regulator of angiogenesis and is expressed by keratinocytes and endothelial cells in capillaries. Interestingly, synergy exists between VEGF-A and PLGF, indicating that both growth factors are important for angiogenesis.⁶⁶

Tumor necrosis factor- α

Along with other pro-inflammatory cytokines (IL-1 α , IL-1 β , and IL-6), TNF- α influences various wound repair processes, including stimulation of keratinocytes, proliferation of fibroblasts, chemotaxis, synthesis and breakdown of ECM protein, and regulation of the immune response.⁹ These cytokines are strongly upregulated during the inflammatory phase of healing and are released by polymorphonuclear leucocytes and macrophages.^{67 68} Wound healing is accelerated in TNF receptor p55-deficient mice, with increased expression of TGF- β 1, VEGF, VEGFR-1, VEGFR-2, and connective tissue growth factor at the wound site and reduced expression of mRNA for adhesion molecules and cytokines.⁶⁹

Interleukin-8

IL-8 is expressed in acute wounds within 4 hours of injury, peaks at around 72 hours, and declines by day 4.⁷⁰ It is a major chemo-attractant for neutrophils, stimulating inflammation and inhibiting contraction of collagen by fibroblasts. High levels of IL-8 are associated with impaired or delayed wound repair.^{71 72} IL-8 is released to a lesser degree in foetal tissue. The resulting reduction in the inflammatory response may contribute to scarless wound repair.⁷³

1.3 Factors influencing wound healing

The potential for wound healing is governed by many extrinsic and intrinsic factors that can be compromised in patients with vascular disease.

Tissue oxygenation, perfusion and anaemia

The role of oxygen in wound healing is discussed in the next section. Dehydration has been shown to affect subcutaneous oxygen tension and severely impair deposition of collagen.^{74 75} Low haematocrit does not correlate with reduced tissue perfusion or deposition of collagen, provided there is no compromise in peripheral perfusion that may compensate for anaemia.⁷⁶

Diabetes

Diabetes reduces the tensile strength of animal wounds and affects tissue oxygenation. However, the effect of the disease on collagen deposition is unclear. No difference in collagen content was found comparing patients with well-controlled type 1 diabetes and healthy controls.⁷⁷ Patients with type 1 diabetes has less accumulated collagen in wounds than patients with type 2 diabetes, and collagen production in the latter group was not different from that in healthy volunteers.⁷⁸ Impaired neutrophil function and a proportionally higher ratio of type III collagen to total collagen due to an inverse relationship between the rate of glycosylation of collagen and the activity of collagenases and proteases might have been responsible for reduced wound strength in a diabetic animal model despite the lack of a difference in collagen deposition.⁷⁹

Smoking

Active smoking reduces tissue perfusion and increases wound complications. Rates of hydroxyproline accumulation and wound contraction in smokers are nearly half those in non-smokers.⁸⁰

Renal disease

Hydroxyproline accumulates at a slow rate in patients with uraemic syndrome.⁸¹ This may be because of less deposition of granulation tissue rather than a specific impairment of collagen synthesis.

Ageing

Ageing is associated with upregulation of MMP-2 and MMP-9 in wounds, an increase in collagenase activity, and decreased concentrations of TGF- β 1, TGF- β 2, PDGF and other crucial growth factors.⁶²⁻⁸² This results in less collagen formation and a reduction in the effects of the inflammatory cascade, thereby affecting angiogenesis, the response of fibroblasts, and production of DNA content.⁷⁵⁻⁸³

Preoperative debility and immune status

The duration of illness before appendectomy correlates inversely with collagen deposition, and patients who undergo appendectomy in the acute setting have 20% less collagen accumulation at the wound site than those undergoing delayed cholecystectomy in the elective setting.⁸⁴ Blood transfusions impair immune function and reduce anastomotic strength in colorectal surgery, enhancing the risk of anastomotic leakage.⁸⁵

Patient with postoperative septic complications produce less hydroxyproline than those with a normal postoperative course.⁴⁰ Infection impairs tissue repair by prolonging the inflammatory phase of healing, inhibiting leukocyte function, and hindering formation of granulation tissue.⁸⁶
⁸⁷ Successful healing correlates with bacterial counts of $<10^5$ organisms/gram of tissue.⁸⁸⁻⁹⁰

Nutrition

Malnutrition and hypoproteinaemia cause decreases in wound tensile strength and collagen deposition, probably because of reduced prolyl hydroxylase activity in the skin.⁹¹⁻⁹² Intravenous nutrition accelerates deposition of collagen in poorly nourished surgical patients.⁹³

Anti-inflammatory drugs and corticosteroids

Corticosteroids and non-steroidal anti-inflammatory drugs reduce collagen synthesis, wound tensile strength, and DNA synthesis, including for TGF- β and insulin-like growth factor-1 (IGF-1).⁹⁴⁻⁹⁶ A single 30 mg/kg dose of glucocorticoids 90 minutes prior to surgery does not affect collagen deposition.⁹⁷

Sex

Women produce at least 50% more collagen than men.⁴⁰

1.4 Role of oxygen in wound healing

In 1969, Hunt *et al* pioneered research on the role of oxygen in wound healing in humans. These authors determined that oxygen is vital for formation of granulation tissue via aerobic metabolism and that oxygen acts as a co-factor for hydroxylation of proline and lysine during synthesis of collagen.⁹⁸ They also concluded that wound tensile strength is directly proportional to the partial pressure of oxygen in wound tissue.^{2 99}

Nonetheless, tissue hypoxia during the proliferative phase initiates the release of growth factors and cytokines, such as TGF- β , VEGF, TNF- α , and endothelin-1.^{100 101} This hypoxic state facilitates angiogenesis and continues until angiogenesis is complete, when blood supply is restored at the end of the proliferative phase.^{2 102-104} Lactate also controls the synthesis of collagen mRNA and hydroxylation of the lysine and proline residues of pro-collagen.¹⁰⁵

Oxygen and inflammation

Oxygen is the substrate for production of reactive oxygen species (ROS) in the inflammatory phase. ROS are produced by neutrophils and macrophages via nicotinamide adenine dinucleotide phosphate oxidase-linked oxygenase.¹⁰⁶ This key enzyme requires oxygen to work optimally. The half-maximal activity (K_m) of ROS production is 45–80 mmHg of oxygen, with maximal production at 300 mmHg.^{107 108} Production of ROS and reactive ions, including leucocyte-derived superoxide ions and hydrogen peroxide, is a process known as the “respiratory burst”.^{109 110} Oxygen concentration is directly proportional to oxygen consumption by neutrophils during the respiratory burst.¹⁰⁷ Hypoxia stimulates initial production of ROS, and oxygen is required to sustain it. Conversely, chronic hypoxia inhibits the process.¹¹¹

Low concentrations of ROS act as a cellular messenger to stimulate release of growth factors, neutrophil chemotaxis, and angiogenesis.^{106 112} Interestingly, excessive levels of ROS can cause tissue injury and sensitise cells to oxidants, resulting in oxidative damage to cellular protein and DNA, which over time induces cell death via apoptosis and necrosis.¹¹³⁻¹¹⁵

The primary role of ROS is to eliminate micro-organisms by oxidative killing, while superoxides break down bacterial membranes and leucocytes produce hydrogen peroxide.¹¹⁶ Previous *in vivo* studies have demonstrated that high-dose oxygen (inspired oxygen concentration [F_iO₂] 80%) intraoperatively and postoperatively (between 2 and 4 hours) reduces the rate of surgical

site infection (SSI) when compared with controls (FiO₂ 30%).¹¹⁷⁻¹¹⁹ The rate of SSI has an inverse relationship with subcutaneous wound oxygen tension.¹²⁰

Several systematic reviews indicate that perioperative oxygen has antibacterial effects.¹²¹⁻¹²⁴ Supplemental oxygen for more than 48 hours postoperatively reduces isolated groin incision SSI in lower limb vascular bypass.¹²⁵ Furthermore, supplemental oxygen works synergistically with antibiotics, specifically aminoglycosides.¹²⁶

Hyperbaric oxygen therapy (HBOT) has been used to deliver 100% oxygen at a pressure of 2.5 atm for durations of around 90 minutes per day.¹²⁷ Systematic reviews suggest that while there is weak evidence that HBOT reduces the need for amputation in patients with diabetic foot ulcers (DFUs), it can be used as an adjunct in selected cases.¹²⁸⁻¹³²

Oxygen and angiogenesis

Neoangiogenesis is regulated by and dependent on growth factors such as VEGF and hypoxia-inducible factor 1 (HIF-1).¹³³ These factors are in turn promoted by ROS, hypoxia, tissue oxygen tension, and lactate.^{104 134-136} Hypoxia also induces VEGF receptor activity.¹³⁷¹³⁸ As for synthesis of collagen and ROS, hypoxia initiates neovascularisation, but oxygen is required for continual release of VEGF.^{136 139 140}

Tissue oxygen tension reflects the balance between tissue oxygen perfusion and consumption, and is in the range of 0–20 mmHg at the wound centre and 60–70 mmHg at the wound periphery.¹⁴¹ Arterial oxygen tension (partial pressure of oxygen in the blood) is typically around 100 mmHg. This gradient promotes diffusion of oxygen from the surrounding normal tissue to the hypoxic tissue.¹⁴² HIF-1a is the regulatory part of the HIF-1a/b heterodimer. It acts as a transcription factor and enters the cell nucleus. HIF-1 binds to hypoxia response elements in gene promoter regions. HIF-1a also upregulates genes involved in glucose metabolism, erythropoiesis, iron transport, control of vessel tone, and angiogenesis.^{137 143 144} Further, HIF-1 regulates homeostasis of oxygen in wound tissue.¹⁴⁵

However, the above theory has been somewhat refuted by HBOT studies, which hypothesise that wound hypoxia is detrimental throughout all phases of wound healing, whereas hyperoxia confers benefits of increased neovascularisation, faster epithelialisation, and more rapid wound closure.^{136 146} Supplemental oxygen (normobaric or hyperbaric) increases ROS, which

have been shown to upregulate VEGF expression in chronic wounds in animals.^{113 147} One explanation for this is that VEGF is induced when normoxia is destabilised and re-establishes higher oxygen tensions no matter how VEGF is induced initially.^{140 148}

Oxygen and growth factors

Production of growth factors is upregulated by both hypoxia and hyperoxia. Secretion of TGF- β 1 mRNA and TGF- β 1 by fibroblasts, and therefore expression of the procollagen-1 gene *COLA1*, is increased by a low oxygen tension and lactate.^{149 150} However, chronic hypoxia slows cell proliferation and release of TGF- β 1 mRNA.¹⁵¹ In addition, ROS induces FGF-2 and is necessary for the function of growth factors, such as EGF.^{142 152 153} Hypoxia decreases the production of IL-2 and IL-8, which play a role in activating neutrophils, macrophages, T-cells, and endothelial cells.¹⁰² Oxygen is also mandatory for synthesis of IGF-1.

Keratinocytes promote re-epithelialisation and increase expression of lamellipodia proteins, which are involved in cell motility. MMP-1 is an interstitial collagenase required for migration of keratinocytes on type I collagen, while MMP-9 is a type IV collagenase.¹⁵⁴ In keratinocytes, hypoxia induces MMP-1 and MMP-9, tissue inhibitors of metalloproteinase, and TGF- β 1 receptors, all of which promote motility of keratinocytes and re-epithelialisation.¹⁵⁵⁻¹⁵⁷

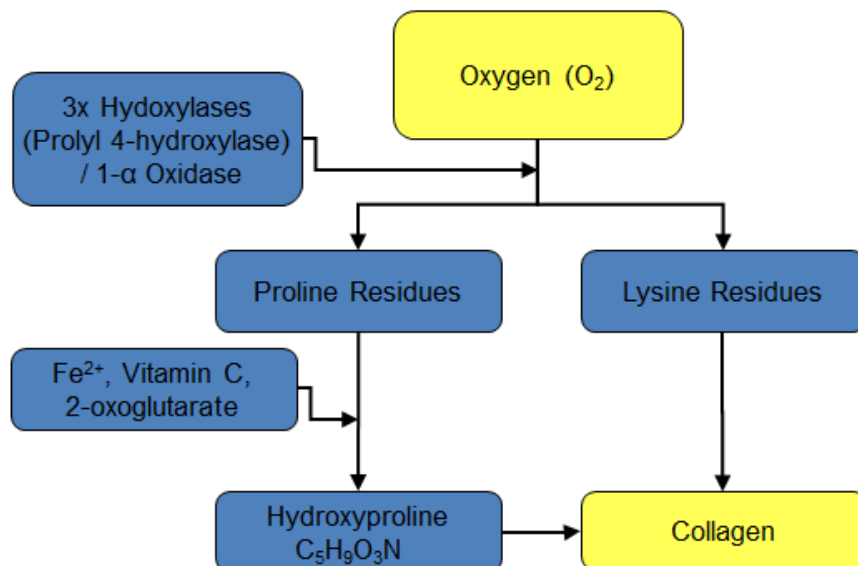


Figure 1. 6. Oxygen, the substrate for collagen synthesis.

Oxygen and collagen

Oxygen is required during biosynthesis of collagen for 3-hydroxylases and 1-oxidases to bind oxygen and insert an oxygen atom in the proline and lysine residues that form the cross-links of collagen (Figure 1.6). The function of the enzymes responsible for hydroxylation of proline (prolyl 4-hydroxylase) and lysine is also directly proportional to tissue oxygenation.³⁶ When the hydroxyproline level is low, the under-hydroxylated pro- α -peptide chains fail to form a triple helix. This causes collagen to unwind.¹⁰⁵ If this collagen is exported out of the endoplasmic reticulum of the fibroblast, it becomes a non-functional protein.^{98 158}

Oxygen may also play a role in wound contraction by triggering the differentiation of fibroblasts into myofibroblasts.¹⁵⁹ Fibroblasts need an oxygen tension of 30–40 mmHg to deposit collagen effectively. Excessive hyperoxia can be detrimental to proliferation of fibroblasts and synthesis of collagen, possibly because of its toxicity to cells.¹⁶⁰

Early animal studies by Niinikoski showed that inhalation of 35%–70% oxygen significantly increases the tensile strength of healing wounds.² *In vitro* studies found reduced production of collagen by fibroblasts and increased MMP-1 in hypoxic wounds, whereas hyperoxia accelerated synthesis of collagen in proportion to the arterial oxygen tension and oxygen gradient.¹⁶¹⁻¹⁶³ This implies that oxygen inhibits MMP-1, promoting wound healing.

HBOT for 4 weeks has been shown to enhance infiltration of fibroblasts and deposition of collagen in wounds.^{164 165} It is unknown if similar findings would be obtained in patients with vascular disease and acute wounds with a high concentration of normobaric oxygen in or wounds with enhanced tissue perfusion.

In summary, while a degree of tissue hypoxia is required in certain parts of the wound healing cascade, enhancing tissue perfusion can amplify production of granulation tissue. However, tissue perfusion can be compromised by peripheral vascular disease (PVD) and diabetes and by disrupted capillary vasculature or relative hypoxia due to increased oxygen demands and cell metabolism.

1.5 Perioperative adjunctive treatments

Three perioperative adjuncts considered for investigation in this thesis that could be applied effectively to promote wound healing and peripheral oxygenation by influencing oxygen delivery, chemical and thermal vasodilation were: supplemental normobaric oxygen, extended active warming, and prostacyclin (prostaglandin [PGI₂]).

Perioperative supplemental oxygen

A pilot study in our vascular unit at Waikato in 2006 showed that high-dose oxygen (F_iO₂ 80%) resulted in increased tissue oxygenation in terms of transcutaneous partial pressure of oxygen (T_{cp}O₂) over an area of the ankle in patients with PVD following infra-inguinal bypass (IIB) surgery.¹⁶⁶ This study won an award at the annual Australasian Vascular Conference in 2007.

Perioperative use of 80% F_iO₂ reduced the rate of SSI by 54% following colorectal surgery when compared with standard 30% oxygen. Analysis of collagen deposition in a subset of these patients revealed no significant change in hydroxyproline.^{118 122} Supplemental perioperative oxygen during lower limb vascular surgery also reduced the risk of SSI.¹²⁵ However, the randomised PROXI trial in 2012 that investigated SSI and high-dose perioperative oxygen in abdominal surgery showed no difference in SSI or pulmonary complications between the treatment group and the control group, but did show increased long-term mortality in the high-dose oxygen group. However, on further investigation, this was only the case for patients undergoing surgery for cancer.^{167 168}

Extended perioperative warming

Inadequate thermoregulation occurs in half of all major surgical procedures because of exposure to the cold environment of the operating theatre, heat loss via the incisional wound, and anaesthesia-induced thermoregulatory impairment, resulting in decreased production of metabolic heat and redistribution of heat from the central to the peripheral compartment.¹⁶⁹ Peripheral vasoconstriction via the sympathetic nervous system occurs with a fall of core temperature as minor as 0.2°C.¹⁶⁹ This decreases tissue oxygen tension, causing hypoxia and a suppressed inflammatory response to wound healing. This results in impaired production of collagen.¹⁶³ Hypothermia also lowers resistance to infection and increases the risk of coagulopathy and myocardial ischaemia.¹⁷⁰ Active systemic and local warming decreases the risk of SSI, intraoperative blood loss, duration of hospital stay, and total hospital costs.¹⁷¹

Applying extended systemic warming 2 hours preoperatively and postoperatively, as well as intraoperatively, increases deposition of collagen at the surgical wound site and reduces the risk of SSI in colorectal surgery.^{172 173} Local radiant heating to 38°C at the acute wound site increases the subcutaneous tissue oxygen tension in healthy volunteers, but collagen deposition is not increased.¹⁷⁴ The degree of heat loss and tissue hypoxia and its consequences is probably greater for a peripheral leg incision than for a central site on the abdomen, especially in patients with PVD.

Perioperative Ilomedin®

Ilomedin® is an intravenous medication that contains iloprost, the first synthetic analogue of prostacyclin, which originates principally from the vascular endothelium (Figure 1.7). Iloprost is a potent vasodilator, platelet suppressant, and mediator between the endothelium, platelets, and leucocytes in the blood vessel wall.^{175 176}

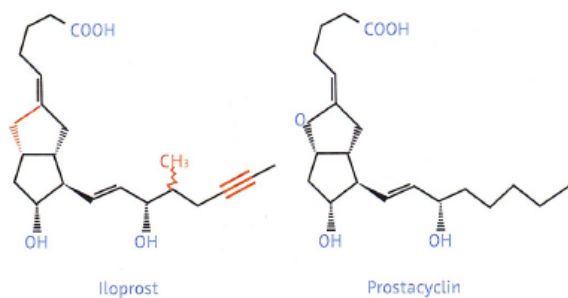


Figure 1. 7. Structural comparison of iloprost and prostacyclin. Sourced from Bayer Schering Pharma AG, 2009.

Microcirculatory disease is caused by an imbalance between prostacyclin, which has dilatory and antiplatelet effects, and thromboxane, which acts as a vasoconstrictor and platelet activator (Figure 1.8). Microcirculatory ischaemia can result from long-standing macrocirculatory disease, from arterial stenosis, or from vasospastic attacks in small vessels. This low tissue perfusion pressure and decreased microcirculatory flow precipitating cellular and biochemical changes can be reversible initially. However, when severe ischaemia, intercurrent infection, or minor injury is superimposed, capillary plugging can occur at the capillary bed as a result of vasoconstriction triggered by endothelial damage via release of

thromboxane A₂, endothelium-derived constricting factors, endothelins, PDGF, and serotonin.¹⁷⁶ In addition, fibrinolytic activity is impaired by inappropriate release of tissue-type plasminogen activator and plasminogen activator inhibitor. This can result in pain, ulceration, and gangrene.

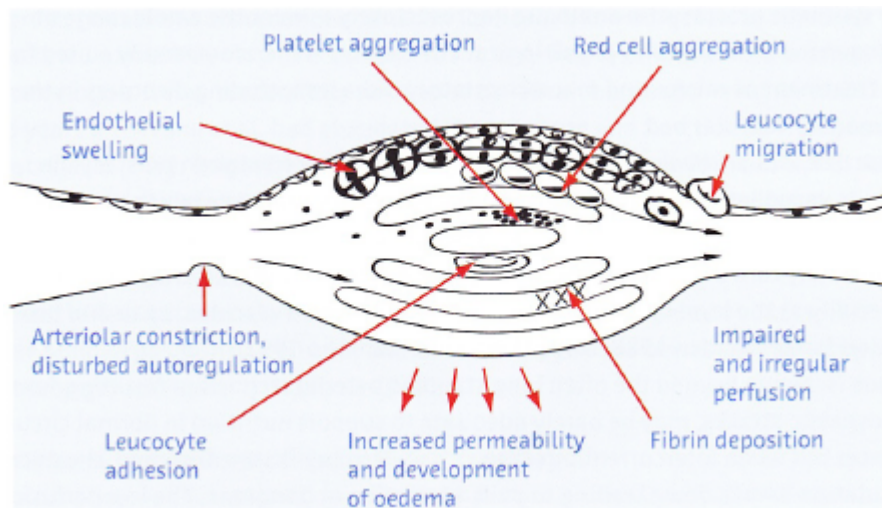


Figure 1. 8. Effects of critical limb ischaemia on the microcirculation. Sourced from Bayer Schering Pharma AG, 2009.¹⁷⁷

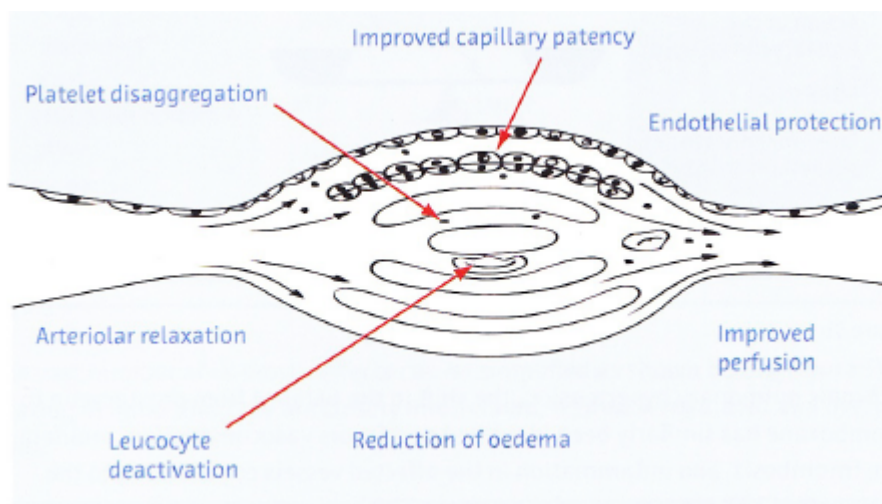


Figure 1. 9. Effects of iloprost on the microcirculation. Sourced from Bayer Schering Pharma AG, 2009.¹⁷⁷

Iloprost activates PGI₂ receptors, stimulating release of adenylate cyclase, and thus cellular production of cyclic adenosine monophosphate¹⁷⁸⁻¹⁸⁰ (Figure 1.9). This induces vasodilation and decreases peripheral resistance, thereby inhibiting platelet activation, repairing and protecting the endothelium, activating endogenous fibrinolysis, and correcting imbalances in the cytokine network.^{181 182} Iloprost has cytoprotective effects that enhance tissue resistance to ischaemia.¹⁸³⁻¹⁸⁵

Vasodilation

Iloprost acts on arterial smooth muscle cells in vascular beds, counteracting thromboxane A₂, leukotrienes and endothelium-derived constricting factor, and promoting release of endothelium-derived relaxing factor and endothelium-derived hyperpolarizing factor.¹⁸⁶⁻¹⁹⁰ Endothelium-derived relaxing factor releases NO, and endothelium-derived hyperpolarizing factor acts on the muscle cell membrane, leading to selective opening of potassium channels. The overall effect is vasodilation (Figure 1.10).

Platelet inhibition

Iloprost binds to PGI₂ receptors on platelets, thereby inhibiting activation, changes in shape, adhesion, and aggregation of platelets, and release of mitogenic factors. This reduces the deposition of platelets on the arteriosclerotic vessel wall.

Vascular endothelium protection

Iloprost has immunomodulatory and anti-inflammatory effects, including inhibition of leucocyte adhesion and accumulation. It also regulates synthesis of TNF- α at both the transcriptional and post-transcriptional levels. Reduced release of TNF- α and intracellular adhesion molecule protects the endothelium. Iloprost restores the permeability of the endothelium by reversing the effects of serotonin and histamine. Iloprost also interacts with macrophages, reducing the release of mitogens and preventing proliferation of smooth muscle cells, thereby inhibiting atherosclerosis.

Iloprost increases urokinase activity by inhibiting tissue plasminogen activator inhibitors, thus enhancing endogenous fibrinolytic and ECM activity. This may reduce the growth and size of thrombi.¹⁹¹

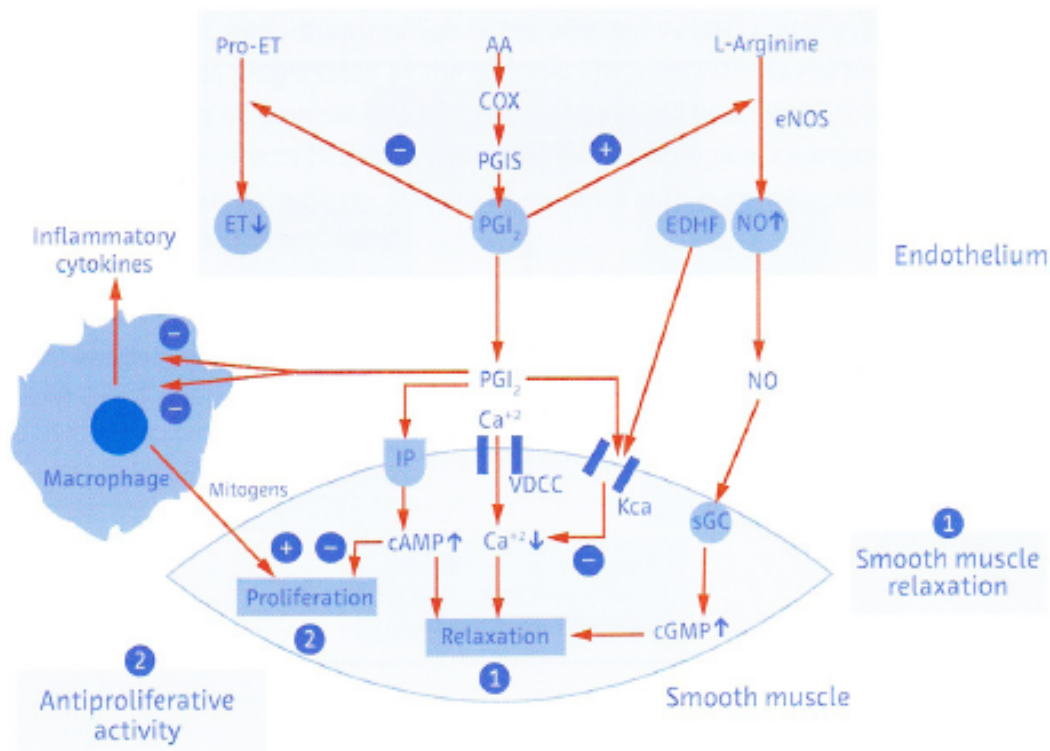


Figure 1. 10. Effect of prostaglandin I₂ (iloprost) on vascular smooth muscle. Sourced from Bayer Schering Pharma AG, 2009.¹⁷⁷ **Abbreviations:** AA, arachidonic acid; cAMP, cyclic adenosine monophosphate; COX, cyclooxygenase; ET, endothelin; EDHF, endothelium-derived hyperpolarizing factor; eNOS, endothelial nitric oxide synthase; NO, nitric oxide; PG, prostaglandin

Clinical studies of iloprost

Intra-arterial or intravenous ilomedin enhances tissue oxygenation.¹⁹² Its half-life and haemodynamic effects in terms of blood pressure, peripheral resistance, and blood flow are around 30 minutes.^{193 194} For patients with end-stage PVD, diabetic angiopathy, or thromboangiitis obliterans (Buerger's disease), where revascularisation would not be indicated, meta-analyses suggest treatment with intravenous iloprost for 2–4 weeks can improve outcome in terms of ulcer healing, relief of rest pain, limb salvage for at least 3–6 months, and survival with both limbs at 6 months (65% versus 45% [placebo], $p < 0.05$).¹⁹⁵⁻¹⁹⁹

A randomised controlled trial (RCT) using a single intra-operative bolus infusion of Iloprost 3,000 ng as an adjunct to IIB, such as femoral-distal bypass, showed improved graft patency at one month and increased survival at 3 months.²⁰⁰⁻²⁰³ However, a meta-analysis by Watson *et al* from the Iloprost Bypass International Study Group concluded that there was limited level

2 evidence due to poor study designs and a lack of RCTs.^{193 204 205} Irrespective of whether a single bolus dose was administered intraoperatively or a short course was given postoperatively, there was no difference in 12-month patency or limb salvage. The only positive finding was improved patency during the first 3 days in femoral-distal bypasses, especially for prosthetic grafts.²⁰⁶

Further investigations of the haemodynamics of bypass grafts identified the “low reflow” phenomenon. This exists postoperatively with low graft velocity during the acute phase and increased thrombogenicity and resistance in the distal vascular bed.²⁰⁵ Low reflow might be a result of increased infiltration of white cells and vascular swelling in the microcirculation because of ischaemia either preoperatively or intraoperatively from arterial clamping. The effects of Ilomedin theoretically minimise this and improve early patency. There is no research on the relationship between Ilomedin and deposition of collagen. Iloprost is also used in patients with Raynaud’s phenomenon and pulmonary hypertension.

The cost of iloprost administration in a hospital setting is NZD \$185 per day, at a ward cost of NZD \$330 per day.²⁰⁷

1.6 Infra-inguinal bypass surgery

For the purposes of this thesis, the incisional wound at the knee during IIB surgery was examined to determine if the afore-mentioned perioperative adjuncts can improve tissue oxygenation and wound healing.

At Waikato Hospital in 2007, 97 IIB procedures were performed, accounting for 25% of all major vascular surgery procedures. Of these, 43 were femoral-popliteal bypasses and 25 were femoral-distal bypasses.

Poor wound healing following IIB increases morbidity, limb loss, and mortality. The incidence of wound complications can be as high as 44%, especially in the case of distal incisional wounds and if there is pre-existing infection in the same limb extremity or comorbidities that impair wound healing.^{208 209} The most feared complications are wound dehiscence and infection, which can potentially expose and infect the graft, rendering the surgery a failure and leading to limb loss. Up to 40% of these wound complications are considered significant, with threatened or actual graft exposure.²¹⁰ A fifth of these patients require at least one readmission as a result of wound complications, adding further burden to the health system of more than USD \$700 per patient with wound complications.^{208 211}

1.7 Peripheral vascular disease

The term “peripheral vascular disease” is often used when referring to atherosclerosis resulting in stenosis or obstruction of the main arteries to the lower extremities and causing inadequate flow of blood supplying oxygen and nutrients to the end organs to sustain their normal functions.

Patients with PVD can be broadly subdivided into three groups according to severity, i.e., those who are asymptomatic, those who have intermittent claudication, and those with critical limb ischaemia (CLI). Accepted classifications include those derived by Fontaine or Rutherford (Appendix A1.2; Figure 9.1)

Asymptomatic PVD is defined as a resting ankle-brachial index (ABI) of ≤ 0.90 in patients who do not experience symptoms. The ABI is a ratio of systolic blood pressure (SBP) of the pedal vessels at the ankle to that of the brachial artery in the upper arm. A resting or exercising ABI ≤ 0.90 may indicate haemodynamically significant arterial stenosis.

Symptomatic PVD includes patients with intermittent claudication or with CLI. The prevalence of intermittent claudication is about 10% in those aged over 70 years.²¹² Most patients with intermittent claudication are managed by lifestyle modification, antiplatelet and statin therapy, and exercise to enhance formation of collateral vessels around the stenoses. Only 5%–10% of cases require surgical intervention to restore the blood supply.²¹³

CLI is limb-threatening and the most common presentation in admissions for vascular surgery. It is defined as chronic ischaemic rest pain of the foot lasting for more than 2 weeks and requiring analgesia, or as ischaemic skin lesions (either ulcers or gangrene) with an ankle systolic BP < 50 mmHg, a toe systolic BP < 30 mmHg, or TcPO₂ at the foot < 40 – 50 mmHg. The diagnosis should be flexible depending on the nature of the disease; for example, in patients with ulcers of mixed aetiology or diabetic neuropathy with reduced pain perception.

The incidence of CLI is 220 per year per million population.²¹³ Independent risk factors associated with a worse outcome are also the major culprits for development of atherosclerosis (i.e. smoking, diabetes, dyslipidaemia, male sex, and older age).

The pathophysiology of PVD is slightly different between patients with and without diabetes. In patients with CLI and diabetes, the occlusive lesions are typically more diffuse and distally

located, and in particular affect the infragenicular arteries (below the knee) including the plantar arch and influencing different angiosomes in the foot. This is different from the occlusive lesions that occur in patients without diabetes, such as heavy smokers, where the lesions are focal, multi-segmental, and proximal. Diffuse distal vessel disease described in the former group is associated with an unfavourable outcome due to “poor run-off”. Collateral formation around the larger arteries is impaired in patients with diabetes, causing tissue downstream to be more susceptible to ischaemia.²¹⁴ Moreover, diabetic patients with CLI often have poor cardiac output and present late as they have been “asymptomatic” for years (or rather their occlusive symptoms have been masked by diabetic neuropathy). The relationship between diabetes and PVD is discussed in more detail later.

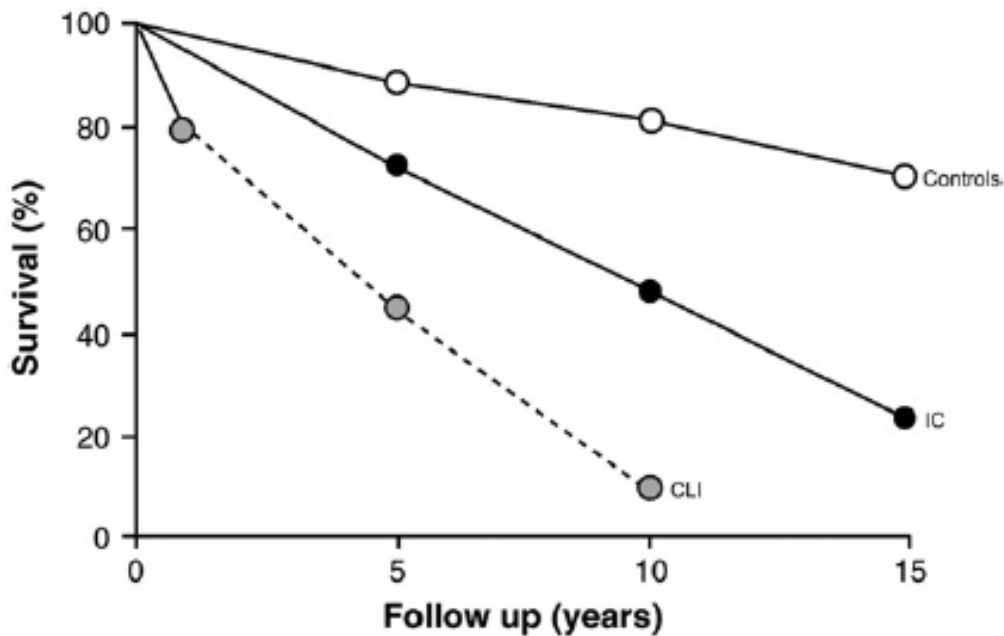


Figure 1. 11. Prognosis of patients with peripheral vascular disease. Sourced from Trans-Atlantic Inter-Society Consensus guidelines, 2009.²¹³

Up to 90% of patients with CLI undergo revascularisation to prevent major amputations.²¹⁵ The prognosis of CLI is poorer than that for intermittent claudication and is associated with a 25% risk of mortality and a 30% major amputation rate at one year. This translates to 45% of patients being alive with both legs after one year (Figure 1.11).

The incidence of major amputations is 500 per year per million population.²¹³ Primary amputation (without previous revascularisation) can be as high as 25% for patients with CLI. These patients usually have non-salvageable disease, with overwhelming infection, uncontrollable rest pain, and/or extensive necrosis that has destroyed the foot, or are unsuitable for revascularisation because they have no “run-off” or are unsafe for anaesthesia. Secondary amputation is indicated when revascularisation options are no longer applicable or when the limb continues to deteriorate despite successful restoration of distal perfusion.

The fate of an amputee is bleak. Only around two thirds of major amputees are fitted with a prosthesis, with a variable number of these patients (16%–96%) successfully achieving independent ambulation by 6–12 months.²¹⁶⁻²²² Moreover, 30% of the amputees who manage to walk at this time no longer use their prostheses by 2 years. Only 60% of below-knee amputations heal by primary intention and 30% of these patients die within 2 years (Figure 1.12). Three quarters of amputees over 75 years of age are unable to return home following surgery, and require additional financial and social support.²²³ Initial rehabilitation usually requires at least 9 months and survival is 70%–80% at 2 years.²¹³

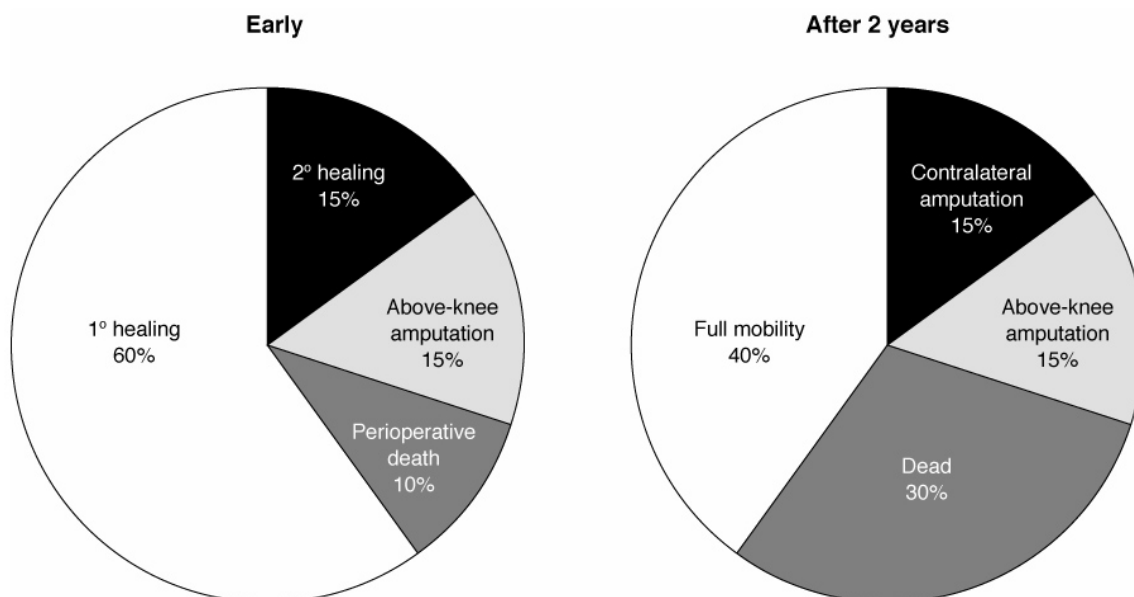


Figure 1. 12. Two-year prognosis following below-knee amputation. Sourced from Trans-Atlantic Inter-Society Consensus guidelines, 2009.²¹³

1.8 Management of infra-inguinal occlusive disease

In CLI, stenoses of the infra-inguinal vessels are more common than aorto-iliac lesions. Nevertheless, treatment of a critical aorto-iliac lesion, if present, should be prioritised to maximize the “inflow” (i.e., the feeding vessels).

Successful revascularisation depends on the extent of disease in the subjacent arterial tree (i.e., inflow, outflow, and severity of disease in the affected segment), the degree of systemic disease (e.g., cardiac output), and the type of procedure performed. Before selecting from the treatment options, the location and morphology of the infra-inguinal lesion should be evaluated.

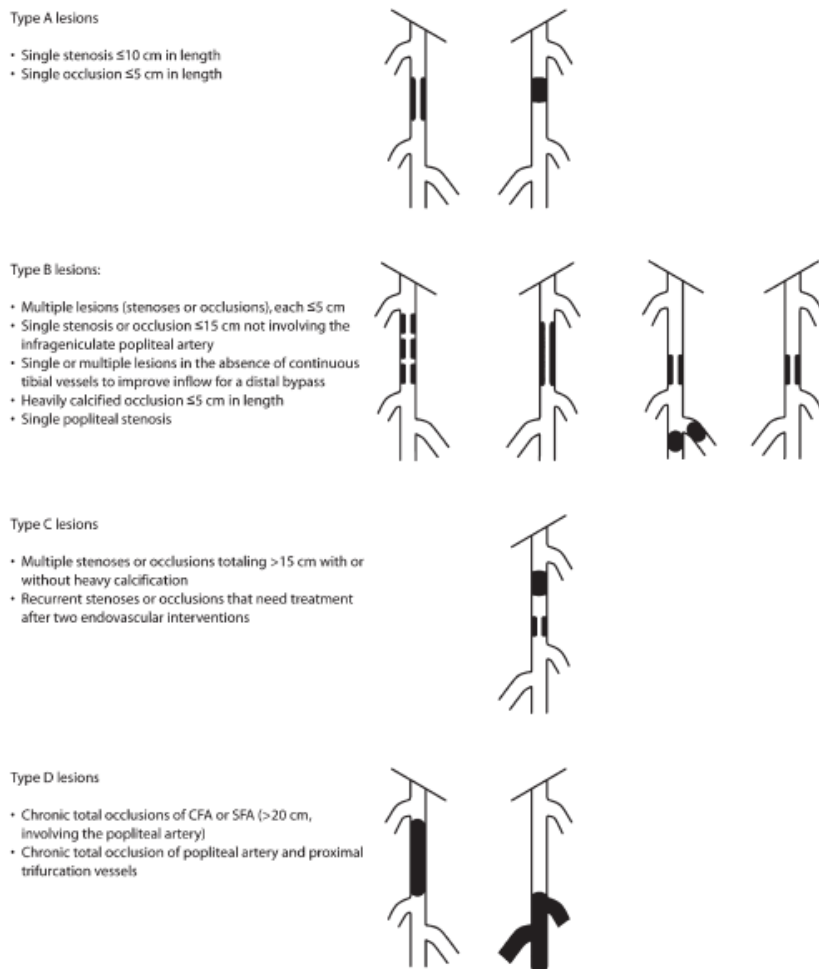


Figure 1. 13. Trans-Atlantic Inter-Society Consensus classification of femoral-popliteal lesions. Sourced from the Trans-Atlantic Inter-Society Consensus guidelines, 2009.²¹³

The Trans-Atlantic Inter-Society Consensus (TASC) classification helps to predict the outcome of revascularisation. A lesion in the femoral-popliteal artery is classified by its severity and length (Figure 1.13). Type A lesions have a better prognosis than type D lesions. There is no classification for the infragenicular arteries (below the knee). Revascularisation of these distal vessels is associated with poor patency, so is typically reserved for limb salvage purposes where a poor outcome is expected.

Surgical interventions for femoral-popliteal lesions can be broadly categorised as endovascular or open surgical bypass procedures. Endovascular treatment of infra-inguinal disease in the form of percutaneous transluminal angioplasty (PTA) and/or stenting usually targets TASC A or B lesions according to the recommendations of the TASC Document on Management of Peripheral Arterial Disease. Compared with bypass surgery, PTA is less invasive with lower morbidity and mortality risks, and has excellent technical and clinical success rates in excess of 95%.²²⁴ PTA and/or stenting of femoral-popliteal lesions achieves acceptable patency rates of approximately 75% at one year, 60% at 3 years, and 50% at 5 years.²²⁴⁻²²⁷

RCTs comparing PTA versus bypass surgery in infra-inguinal PVD are rare. One of the reasons for this is that the indications for bypass surgery and PTA are different. A Cochrane review in 2008 compared PTA with bypass surgery based on four landmark trials, including BASIL and the Veterans Study.²²⁸⁻²³¹ Essentially, there was insufficient evidence to suggest superiority of one intervention over the other with regard to outcome parameters, including mortality, limb salvage, or complication rates. Patients who underwent bypass surgery had a higher 12-month primary patency rate (odds ratio 0.62). This benefit did not last beyond 4 years, according to the findings of the Veterans Study.

BASIL was a landmark RCT comparing the “bypass first” and “angioplasty first” approaches in patients with severe limb ischaemia. The initial paper in 2005 did not suggest any difference in clinical outcome between the two treatment arms. However, a second paper was published in 2010 with a longer follow-up of 3 years,²²⁹ although 56% of the study participants had died and there was no difference between the treatment groups in terms of overall survival or amputation-free survival, those who underwent bypass surgery first and survived for at least 2 years had significantly better overall survival (an additional 7.3 months) and showed a trend towards improved amputation-free survival. Therefore, for severe PVD and CLI (TASC C or

D), bypass surgery appears to achieve better primary patency and possibly a more favourable long-term outcome.

When planning for IIB surgery, patent and uncompromised inflow and outflow to the foot is ideal. The quality of outflow is a more important determinant of patency than the level of the distal anastomosis. Common proximal anastomotic sites are the common femoral artery and superficial femoral artery, whereas distal anastomoses usually involve the above-knee popliteal artery, below-knee popliteal artery, tibial or peroneal vessels, or plantar arteries.

The conduit used is also an independent prognostic factor. Veins (reversed, non-reversed, or in situ) typically have better long-term patency than prosthetic grafts, other than in bypass to above-knee vessels where the two conduits have near-equivalent early patency. Polytetrafluoroethylene (PTFE) grafts to the infra-popliteal arteries are less successful, with a primary patency rate of 30.5% and a secondary patency rate of 39.7% at 5 years.²³² This patency may be improved by adding a “cuff” or a hood of vein at the distal anastomosis below the knee.^{233 234} The consequences of a prosthetic graft occlusion are more sinister than those of a vein graft occlusion.²³⁵ This does not include the prosthetic material becoming infected, which may require the prosthesis to be explanted, thereby increasing morbidity and mortality. PTFE grafting is reserved for when there are no suitable veins available, including contralateral leg veins, arm veins, or even composite and spliced veins.

In general, a quarter of infra-inguinal bypasses need revision within the first year, and the limb salvage rate can be as low as 85% at one year.²⁰⁸ About three-quarters of patients are still living independently at home at 3 years following surgery and a similar proportion remains ambulatory.²³⁶ Should the bypass graft occlude or fail to re-establish patency, limb salvage rates at 2 years are 100% for a bypass constructed for claudication, 55% for a bypass for rest pain, and only 34% for tissue loss. Early occlusion of a graft (≤ 30 days) is associated with a poor 2-year limb salvage rate of 25%.²³⁷

1.9 Peripheral vascular disease in New Zealand

PVD is especially problematic in New Zealand and places a significant burden on quality of life, the workforce, the health system, and society. This burden is expected to worsen as the population ages.

New Zealand is the third most obese nation worldwide, and has the fourth highest rate of diabetes per capita. More than 25% of the population is considered to be obese (body mass index >30).²³⁸ In 2013, there were 245,000 people with diabetes in New Zealand, and the prevalence of the disease was 7.0%.^{239 240} Diabetes is the main reason for lower limb amputation in this country.²⁴¹

Our indigenous Māori population, which makes up 20% of the total population, is at higher risk of atherosclerotic disease than Whites.²⁴² Māori and Pacific Islanders have a higher prevalence of diabetes (diagnosed or undiagnosed) and related risk factors (e.g., obesity, physical inactivity, insulin resistance, and metabolic syndrome) when compared with Whites.²⁴³⁻²⁴⁶ The prevalence of diabetes is higher among the obese population at 14.2% and Māori (7%) and Pacific Islanders (8.1%) than in other ethnic groups (4.9%).²³⁹ There is conflicting evidence regarding the relationship of smoking in the Māori population. Two studies reported low cigarette smoking rates,^{246 247} but another study reported a higher prevalence of smoking among Māori with diabetes than in their non-Māori counterparts (35% and 13%, respectively).²⁴⁸

Diabetes-related complications are over-represented in Māori when compared with Whites.²⁴⁹ The age-adjusted mortality rates for diabetes-related illnesses, including cardiovascular disease, cancer, and renal disease, are higher in Māori, in particular Māori women.²⁴⁵ Diabetes accounts for 20% of all deaths among Māori as compared with 4% in other New Zealanders.²⁵⁰

Compared with Whites, the Māori and Pacific Island populations are at increased risk of diabetic foot, with a higher prevalence, a younger age at presentation than Whites (53 and 56 years versus 69 years, respectively), and a worse outcome.^{251 252} The relative risk for diabetes-related amputation is 6-fold higher for Māori than for non-Māori.²⁴⁰ Māori have been reported to be less likely to comply with diabetes-related medical care due to poor perception of risk.²⁴⁷ With the Māori and Pacific Islanders in New Zealand living in an environment of tobacco use and socioeconomic disparity,²⁴² and the latter leading to poor compliance and

inadequate access to medical attention, there is a major threat to their feet despite primary and secondary prevention measures, including education, diabetic screening, and podiatry cares.^{253 254}

The economic cost of managing DFU is high. Payne *et al* found that hospital admissions for diabetic foot are increasing in New Zealand and have a longer hospital stay when compared with other vascular admissions, with NZD \$10–11 million spent on inpatient management of DFU in 1993 alone.²⁵⁵ Further, in a report from Wellington, Scott *et al* estimated hospital costs of NZD \$13.1 million for admissions with CLI and prostheses, and a cost of NZD \$2.8 million for loss of output or productivity in 1994.²⁰⁷ Thirty-two percent of patients requiring amputations in New Zealand are in the working age group.²⁰⁷ Thompson *et al* calculated the average inpatient cost per diabetic foot admission at Middlemore Hospital, Auckland, in 1993 to be \$12,500, with a total annual cost of over \$600,000.²⁵¹ The cost of a PTA is \$10,000, a bypass surgery costs \$20,000, and an amputation costs \$25,000.^{207 213} The total cost per patient should be multiplied by a factor of 2 to 4 to account for further procedures, complications, and rehabilitation.

1.10 Tissue perfusion

Patients with PVD typically have impaired oxygen uptake and delivery mechanisms, and may have concomitant cardiorespiratory disease, peripheral neuropathy, an impaired vasomotor response, arteriovenous (AV) shunting, and/or dysfunctional thermoregulation.

Microcirculation in the skin tissue involves a complex system of microvascular flow regulation and is a defence mechanism. It is composed of terminal arterioles, capillaries, venules and lymphatic capillaries. The arterioles (10–100 μm) are surrounded by innervated smooth muscles. Capillaries (5–8 μm in diameter) have no smooth muscle and venules (10–200 μm) have little smooth muscle.^{256 257} The microcirculation includes extrinsic neurogenic mechanisms (actions of noradrenaline and adrenaline at alpha and beta adrenergic receptors) and intrinsic local mediators, and is modulated by factors circulating in the humoral pathway or bloodstream (e.g., renin-angiotensin and vasopressin). The endothelium participates in regulation of capillary flow by releasing vasodilatory mediators (e.g., prostacyclin and NO) and contractile factors (e.g., endothelins). In normal individuals, only 15% of total blood flow in the foot is required to provide adequate capillary exchange for oxygen and nutrients in tissues.²⁵⁸ The remaining blood flow has a thermoregulatory function.

Patients with CLI develop microcirculatory defects, including endothelial dysfunction, altered thrombotic function, macrophage activation, and inflammation. This causes maldistribution of the microcirculation as well as a reduction in total blood flow. T_{cpO_2} in the lower extremity is less in patients with PVD than in healthy individuals.²⁵⁹

Therefore, while the primary aim of treatment for CLI is to correct the pathology of the macrocirculation (i.e., circulation of blood to the organs), it is equally important to assess and normalise microcirculatory changes in the tissue.

1.11 Assessment of tissue oxygenation

Measurement of tissue oxygenation is a component in the evaluation of PVD to determine the severity of tissue hypoxia and predict tissue viability. There is no gold standard for its assessment. Most clinicians use their clinical judgement at the bedside. Various modes of arteriography (e.g., duplex ultrasound, computed tomographic angiography, magnetic resonance angiography, and digital subtraction angiography) can be used to outline the major vessels that are patent and can identify stenotic or occlusive lesions within the vessel that may contribute to tissue hypoxia, but offer no indication of the adequacy of microvascular perfusion.

Measurement of toe pressure

Toe pressures measure systolic BP of the toe arteries by applying a miniature cuff at the base of the toe. Systolic BP >45 mmHg is a good predictor of wound healing, even in patients with diabetes and renal disease.²⁶⁰ Nevertheless, the reproducibility of toe pressure measurements varies in the literature; vascular patients frequently present with necrotic toe ulcers or previous toe amputations, rendering toe pressures a difficult marker to analyse in studies.

Laser Doppler flowmetry

Laser Doppler flowmetry measures haemodynamics and quantifies blood flow in human tissues, including skin. A low-power laser diode generates light of wavelength 780 nm that penetrates a small area of skin up to 0.5–1 mm in depth.²⁶¹ The beam is scattered with a Doppler shift by haemoglobin and returns to be concentrated by a detector.²⁶² However, laser Doppler flowmetry is not readily available.

Laser angiography

Indocyanine green (ICG) is a fluorescent cyanine dye with a peak spectral absorption at about 800 nm and a half-life of 150–180 seconds. It binds tightly to plasma proteins and is confined to the vascular system.²⁶³ ICG is used as a marker in assessment of tissue perfusion. Near-infrared light generates excitation of the fluorescence. A digital video camera allows absorption of the ICG fluorescence to be recorded in real time. ICG angiography has been used in patients with vascular disease to predict tissue viability and assess perfusion before and after vascular intervention.^{264 265} ICG is administered intravenously and patients can experience side effects. The SPY camera system is not readily available and expensive.

Transcutaneous oximetry measurement

Transcutaneous oximetry measurement (TCOM) is well established in certain clinical settings, including paediatric intensive care, respiratory, anaesthesiology, and hyperbaric medicine, and is regarded as a useful tool for assessing the peripheral circulation in vascular and plastics surgery.

TCOM measures oxygen tension (partial pressure) on the skin surface under an electrode.²⁶⁶ Invasive electrodes were first pioneered by Clark and then miniaturised by Silver.^{267 268} Fifty years ago, Hunt was the first to describe measurement of tissue oxygenation in humans.²⁶⁹ A decade later, “non-invasive” TCOM probes were developed that required physical contact between the skin and a probe. A plastic ring filled with a layer of contact fluid is placed over an area of interest and the electrode is placed into the ring. Nowadays, TCOM can cater for both transcutaneous partial pressure of oxygen ($TcpO_2$) and transcutaneous partial pressure of carbon dioxide ($TcpCO_2$).²⁷⁰ TCOM estimates tissue oxygenation by measuring the diffusion of extracellular oxygen and carbon dioxide into a heated sensor on the skin.²⁷¹

Tissue oxygenation of a limb responds to clinical situations, e.g., positional changes, with increases in $TcpO_2$ in a dependent position and decreases with elevation. $TcpO_2$ also falls when the skin is undermined and stretched.²⁷² $TcpO_2$ increases significantly in normal subjects when breathing an F_iO_2 of 100% oxygen.²⁷³ In individuals with PVD, $TcpO_2$ falls during and after exercise.²⁷⁴ Similarly, a $TcpO_2$ of <30 mmHg despite breathing 100% normobaric oxygen is consistent with severe PVD. Many TCOM studies are based on HBOT. In some patients, HBOT is the only method that can increase $TcpO_2$ for healing. $TcpO_2$ increases with the partial pressure of arterial oxygen (P_aO_2) which is in turn increased by the partial pressure of inspired oxygen (P_iO_2) when oxygen is delivered at greater than 1 atm.^{275 276}

In patients with severe ischaemia, $TcpO_2$ is more sensitive than the ABI in those with renal disease and/or diabetes, because it detects impaired blood flow from both macrovascular and microvascular disease.²⁷⁷⁻²⁷⁹ TCOM also has better predictive capability than laser Doppler flowmetry or segmental pressure.²⁵³

Lower extremity $TcpO_2$ is sometimes used clinically to assess wound healing potential and to review therapeutic results in ischaemic legs. Tissue hypoxia ($TcpO_2$ <30 mmHg) disrupts all phases of wound healing, leading to anaerobic metabolism, which creates acidosis and results

in inadequate production of adenosine triphosphate to maintain cellular function.¹²⁷ Wounds with a $T_{cpO_2} > 40$ mmHg generally heal.²⁸⁰⁻²⁸² The predictive index has a sensitivity and specificity of 85% and 92%, respectively.²⁸² Patients with diabetes and renal failure may require a higher T_{cpO_2} of > 50 mmHg for successful healing.^{283 284} An increase in T_{cpO_2} of > 40 mmHg after revascularisation is indicative of significant improvement.²⁸⁵ T_{cpO_2} (or T_{cpCO_2}) is also used as an indirect measurement of the P_{aO_2} , (or P_{aCO_2}) of arterial blood, whether dissolved or bound to haemoglobin.

There are limitations with TCOM. Wound T_{cpO_2} measured by TCOM is the oxygen tension in the skin surrounding the wound and is not a direct measurement of wound oxygen tension (P_wO_2). Wound oxygen tension is likely to be lower than the T_{cpO_2} adjacent to the wound. Moreover, TCOM measures T_{cpO_2} at a single site the size of an electrode (about 1 cm in diameter). Mean T_{cpO_2} values from two or more adjacent sites in a wound are better predictors of healing potential than single site values. However, assessment of multiple sites can be impractical and time-consuming, given that a single reading may take up to 20 minutes.²⁸⁶ Intra-operator variability with TCOM is 10% for T_{cpO_2} and 5% for T_{cpCO_2} .^{287 288}

Guidelines have been published for the use of TCOM.²⁸⁹⁻²⁹¹ Most aspects are adequately described. Landmark papers on TCOM have been published by Sheffield *et al*, Smart *et al*, and Fife *et al*, who have provided comprehensive literature reviews of its use, reference ranges for normal and diseased individuals, and previous research findings, such as its value for predicting amputation and wound healing.

However, there are no recommendations regarding the length of time that the probe is required to be in contact with the skin in order to achieve reliable absolute measurements. A reason for this is that TCOM is usually used for continuous measurements to detect unexpected changes in oxygenation in patients with sleep apnoea and in neonates to monitor oxygen levels without needing to perform regular arterial blood gas measurements. Some authors have described recording measurements at periods “between 10 and 20 minutes” when the gas exchange between the probe and skin reaches equilibrium; while others have taken recordings only when measurements cease to fluctuate. Recording when measurements cease to fluctuate is not precise.

The only documentation in the guidelines regarding the duration required for the electrode to reach equilibrium was found in Sheffield *et al*.²⁷³ This was suggested to be around 10–15

minutes in subjects with normal perfusion and 15–20 minutes in those with a compromised circulation. This is referenced to a “personal communication” with Vesterager *et al*. The relationship between $TcpO_2$ and time taken to reach equilibrium of the electrode was also discussed. A typical dip in measurements at around 8 minutes was described, where $TcpO_2$ reached the lowest value and subsequently rebounded to equilibrium at around 15 minutes (Figure 1.14). Again, exact referencing was not found, and this appeared to be based on a “drawing” by Vesterager *et al* as part of their “personal communication”.

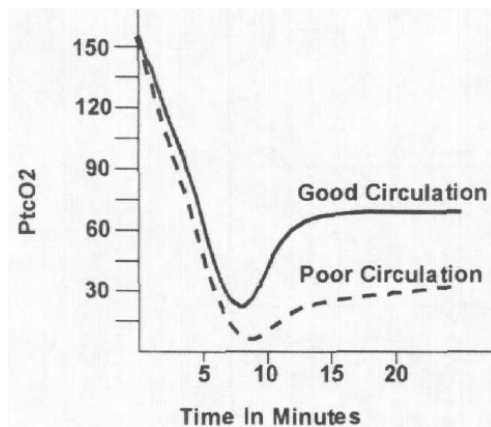


Figure 1. 14. Proposed electrode behaviour during equilibrium. Sourced from Sheffield *et al*, 1998.²⁷³

Sheffield *et al* observed that “TCOM is much an art than science”. Technical limitations were also described. The issues described included how time-consuming, labour-intensive, and operator-dependent TCOM was in terms of achieving consistent results. Sheffield *et al* recommended 45 minutes of reading per limb, and performed leg elevation and oxygen challenge tests to determine if the hypoxia was due to large or small vessel disease and if perfusion would respond to hyperoxaemia, such as HBOT. With the newer TCOM4 model, simultaneous measurements can be taken using a solo monitor to reduce the time needed to complete the procedure.

Sheffield *et al* also commented that “No single value can be specified ‘normal’ oxygen tension for all tissue. Rather there exists a series of gradients, the steepness of which varies with arterial oxygen tension, type of tissue, inter-capillary distance and cellular metabolic rate”.²⁷³ $TcpO_2$ values vary according to the patient population being studied, the technique used, the site of measurement, the position of the limb, and the therapeutic intervention applied. This

variability can be as high as 10%. TCOM measurements are considered reproducible because this variability does not appear to affect decisions in clinical practice.²⁸⁸

Some authors recommend use of a reference point to interpret TCOM readings, for example, on the chest to calculate the regional perfusion index (RPI) or comparing the affected limb with its contralateral partner to determine the bilateral perfusion index (BPI).²⁷³ Using a reference point could reduce bias from central or external causes when interpreting changes in peripheral perfusion. Chest readings are not significantly different from leg oxygenation in the healthy population.²⁷⁶

However, the measurement error can be doubled when a reference point is used. Smart, Sheffield and Fife advocated interpreting the raw actual values rather than the relative values when predicting healing potential. Others demonstrated incongruence between values for the lower limb and those for the chest.^{288 290} Theoretically, RPI can determine whether tissue hypoxia is due to arterial hypoxaemia.²⁹² However, use of a chest reference value is unreliable and abnormally low in certain patients, such as those with previous sternotomy. This can create a spuriously high RPI, rendering it unhelpful in patients with vascular disease.

TCOM technology

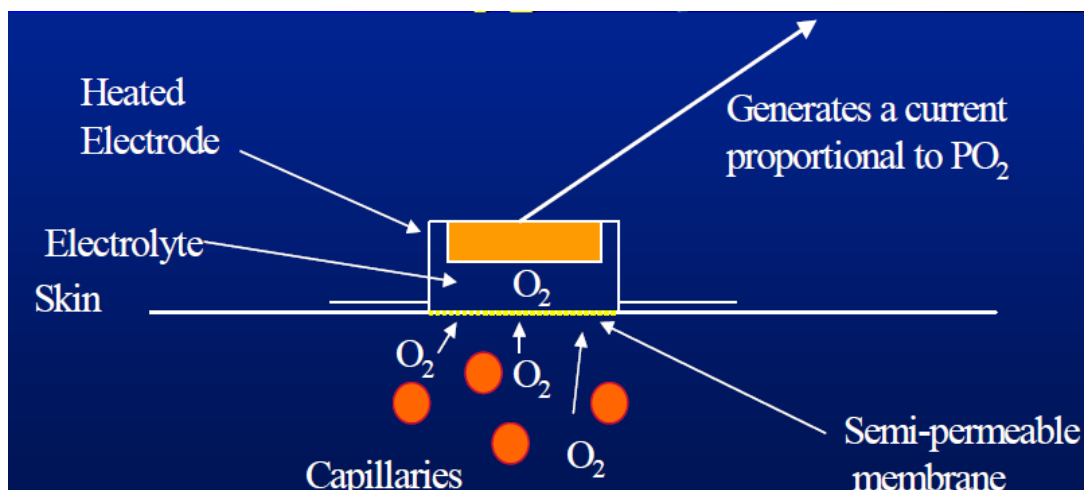


Figure 1. 15. A schematic diagram demonstrating how a transcutaneous oximetry measurement electrode works. Sourced from Smart et al, 2006.²⁸⁵

The TCOM system contains a thermostatically controlled heating element with a preset temperature range of 37.0°C–45.0°C (Figure 1.15). The electrode can combine a pO₂ sensor (Clark-type) and a pCO₂ sensor (Stow-Severinghaus). A Clark electrode is composed of a platinum cathode and a silver anode immersed in an electrolyte solution with an overlying oxygen-permeable membrane. Molecular oxygen is reduced at the cathode. With voltage applied between the anode and cathode, the current generated by oxygen reduction is proportional to the T_{cp}O₂.²⁹³ The electrode measures the T_{cp}O₂ in a sealing ring chamber which reaches equilibrium with T_{cp}O₂ at the skin surface over time. The Severinghaus electrode calculates the pCO₂ electrochemically by a change in pH of the electrolyte solution. Additionally, a temperature correction is used to address the epithelial carbon dioxide produced by heating the skin.

Several factors can influence readings, and include:

- P_aO₂ (or P_aCO₂)
- Capillary blood flow in the skin under the electrode
- Oxygen consumption and carbon dioxide production by the skin
- Oxygen consumption by the electrode
- Temperature gradients in the skin
- Structural and diffusive properties of the skin (e.g., skin thickness, oedema, and inflammation).

Imprecision of TCOM values may also be due to “electrode drift” caused by wear and tear of the electrode membrane, variations in pressure on the electrode (such as direct pressure on the electrode), and skin properties.

TCOM electrodes are heated during measurement because the technique:

- Induces capillary hyperperfusion of the skin under the electrode in both the stratum papillare and the deeper dermal microcirculation, which has multiple arterial and venous plexuses. This reduces the arteriovenous differences in T_{cp}O₂ and T_{cp}CO₂ and provides more accurate values for true P_aO₂ or P_aCO₂.
- Lowers blood solubility of oxygen and carbon dioxide.

- Causes a right shift in the oxygen-haemoglobin dissociation curve, lowering the haemoglobin-oxygen affinity and increasing dissociation of carbonic acid. This increases P_{aO_2} or P_{aCO_2} in the heated blood and therefore increases $TcpO_2$ and $TcpCO_2$.
- Increases gas diffusion through the skin due to enhanced solubility of the lipid layer of the epidermis.
- Increases oxygen consumption and carbon dioxide production (metabolic rate) at the skin by 4%–5% per degree Celsius.²⁹⁴

OxyVu™

OxyVu™, a hyperspectral transcutaneous oxygenation (HTCOM) measurement system, uses “hyperspectral technology” to deliver a two-dimensional, colour-coded map of “oxygen anatomy” over regions of interest in a non-invasive manner. This two-dimensional region can vary from as large as for the entire foot or be as specific as for an ulcer at the toe.



Figure 1. 16. Photograph of the OxyVu-2™ system. (Retrieved from <http://www.hypermed-inc.com>)

The OxyVu (HyperMed Inc, Boston, MA, USA) was released in 2006, and is a mobile integrated computer with a camera device (Figure 1.16). A “target”, i.e., a small sticker, is placed at the region of interest, such as the sole of the foot. The mounted camera produces two red dots that allow the target to be focussed on at a fixed focal distance of 12 inches. The camera then produces light at various wavelengths that penetrates the skin to a depth of 1–2 mm to obtain information from the subpapillary plexus (Figure 1.17). The computer software detects the presence of chromophores (“fingerprint of colour”) that are uniquely specific to oxyhaemoglobin and deoxyhaemoglobin. This process is repeated at each pixel of the digital picture with a resolution of 90 μm , producing a spectrum of colours around the regions of interest that correlates with the density of oxyhaemoglobin and deoxyhaemoglobin that can then be quantified. The hyperspectral image provides quantitative values for transcutaneous oxyhaemoglobin (HT-Oxy) and deoxyhaemoglobin (HT-Deoxy) within 15 seconds. The OxyVu also measures skin temperature using a remote infrared temperature sensor on the imaging unit, adding a new dimension to analysis of tissue oxygenation. Currently, no other devices provide the information gleaned by OxyVu.

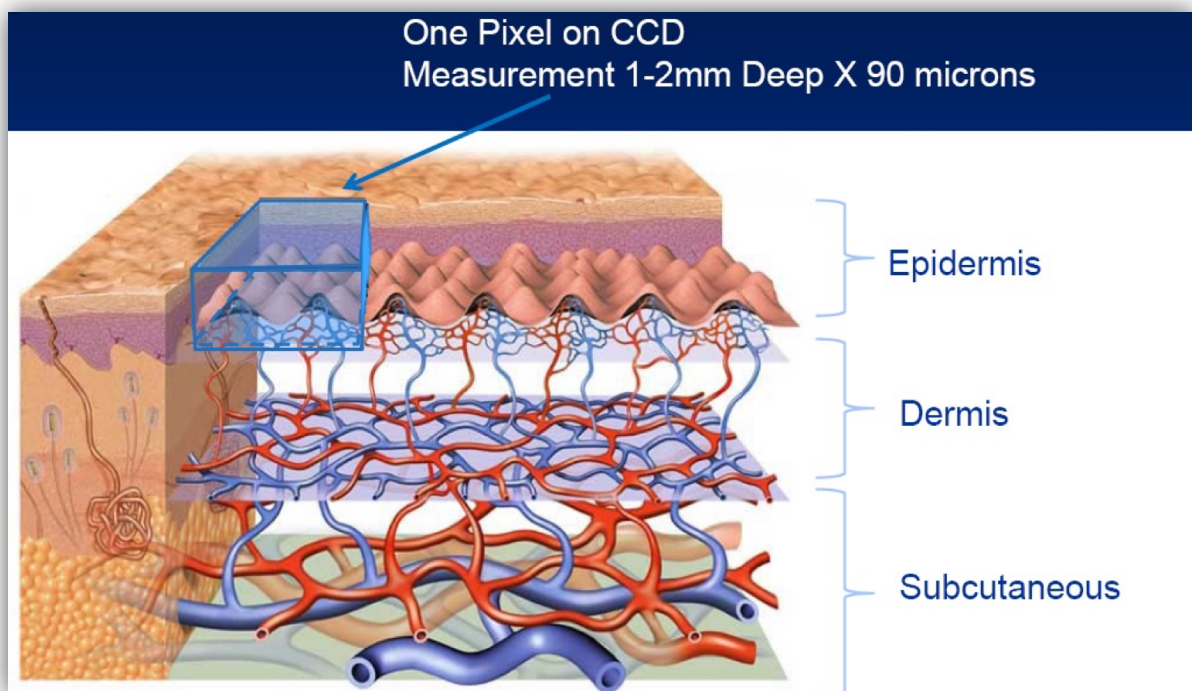


Figure 1. 17. Diagram illustrating how the OxyVu™ works. (Retrieved from <http://www.hypermed-inc.com>).²⁹⁵

Hyperspectral technology

Hyperspectral technology is a complicated process. Essentially, light rays hitting human skin are reflected back to a camera depending on the refraction index between air and the stratum corneum. This phenomenon of light reflecting off two discrete interfaces is called Fresnel reflection.²⁹⁶ However, some of this light energy is absorbed by chromophores in the dermis and the epidermis, or scattered. The primary chromophores in the skin showing peaks within the visible light spectrum are oxyhaemoglobin, deoxyhaemoglobin, and melanin.²⁹⁷⁻²⁹⁹ The sum of light energy observed by the detector is that of Fresnel reflection and diffuse reflectance. The latter corresponds to light that enters the tissue and re-emerges out of the tissue toward the detector. If skin is illuminated by polarised light, the light reflected by the surface remains polarised (diffuse reflectance).³⁰⁰ However, the re-emerging light is depolarised due to scattering in the tissue (Fresnel reflection).

According to previous work on reflectance spectroscopy, the spectral molar absorption coefficients of oxyhaemoglobin and deoxyhaemoglobin are fixed and different. Deoxyhaemoglobin has a single absorption peak around 554 nm, whereas oxyhaemoglobin shows absorption peaks around 542 nm and 578 nm²⁹⁹ (Figures 1.18 and 1.19).

OxyVu exploits this uniqueness and uses hyperspectral imaging to detect diffuse reflectance. OxyVu records a series of two-dimensional images at 15 equally spaced and specific wavelength points (λ) between 500 nm and 660 nm.³⁰¹ Seven broadband visible light-emitting diodes (LEDs) with collimating wide lenses are radially arranged around and cross-polarised relative to the collection optics. The Fresnel reflection in the image is eliminated by placing a linear polariser film set between two acrylic sheets in front of the LED assembly. The detection system is designed to have a 12-inch focal length and a spatial resolution of 100 μm .

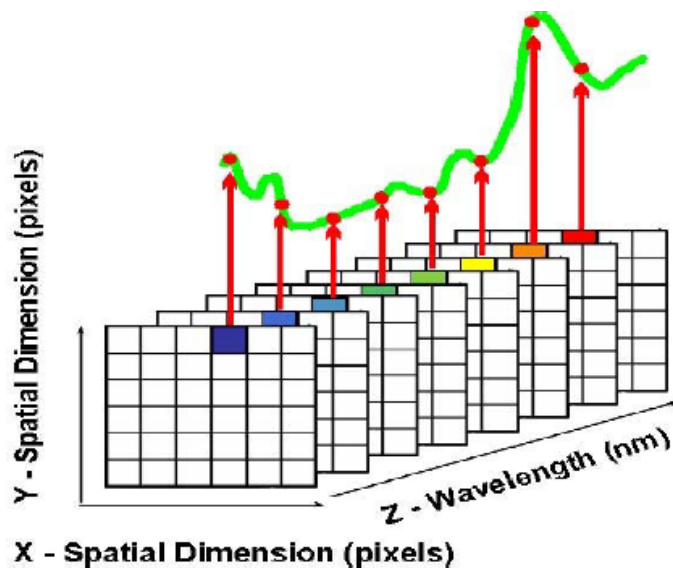


Figure 1. 18. OxyVu™ using different wavelengths to detect specific chromophores. (Retrieved from <http://www.hypermed-inc.com>).³⁰¹

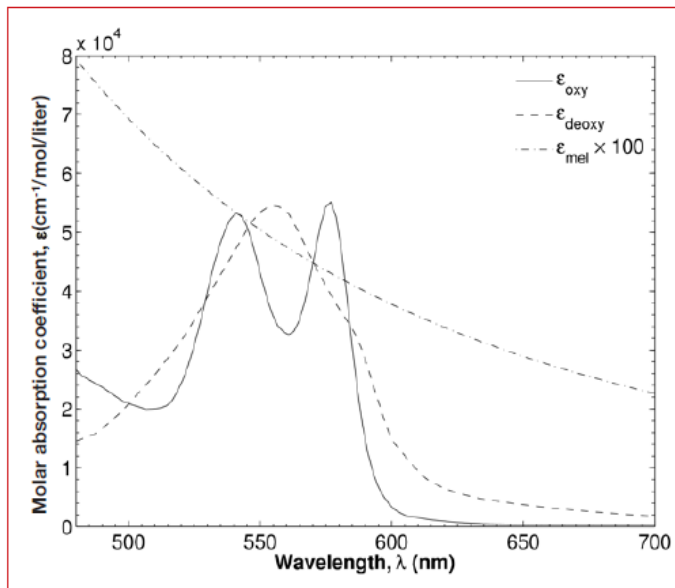


Figure 1. 19. Graph demonstrating the chromophores of oxyhaemoglobin and deoxyhaemoglobin. (Retrieved from <http://www.hypermed-inc.com>).³⁰¹

With sophisticated computer software, OxyVu transforms each pixel of the picture into a three-dimensional “hypercube” where the x and y axes are the two spatial coordinates and λ is the spectral coordinate. Analysis of the hypercube can reveal the local concentration of tissue chromophores.

With further mathematical modelling and scaling the oxyhaemoglobin concentration (HT-Oxy) to be 50 based on the average for a population of healthy subjects, HT-Oxy(x,y), HT-Deoxy(x,y), and HT-melanin(x,y) can be estimated in arbitrary units (AU), as well as the total haemoglobin concentration (HT-Sum) and oxyhaemoglobin saturation (HT-Sat) where HT-Sum = HT-Oxy + HT-Deoxy and HT-Sat = HT-Oxy/HT-Sum, respectively³⁰² (Figure 1.20).

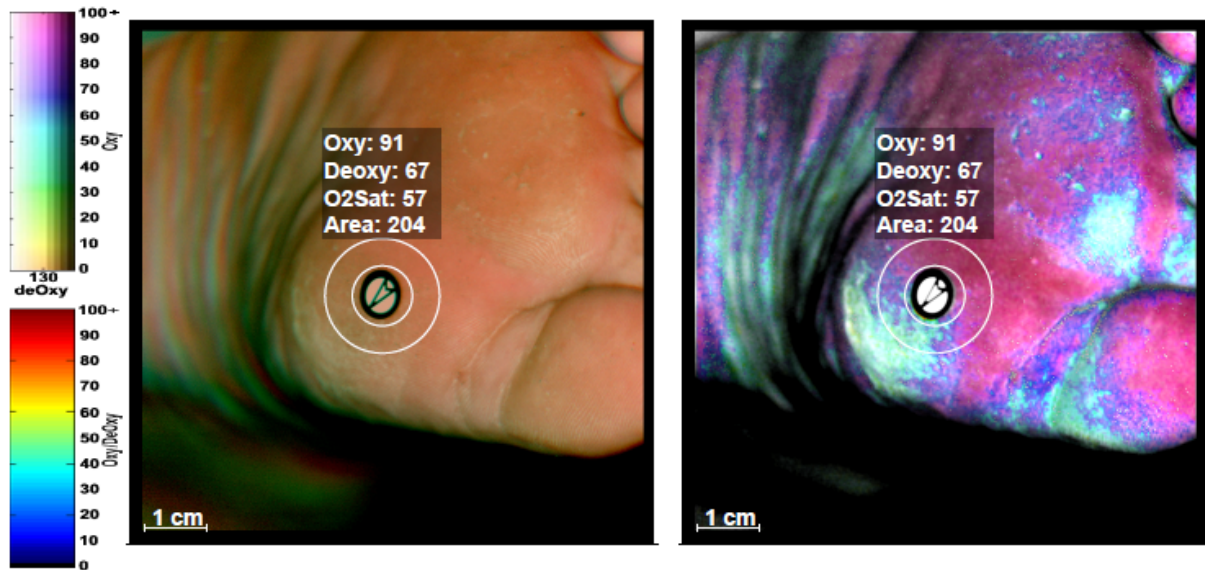


Figure 1. 20. Example of an OxyVu™ reading.

The readings do not account for melanin concentration, epidermal thickness, or the scattering properties of the tissue. Another advanced mathematical model is used to refine these diffuse reflectance measurements and simultaneously determine HT-Sat, blood volume fraction, melanin concentration, and the tissue scattering coefficient.³⁰³ Several assumptions are made, including the epidermis being a plane-parallel slab supported by a semi-infinite layer of dermis and the tissue scattering coefficient being identical for the dermis and epidermis.²⁹⁹ The spectral absorption coefficient of the dermis is determined by the absorption of blood and tissue, which depends on the blood volume fraction and the concentrations of oxyhaemoglobin and deoxyhaemoglobin.³⁰⁴ This coefficient is successfully applied to reflectance measurements in different levels of pigmented skin.³⁰⁵ This results in consistent measurements irrespective of the racial groups, anatomical location, and tanning status.^{295 306}

Previous clinical studies with OxyVu

OxyVu was validated against high-resolution spectrometry at eight different anatomical sites before and after pressure cuff-induced ischaemia in 19 healthy subjects.³⁰⁷ The findings showed good congruence when comparing OxyVu and high-resolution spectrometry, with correlation coefficients of 0.86 and 0.88, respectively.³⁰⁸ OxyVu recorded improved tissue oxygenation of the lower limb following IIB surgery³⁰⁹ and was used to predict the optimal level of major lower limb amputations.

When this thesis was started in 2008, there were two clinical research papers that used HTCOM, both of which were published by the same research group. Khaodhiar *et al* in *The Lancet* (2005), showed a difference in HT-Sat at the forearm and foot in 108 patients with no diabetes and in patients with diabetes with and without neuropathy.³⁰⁹ These investigators showed that tissue oxygenation was worst in terms of low HT-Oxy, HT-Sat, and high HT-Deoxy in patients with diabetic neuropathy. There was also an increase in HT-Sat when tissue was vasodilated by iontophoresis.

Khaodhiar *et al* (2007) performed a similar study, but compared ten patients with type 1 diabetes and ulcers, 13 patients with type 1 diabetes without ulcers, and 14 healthy patients.³¹⁰ The patients with ulcers were monitored for 6 months to determine healing potential. HTCOM was also compared with TCOM, laser Doppler flowmetry, and ABI. HTCOM was the only method that showed lower HT-Oxy and HT-Deoxy surrounding the ulcer. HT-Oxy at the metatarsal site of the plantar foot was lower in patients with diabetes and ulcers than in controls, but no difference was demonstrated for HT-Deoxy. The HT-Healing Index was also defined based on DFU healing at 6 months. Greenman *et al* concluded that the OxyVu has a sensitivity and specificity of 93% and 86%, respectively, for predicting DFU healing based on readings from the first visit. Of note, patients with severe PVD requiring surgical intervention, heart failure with lower extremity oedema, a history of a non-resolved cerebrovascular event, uncontrolled hypertension, end-stage renal failure, or any other chronic illness or medications that affect wound healing were excluded from the study.

By 2014, six further clinical studies using HTCOM were identified. Nouvong *et al* (2009) extended the pilot study conducted by Khaodhiar *et al* to a study that included 73 DFUs in 54 patients with type 1 or type 2 diabetes. Again the study derived the HT-Healing Index, with a sensitivity, specificity, and positive predictive value of 86%, 88%, and 96%, respectively. HT-

Oxy and HT-Sat at the ulcer border were lower in ulcers that did not heal in 6 months than in those that healed during this time. No differences in HTCOM at the dorsum of the foot were found between the two groups. This study differed from the pilot study in that OxyVu readings were taken from the dorsum of the foot.

Neville *et al* (2009) studied normative perfusion values at eleven separate anatomical regions in 194 subjects without PVD using the OxyVu.³¹¹ While HT-Oxy, HT-Deoxy, and HT-Sat varied according to anatomical location, the plantar and palmar surfaces demonstrated the highest baseline perfusion. Although not a statistically significant finding, men had higher HT-Oxy, HT-Sat, and lower HT-Deoxy. Insignificant differences were found in measurements 8 hours apart. Ischaemia induced by cuff inflation revealed a decrease in HT-Oxy and an increase in HT-Deoxy. After release of the ischaemic cuff, rebound perfusion increased HT-Oxy to above baseline while HT-Deoxy returned to baseline levels with reperfusion. The pattern of HT-Sat followed that of HT-Oxy. Similar findings were reported by Nagaoka *et al* when the brachial artery was compressed and oxygenation measurements were made at the middle finger.³¹²

Jafari-Saraf *et al* (2010) compared hyperspectral readings with the ABI in 85 limbs, of which 53 had ABI ≥ 0.9 , 22 had ABI 0.45–0.9, and 10 had ABI ≤ 0.45 .³¹³ Those with non-compressible ABIs were excluded. HT-Oxy and HT-Sat were measured at three points on the dorsum of the foot as well as on the ipsilateral forearm. Readings at the ipsilateral forearm was used as the reference point. The validity of this method is not certain. HT-Oxy, HT-Sat, and their “normalised” values by comparison with the forearm measurement did not correlate with ABI in any of the three categories described or as a continuous variable.

Jafari-Saraf *et al* (2012) compared HTCOM with TCOM in 23 sections of the foot (dorsal and plantar) and wrist (volar) in four healthy volunteers.³⁰⁷ They compared oxygenation of these sites when baseline probe temperature was fixed at 37°C, then at 41°C and 45°C. HT-Oxy, HT-Sat, and HT-Sum increased with increasing temperature up to 45°C. HT-Deoxy did not vary with temperature. Only HT-Sat showed a difference between baseline and at 37°C. At 37°C, TcpO₂ correlated with HT-Oxy ($R=0.35$), HT-Deoxy ($R=0.63$), and HT-Sum ($R=0.60$). As temperature increased to 45°C, this correlation progressively weakened or disappeared. At 45°C, TcpO₂ only correlated significantly with HT-Sat ($R=0.28$), with no association at 37°C. Interestingly, TcpO₂ tended to correlate positively with HT-Deoxy, meaning that as oxygen tension increased, so did deoxyhaemoglobin.

Chin *et al* (2011) investigated the relationship between HTCOM and the severity of PVD in 46 patients (92 limbs) without PVD and 65 patients (130 limbs) with PVD.³¹⁴ The definition of PVD was based on ABI and Doppler waveforms qualified by four vascular technicians. The presence of PVD was defined based on Doppler waveforms, i.e., triphasic, biphasic and monophasic. It was unclear if their patients with PVD were symptomatic or if their Doppler findings were regulated by two or more technicians. Hyperspectral readings (HT-Oxy, HT-Deoxy, and skin temperature) were made at nine different sites on each limb at the calf, ankle, heel, and the dorsal and plantar foot. These nine sites were angiosomes of specific vascular beds supplied by major named arteries as described by Galiano *et al*.³¹⁵ Hyperspectral oxygenation was also recorded with the participant lying on a bed with the head of the bed elevated to 45°. It is assumed that ABI was measured supine.

HT-Deoxy at the plantar metatarsal, arch, and heel was significantly lower in the PVD group (monophasic or biphasic flow) than in the non-PVD group (triphasic flow). When HT-Deoxy at the three sites was compared with ABI using linear regression, there was a significant correlation but in an inverse direction to their other findings, suggesting that as ABI increased, HT-Deoxy decreased. HT-Oxy was not sensitive to the presence or severity of PVD or ABI. Of interest, Chin *et al* also compared hyperspectral readings with the toe pressure index, and showed a correlation with HT-Oxy at the plantar metatarsal ($R=0.31$, $p=0.001$). No correlations were detected with skin temperature.

Raju *et al* utilised OxyVu to demonstrate differences in tissue oxygenation (HT-Sat) at different parts of the body, from the forehead to the ankle, in healthy volunteers standing erect or lying supine.³¹⁶ Their sample size was not stated, and the number of patients scanned per location varied from 10 to 29. It showed higher HT-Sum from the ankles to the xiphisternum in the erect position when compared with the supine position, indicating an increased microvascular volume resulting from congestion. HT-Sat was also lower between the ankles and the mid abdomen in the erect position. Calf pump action did not affect tissue oxygenation.

1.12 Diabetic foot

Diabetes mellitus is a common disease that affects 194 million people globally, and this figure is expected to increase to 344 million by the year 2030.^{317 318} Diabetic foot is defined as the foot of a diabetic patient with ulceration, infection, and/or destruction of the deep tissues associated with neurological abnormalities and various degrees of PVD in the lower limb.³¹⁹ Diabetic foot problems account for nearly 50% of all diabetes-related hospital days.³²⁰ DFUs are one of the most common and serious sequelae of diabetes, alongside neuropathy, angiopathy, retinopathy and nephropathy.

The prevalence of DFU in developed countries is approximately 4%–10%, with an annual incidence of 2.2%–5.9%.³²¹ The lifetime risk of developing DFU could be as high as 25%.³²² The prevalence of DFU is higher (5%–10%) in older individuals with type 2 diabetes and in Whites than in Indian Asians.³²³ PVD is twice as common in diabetic patients when compared with their nondiabetic counterparts. For every 1% increase in glycated haemoglobin (HbA_{1c}), there is a 26% increased risk of PVD.³²⁴ PVD is more aggressive in patients with diabetes.³²⁵ DFUs are often located on the plantar aspect of the toes or foot. If left untreated, foot ulcers may lead to infection and deep tissue necrosis. Between 14% and 24% of patients with DFU require an amputation.³²⁶ The rate of lower limb amputation is 15 times higher in diabetic patients than in individuals without diabetes.³²⁷ Eighty-five percent of diabetes-related amputations are preceded by a gangrenous or infected foot ulcer.^{323 328} The incidence of major amputation is 1% per year for patients with diabetes who are older than the age of 65 years. The annual rate is higher in type 2 diabetes (5%).³²⁹ Survival following amputation does not seem to be worse for those with diabetes.^{329 330} Up to 85% of these amputations could be prevented.³³¹

Therefore, treatment of diabetic foot is a high priority when attempting to prevent limb loss. Adequate glucose control, local wound care, relief of pressure using appropriate footwear, evaluation of the vascular supply and subsequent revascularisation, and appropriate antibiotic therapy are critical. Despite adequate revascularisation and foot care, the ulcer may not heal due to extensive infection or irreversible ischaemia. Surgical debridement of the ulcer or distal amputation may be required to save the foot. Methods to enhance the healing process in the acute wound may improve limb salvage and survival.

Pathophysiology of DFU

Increased production of advanced glycation end products and vascular superoxide from hyperglycaemia, thereby causing endothelial toxicity and inactivating nitric oxide (NO), has been hypothesised to contribute to vascular dysfunction of the vessels and nerves. This results in atherosclerosis, thickening of the basement membranes of capillaries, hardening of arteriolar walls, and endothelial proliferation, which have been implicated in the pathogenesis of diabetic complications.³²⁰

The concept of predisposing, precipitating and aggravating factors in the development of diabetic foot problems has important implications for management of patients with predisposing factors. Foot lesions will not develop unless exposed to a precipitating factor, and even at this stage, resolution of the problem can be expected if the effects of the potential aggravating factor can be avoided.²⁵⁶

Predisposing factors

- Vascular disease
 - Atherosclerosis: This is the most important factor in about half of DFU cases. If the blood supply is inadequate, minor wounds will not heal and there may be ischaemic rest pain. Neuropathy frequently co-exists and masks the pain, but tissue damage and infection may progress unnoticed.
 - Calcification of arteries: This typically occurs in the tunica media and intima (Monckeberg's arteriosclerosis). This is an indicator of a prolonged diabetic metabolic disturbance but there is no direct evidence that it causes foot problems.
 - Microangiopathy: Ischaemic lesions could develop in the event that local blood flow is reduced. The rigidity of the vessel walls might decrease the ability of the microcirculation to respond to injury and mount an adequate inflammatory response.
- Neuropathy
 - Loss of pain perception (sensory): loss of sensation and ischaemia are the two most important factors in the development of DFU. Impaired pain perception leads to loss of tissue initiated by small unrecognised lesions. There is no direct evidence that neuropathy increases the risk of infection.

- Paralysis of the intrinsic muscles of the foot (motor): This results in an imbalance between the flexor and extensor mechanisms, toe clawing, increased prominence of the metatarsal heads, and a decreased effective weight-bearing area under the forefoot. These abnormal forces may cause soft tissue and bony deformity.
- Autonomic neuropathy:
 - Failure of reflex dilation in response to local injury.
 - Abnormal vasoconstriction in response to cold.
 - Loss of sweat and sebaceous gland functions leading to dry skin which predisposes to skin cracks, fissures, and infection.
 - Increased AV shunting. This requires a greater increase in tissue perfusion to maintain intact skin and healing.
- Increased risk of infection
 - Decreased immune resistance.³³²

Precipitating factors

- Physical injury
 - A puncture wound or localised pressure areas arising from, e.g., tight shoes.
- Mechanical trauma
 - e.g., from walking. Progressive atrophy of connective tissue in the skin as a result of decreased proliferation of fibroblasts in patients with diabetes is the critical intermediate event leading to formation of a DFU.^{333 334}
- Heat
 - If there is reduced perception of temperature and loss of pain sensation.
- Chemical
 - Application of corrosive substances, e.g., those found in corn plasters.

Aggravating factors

- Infection
 - Causes more damaged tissue, possibly because of:
 - Abnormal cellular and humoral responses to inflammation
 - Decreased efficiency of repair mechanisms, in particular collagen formation
 - An environment being created that allows growth of anaerobic bacteria.

- Ischaemia
 - Also acts as an aggravating factor because healing is impaired by an inability to increase the local blood supply; ischaemia also promotes spread of infection.
- Neuropathy.
 - Loss of pain sensation acts as an aggravating factor by increasing the risk of mechanical injury and allowing infection to continue unnoticed. Over time, a limb-threatening condition called Charcot neuropathic osteoarthropathy can develop; this is a condition involving the interaction of several components (diabetes, neuropathy, trauma, and metabolic abnormalities of bone) affecting the bones, joints, and soft tissues of the foot and ankle, and results in an acute localised inflammatory condition that may lead to bone destruction, subluxation, dislocation, and deformity. The hallmark deformity is midfoot collapse with a “rocker bottom” foot.

Other risk factors associated with DFU include nephropathy, retinopathy, plantar callus formation, history of ulceration or amputation, old age, a long history of diabetes, poor glucose control, peripheral oedema, low socioeconomic status, poor health care, and low educational status.³³⁵

In general, approximately 20% of patients with DFU primarily have inadequate arterial blood flow, while 50% primarily have neuropathy, and approximately 80% have both conditions.³³⁶
³³⁷ Vascular disease and neuropathy cannot be reversed, although their development may be delayed. The precipitating factors are preventable, e.g., by rigorous avoidance of physical trauma.

Diabetic angiopathy is typically described as a diffuse disease affecting the large, medium and small vessels. The term “small vessel disease” may have several meanings:

1. Disease of the arterioles and capillaries (i.e., “microangiopathy”).
2. Disease of the tibial arteries; to vascular surgeons, this is “small vessel disease” that typically occurs in patients with diabetes and has prognostic features
3. The metatarsal and digital arteries are also affected by diabetes in a way that resembles atherosclerosis.

The microangiopathy associated with diabetes can cause haemodynamic changes at the level of the arteriolar and capillary vessels. An increase in blood flow is characteristically found early

in diabetes, resulting in capillary hypertension and damage to the microvascular endothelium.

Factors that contribute to this microangiopathy include:

1. An increased metabolic rate in poorly controlled diabetes, causing more heat to be lost from the skin.
2. A chronic increase in the plasma and extracellular fluid volume, causing capillary leakage
3. Alterations in the action of vasoactive substances.
 - a. Decreased plasma renin activity
 - b. Decreased sensitivity of blood vessels to angiotensin II
 - c. Decreased responsiveness to noradrenaline.
4. Increased production of vasodilator substances (prostacyclin and prostaglandin E)
5. Hyperglycaemia and increased glucagon and growth hormone levels, causing vasodilatation
6. Precapillary sphincter dysfunction.
7. Tissue hypoxia, causing local vasodilatation.
8. Denervation as a result of autonomic neuropathy, also causing vasodilatation.

It is probable that increased blood flow via AV shunting is an important mechanism for hyperperfusion in the limbs. AV shunts are present in the digits and plantar surfaces of the feet. They are 20–70 microns in diameter and when open provide a low resistance pathway between the small arteries and veins. Their diameter is controlled by the sympathetic nervous system. In the setting of neuropathy, autonomic control of the vascular sphincter mechanisms regulating flow through these shunts is lost. An increase in blood flow through the AV shunt has important effects on capillary function, i.e., a reduction in capillary blood flow due to stealing of blood by the shunt and increased pressure in the post-capillary venules, which would decrease the perfusion pressure. This impairs diffusion of oxygen, migration of leukocytes, and capillary permeability. The latter also causes oedema. Paradoxically, increased blood flow via AV shunting can result in a relatively warm foot, which can falsely reassure the clinician.

1.13 Local wound management

Providing there is adequate blood supply to a wound, the main objective in terms of management would be to apply appropriate wound dressings dictated by the condition of the wound. Local wound care requires cleansing, irrigation, debridement of the wound and surrounding tissues, and application of appropriate wound dressings. Surgical wound debridement with removal of surface debris and necrotic material is considered the most effective method; however, this may require anaesthesia. Other methods are:

- mechanical (wet-to-dry gauze dressings, Mesalt®, irrigation, pulsatile lavage)
- autolytic (moist interactive dressings, i.e., hydrogels, alginates, and hydrocolloids)
- enzymatic (collagenase, papain, urokinase).

Relief of pressure (mechanical off-loading) at the wound site is equally important. Total contact casts for patients with DFU appear to be the most efficacious.³³⁸

Dressings cover the wound and insulate it from the environment. Ideally, they should:

- maintain humidity at the wound/dressing interface to provide a moist environment that optimizes wound regeneration and repair
- remove exudates and toxic components
- allow gas exchange
- provide thermal insulation
- prevent secondary infection
- be able to be removed without trauma at dressing changes
- allow monitoring of the wound
- be comfortable and easy to use
- be small enough to allow use of footwear.

No single dressing meets all the above requirements. Choice between the types of dressing available for the various wounds is an art and varies between hospitals and surgeons. Available dressing materials are broadly classified into films, foams, hydrogels (Intrasite®), hydrocolloids (Duoderm®), alginates (Kaltostat®), hydrofibres (Aquacel®), cadexomer dressings with iodine (Iodosorb®), and medicated dressings. Use of local growth factors has produced some early promising results, in particular becaplermin (recombinant PDGF).³³⁹

Hydrogels and hydrofibres are commonly used at our institution. They have wound debriding properties and provide an ideal wound environment when used appropriately. Hydrogels provide moisture at the wound site, whereas hydrofibres absorb the excess exudate and stimulate proliferation of keratocytes as well as immobilising bacteria and delaying bacterial growth. The presence of ionic silver in these dressings can also reduce the bacterial load.³⁴⁰ Saline-soaked dressings are deemed obsolete at our institution.

Vermuelen *et al* published a Cochrane systematic review in 2005 addressing the evidence for use of topical dressings for surgical wound healing.³⁴¹ They found no difference between the alginate, hydrocolloid and gauze dressings in terms of wound healing rates, that gauze dressings were more painful and associated with less patient satisfaction, and that the cost of a dressing change was not cheaper than other modalities. There has been limited research compared modern traditional dressings with gauze for surgical wound healing. It is hypothesised that gauze dressings can prolong the inflammatory phase of wound healing, induce localised hypothermia, and increase the risk of infection.³⁴²

Over the last decade, there has been increasing use of topical negative pressure (TNP) therapy, which substitutes for traditional dressings. This treatment has seen a paradigm shift in the management of many types of wound in hospitals worldwide. However, the clinical efficacy of TNP remains debatable. Systematic reviews have concluded that there is no evidence, especially at a scientific level, of TNP being of benefit for vascular wounds, where the potential for healing is often compromised.³⁴³⁻³⁴⁵

1.14 Topical negative pressure therapy

In recent years, wound management has become more refined, with innovative strategies now available to target the various stages of wound healing. TNP therapy is one of these strategies. Historically, TNP is well known to cause tissue hyperaemia, and has been used for this purpose in Chinese medicine for thousands of years.³⁴⁶

In 1993, Fleischmann *et al* applied TNP to wounds via a foam dressing for an extended period in patients with open fractures and suggested that TNP promotes production of granulation tissue in healing wounds and reduces the risk of infection.³⁴⁷ Negative pressure was achieved using a wall suction apparatus or surgical vacuum bottle, which proved cumbersome and restricting, and negative pressure levels were difficult to control.

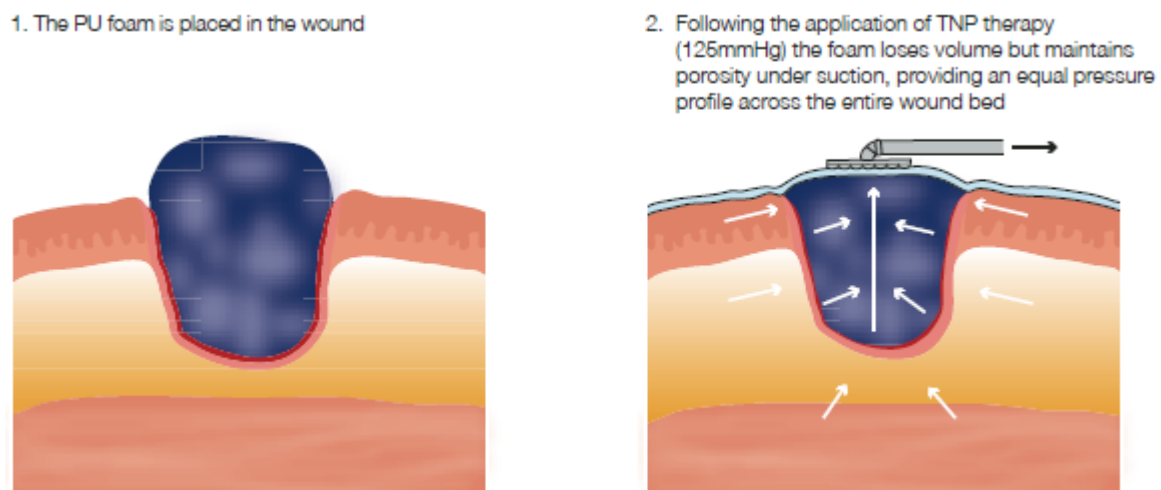


Figure 1. 21. Application of VAC® foam. Sourced from Bovill *et al*, 2008.³⁴⁸ **Abbreviations:** PU, polyurethane; TNP, topical negative pressure.

The Vacuum-Assisted Closure (VAC®) device is a form of TNP therapy that was pioneered by Argenta and Morykwas in 1997³⁴⁹ (Figure 1.21). It has gained popularity in many wound care settings, including chronic wounds, diabetic wounds, pressure ulcers, skin grafts, and acute surgical wounds. This technique involves application of a polyurethane or PVA foam dressing with large open pores (400–600 μm) that maintain porosity over the wound. The foam dressing is connected to a suction device delivering a uniform controlled negative pressure of –50 to –125 mmHg either continuously or intermittently across the wound bed. Examples of other TNP therapy systems are Wound Assist™, Renasys™, Exsudex™, and Venturi™. The majority of clinical studies, however, have used the VAC device.

The negative pressure applies mechanical forces to the wound known as macro-strain (visible stretch) and micro-strain (micro-deformation at the cellular level causing cell stretch).³⁵⁰ The effect is a sophisticated, sterile, closed dressing that provides a moist healing environment and alters the physiological and chemical environment.

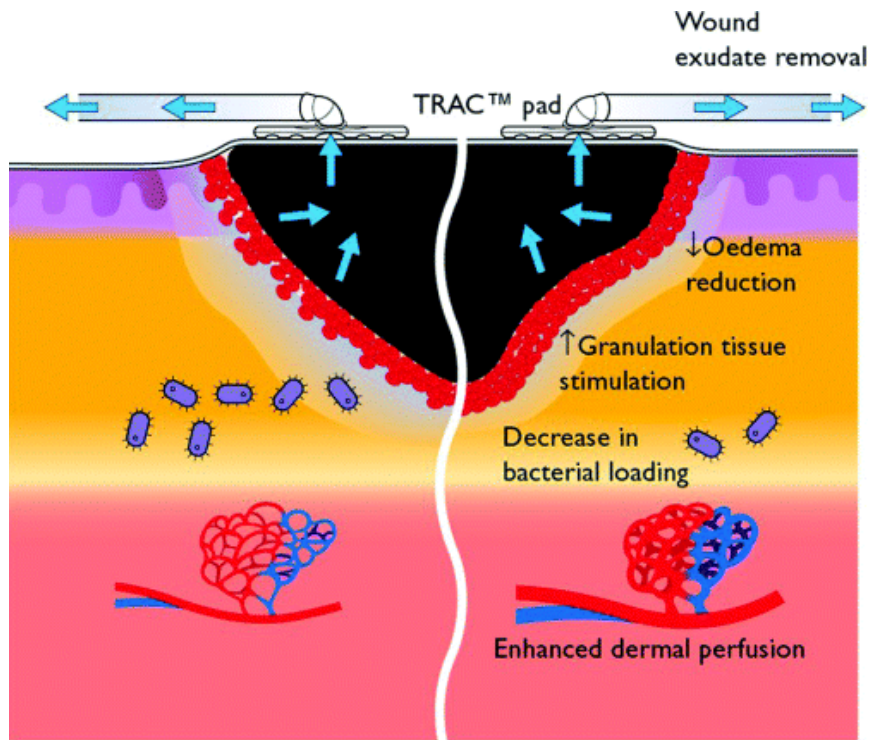


Figure 1. 22. Effects of topical negative pressure therapy. Source from Banwell et al, 2004.³⁵¹

TNP is thought to promote healing by:

- Increasing local blood flow and tissue perfusion
- Reducing oedema
- Stimulating formation of granulation tissue
- Stimulating cell proliferation
- Removing soluble inhibitors of healing from the wound
- Reducing bacterial load
- Contracting the edges of the wound
- Preventing wound infection by avoiding handling (Figure 1.22).³⁵²

Enhanced formation of granulation tissue

Morykwas *et al* compared the efficacy of TNP therapy with that of standard saline-soaked gauze in a porcine model and measured the correlation between change in wound volume over time and rate of formation of granulation tissue. Enhanced formation of granulation tissue was observed with continuous and intermittent application of TNP (63% and 103%, respectively).³⁵³ Intermittent treatment (5 minutes on and 2 minutes off) is more effective than continuous treatment because wound cells can become acclimatised to the constant physical forces applied with continuous therapy, whereas intermittent therapy increases tissue perfusion by inactivating capillary autoregulation, which prevents vasoconstriction and allows proliferating cells time to rest between cell cycles. Constant stimulation with negative pressure can also switch off the mitotic process. Many clinicians use continuous pressure for the first 48 hours before switching to the intermittent mode.

Increased tissue perfusion and less oedema

TNP at -125 mmHg increases capillary blood flow by up to four-fold.^{349 354} Malmstro *et al* published several papers relating to microvascular blood flow at the wound edge during TNP as measured by laser Doppler flowmetry in pigs with no vascular disease.³⁵⁵⁻³⁵⁹ In summary, cutaneous blood flow nearly doubled at 2.5 cm from the skin edge, but was halved at 0.5 cm from the skin edge as a direct result of negative pressure. The degree of reduction was proportional to the increase in pressure applied and it was found that cutaneous blood flow increased at a low pressure. This is one of the reasons why intermittent suction is considered superior to continuous suction for TNP. Excessive negative pressure of >400 mmHg has an opposite effect, inhibiting flow and leading to capillary distortion. Tissue perfusion is increased directly by negative pressure and indirectly by removing interstitial fluid and influencing vasomotor tone and vasoactive mediators; however, the latter would be difficult to quantify experimentally, so is theoretical only.

Different types of wound fillers for TNP (e.g., black polyurethane foam, white PVA foam, green foam, gauze-based filler, and pathogen-binding mesh) were also compared.³⁶⁰ Polyurethane foam was more effective than PVA foam because of the relatively smaller pore size in the PVA product. Cutaneous blood flow and wound contraction were similar. Wound fluid was more efficiently removed when pathogen-binding mesh was used.

Stimulation of cell proliferation

Mechanical stress on the ECM induces cell proliferation and cell division. Negative pressure induces tissue micro-deformations within the wound.³⁶¹ Mechanical stretching of the cells alters the cytoskeleton, thereby disrupting the integrin bridges and upregulating the release of intracellular secondary messengers, which in turn stimulate cell proliferation, angiogenesis, and epithelialisation.³⁶²⁻³⁶⁴ In addition, the vacuum created causes the foam to shrink, which draws the wound margins to the centre, facilitating wound closure.³⁴⁹

Removal of wound exudate and interstitial fluid

Optimal wound healing depends on the balance between positive growth factors and inhibitory inflammatory cytokines. Many up and coming medical products that target chronic wound healing, in particular topical growth factor products, support this concept. TNP therapy may induce an interstitial fluid gradient, thereby reducing oedema, indirectly stimulating perfusion by decompressing small capillaries, and directly removing harmful components (such as cytokines and matrix MMPs), ultimately promoting secondary intention healing.³⁶³⁻³⁶⁶

Animal studies have compared cytokine and growth factor levels in wounds treated with TNP and those in wounds treated with traditional dressings. The evidence is mixed, but suggests growth factors are upregulated and levels of inhibitory cytokines are decreased, thereby promoting healing.³⁶⁷ One study showed decreased levels of TGF- β , TNF- α , and IL-8 in the TNP group, which healed more rapidly. Although the absolute TGF- β level was lower in the TNP group, the TGF- β to TNF- α ratio was much greater.³⁶⁸ Another animal study showed increased VEGF and FGF-2 in the TNP group.³⁶⁹ VEGF and IL-8 levels were higher when human traumatic wounds were treated with TNP.³⁷⁰ In 2014, Yang *et al* reported a study that found upregulation of FGF-2 and extracellular signal-regulated kinase (ERK) 1/2 in human diabetic foot wounds.³⁷¹

Removal of bacterial load

Morykwas *et al* demonstrated that TNP decreased the bacterial load in a porcine wound model by a factor of 10^3 over 5 days compared with the control, especially following inoculation with *Staphylococcus aureus* and *Staphylococcus epidermidis*.³⁵³ The mechanism may involve increased blood flow supplying oxygen and leucocytes, decreased interstitial oedema, and

removal of bacterial by-products, such as harmful enzymes (elastase and collagenase), from the wound bed.

Clinical evidence for TNP

Several systematic reviews published in recent years have yielded inconclusive evidence for the superiority and widespread use of TNP in vascular foot wounds. The authors of these reviews have criticised the lack of quality level 2 evidence for effects on wound healing and called for further controlled trials. Most of these reviews were based on a small number of RCTs and examined time to complete healing, the proportion of wound tissue healed, time to secondary closure, wound complications, two-dimensional size in terms of surface area or depth, survival, quality of life, and/or economic costs.

When determining the clinical effectiveness of TNP therapy, the rate of production of granulation tissue is the most relevant and sensitive surrogate marker. Only four RCTs investigated change in wound size over time, and yielded mixed results. The studies were too heterogeneous to analyse. McCallon *et al* focused on reduction in surface area and time taken for the ulcer to heal, and did not show a significant difference between the treatment and control groups.³⁷² In contrast, in a study by Etoz *et al* that included 24 patients with DFU, reduction in wound surface area and time taken for the wound bed to be covered with granulation tissue were more rapid in the TNP group than in the group treated with saline gauze dressings.³⁷³

Study	No. of patients	Control	Time	Results	Statistical significance
Ford <i>et al</i> . ^[25]	28	HP	6 weeks	Mean reduction in wound volume: VAC 51.8%; HP 42.1%	p = 0.46
Joseph <i>et al</i> . ^[22]	24	WM	6 weeks	Decrease in wound volume/depth: VAC 78%/66%; WM 30%/20%	Volume p = 0.038; depth p < 0.00001
McCallon <i>et al</i> . ^[24]	10	WM	Not recorded	Surface area decrease: VAC 28.4 ± 24.3%; WM 9.5 ± 16.9% <i>increase</i>	No statistical significance
Edington <i>et al</i> . ^[23]	6	WM	4 weeks	Decrease in wound volume/depth: VAC 50%/49%; WM 0%/8%	Volume p > 0.05; depth p < 0.05

HP = Healthpoint® system of wound gel products; WM = wet to moist saline dressing.

Table 1. 1. Summary of clinical studies on topical negative pressure therapy and wound dimension assessment Sourced from Venturi *et al*, 2005.³⁵²

Most wounds are three-dimensional and irregular in shape. Deposition of granulation tissue starts at the wound base and leads to changes in depth prior to contraction of the wound edges. Therefore, measurement of volume is more reliable in evaluation of wound healing. Ford *et al*, Joseph *et al*, and Eginton *et al* investigated wound volume and the results are summarised in Table 1.1.

Eginton *et al* compared TNP with hydrocolloid wound gel and gauze dressings in diabetic foot wounds.³⁷⁴ Only 6 of their 10 patients (representing 7 wounds) completed the study. All wounds were randomised to TNP for the first 2 weeks followed by traditional dressings for another 2 weeks or vice versa. Wound dimensions were recorded using computerised planimetry from digital photographs on a weekly basis for 4 weeks. According to their protocol, wounds were subjected to continuous negative pressure of –125 mmHg. Whilst TNP was shown to decrease wound volume and depth to a significantly greater degree than moist gauze dressings, all wounds received 2 weeks of TNP and traditional dressings.

Joseph *et al* studied 36 wounds that were not arterial in nature.³⁷⁵ Eighty percent were pressure wounds, and the remaining 20% included venous ulcers, dehisced wounds, traumatic wounds, and post-radiation wounds. Eighteen of the wounds were treated with saline-soaked gauze dressings three times a day and the remainder were randomised to TNP therapy. It appeared that the same type of wound dressing was used throughout the study. Wound volumes were assessed by volume displacement of alginate impression moulds. Volume reduction was greater in the TNP group at 3 and 6 weeks. Punch biopsies were taken for histology. The chief characteristic of the TNP group was formation of granulation tissue, whereas inflammation and fibrosis were seen in wounds treated by gauze dressings. Further, there were more complications, including infection and fistulae, in the control group.

A randomised study by Ford *et al* included 35 pressure wounds, 8 of which were located below the ankle.³⁷⁶ For wounds allocated to traditional dressings, those with substantial exudate received Iodosorb® or Iodoflex®, whereas the others were treated with Panafil®. Panafil is a topical dressing containing papain and urea, both of which break down proteins and debride wounds. Wound volumes were measured by volume displacement of plaster impressions. Tissue biopsy and wound assessments were conducted at 3 and 6 weeks. One 6-week trial of treatment was completed in three wounds followed by a second 6-week trial of the alternative treatment. The mean reduction in volume displacement was not different between

the groups (52% in the TNP group versus 42% in the control group; $p=0.46$). There was also no difference in the numbers of polymorphonuclear leucocytes or lymphocytes present.

Of note, the wounds were assessed by independent investigators in a “blinded” fashion in these studies. However, it would not be difficult to differentiate between wounds dressed by TNP and those dressed using traditional methods.

Noble-Bell *et al* focused on TNP therapy for DFUs in their systematic review,³⁴⁵ and concluded that “... while all the studies included in the review indicated that TNP therapy is more effective than conventional dressings, the quality of the studies were weak and the nature of the inquiries in terms of outcome and patient selection divergent ...”. Ubbink *et al* and Vikatmaa *et al* also commented on DFUs in their systematic review, but their conclusion concerning the effectiveness of TNP was more reserved.^{343 377} The criticism in all the reviews was the presence of only one study that investigated postoperative TNP therapy in partially amputated diabetic foot wounds, which are the most clinically relevant in vascular surgery. Armstrong *et al* compared TNP with modern moist wound treatment in 162 patients with transmetatarsal amputation wounds. More patients in the TNP group achieved 100% re-epithelialisation than in the control group (56% versus 39%, respectively, $p=0.04$) and within a shorter time period.³⁷⁸

Following these reviews, Paola *et al* completed two RCTs of the treatment of diabetic foot wounds post debridement (one studying the time to secondary closure and the other healing by secondary intention).³⁷⁹ The latter study compared TNP with modern (non-gauze) dressing in 130 patients, with the endpoints of time needed for complete coverage of exposed bone with granulation tissue, healing time, and number of surgical procedures. While TNP was superior, the endpoints were arguably weak and prone to bias.

There were five studies identified in a 2013 Cochrane systematic review that evaluated TNP in the treatment of post-amputation wounds in patients with diabetes and debrided DFU wounds.³⁸⁰ Again, although there was a suggestion that TNP was better than traditional dressings (both gauze and non-gauze) in terms of wound healing, the studies were weak, small, and at risk of performance bias.

As a result of the inconsistent evidence, the clinical use of TNP therapy varies amongst institutions and surgeons. Some do not favour TNP therapy because they assume it to be costly; the TNP suction device and its related products are expensive, but systematic reviews

did not reveal a difference in cost.^{343 381 382} Vuerstack *et al* suggested that TNP therapy is less costly than conventional dressings (\$3881 and \$5452, respectively; p=0.001).³⁸³ Further Driver *et al* deduced that TNP is more cost-effective than traditional dressings regardless of whether the wound heals (\$1227 versus \$1695, respectively, per 1 cm² of wound closure) or does not heal (\$1633 versus \$2927 per 1 cm² of wound closure].³⁸⁴

1.15 Assessment of wound dimensions

Wound healing rates should be assessed objectively and quantitatively. The clinical tools most commonly used to measure wound dimensions include wound tracing and width and length measurements, which lack accuracy, and the image of the wound in three-dimensional form is often misrepresented.

Previously validated methods for wound volumetric measurements include formation of wound moulds (a “plastic” mould used to fill a wound that can then be removed to determine wound volume) and fluid installation (volume of saline injected over a wound, enclosed by cling-film). These are crude, messy, impractical, and labour-intensive, and often involve contact with the wound, thereby increasing the risk of infection. A three-dimensional (Kundin) wound gauge assumes the wound to conform to a cone and cylindrical contour, and thus neglects the irregular nature of wounds.

Stereophotographic and optoelectric systems use cameras to reconstruct the shape of the wound in a three-dimensional space without contacting the wound. Early models were inaccurate and subjective, as well as being bulky, heavy, and expensive.³⁸⁵ With evolving technology that uses cubic spline interpolation to interpret the curvature of the wound and a digital photography system, wound surfaces can be meticulously reconstructed, with volumetric measurements being more objective and reproducible.³⁸⁶

Computed tomography (CT) is considered to be the gold standard for assessment of wound dimensions. Wound volume and depth are calculated via three-dimensional reconstruction without contrast. However, CT scanning would be impractical and resource-consuming for longitudinal wound monitoring, with adverse effects from radiation exposure.

The ARANZ Medical Silhouette Mobile™ (SM) (Figure 1.23) is an innovative hand-held personal digital assistant (PDA)-based wound imaging and documentation device that combines a digital camera and structured lighting in the form of two laser beams to automatically correct for image scale and skin curvature, allowing quantitative, objective, rapid, and noncontact measurements of the wound surface area and cross-sectional depth. The SM correlates these measurements with past and present measurements to give a statistical, graphical, and photographic representation of the progress of the wound. The

scanner has been used in clinical trials in patients with leg ulcers; however there is limited evidence of its accuracy and reliability.

The FastSCAN Cobra® (FS) (Polhemus Inc, Colchester, VT, USA) is another non-invasive hand-held laser scanner (Figure 1.24) combined with tracking software that has been recently introduced. The PS was also developed by ARANZ in New Zealand. It uses a built-in “class A” laser line scanner (“laser wand”) that sweeps repeatedly over the object, and a miniature hand-piece camera registers the three-dimensional spatial coordinates of the surface points by utilising electromagnetic fields, enabling reconstruction of an exact three-dimensional digital surface map of the ulcer and wound edge contour in real time. Advanced computer software, known as Delta®, can then quantify the wound volume from the wound profile. This appears to be the most practical, modern, and reliable device available for objective wound volume measurement that has been validated, albeit not in human wounds.³⁸⁷ Based on a small study of 30 upper limbs in healthy volunteers, inter-operator reliability was up to 95% and intra-operator reliability was 72%; the latter was thought to be due to poorer quality scans and the fact that the entire upper limb, including the hand, was imaged rather than targeting a smaller wound volume. The FS also appeared to overstate volume when compared with the fluid displacement method.³⁸⁸ The significance of this is unclear because fluid displacement is a crude method for assessment of volume.



Figure 1. 23. Image of the Silhouette Mobile™.³⁸⁹ (Retrieved from <http://www.aranzmedical.com>)



Figure 1. 24. Image of the FastScan™.³⁸⁹

2 Objectives

2.1 Aims

The main goal of this thesis was to provide a scientific basis for the various clinical practices used to improve the microcirculation and wound healing in patients with peripheral vascular disease (PVD) by influencing oxygen delivery to peripheral areas of the wound, which is believed to be key to the potential for the wound to heal. This could be achieved by supplemental oxygen, supplying more oxygenated blood to the wound as a result of either chemical or thermal vasodilation, or by drawing blood to the wound by negative pressure. The aspects of clinical practice and adjuncts investigated were high-dose oxygen, Ilomedin, and active warming during IIB surgery, and TNP therapy in diabetic foot wounds.

Because various innovative devices (i.e., OxyVu™, FS, and SM) were used to measure tissue oxygenation and rate of wound volume reduction, the reliability and feasibility of these instruments needed to be determined to be able to explore their potential in the field of research.

2.2 Summary of studies

Four key studies were included:

1. *Validation of OxyVu™: a hyperspectral transcutaneous oxygenation measurement device*

This was an observational study comparing the OxyVu with TCOM, the ABI, and severity of PVD, and assessing their correlations. The intra-operator and inter-operator reliability of the OxyVu were also evaluated. HT-Sat was hypothesised to be the most sensitive marker of tissue oxygenation because it accounts for both oxyhaemoglobin (oxygen delivery) and deoxyhaemoglobin (oxygen consumption).

2. *Effects of peri-operative Warming, Oxygen and Ilomedin (PGI-2) on Oxygenation and Wound Healing in Infrainguinal Bypass Surgery (WOIOW study)*

An RCT of the effects of supplemental oxygen and thermal and chemical vasodilation on tissue oxygenation and wound healing was performed in patients undergoing revascularisation surgery to elucidate the roles of key molecular markers of wound healing, i.e., hydroxyproline, growth factors in the wound healing cascade, and their mRNAs in relation to perturbations of oxygenation and vascular perfusion.

The hypothesis was that perioperative high-dose oxygen (inspired oxygen of 80%), extended warming (2 hours before, during, and 2 hours after surgery), and perioperative Ilomedin would improve tissue oxygenation and wound healing following IIB surgery.

3. *Validation of FastScan™ and Silhouette Mobile™: portable wound volumetric measurement devices*

An observational study was performed in vascular patients with open wounds and ulcers of the lower limb to assess the correlation of FS and SM measurements with those from three-dimensional computed tomography reconstruction, as well as intra-operator and inter-operator reliability.

4. Effects of TNP therapy on tissue oxygenation and wound healing in diabetic foot wounds

A randomised controlled trial comparing TNP therapy with traditional wound dressings was performed in patients with acute diabetic foot wounds to investigate the molecular mechanisms of TNP therapy, focusing on healing rate, change in collagen deposition, the balance between growth factors and inhibitory cytokines, and tissue oxygenation.

The hypotheses were:

- TNP would enhance the rate of healing of acute arterial wounds in terms of wound volume and hydroxyproline levels when compared with traditional dressings. Volumetric reduction was the primary outcome
- TNP would alter the balance of growth factors and cytokines in the wound environment, thereby promoting formation of granulation tissue
- TNP would enhance the dynamics of blood flow around the wound to a greater extent than traditional dressings.

3 Methods

3.1 Validation of OxyVu™

Ethical approval to carry out this study was obtained from the local Northern Y ethics committee (NTY/08/08/082). The study was divided into three stages.

1. Comparing OxyVu™ with TCOM, ABI, and severity of PVD

Healthy volunteers and patients with or without PVD of the lower limbs and admitted to the vascular unit at Waikato Hospital, New Zealand, were recruited. Exclusion criteria included age under 18 years, cellulitis or ulcers on the skin overlying the head of the first metatarsal bone (region of interest in this study), a history of major amputation, lymphoedema of the lower limb, severe dementia, or methicillin-resistant *Staphylococcus aureus*.

Patient demographics, severity of PVD, hyperspectral oxygenation (OxyVu™), T_{cp}O₂ and T_{cp}CO₂ (TCOM3), and ankle-brachial index (ABI) were recorded using hand-held Doppler devices.

The Rutherford classification was used to assess the severity of PVD. As per the TASC II guidelines, category 5 was defined as minor tissue loss, i.e., ischaemic ulceration not exceeding ulceration of the digits of the foot, and category 6 was defined as major tissue loss with severe ischaemic ulcers or frank gangrene.²¹³ The volunteers were asymptomatic and therefore scored zero. To assist with the statistical analyses, Rutherford categories 1, 2, and 3 were grouped into “claudicants” and similarly Rutherford categories 4, 5, and 6 into “critical limb ischaemia” (CLI). For the purposes of the study, this classification was called the Simplified Severity Score (SSS), whereby a scoring system of 0, 1, and 2 was applied, with 0 being “volunteers” (i.e., asymptomatic), 1 being “claudicants”, and 2 being “critical limb ischaemia”.

Hyperspectral oxygenation, T_{cp}O₂, and T_{cp}CO₂ were measured in both lower limbs at a standardised point over the head of the first metatarsal on the plantar aspect. Relative values from the mirror image site on the opposite limb were used to calculate the bilateral perfusion index (BPI) by comparing readings from the diseased limb with those of the contralateral limb, as described by Sheffield *et al* and Fife *et al*.^{273 290} For the purpose of the study, the left limb of the healthy volunteers was considered “diseased”. Due to limited resources at the start of

this research it was not until the second stage of the study that there were two functioning TCOM electrodes to allow simultaneous recordings, thereby reducing the duration of each study session. The additional electrode enabled chest measurements to be recorded to define the regional perfusion index, i.e., the limb-to-chest ratio.

Oxygenation measurements were recorded with each participant lying in a supine position on a flat bed in a room set at a fixed ambient temperature. Detailed operating manuals for the OxyVu, TCOM and ABI are described in sections 3.7.1 to 3.7.3.

TCOM measurements were recorded at 15-minute intervals. There are various guidelines for the use of TCOM. However, no clear recommendations exist regarding the duration needed for the electrode to equilibrate in order to obtain recording values. A sub-study was conducted as part of this thesis for standardisation of the contact time for the electrodes to facilitate interpretation and minimise error (Chapter 10). After studying minute-by-minute TCOM measurements in the 82 limbs, the difference in proportional change of $TcpO_2$ between minutes 14 and 15 was 0.8% and that for $TcpCO_2$ was 2.9%. Therefore, 15 minutes were set as the duration required for the electrode to equilibrate.

The correlations between OxyVu and TCOM, ABI of the diseased limb, and severity of PVD were evaluated.

2. Evaluation of inter-operator variability

OxyVu readings were recorded by two trained operators. Recordings by the two operators were made within a 2-minute period. The operators were blinded to the location of the “target” placed by the other operator, which was set at the head of the first metatarsophalangeal joint. The operators placed the target sticker themselves to imitate clinical settings and eliminate bias. The intraclass correlation coefficient (ICC) was used to determine inter-operator variability. Reliability of a measurement is defined as the ratio of the variance of the “true” values between individuals to the variance of the observed values, which is a combination of the variation between individuals and measurement error.³⁹⁰ The ICC has a range from 0 to 1. The latter indicates complete reliability with no measurement error.

3. *Evaluation of intra-operator variability*

Hyperspectral readings were measured consecutively over 36 minutes at 2-minute intervals for two patients (one patient with PVD and the other with no known PVD). The target sticker and camera were fixed and not moved during the assessment to eliminate operator bias. The within-subject coefficient of variance described by Bland *et al*³⁹¹ was used to define the intra-operator variability.

3.2 Wound healing and oxygenation in IIB surgery

Study design

The hypotheses were tested within an overall framework of a randomised controlled trial. Ethical approval were obtained from the local Northern Y ethics committee (NTY/08/04/032). As shown in Table 3.1, participants were randomly allocated to one of four groups:

- An oxygen group (FiO₂ 80% without extended warming and Ilomedin®)
- An Ilomedin group (FiO₂ 30% with Ilomedin intraoperatively and postoperatively, without extended warming)
- A temperature group (FiO₂ 30% with preoperative and postoperative active systemic warming and without Ilomedin)
- A control group (FiO₂ 30% without extended warming or Ilomedin, i.e., current practice)

GROUP	OXYGEN	ILOMEDIN	TEMPERATURE	CONTROL
FiO₂	80%	30%	30%	30%
Warming (during surgery)	✓	✓	✓	✓
Warming (2 hours before and after surgery)	x	x	✓	x
Ilomedin®	x	✓	x	x

Table 3. 1. Interventions received in each study arm.

Each treatment group was designed to control variables other than the treatment tested in that arm. Randomisation codes were formulated by Statistical Package for the Social Sciences (SPSS) software on a 1:1 basis. Participants were blinded as to their group allocation, although concealment was difficult in the temperature group.

Main outcome

The primary endpoint was wound healing, assessed by incorporation of hydroxyproline (OHP) into embedded implants.

Secondary endpoints included levels of growth factors, including TGF-β, FGF-2, and VEGF, and their mRNA expression in the wound tissue, and tissue oxygenation of the acute surgical wound and foot for up to 30 days postoperatively as measured by OxyVu and TCOM.

Sample size calculation

Goodson and Hunt³⁹ studied 40 ePTFE implants in 30 healthy participants. Accumulation of OHP was found to start as early as 8 hours and to increase slowly over 5 days. After day 5, it increased exponentially. At day 5, there was significant accumulation of OHP and the standard deviation was the smallest (0.30 ± 0.08 µg OHP per cm tubing) at this time when compared with day 7 and beyond.

A minimum of 100 patients was required, with 25 participants in each group, to detect a mean increase of 0.075 µg OHP per cm tubing on day 5 in each treatment group when compared with controls, with a power of 90% and a significance level of 5%. A 25% absolute increment in OHP content was deemed to be clinically significant. In 2007, the throughput of eligible patients in the unit where this research was conducted was around 70 per year. Assuming a 60% recruitment rate, a recruitment period of 24 months was allocated.

Patient selection and exclusion criteria

Patients undergoing IIB surgery at Waikato Hospital were considered. Patients were excluded if they had untreated critically stenotic lesions proximally, chronic obstructive pulmonary disease with retention of carbon dioxide, a history of previous exposure to bleomycin, use of Ilomedin, corticosteroids, or immunosuppressants in the 4 weeks prior to surgery, sensitivity to Ilomedin, or a history of methicillin-resistant *S. aureus*.

Preoperative period

The necessary information regarding the study was provided to the surgical team, anaesthetic team, and the nursing staff caring for the patients to ensure that the study protocol was adhered to and to assure quality control. Relevant demographic information was collected, including age, comorbidities, severity of PVD, pre-existing infections, cardiovascular risk factors, ABI, body mass index, and drug history, in particular use of steroids and any recent Ilomedin administration.

The number of patent crural vessels, or “run-offs”, was determined using preoperative imaging either in the form of digital subtraction arteriography (DSA), magnetic resonance angiography (MRA), computed tomographic angiography (CTA), or arterial duplex scan. In settings where more than one modality of imaging was available, the most accepted imaging method was

used. This was in the specific order listed above, with DSA set as the gold standard and duplex being the least reliable. The score was out of 3, i.e., 1 per crural vessel. A score of 1 was defined as a patent vessel without critical stenosis; 0.5 as a vessel with one or more critical stenoses; and zero as a vessel with any length of chronic total occlusion regardless of the length or presence of collateral flow. Rutherford's recommended "run-off" weighting was not applied because it was difficult to assess the exact degree of stenosis or length of occlusion.³⁹²

Each patient was randomly allocated to one of four groups. Randomisation were generated electronically. The results were placed in an envelope and sealed by a person not connected with the study. The envelope was opened by the anaesthetist at least 2 hours prior to induction of anaesthesia.

HTCOM, TCOM and ABI were recorded at least 2 hours prior to surgery as described in sections 3.7.1 to 3.7.3. The locations of the lower limb measurements were standardised at the medial aspect of the knee where the distal skin incision would lie and the plantar foot over the head of the first metatarsal. The BPI was the ratio between oxygenation of the "diseased" foot (the side of the surgical bypass) and the contralateral foot.

A forced-air warming device (Bair Hugger®) was used to cover the body from the neck to the toes on each patient in the temperature group and set at 38°C ("medium") 2 hours prior to induction of anaesthesia. Core temperature was monitored using a tympanic thermometer every 30 minutes in this group.

Perioperative period

Anaesthesia was induced in the manner preferred by the anaesthetist. Corticosteroids were not administered. Chlorhexidine and alcohol (Chloraprep®) were used as skin preparation in all patients, along with a standard protocol for antibiotic prophylaxis at induction. The antibiotic prophylaxis was to continue for 24 hours (1g cefazolin intravenously or erythromycin if contraindicated). Surgery was performed in the manner preferred by the surgeon.

A Bair Hugger® set at 38°C was placed on all participants intraoperatively irrespective of the allocation group from the neck to the level of the umbilicus and including both upper limbs, unless arm veins were to be harvested. The theatre environment was standardised by a room temperature set at 21°C and warmed intravenous fluids. FiO₂ was set at 30% or 80% as

determined by randomisation and maintained throughout surgery after induction of anaesthesia.

For patients in the Ilomedin group, 50 µg of Ilomedin was prepared with 250 mL of normal saline; 3,000 ng of Ilomedin in 15 mL of the mixture was slowly infused intra-arterially into the bypass graft intraoperatively using an 18 gauge cannula once the anastomoses of the graft were completed. The remaining Ilomedin was infused intravenously, starting immediately postoperatively whilst in recovery, at a rate of 10–40 mL per hour as tolerated for 6 hours according to the unit's protocol (Appendix A.5). If the core temperature exceeded 38°C during surgery, the temperature of the Bair Hugger® could be turned down.

Prior to skin closure, an ePTFE tube (Maquet™, Hudson, NH, USA) 5 cm in length, 2 mm in diameter, 1 mm in thickness, and a pore size of 60 µm, as well as a 1 cm³ cubed-shaped viscose cellular sponge were implanted subcutaneously parallel to the wound incision with the proximal end flush with the skin (Figure 3.1). The location was standardised at the incision close to the knee. A 3/0 nylon suture was placed at one end of the implant to act as a marker and to aid removal at a later stage. Another 3/0 nylon stitch was secured to cover the end of the ePTFE tube with the surrounding skin to minimise the risk of infection.

Intraoperatively, the anaesthetist provided appropriate inspired concentrations of oxygen under general anaesthesia. Changes in FiO₂ were allowed at completion of the operation when the anaesthetic was reversed. During the first 2 hours postoperatively, FiO₂ was maintained at 30% or 80% according to the randomisation protocol.

Postoperatively, or if regional anaesthesia was used, a high-concentration non-rebreather oxygen mask (Salter Labs, Arvin, CA, USA) at a total flow rate of 16 L/min was used with a Bird® oxygen blender (BD, Franklin Lakes, NJ, USA) to provide the desired oxygen concentration. After 2 hours, all patients could breathe room air or supplemental oxygen as required to maintain oxygen saturation above 92%.

Core temperatures were monitored before, immediately after, and at 30-minute intervals following surgery for 2 hours using a tympanic thermometer. Intraoperative temperatures were also recorded at 30-minute intervals while the patient was anaesthetised using a nasopharyngeal temperature probe that allowed continuous monitoring. Each patient in the

temperature group had a Bair Hugger® placed over the entire body and set at 38°C for 2 hours postoperatively.

The estimated blood loss, duration of surgery, and V-POSSUM (Vascular-Physiological and Operative Severity Score for the enUmeration of Mortality and morbidity) score were recorded. Fluids and pain management were prescribed at the discretion of the anaesthetist. V-POSSUM estimates patient morbidity and is a predictor of mortality. The physiological score and operative score were recorded prospectively by the anaesthetists intraoperatively. A summary of the scores is shown in Appendix A.1.3. (Figure 9.2 and 9.3)

Significant oxygen toxicity may occur after 12 hours of FiO₂ at 100%, 24 hours at 80%, and 36 hours at 60%.³⁹³ Patients undergoing operations lasting more than 10 hours were excluded from the study, and those requiring intraoperative changes in FiO₂ to maintain oxygen saturation that deviated from the study protocol by greater than 10% were also excluded.

Postoperative management




		
<p>Graft implanted subcutaneously along the wound with the end flushed to the skin. A 3/0 nylon suture is used to close the skin over the implant.</p>	<p>On day 5, the nylon suture is cut, the skin released, and the proximal end of the graft with the “marker” nylon suture exposed to aid its extraction.</p>	<p>The ePTFE tube is extracted with care under sterile technique and local anaesthesia. The implants were placed in a sterile pot and stored in -80°C.</p>

Figure 3. 1. Illustration of implanting and explanting the expanded polytetrafluoroethylene tubing from the surgical wound.

Using sterile technique under local anaesthesia with EMLA® 5% cream (lignocaine and prilocaine; AstraZeneca, Cambridge, UK), the embedded implants were harvested on day 5. The nylon suture was cut to expose the end of the expanded PTFE tube. The implants were extracted by applying gentle pressure on the nylon suture acting as a “marker”. These were then transferred to a sterile pot, and immediately stored below -80°C in the laboratory at Waikato Hospital. The open wound was closed with 3/0 nylon, and this suture was removed

at the day 14 wound assessment visit. Day 5 was chosen for harvesting the embedded implants to balance the risk of wound complications or graft infections and the benefit of accumulating more OHP.

Analysis of OHP (expressed in $\mu\text{g}/\text{cm}$ of tubing) was carried out for a 4.0 cm segment of the 5 cm expanded PTFE implants. The granulation tissue in the remaining 1.0 cm was used to quantify mRNA expression of relevant growth factors by polymerase chain reaction (PCR).³⁹⁴ To ensure reproducibility and consistent quantification, the PTFE tubes were cut 4 cm from the start from the suture marker end in a standardised manner. Wound fluid from the viscose sponge was analysed for growth factors.³⁹⁵ The methods used for these analyses are described in sections 3.6.1 to 3.6.3.

Tissue oxygenation was measured using OxyVu on days 1 and 3 postoperatively. Transcutaneous oxygenation at the incision site on the knee was measured at six areas surrounding the site of the ePTFE implant. Two of the “targets” were placed anteriorly, two posteriorly, one superiorly, and another inferiorly (Figure 3.2). The average of these measurements was used for the analyses. A complete scan using OxyVu, TCOM3 oxygenation measurement, and calculation of ABI were performed on days 5, 14, and 30 in the follow-up clinic.

Postoperative management was provided in the usual fashion without prejudice for participation. Surgical wounds were assessed for complications during hospitalisation. Patients were followed up on days 14 and 30 by the author and beyond at the discretion of the clinical team. The duration of participation in this study was 30 days postoperatively. Bypass vein grafts were routinely surveyed at 6-monthly intervals for 2 years. Clinical notes were retrospectively reviewed in June 2013. Graft blockage, failure, re-interventions, limb loss, and deaths were recorded.



Figure 3. 2. Location of the expanded polytetrafluoroethylene implant along surgical wound (red) and sites where oxygenation was measured using OxyVu™ (blue).

3.3 Validation of FastScan™ and Silhouette Mobile™

This study was approved by the local Northern Y ethics committee (NTY/09/08/080).

A pilot study was conducted in vascular patients with wounds or ulcers of the lower limbs. Wound dimensions were measured using the FS and SM, and the readings were compared with those obtained by three-dimensional CT reconstruction, which was assumed to be the gold standard. Patients with wounds or ulcers were recruited irrespective of aetiology from the ward and from the outpatient diabetic foot clinic. Patients with known methicillin-resistant *S. aureus* were excluded.

Consented participants underwent a targeted CT scan of the lower limb focussing around the region of the ulcer(s) or wound(s). Wound dressings were removed, and the wound was then cleaned and covered in transparent cling-film. The cling-film technique was adopted because packing and wound dressings would have disrupted the wound-surface interface on CT imaging. The film also protects such wounds and prevents desiccation as a result of prolonged exposure to air.

Immediately following CT, the wounds were scanned using the laser devices. The relevant protocols are found in sections 3.7.4 and 3.7.5. Each wound was scanned by three different operators using the FS and SM. Each operator scanned the same wound three times. Surface area, maximum depth, and volume measurements were obtained from the FS and SM images. These were compared with similar measurements obtained from CT images using three-dimensional reconstruction software (Siemens) by a single operator. The same single operator measured the dimensions of each wound three times, and the average values were used for analyses. Details on the application of the reconstruction software can be found in Section 3.7.6. The maximum depth was chosen to be the comparative measure rather than the “average depth”. Three depth measurements were taken per reading, and were averaged to give one maximum depth figure. No wounds were debrided significantly during the scanning process.

3.4 Wound healing and tissue oxygenation in TNP therapy

Study design

Ethical approval was secured from the Northern Y ethics committee (NTY/08/11/104).

The inclusion criterion was an acute surgical wound of the lower extremity:

- Following surgical debridement or minor amputation (defined as any amputation below the level of the ankle joint)
- With an adequate blood supply and not requiring a further revascularisation procedure
- Deemed suitable for TNP therapy.

Exclusion criteria were:

- Treatment with corticosteroids, immunosuppressive drugs, chemotherapy, TNP therapy, hyperbaric medicine, growth factors, or other bioengineered tissue products in the previous 30 days
- An acute wound with signs of infection or osteomyelitis, or necrotic tissue that would not be suitable for TNP therapy
- Known ankle pressure <50 mmHg or toe pressure <30 mmHg
- Being unsuitable for the trial in the opinion of the operating surgeon.

Consented patients were randomly allocated to a treatment group (to receive TNP as per routine practice) or to a control group (to receive regular modern topical dressings). Randomisation codes were formulated by SPSS software on a 1:1 basis. Neither the author nor the patients were blinded; however, the outcomes were objectively measured.

Main outcomes

The primary endpoint was volumetric assessment of the wound at 2 weeks using FS. Secondary endpoints included biochemical analyses of OHP levels, growth factors, including TGF- β , FGF-2 and VEGF, and inhibitory cytokines such as tumor necrosis factor alpha (TNF- α) and interleukin (IL)-8, at baseline and on day 14. Tissue oxygenation surrounding the wound as measured by OxyVu was compared between baseline and day 14. Limb loss rates were recorded at 3 months.

Sample size calculation

A minimum of 64 patients was required (n=32 in each group) to be able to detect more rapid wound healing in the TNP group at 2 weeks with an absolute mean difference of 20% in wound volume when compared with the control group.³⁷⁴ This was set at 80% power and a significance level of 5%. Patient recruitment was planned to last for 18 months.

Protocol

On day 0, relevant demographic information was collected, including age, comorbidities, cardiovascular risk factors, ABI, body mass index, and drug history, in particular use of steroids.

The wound was presented within 48 hours of surgical debridement and cleaned appropriately to prepare for dressing application as per routine management. Light debridement over the wound surface was permitted to remove debris or slough if necessary. Dimensions of the ulcer was measured using FS at baseline as per Section 3.7.4. Three punch needle biopsies were extracted from the centre of the wound using a 3 mm punch needle under aseptic technique. "Urogel" containing lignocaine was applied topically if required. Tissue samples were placed in a sterile test tube and placed in a freezer at -80°C for analysis of OHP. Two tissue oxygenation measurements were obtained (one from each end of the wound) using OxyVu as described in Section 3.7.1. TCOM was not used because it would have added an additional 45 minutes to the assessment and aired the wound unnecessarily.

In the treatment group, TNP was applied in the usual fashion by ward nurses. The settings were set at continuous suction (-125 mmHg) for the first 24 hours and for intermittent suction thereafter. In the control group, modern traditional dressings were applied: typically topical hydrofibre or hydrogel dressings guided by the condition of the wound. Dressings were changed every 48 hours in each group unless advised by the surgeon or the wound care nurse specialists.

On day 2, the entire wound dressing or foam sponge was extracted. No fluids (e.g., local anaesthetics or saline) were infiltrated into the dressing. A section of the dressing or foam that was in direct contact near the centre of the wound bed was sampled. The sample was inserted into a test tube and then placed into a centrifuge to be spun at 4,000 rpm for 10 minutes at

4°C to drain the wound fluid. The fluid was pipetted across to a sterile test tube and snap-frozen at –80°C for measurement of growth factors and cytokines.

This was an intention-to-treat study. TNP was switched to traditional dressings before day 14 if the surgeon could no longer justify its use clinically, such as when the wound was filled with significant granulation tissue, to imitate “real-world” clinical decision-making. Patients were allowed to be discharged prior to day 14 with wound dressings changed by district nurses or the ward nurses if an arrangement was made. Patients were excluded if the study protocol was violated or if the wound required significant debridement or failed to progress during the study period. Participants were required to attend the wound assessment clinic on day 14 to complete the study. Delayed skin closure with split skin grafts to the acute wound was not a common practice in the unit.

On day 14, wound dimension measurements were repeated using FS. Wound fluid was extracted from the wound dressings. Three punch needle biopsies at the centre of the wound bed were taken for assessment of OHP. Tissue oxygenation measurements around the wound were recorded.

Patients were either reviewed in the outpatient clinic at 12 months or were followed up by telephone to record the progress of the wound.

Biochemical analyses were conducted as per sections 3.6.1 to 3.6.3. Each wound imaging using FS was repeated three times and the mean values were used for analyses. Wound dimensions were quantified using the Delta software. Measurable outcomes included: wound “body” surface area (area of the wound surface); wound “cap” surface area (area of the wound defect at the skin surface); maximum depth; mean depth; and volume.

3.5 Statistical methods

Data were collected in Excel®. Statistical analyses were performed using SPSS version 22 software (IBM Corporation, Armonk, NY, USA). A type I error of 5% ($P \leq 0.05$, two-tailed) was considered to be statistically significant.

Descriptive statistics were described in terms of the range, mean or median and standard deviation. Kurtosis and skewness were evaluated for continuous variables. The coefficient of kurtosis measures the spread of values. For a normal distribution, the coefficient of kurtosis would be less than 3. If the distribution is more spread out, the coefficient would be greater than 3.³⁹⁰ For a symmetrical distribution, the coefficient of skewness would be zero; positive values correspond to a right-skewed distribution and vice versa.

When comparing the means of two groups of continuous variables, parametric analysis (the Student's *t*-test) was used assuming the data followed a normal distribution. Bonferroni correction was applied in the WOLOW study where there were multiple "hypotheses" with three comparison groups (i.e., three treatment arms and one control). In the setting of comparing means for discrete variables, Chi-squared and Fisher's Exact tests were applied depending on the size of the sample. Analysis of variance (two-way repeated measures) or the Kruskal-Wallis test was used to compare the means of more than two groups. The latter was used in the WOLOW study to test for any potentially significant difference in basic demographics between the groups.

Pearson's and Spearman's correlation tests were used to test for an association between variables depending on whether they were continuous or ordinal-scale (ranked; such as the severity of PVD using the SSS scale in the Validation of OxyVu study).

A logistic regression model was used to perform multivariate analysis and to detect confounding factors. The regression model was also used to determine the gradient of change in core temperature for patients in the "temperature" group in the WOLOW study.

Kaplan-Meier plots were used for the survival analyses, such as for graft patency, limb survival and patient survival.

Random systematic errors in assessing the reliability of the devices were expressed as a ratio of total variance to calculate the intraclass correlation coefficients (ICCs). These coefficients

determine how strongly repeated measurements relate to each other.³⁹⁶ ICCs and the Bland-Altman test were used to assess inter-operator and intra-operator variability. The within-subject coefficient of variation defined the intra-operator reliability in the Validation of OxyVu study.

A single ICC would indicate the reliability of one operator, whereas the average ICC would indicate the reliability when recordings were made by two or more operators (or attempts). The latter would be a higher value and hence more “reliable”.

Inter-operator variability could be the result of errors on the part of the instrument (e.g., OxyVu) or the operator. Systematic bias is a tendency to overestimate or underestimate the “true value”. By studying the mean difference in OxyVu measurements between the two operators (A and B), such bias could be detected.

A receiver operating characteristic (ROC) curve was used as part of the Validation of OxyVu study described in Appendix 6.4 to determine the sensitivity and specificity of using HT-Sum to diagnose anaemia.

Power and sample size calculation was evaluated using an interactive software program designed by Dupont and Plummer (PS: Power and Sample Size Calculation). The program can be downloaded from:

<http://biostat.mc.vanderbilt.edu/wiki/Main/PowerSampleSize>

3.6 Laboratory investigations

3.6.1 Hydroxyproline assays

These assays were completed under the supervision of Dr Christina Buchanan, a post-doctoral research fellow in the Department of Molecular Medicine and Pathology at the University of Auckland, who has previous experience in OHP assays. The protocol used is described below; it was based on key OHP studies by Chiariello *et al* and Jorgensen *et al*,^{14, 397} and was validated in a further study at the University of Auckland recently published by Dr Buchanan.³⁹⁸

Protocol

1. All tissue samples were placed in a plain test tube and snap-frozen at -70°C to -80°C as soon as they were harvested from the study participants. The samples were placed in a freezer in the clinical laboratory at Waikato Hospital.
2. The test tubes were thawed on the day of analysis.
3. The dimensions of the samples were quantified. For those in the ePTFE tube, the length of the tube was measured. For the tissue biopsy samples, the dried weight of the tissues was measured.
4. Each sample was placed in a 100 mm length borosilicate Kimax®-capped culture tube (the tissues could be spliced into smaller pieces).
5. The tissues were hydrolysed with 1 mL of 6 M hydrochloric acid; the culture tubes were placed in an oven set at 105°C overnight (for at least 16 hours), ensuring that the tubes were well-secured with the cap (Figure 3.3)
6. Each solute containing the OHP was carefully pipetted out in a fume hood into a 1 mL microtube without a cap
7. The microtubes were placed in the SpeedVac® which dried the solvent at 40°C under constant sub-atmospheric pressure. (Figure 3.4)
8. The solvent containing the OHP was completely crystallised. This process could take up to 24 hours depending on the number of samples placed in the SpeedVac.

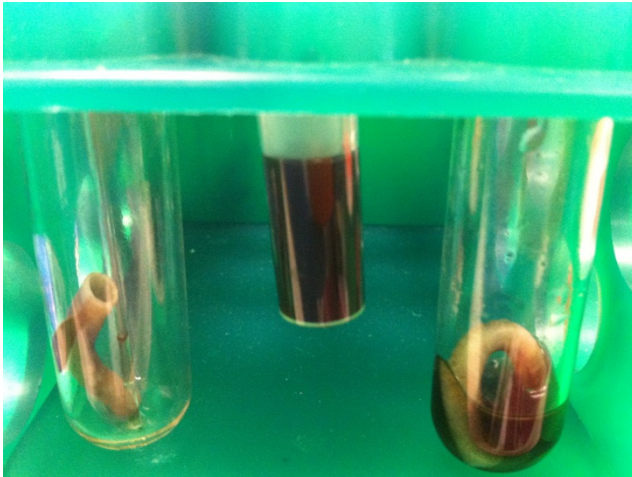


Figure 3. 3. Expanded polytetrafluoroethylene tube hydrolysed in 6 M hydrochloric acid (right), hydroxyproline solute in microtube (centre), and expanded polytetrafluoroethylene tube following hydrolysis (left).



Figure 3. 4. Photograph of the SpeedVac®.

9. The crystals were dissolved into 1 mL of sterile Milli-Q™ water.
 10. This was then neutralised with 45 μ L of 5 M sodium hydroxide and the pH was adjusted to around 6.
 11. 1 mL of isopropanol (isopropyl alcohol [IPA]) was added.
 12. The microtube was centrifuged at 2,000 rpm for 5 minutes.
 13. Various reagents were prepared:
 - a. Acetate/citrate buffer in IPA
- Mix 200 mL of Milli-Q water with the following:

- i. 0.7 M of sodium acetate (molecular weight 82) – 11.48 g
 - ii. 0.2 M of trisodium citrate (molecular weight 294) – 11.76 g
 - iii. 0.045 M citric acid (molecular weight 210) – 1.89 g
 - iv. Dilute six parts of the above solution to four parts of IPA before use.
 - b. Chloramine T (oxidative agent for OHP)
Prepare 300 mM in 10 mL of acetate/citrate buffer in IPA (molecular weight 228) – 0.684 g of salt
 - c. Ehrlich's reagent (stains the oxidised OHP compound)
Prepare 3.5 M in 100 mL of 72% perchloric acid (molecular weight 149.19) – 5.22 g.
Store solution in the dark and wrap the storage tube in aluminium foil.
Dilute one part of the above solution in four parts of IPA before use.
Store in the dark as above.
 - d. Half-strength IPA
Add one part of IPA to one part of Milli-Q water.
14. The standards were prepared:
 - a. Formulate 100 µg/mL of OHP.
 - i. 0.00965 g of pure OHP in 1 mL of Milli-Q water (9,650 µg/mL).
 - ii. Mix 10 µL of the pure OHP solution in 955 µL of half-strength IPA.
 - b. 1:1 serial dilution
 - i. 100 µg/mL → 50 → 25 → 12.5 → 6.25 → 3.125 → 1.56 → 0.78 → blank.
15. 120 µL of tissue sample were taken from step 12 into a new 1 mL microtube for OHP assay.
16. 280 µL of acetate/citrate/IPA buffer was added.
17. 100 µL of chloramine T was added.
18. Microtubes were incubated for 5 minutes at room temperature to allow OHP to oxidise.
19. 1.3 mL of Ehrlich's reagent were added into each microtube.
20. Microtubes were placed in a hot water bath set at 60°C for 30 minutes.
21. The tubes were cooled for 5 minutes.
22. The content of OHP (µg/mL) was quantified using spectrometry to measure absorbance at 558 nm. This was performed in bulk using a 96-microwell plate with 100 µL of the sample solution from step 21 (Figure 3.5). Spectrometric analyses should not be delayed as Ehrlich's reagent continues to react over time.

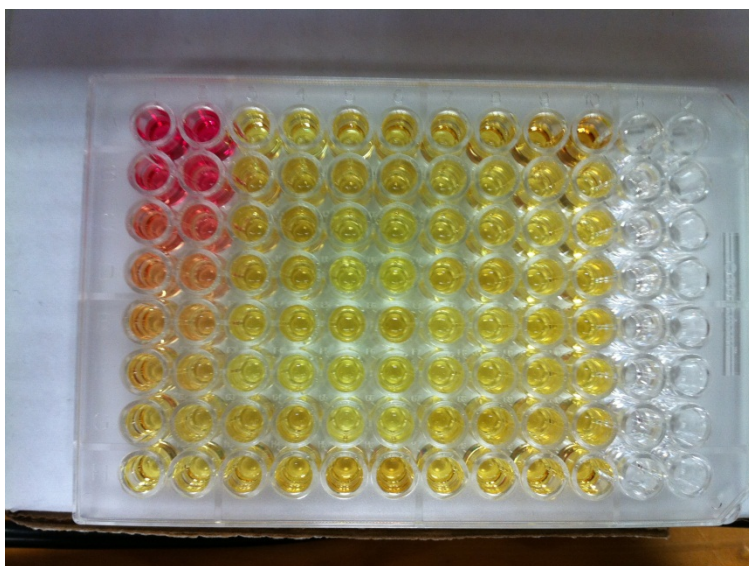


Figure 3. 5. Example of the 96-microwell plate containing standards and samples prior to spectrometry.

23. A standard curve was generated using the readings from standards.
24. OHP levels ($\mu\text{g/mL}$) were interpreted using the gradient of the standard curve ($y=mx + c$) multiplied by the volume of sample (mL) per well.
25. Measurements were divided by weight (or length of tubing) to obtain absolute OHP levels per weight or cm of tubing. To determine the amount of collagen, OHP levels were multiplied by 7.46 because collagen consisted of approximately 13.4% OHP.³⁹⁹

3.6.2 Analysis of growth factors and cytokines

This section was conducted at the Auckland Cancer Society Research Centre at the Grafton Campus, University of Auckland, under the supervision of Dr Sofian Tijono.

Preparation of wound fluid sample (WOIOW study)

1. Wound fluid saturated in a 1 cm³ PVA sponge was stored in a 1.7 cm³ sterile microtube when harvested from patients.
2. Samples were snap-frozen in a freezer at –80°C.
3. Prior to thawing on the day of analysis, the tip of each microtube was carefully cut, producing a small opening at the tip.
4. Once thawed, each microtube was placed in the neck of a narrow 5 cm³ plastic test tube.
5. Each microtube with a plastic test tube sitting in situ was centrifuged at 4,000 rpm and 4°C for 10 minutes.
6. Microtubes with a desaturated sponge were discarded.
7. Wound fluid drained into the 5 cm³ plastic test tube was pipetted into a new microtube.
8. Re-freezing wound fluid was avoided, with the analysis performed on the same day. Multiple freeze/thaw cycles could have impaired the quality of the sample.

Preparation of wound fluid sample (TNP study)

1. A section of the wound dressing or foam was sampled from the patient during their “dressing change” in the ward.
2. This dressing sample was placed into a 5 mL sterile capped plastic pot.
3. This pot was placed into a specially designed 20 mL test tube. The cap of the tube was modified to snugly fit the pot and secured by the cap of the pot.
4. This combination device was centrifuged at 4,000 rpm and 4°C for 10 minutes.
5. The wound fluid drained into the plastic test tube was pipetted into a new microtube.
6. This was then snap-frozen at –80°C.

Analysis of TGF- β 1

An enzyme-linked immunosorbent assay (ELISA) technique was used for quantitative detection of human TGF- β 1. A detailed protocol is provided in the analysis kit for eBioscience® Platinum ELISA. The principles of ELISA were as follows:

- TGF- β 1 in the wound fluid was bound to the anti-TGF β 1 coating antibodies adsorbed to the microwells.
- Biotin-conjugated anti-TGF β 1 antibody was added to bind to the human TGF- β 1 captured by the first antibody. Unbound biotin-conjugated anti-TGF β 1 was washed out.
- Streptavidin-horseradish peroxidase was added to bind to the biotin-conjugated anti-TGF β 1 antibody. Unbound streptavidin-horseradish peroxidase was washed out.
- A substrate solution reactive with horseradish peroxidase (tetramethyl-benzidine) was added. A coloured product was formed in proportion to the amount of human TGF- β 1 in the sample. The reaction was terminated by addition of 1 M phosphoric acid.
- Absorbance was measured at 450 nm using spectrometric analysis. The concentration of TGF- β 1 in each sample was determined from the standard curve prepared from seven standard dilutions.

Analyses of VEGF, FGF-2, IL-8 and TNF- α

Milliplex® is based on Luminex® technology that performs bioassays on the surface of fluorescent-coded beads known as microspheres. When an analyte is captured by the bead, a biotinylated detection antibody is introduced. The reaction mixture is then incubated with streptavidin-phycoerythrin conjugate, the reporter molecule, to complete the reaction on the surface of each microsphere. The microspheres are allowed to pass rapidly through a laser which excites the internal dyes marking the microsphere set. A second laser excites phycoerythrin, the fluorescent dye on the reporter molecule. Finally, digital signal processors identify each individual microsphere and quantifies the result of the bioassays based on fluorescent reporter signals.

The ability to add multiple conjugated beads to each sample enabled multiplexing of many types of bioassay from a single sample of 25 μ L, which is critical in studies with a small sample volume. Unfortunately, TGF- β 1 is not available in Milliplex® so was performed using the traditional ELISA technique. The immunoassay procedure was followed as per the protocol produced by Millipore®.

3.6.3 Analysis of growth factor mRNA

This was conducted in the Department of Molecular Genetics at the University of Waikato under the supervision of Dr Ray Cursons. There was an option to process the tissues using development kits produced by various companies. However, it was more cost-effective to analyse the samples using conventional methods. In addition, this would allow better preservation of DNA quality and thus more accurate results.

Isolation of RNA from tissue

1. 1 cm of the ePTFE tube was cut when the implant was harvested from the patient.
2. This was then placed in a 1 cm³ microtube soaked with 0.5 mL of RNA Later® to cover the ePTFE tube.
3. The sample was snap-frozen at -80°C.
4. On the day of analysis, tissue samples were thawed from the freezer.
5. The RNA Later was pipetted out of the microtube.
6. 500 µL of 5 M guanidine thiocyanate (GITC) was added to the microtube and left overnight. Tissue were flushed out of the tube with the GITC. Tissue was homogenised if needed. GITC is a strong denaturant and inhibits RNase. This provides a purer sample in aqueous form.
7. 50 µL (1/10 of volume) of 2 M sodium acetate at pH 4.0 was added and shaken gently. This made the RNA soluble and separated it from DNA.
8. 500 µL of phenol at pH 4.3 was added and shaken gently. Cell membranes were destroyed and dissolved.
9. The microtube was placed in a rotator wheel for 5 minutes.
10. 200 µL of chloroform was then added, and the debris precipitated in the interface.
11. The microtube was placed on ice and then centrifuged at 4°C for 10 minutes.
12. The top aqueous layer containing the GITC was extracted. Total RNA was dissolved in GITC.
13. Steps 8–12 were repeated to further purify the total RNA.
14. 500 µL (1 mL/mL) of IPA was added to precipitate the tRNA.
15. The microtube was placed in a freezer at -20°C for one hour to intensify the precipitation process.
16. The microtube was centrifuged at 4°C for 20 minutes.
17. The IPA was gently tipped out, leaving behind the precipitated RNA.

18. 1 mL of 70% ethanol was added to dissolve the precipitated RNA.
19. The microtube was centrifuged at 4°C for 5 minutes.
20. The ethanol was tipped out to remove unwanted salts.
21. The microtube was centrifuged at 4°C for 10 seconds.
22. The remaining ethanol was pipetted out. RNA pellets were sometimes visible at this stage.
23. Ethanol was left to dry in a fume cupboard for about 15 minutes.
24. 15 µL of TRIS manganese and 1 µL of DNase were added.
 - TRIS acted as a buffer and made the RNA sensitive.
 - DNase broke down the DNA.
25. The microtube was placed in a vortex machine and spun rapidly for 10 seconds.
26. The microtube was placed on a ThermoMixer™ set at 800 rpm for 30 minutes at 37°C.
27. 1.5 µL of DNase stop solution was added.
28. The microtube was placed in a vortex machine and spun rapidly for 10 seconds.
29. The microtube was placed on a ThermoMixer at 65°C set at 800 rpm for 10 minutes.
30. 2 µL of the sample was used for Nanodrop® spectrometry. (Figure 3.6)
 - Nanodrop was used to test the purity and concentration of the mRNA sample. Absorbance 260/280 (a_{260/280}) should be more than >1.6.
 - More than 1 µg of mRNA was required for production of cDNA.

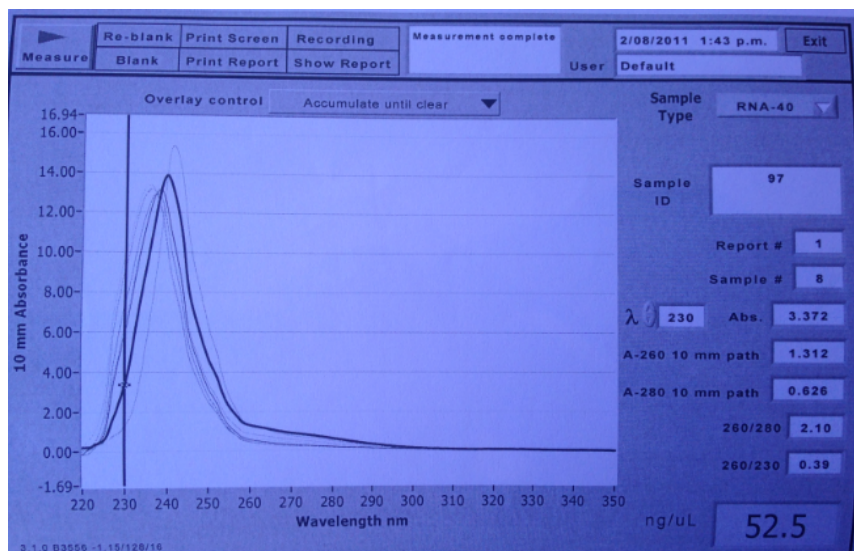


Figure 3. 6. An example of a Nanodrop® report for an RNA sample from one of the study participants.

Production of cDNA from mRNA

1. MasterMix A and B were prepared.
 - a. MasterMix A:
 - “n” μL of total RNA (to make approximately 1 μg of RNA)
 - 1 μL of oligo DDT (16 Ts)
 - Treated H_2O to make up 10 μL
 - b. MasterMix B:
 - 4 μL of 5 \times buffer (37°C)
 - 1 μL of reverse transcriptase (RT)
 - 1 μL DTT (catalyst for RT)
 - 1 μL 10 mM dNTPs (substrates)
 - Treated H_2O to make up 10 μL
 - In total RNA, only 5% is mRNA; 12% is transfer RNA and 80% is ribosomal RNA. mRNA has a specific marker at 3' that has 30 AAAAA. Therefore, oligo DDT acts as an mRNA primer that targets mRNA.
2. In an ultraviolet light box, Mastermix A was added into a microtube. This was shaken and flushed several times.
3. The sample was incubated in the DNA Engine at 70°C for 5 minutes.
4. The sample was then cooled on ice for 10 minutes.
5. Mastermix B was added to the microtube. This was shaken and flushed several times.
6. The sample was incubated in the DNA Engine at 50°C for 60 minutes.
7. The sample was incubated in the DNA Engine at 85°C for 10 minutes.

Preparation of primers

1. “n” μL of TE was added to the primer powder. “n” was defined as $10\times$ the concentration of primer powder (nmoles). The sequences are described in Table 3.2.
2. This was then diluted with TE by 1/10 (i.e., 10 μL of primer and 90 μL of TE).

GENE	PRIMER SEQUENCE
TGFB_F	5'-GCA GAA GTT GGC ATG GTA GC-3'
TGFB_R	5'-CCC TGG ACA CCA ACT ATT GC-3'
VEGF_F	5'-GCT ACT GCC ATC CAA TCG AG-3'
VEGF_R	5'-GGT GAG GTT TGA TCC GCA TA-3'
FGF-2_F	5'-CCT CTT CCT GCG CAT CCA C-3'
FGF-2_R	5'-CCT TCA TAG CCA GGT AAC GG-3'
TBP_F (house-keeping gene)	5'-GTT CTG AAT AGG CTG TGG GG-3'
TBP_R	5'-ACA ACA GCC TGC CAC CTT AC-3'

Table 3. 2. Code for relevant primers.

RT-PCR procedure

1. 20 μL of PCR Mastermix, 0.1 μL Taq™ Hot Firepol™ polymerase, 0.5 μL of forward primer and 0.5 μL of reverse primer were added to 1 μL of cDNA (20 μL reaction).
2. This was then shaken well and placed in a vortex for 10 seconds.
3. The mixture was placed in a DNA engine to commence PCR.
 - a. 95°C for 3 minutes (to denature or unravel cDNA)
 - b. 95°C for 20 seconds
 - c. 55°C for 20 seconds (for primers to attach onto genes)
 - d. 72°C for 30 seconds [for Hot FirePol polymerase to optimize productivity (thermophilic)]
 - e. The above three steps were repeated for 39 cycles.
 - f. The mixture was kept at 68°C for 5 minutes (to extend remaining cDNA).
4. 50 mL of 2% agarose gel was prepared by heating 1 g of agarose to 50 mL of Tris acetate EDTA; 2% is optimum for target DNA around 100–200 kb.

5. 3 μL of ethidium bromide was added to the gel solution. Ethidium bromide binds to “minor grooves” of DNA and reacts to ultraviolet light to enable reading.
6. The gel solution was poured onto a plate and allowed to settle for 30 minutes.
7. 10 μL of cDNA mix was mixed with 2 μL of blue dye.
8. 10 μL was pipetted into a well on the gel plate.
9. 6 μL of 100 bp DNA ladder was added into each row of the well. This would derive the unit of measurement.
10. Electrophoresis was commenced at 100 V for 30 minutes.
11. The gel was read on an ultraviolet light box and a photograph was taken (Figure 3.7).

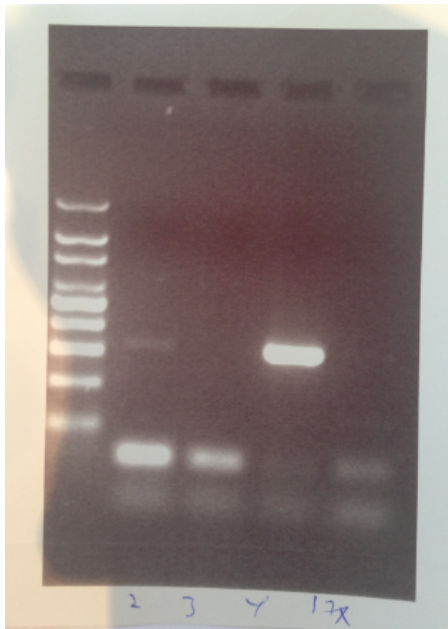


Figure 3. 7. An example of gel electrophoresis following reverse-transcriptase polymerase chain reaction of a sample from four of the study participants.

Quantitative PCR procedure

1. All wells on a 32-well PCR plate were labelled.
2. 1 μL of cDNA, 20 μL of PCR Mastermix, 0.1 μL of Taq Hot Firepol polymerase, 0.5 μL of forward primer and 0.5 μL of reverse primer were added into each well.
3. The plate was placed into the quantitative PCR machine for analysis.
4. Interpret result to quantify cDNA levels.

3.7 Operating devices

3.7.1 OxyVu™

1. Subjects were imaged lying supine on a standard flat examination bed.
2. They were requested to rest and become acclimatised on the bed for 15 minutes prior to measurements in a small quiet room with room temperature set at 20°C–23°C using air conditioning.
3. A target (plastic sticker) was placed near the centre of the imager's region of interest (e.g., a foot)
4. OxyVu was turned on and set at the appropriate settings and labels.
5. To normalise and correct for spectral variation in illumination intensity and collector sensitivity, the hyperspectral imager was calibrated to a well-characterised highly and diffusely reflecting standard known as a "Check Pad" prior to imaging each new subject.
6. Subjects were required to lie still during the 15 seconds of hypercube acquisition to prevent movement. For each measurement site, OxyVu would collect two hypercubes corresponding to either background or LED-illuminated conditions. The spectral separator was tuned to 15 equally spaced wavelengths between 500 nm and 660 nm, while the camera measured the tissue reflectance to determine the absorbance of the tissues. The LEDs were switched off and on to produce both illumination conditions. Acquisition at each wavelength lasted for approximately one second.
7. Hyperspectral oxygenation values were calculated by the OxyVu over a fixed area of 204 mm² 1 cm around a "target" in a doughnut contour. Oxyhaemoglobin, deoxyhaemoglobin, and oxyhaemoglobin saturation, along with skin temperature values, were provided for each image (Figures 3.8 and 3.9).
8. It was important that the OxyVu readings were recorded prior to TCOM measurements because the latter involved heating the skin at the region of interest to 44°C for more than 15 minutes.

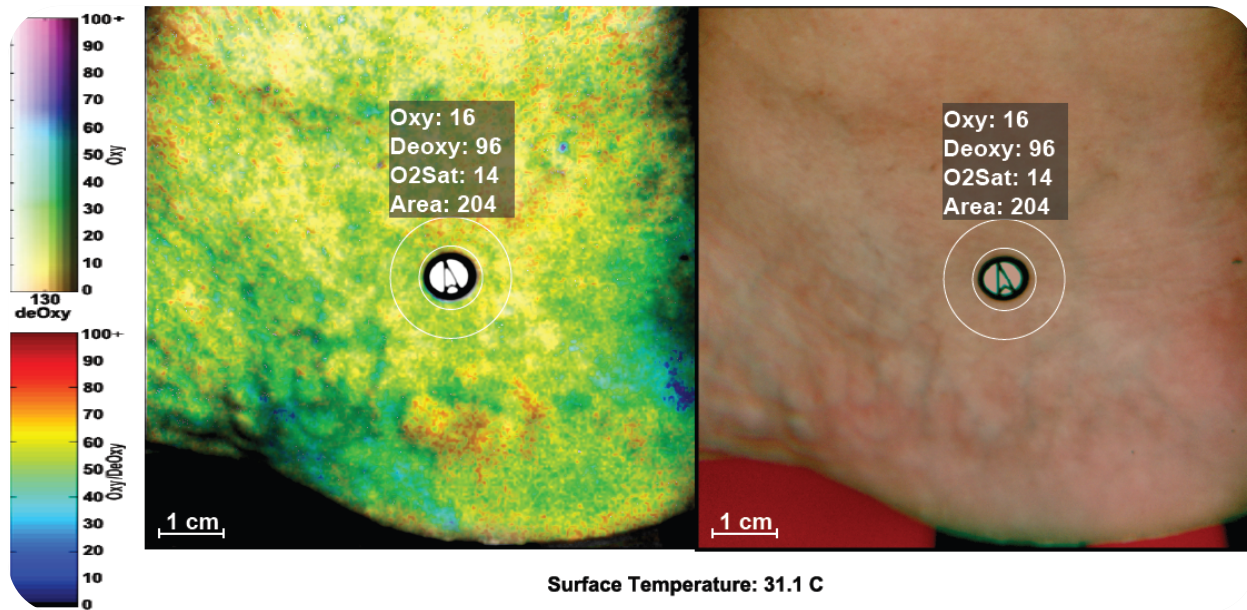


Figure 3. 8. Example of an OxyVu™ reading.



Figure 3. 9. Operating the OxyVu™. The region of interest (i.e., the foot) was imaged from the camera box attached to the OxyVu machine. This was then processed and displayed on the screen as per Figure 3.8, providing oxygenation measurements. The patient was placed supine in a small quiet room with the temperature set at 20°C–23°C.

3.7.2 Transcutaneous oxygenation measurement

The TCOM protocol described below was derived from the manufacturer's manual for the TCM3 transcutaneous pO₂ monitoring system (Radiometer Medical ApS, Brønshøj, Copenhagen) and the TCOM guidelines published in the literature.^{273 400}

1. Subjects were imaged lying supine on a standard flat examination bed.
2. They were requested to rest and be acclimatised on the bed for 15 minutes prior to measurement in a small quiet room with room temperature set at 20°C–23°C using air conditioning.
3. All devices were switched on and connected appropriately.
4. The electrode membrane was kept relatively fresh.
5. Electrode calibrations were performed immediately before use. Any fluid droplets on the outer surface of the electrode membrane were removed before calibration. Calibration was done using a certified gas mixture with known fractions of oxygen (20.9%) and carbon dioxide (5%), balanced with nitrogen. At a sea level atmospheric pressure of 101 kPa (approximately 760 mmHg), this would correspond to a pO₂ of 159 mmHg and a pCO₂ of 38 mmHg. A stable calibration value should be attained within 3–10 minutes. When this was completed, pO₂ and pCO₂ values displayed on the machine should not drift for more than 1% per hour. This phenomenon, called the “electrode drift” rate, might indicate wear and tear of the membrane or the electrode.
6. The electrode was heated to and maintained at 44°C from calibration and throughout the duration of measurement. The temperature used is recommended by the TCOM guidelines for combined T_{cp}O₂ and T_{cp}CO₂ electrodes²⁸⁹⁻²⁹¹ to optimise the skin condition for measurement without the side effects of skin burns. Deviation from 44°C could lead to a bias of 4% error per degree Celsius. The probe temperature should not deviate by more than 0.6°C for longer than 20 seconds.
7. Optimal measuring conditions should be obtained in skin areas with a high density of capillaries, ample capillary blood flow, a thin epidermis, and little or no fat deposits. The plantar aspect of the foot over the head of the first metatarsophalangeal joint and the sternum of the chest were chosen. Body hair was removed to ensure better adhesion. The skin was cleaned with alcohol swabs prior to application of a self-adhesive fixation ring. One to two drops of contact fluid was placed within the fixation ring. This thin layer of glycerol fluid prevents the presence of air between the electrode

and the skin and improves the accuracy of the sensor and makes the diffusion of gases more efficient.

8. The electrode was then snap-fixed onto the ring in direct contact with the skin area of interest to commence TCOM. The ring must create enough of a seal to prevent leaks or formation of air bubbles, as ambient air reaching the sensor would affect measured values (Figure 3.10).
9. When equilibrium was reached and measurements were recorded at minute 15, the electrode was removed from the ring. It could be replaced into another fixation ring that was moistened with contact fluid at another area of interest if the last calibration was less than 4 hours earlier.
10. If OxyVu and TCOM measurements were required at the same site; OxyVu had to precede TCOM because tissue oxygenation might be affected by the rise in skin temperature caused by the heated TCOM probes.

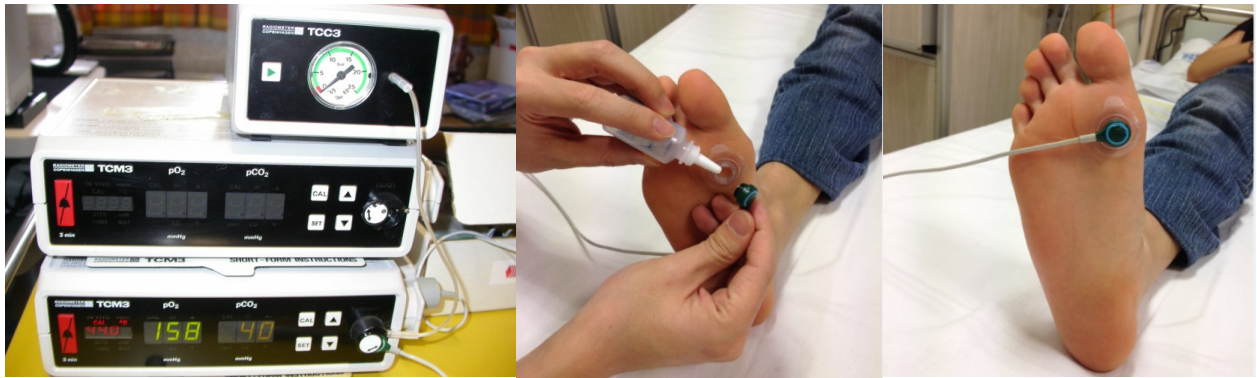


Figure 3. 10. Transcutaneous oxygenation measurement monitor.

3.7.3 Ankle-brachial pressure index

Systolic pressures in the arteries at the ankle level are measured routinely in patients with PVD. A common method of measurement is to use a sphygmomanometer cuff placed just above the ankle with the patient supine. A hand-held Doppler instrument was used to measure the systolic pressure of the posterior tibial and dorsalis pedis arteries of each leg. These pressures were then “normalised” to the higher brachial pressure of either arm to form the ABI (Figures 3.11 and 3.12).

The ABI is a good indicator of the severity of PVD. The systolic BP of the lower limb should be similar to that of the upper limb in healthy individuals, who have an ABI between 0.9 and 1.3. An ABI between 0.4 and 0.9 is considered to indicate mild or moderate PVD. An ABI of <0.4, where the systolic BP of the lower limb is markedly less than that of the upper limb, is indicative of severe PVD.⁴⁰¹

In individuals with symptomatic PVD, an ABI of <0.90 is 95% sensitive in detecting arteriogram-positive lesions and almost 100% specific in identifying individuals without PVD.²¹³ In claudicants, an ABI of <0.50 is associated with twice the mortality of that associated with an ABI of >0.50.⁴⁰² Based on the Edinburgh Artery Study, ABI is a good predictor of nonfatal and fatal cardiovascular events as well as total mortality. Each decrease in ABI of 0.10 is associated with a 10% increase in relative risk for a major cardiovascular event.⁴⁰³ An ABI of \leq 0.90 doubles the 10-year mortality rate, risk of cardiovascular mortality, and major coronary event rates.⁴⁰⁴ In patients with type 2 diabetes, a low ABI correlates with a high 5-year risk of a cardiovascular event.⁴⁰⁵

The ABI does have some shortcomings. Again, it is an assessment of the macrovascular circulation of the pedal arteries; it does not account for microvascular disease and does not provide information about the effects of an arterial obstruction in specific tissue regions. More importantly, systolic BP is a measurement when the artery is fully compressed by the cuff at a certain pressure. In elderly patients and in those with diabetes or renal disease, the artery walls are often heavily calcified, so the ankle vessels are difficult to compress or are not compressible at cuff pressures >300 mmHg. This leads to a false interpretation of the elevation of ankle pressure with an ABI of >1.3.



Figure 3. 11. Measurement of ankle-brachial pressure index.

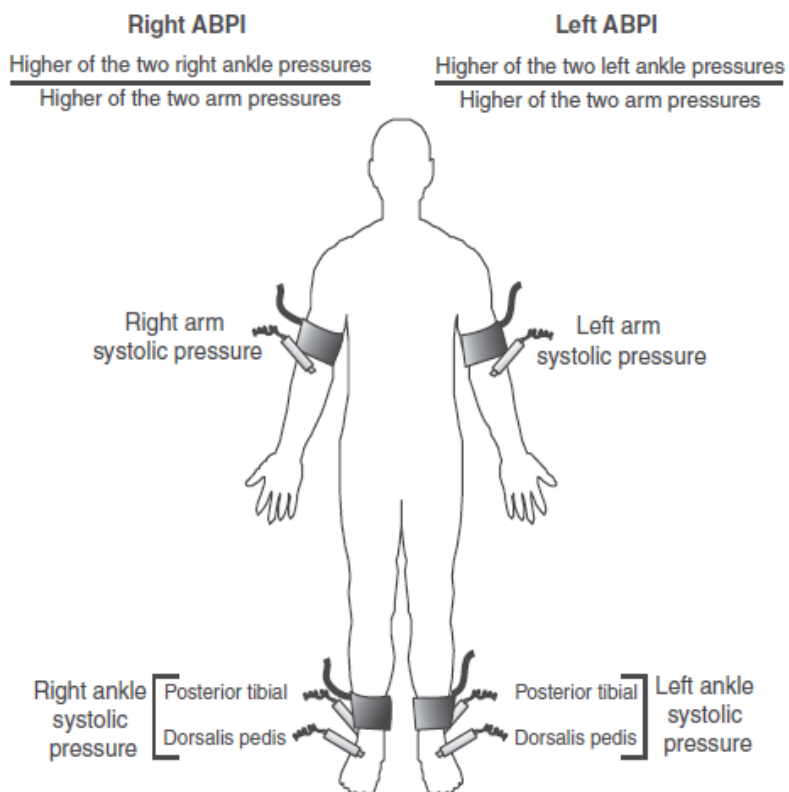
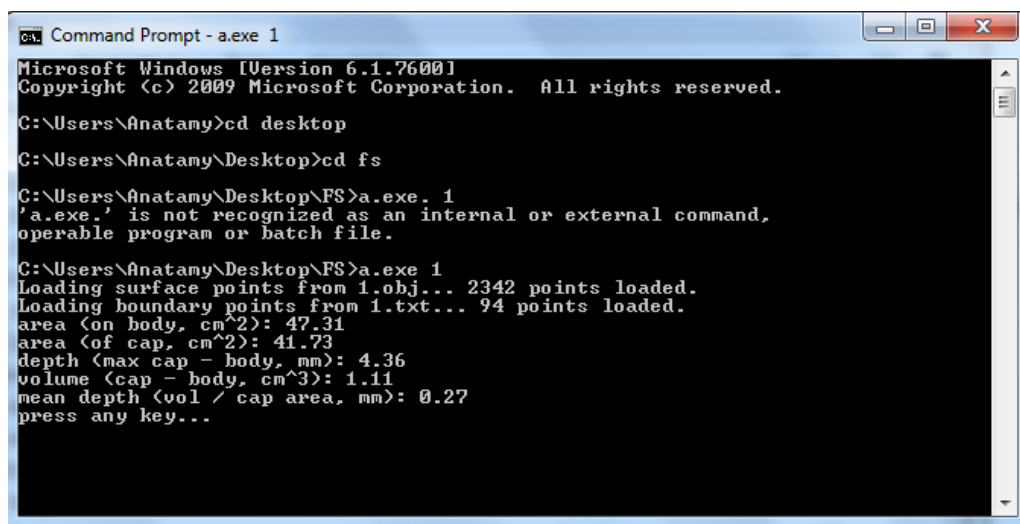


Figure 3. 12. Image explaining measurement of the ankle-brachial pressure index. Sourced from Norman et al, 2004) ⁴⁰⁶

3.7.4 FastSCAN™

1. The wound was exposed entirely with the patient in the supine or prone position depending on the location of the ulcer.
2. The laptop computer connected to the FS device was turned on with the imaging software uploaded.
3. A calibrating device was attached firmly on the skin near the region of interest. This was scanned by the laser scanner, which marked the “zero axis”.
4. Once calibrated, the laser scanner swept across the wound repeatedly until a clear three-dimensional image of the wound was produced on the computer screen. To achieve this successfully, the “brightness” dial might need to be adjusted. The difference in colour of the skin and of the wound interface, as well as the surrounding light ambience can affect the quality of the image.
5. “Stylus” markers were then placed on the wound edge, again using a laser pen. These styluses would only be visible on the screen and were used to aid volumetric measurements later.
6. The images were then saved and opened in a separate software programme (Delta®) where the images were cropped and fashioned appropriately to be used for volumetric measurements.
7. Dimensional measurements were provided using the FastScan Volumator designed by ARANZ (Figure 3.13).



```
cs> Command Prompt - a.exe 1
Microsoft Windows [Version 6.1.7600]
Copyright (c) 2009 Microsoft Corporation. All rights reserved.

C:\Users\Anatamy>cd desktop
C:\Users\Anatamy\Desktop>cd fs
C:\Users\Anatamy\Desktop\FS>a.exe. 1
'a.exe.' is not recognized as an internal or external command,
operable program or batch file.

C:\Users\Anatamy\Desktop\FS>a.exe 1
Loading surface points from 1.obj... 2342 points loaded.
Loading boundary points from 1.txt... 94 points loaded.
area (on body, cm^2): 47.31
area (of cap, cm^2): 41.73
depth (max cap - body, mm): 4.36
volume (cap - body, cm^3): 1.11
mean depth (vol / cap area, mm): 0.27
press any key...
```

Figure 3. 13. Example of wound dimension analysis using the FastScan Volumator.

3.7.5 Silhouette Mobile™

1. With the patient in the supine or prone position depending on the location of the ulcer, the wound was exposed entirely.
2. The SM laser and camera device was attached to the PDA and switched on (Figure 3.14).
3. Data including demographic details were entered into the built-in software at the patient's bedside. Wound data including site, aetiology, and wound bed characteristics could also be recorded.
4. The operator then captured an image of the wound by placing the region of interest in between the two laser lines provided by the device. This measured the length and width of the wound.
5. Settings were then changed to measure depth where another image marked by one laser line across the plane of maximum depth was captured. This was repeated three times to record depth at three different planes of the wound.
6. Its confines were determined using a stylus pen on the PDA touch screen.
7. The software would automatically generate wound measurements of surface area, depth and volume, and wound edge contour. The image was then saved and could be correlated with previous images to produce a graphical report of wound progress.

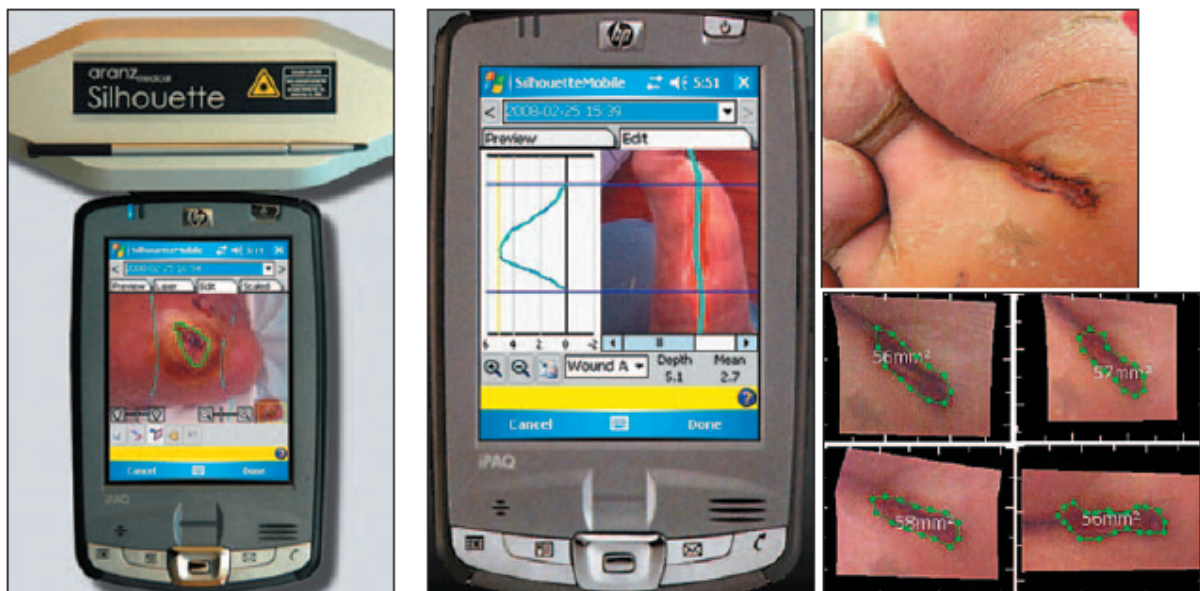


Figure 3. 14. Image of Silhouette Mobile™ (retrieved from <http://www.aranzmedical.com>)

3.7.6 Three-dimensional CT reconstruction

Volumetric measurement software provided by Siemens was used. This was accessible at the Department of Radiology, Waikato Hospital.

Protocol

1. Open the CT images of the wound.
2. Adjust the upper Hounsfield unit (HU) value to 160 and lower HU value to -1,024 (to cancel excluded air).
3. Click the Applications tab > Volume.
4. Target the wound surfaces by adjusting the axial, coronal and sagittal planes.
5. Outline the wound margin in the three-dimensional planes.
6. After finishing the manipulation, click START EVALUATION to measure dimensions for the reconstructed wound.

4 Results: Validation of OxyVu™

Evaluating inter-operator reliability

One hundred and twenty limbs in 62 patients were studied. Thirty patients presented with symptoms of PVD; the remainder were patients with no known PVD (11 vascular patients admitted for reasons other than PVD, and 21 preoperative patients undergoing elective cardiothoracic surgery). The vascular and cardiothoracic departments shared the same ward in the hospital.

Figures 4.1–4.4 show the correlation of the various OxyVu measurements between the two operators for the 120 limbs. When the measurements were paired, the ICC could be derived by the Pearson coefficient (R), with each pair assessed twice, once in the reversed order.

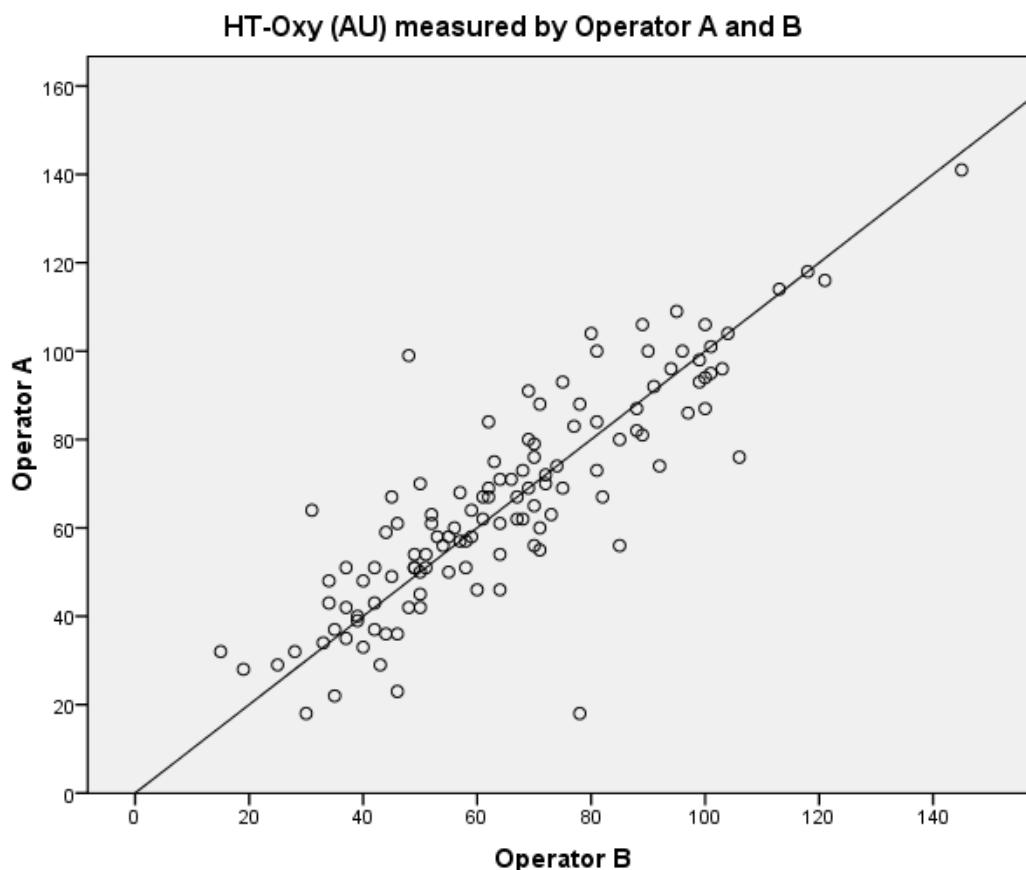


Figure 4. 1 Scatter plot showing the variation in HT-Oxy measurements between the two operators.

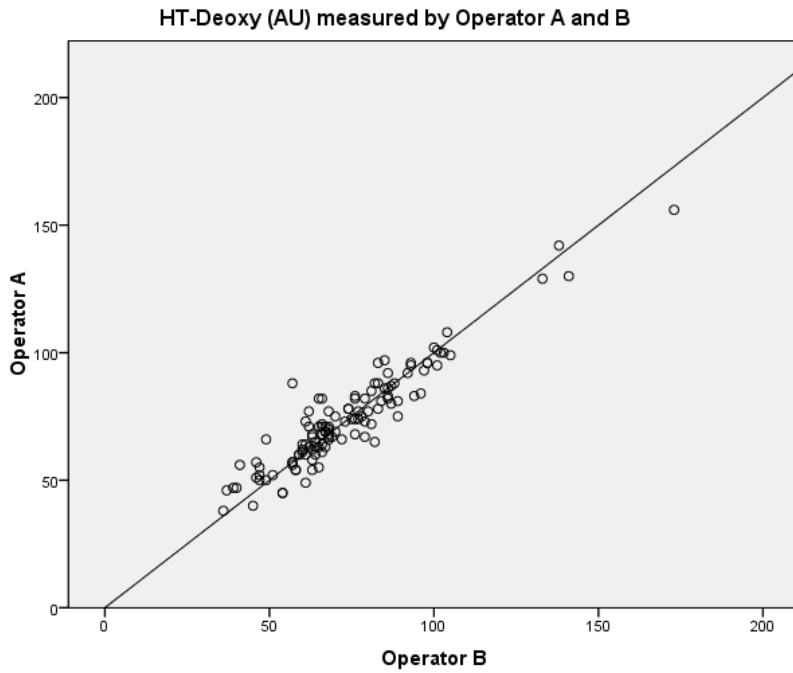


Figure 4. 2. Scatter plot showing the variation in HT-Deoxy measurements between the two operators.

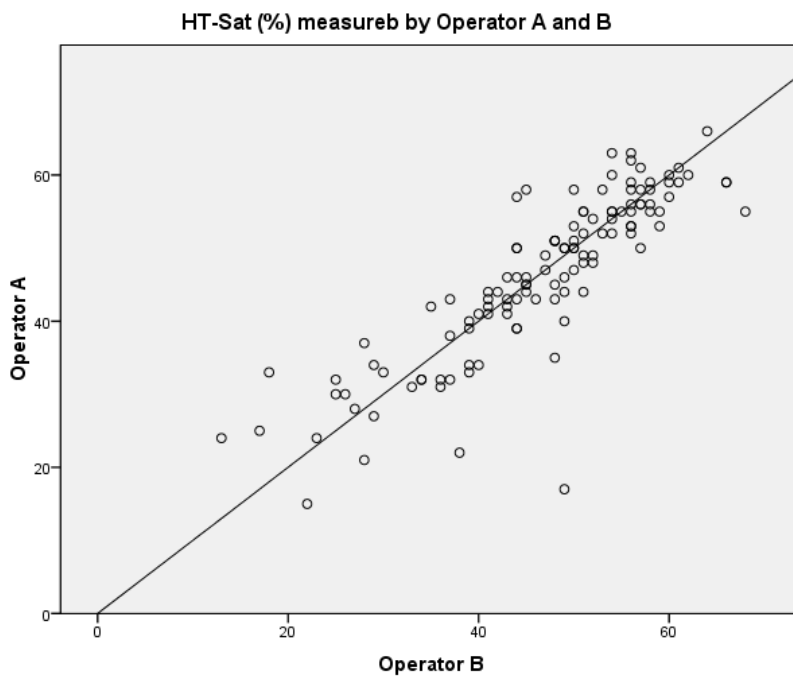


Figure 4. 3. Scatter plot showing the variation in HT-Sat measurements between the two operators.

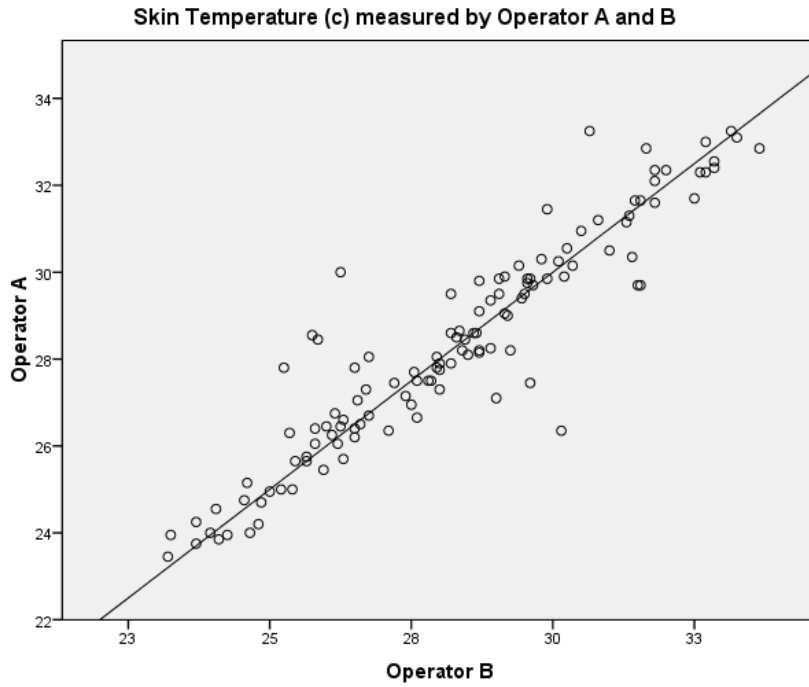


Figure 4. 4. Scatter plot showing the variation in skin temperature measurements between the two operators.

The single-measure ICC and average ICC of the four OxyVu measurements are listed in Table 4.1. Overall, inter-operator reliability when recordings were made by a single operator ranged from 86% to 94%.

	SINGLE ICC (95% CI)	AVERAGE ICC (95% CI)
HT-Oxy	0.86 (0.80–0.90)	0.92 (0.89–0.95)
HT-Deoxy	0.94 (0.91–0.96)	0.97 (0.95–0.98)
HT-Sat	0.86 (0.81–0.91)	0.93 (0.90–0.95)
Skin temperature	0.94 (0.91–0.96)	0.97 (0.95–0.98)

Table 4. 1. Summary of ICC values and 95% CIs for OxyVu™ measurements. **Abbreviations:** ICC, intraclass correlation coefficient; CI, confidence interval

Figure 4.5 is a Bland-Altman plot showing the difference in HT-Oxy measurements between operators A and B plotted against the mean HT-Oxy for the two operators. The three horizontal lines represent the mean \pm 2 SE. The results show that HT-Oxy measured by operator A was on average 0.87 arbitrary units higher than that measured by operator B, which is insignificant. The mean difference in measurements for the other variables between the two operators is described in Table 4.2.

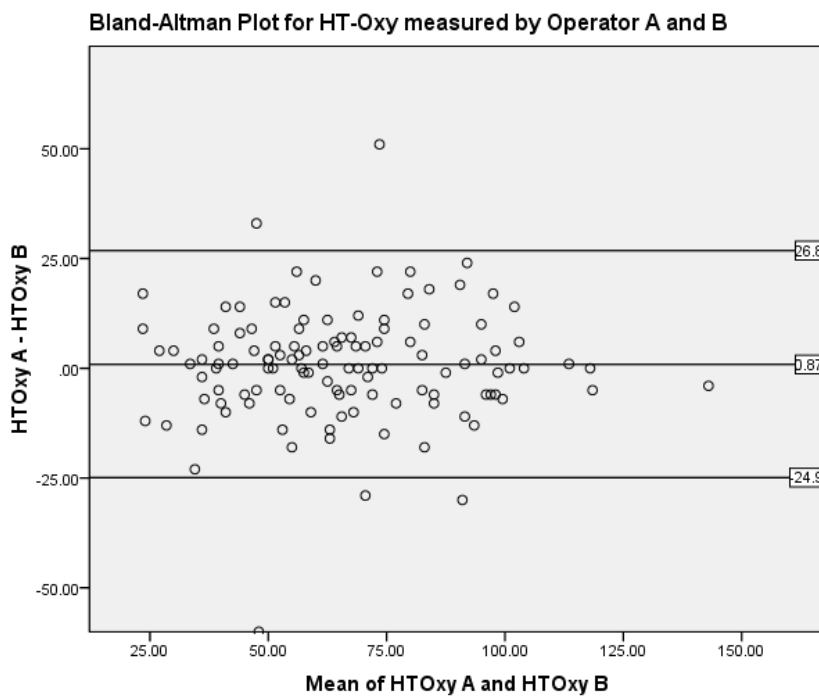


Figure 4. 5. Bland-Altman (scatter) plot for HT-Oxy measured by the two operators.

	Mean difference in measurements between operators	SE of difference in measurements between operators
HT-Oxy	0.87	12.9
HT-Deoxy	0.51	7.3
HT-Sat	-0.26	5.8
Temperature	0.08	0.9

Table 4. 2. Summary of mean differences in OxyVu™ measurements between the two operators. **Abbreviation:** SE, standard error

Evaluating intra-operator reliability

Consecutive OxyVu foot measurements were recorded for two volunteers (individuals A and B) at 2-minute intervals for 36 minutes. The numerical difference between a reading and that from 2 minutes earlier was used to calculate variation. This was equivalent to 36 comparisons ([36 minutes/2 minutes] * 2 limbs). The mean difference in the comparisons for each variable (e.g., $HT-Oxy_t - HT-Oxy_{t-2}$, where “t” is time) was not statistically significant (Table 4.3).

	HT-OXY (AU)	HT-DEOXY (AU)	HT-SAT (%)	TEMP (°C)
Mean difference of comparisons	-0.44	-0.44	0.08	0.06

Table 4. 3. Summary of mean differences in OxyVu measurements for each comparison. **Abbreviation:** AU, arbitrary units

Figures 4.6-4.7 show the mean \pm 95% CI for each of the OxyVu variables in individuals A and B. The variation over 36 minutes was small as indicated by the small 95% CI.

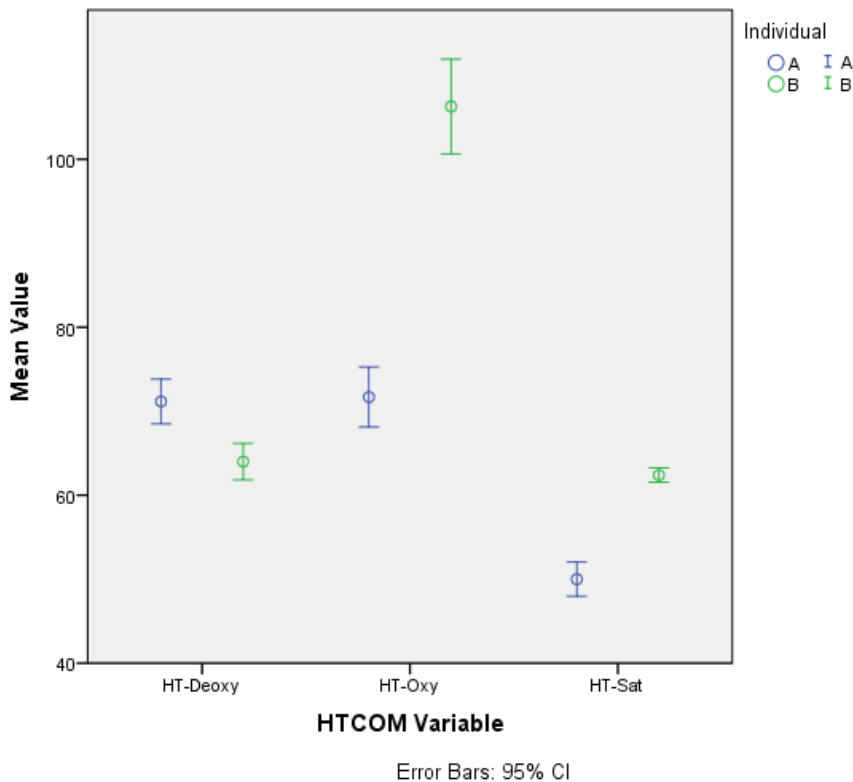


Figure 4. 6. Error bar graph showing the mean \pm 95% CI of HTCOM readings in the lower limb of individuals A and B. **Abbreviation:** CI, confidence interval.

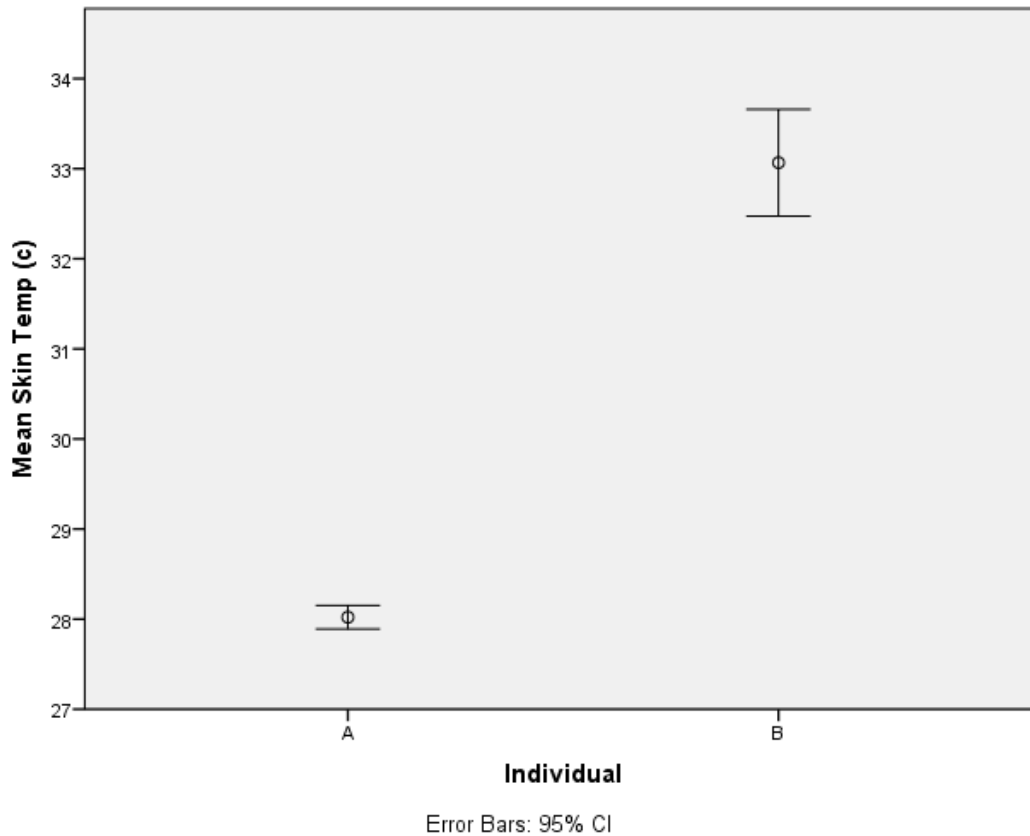


Figure 4. 7. Error bar graph showing the mean \pm 95% CI for skin temperature in the lower limb of individuals A and B. **Abbreviation:** CI, confidence interval

The within-subject coefficient of variation defined the intra-operator reliability. The intra-operator reliability of the hyperspectral oxygenation measurements ranged from 92% to 94% (Table 4.4).

	HT-OXY	HT-DEOXY	HT-SAT	SKIN TEMPERATURE
CV	0.92	0.94	0.94	0.990
95% CI	0.89–0.95	0.92–0.96	0.92-0.96	0.986–0.993

Table 4. 4. Summary of CV and 95% CI for OxyVu™ measurements. **Abbreviations:** CI, confidence interval; CV, coefficient of variation

Comparing HTCOT to TCOM, skin temperature, ABI and severity of PVD

One hundred and fifty patients with PVD of the lower limbs and 20 healthy volunteers participated in this research. The volunteers were mainly medical and nursing staff members in the ward who did not have a history of PVD. Basic demographic data were gathered from patient histories and medical records (Table 4.5). Figure 4.8 shows the distribution of the participants according to Rutherford classification. More than three-quarters (115/150) of the patients with PVD had CLI with rest pain and ulcers. Study sessions typically took 45 minutes to complete. The OxyVu measurement component would not have taken more than one minute. Most of the time was spent operating the TCOM device and taking measurements for both feet.

	VASCULAR (N=150)	VOLUNTEERS (N=20)
Median age (range)	72 (35–91)	36 (23–65)
Male	101 (67%)	7 (35%)
Whites	128 (85%)	13 (65%)
Active smoker	28 (19%)	5 (25%)
Ex-smoker (>6 months)	85 (57%)	2 (10%)
Diabetes on medications	52 (35%)	0
Previous angioplasty	58 (39%)	0
Previous IIB	49 (33%)	0
Previous minor amputation	20 (13%)	0
Renal disease (eGFR <60)	22 (15%)	0
ESRF on dialysis	6 (4%)	0
Hypertension	122 (81%)	3 (15%)
Dyslipidaemia	111 (74%)	3 (15%)
IHD	71 (47%)	1 (5%)
Previous CABG	24 (16%)	0
TIA/CVA	40 (27%)	0
COPD	14 (9%)	0

Table 4. 5. Basic demographics of participants. **Abbreviations:** eGFR, estimated glomerular filtration rate; CABG, coronary artery bypass grafting; COPD, chronic obstructive pulmonary disease; CVA, cerebrovascular accident; ESRF, end-stage renal failure; IIB, infra-inguinal bypass; IHD, ischaemic heart disease; TIA, transient ischaemic attack.

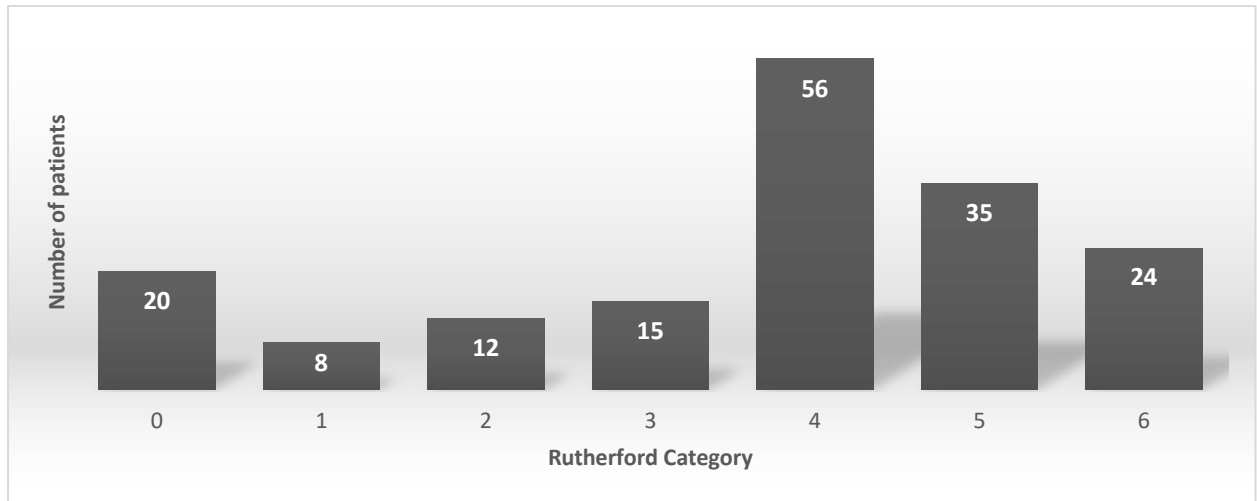


Figure 4. 8. Distribution of the study population according to severity of peripheral vascular disease.

Estimation of kurtosis and skewness for the variables

Table 4.6 describes the kurtosis and skewness of each of the continuous measurements. TcpCO₂ had a kurtosis coefficient of 8.0, suggesting it did not follow the normal distribution, which has a positive skewness of 2.3. On further interrogation of the data, there was an anomaly with one of the patients in Rutherford category 5 who had a TcpCO₂ of 120 mmHg and an ABI of 0.5 (Figure 4.9). When the data for this patient were removed, the coefficient of kurtosis readjusted to 2.2 with a positive skewness of 1.3.

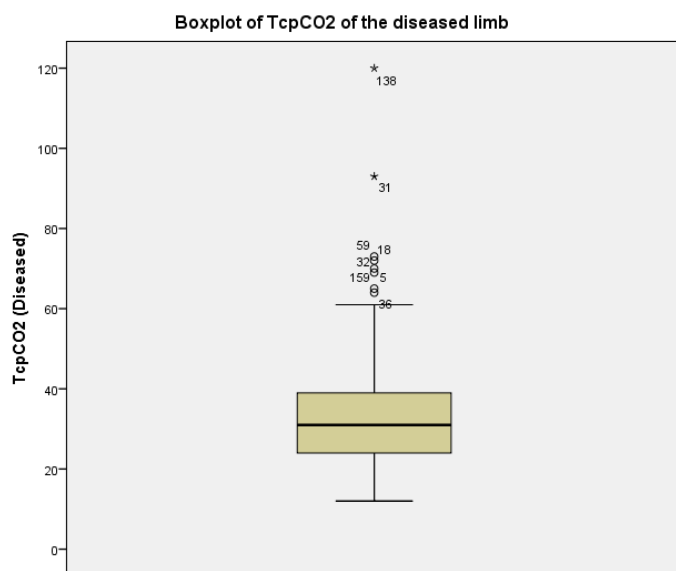


Figure 4. 9. TcpCO₂ in the diseased limb for all patients including the outlier.

VARIABLES		SKEWNESS	KURTOSIS
Age		-1.12	1.14
Diseased limb	HT-Oxy	0.27	0.19
	HT-Deoxy	1.04	1.50
	HT-Sat	-0.99	1.06
Contralateral limb	HT-Oxy	0.24	-0.32
	HT-Deoxy	0.62	0.84
	HT-Sat	-0.59	0.19
Chest	HT-Oxy	0.75	0.35
	HT-Deoxy	1.40	2.95
	HT-Sat	-0.80	0.84
Temperature	Diseased limb	0.01	-0.73
	Contralateral limb	-0.03	-0.69
	Chest	-0.88	1.50
ABI	Diseased limb	0.40	0.11
	Contralateral limb	0.40	0.60
Diseased limb	TcpO₂	-0.38	0.06
	TcpCO₂	2.27	7.95
Contralateral limb	TcpO₂	0.12	0.05
	TcpCO₂	-0.04	0.58
Chest	TcpO₂	-0.28	0.22
	TcpCO₂	0.62	0.87

Table 4. 6. Summary of skewness and kurtosis for all continuous variables.

OxyVu™ measurements in diseased limb and contralateral limb

In the 150 patients with PVD, HT-Deoxy was higher and HT-Sat was lower in the diseased limb, while there was no difference in HT-Oxy (Table 4.7). Skin temperature in the diseased limb was also lower.

	MEAN	RANGE	SD	P-VALUE
HT-Oxy (diseased)	76.4	11–145	24.4	0.31
HT-Oxy (contralateral)	77.7	26–123	21.4	
HT-Deoxy (diseased)	80.9	40–144	19.8	<0.001
HT-Deoxy (contralateral)	74.1	32–124	16.8	
HT-Sat (diseased)	47.8	11–62	10.6	0.007
HT-Sat (contralateral)	50.6	24–66	8.5	
Temperature (diseased)	28.9	23.7–34.6	2.6	0.036
Temperature (contralateral)	29.4	23.6–35.2	2.8	

Table 4. 7. Summary of OxyVu™ findings in patients with peripheral vascular disease. **Abbreviation:** SD, standard deviation

	MEAN	RANGE	SD	P-VALUE
Oxy-BPI	1.00	0.19–2.13	0.26	<0.001
Deoxy-BPI	1.12	0.63–2.88	0.27	
Sat-BPI	0.957	0.21–1.94	0.21	
Temp-BPI	0.985	0.73–1.23	0.081	

Table 4. 8 Summary of OxyVu™ findings with regard to BPI in vascular patients. **Abbreviations:** BPI, bilateral perfusion index; SD, standard deviation

In healthy individuals, the bilateral perfusion index (BPI) for HT-Oxy (Oxy-BPI) and BPI for HT-Deoxy (Deoxy-BPI) should be 1. In patients with PVD, Oxy-BPI would be expected to be less than 1, whereas Deoxy-BPI would be more than 1. In our PVD cohort, Oxy-BPI was 1, but Deoxy-BPI was 1.12. BPI for HT-Sat (Sat-BPI) was 0.96 (Table 4.8). The mean Oxy-BPI and Deoxy-BPI values were significantly different. Meanwhile, no difference was found in OxyVu measurements between the left and right limbs in the volunteer group (Tables 4.9 and 4.10).

These findings suggest that the OxyVu is able to detect a difference in tissue perfusion between a diseased limb and the contralateral limb.

	MEAN	RANGE	SD	P-VALUE
HT-Oxy (left)	100	49–160	31.3	0.19
HT-Oxy (right)	97.1	56–149	27.8	
HT-Deoxy (left)	71.2	49–101	13.2	0.43
HT-Deoxy (right)	70.4	46–100	13.6	
HT-Sat (left)	56.9	41–68	8.4	0.28
HT-Sat (right)	56.7	43–69	8.2	
Temperature (left)	30.4	25.1–35.0	2.3	0.32
Temperature (right)	30.5	24.4–35.35	2.8	

Table 4. 9. Summary of OxyVu findings in volunteers. **Abbreviation:** SD, standard deviation

	MEAN	RANGE	SD	P-VALUE
Oxy-BPI	1.02	0.87–1.24	0.11	0.25
Deoxy-BPI	1.02	0.76–1.19	0.11	
Sat-BPI	1.00	0.87–1.26	0.08	
Temp-BPI	1.01	0.97–1.09	0.03	

Table 4. 10. Summary of OxyVu BPI findings in volunteers. **Abbreviations:** BPI, bilateral perfusion index; SD, standard deviation

Comparing OxyVu™ measurements of lower limb to the chest

OxyVu measurements for the chest were carried out in 71 (47%) of the 150 patients with PVD and were used as a reference point for calculation of RPI. No chest readings were taken from volunteers. Seventy-six percent of study participants with chest recordings had CLI (54/71; Figure 4.10); the 150 vascular patients contained a similar proportion of patients with CLI.

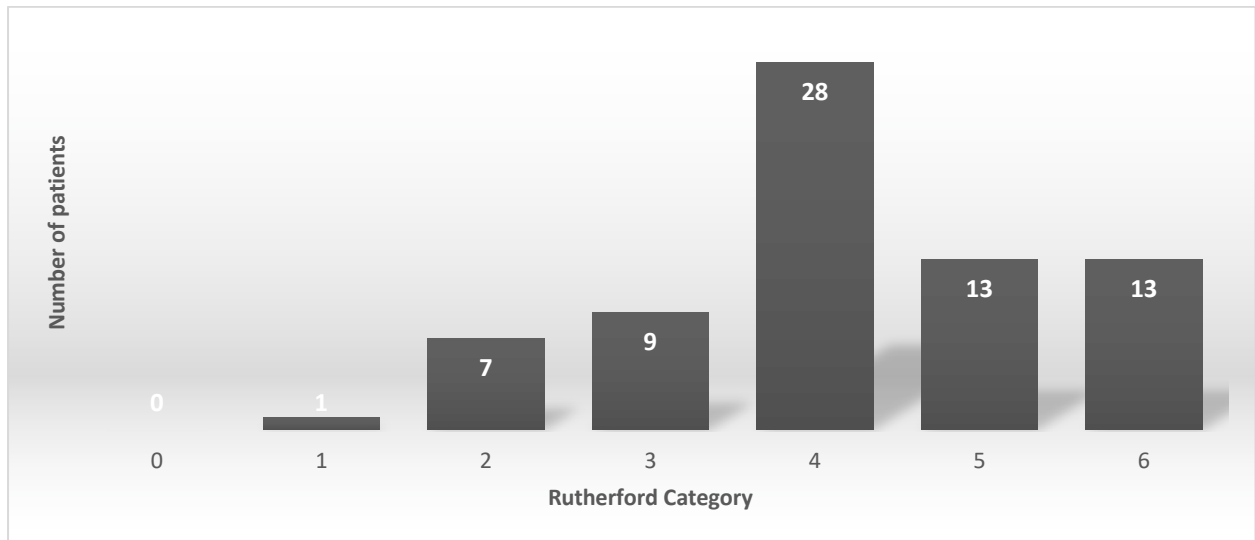


Figure 4. 10. Number of patients who had chest OxyVu™ measurements according to their Rutherford classification.

Like TCOM, where values differed between different anatomical sites, hyperspectral oxygenation in the chest differed from that in the “contralateral” limb (Tables 4.7 and 4.11). HT-Oxy, HT-Deoxy, and HT-Sat were lower in the chest ($p \leq 0.001$, $p \leq 0.001$, and $p = 0.02$, respectively), whereas skin temperature was higher ($p \leq 0.001$); as a result, the values for BPI and RPI were different.

CHEST READINGS	MEAN	RANGE	SD
HT-Oxy	47.1	16–114	21.4
HT-Deoxy	48.2	27–106	14.9
HT-Sat	47.8	14–69	10.0
Skin temperature	33.7	29.8–35.9	1.15

Table 4. 11. Hyperspectral readings at the chest. **Abbreviation:** SD, standard deviation

Although the mean Oxy-RPI was 2.04, suggesting that the amount of oxyhaemoglobin in the diseased limb was approximately twice that in the chest due to the complex plantar capillary plexus, this was offset by a higher level of deoxyhaemoglobin in the diseased limb (Deoxy-RPI 1.84), giving a mean Sat-BPI of 1.05 (Table 4.12). Nevertheless, BPI correlated with RPI, in particular for HT-Oxy, HT-Sat, and skin temperature (Table 4.13).

RPI	MEAN	RANGE	SD
Oxy RPI	2.04	0.19–6.7	1.19
Deoxy RPI	1.84	0.72–3.3	0.55
Sat RPI	1.05	0.21–1.9	0.31
Temp RPI	0.85	0.69–1.03	0.08

Table 4. 12. Summary of OxyVu™ findings with regard to RPI in vascular patients. **Abbreviations:** RPI, regional perfusion index; SD, standard deviation

		OXY BPI	DEOXY BPI	SAT BPI	TEMP BPI
Oxy RPI	(R)	0.32			
	(p)	0.007			
Deoxy RPI	(R)		0.22		
	(p)		0.07		
Sat RPI	(R)			0.28	
	(p)			0.02	
Temp RPI	(R)				0.32
	(p)				0.007

Table 4. 13. Correlation between RPI and BPI describing correlation coefficients and p-values. **Abbreviations:** BPI, bilateral perfusion index; RPI, regional perfusion index

Correlation between OxyVu™ readings and severity of PVD

When the study population was subdivided according to Rutherford classification, it was expected that HT-Oxy, HT-Sat, and skin temperature would show a downward trend in the diseased limb and that HT-Deoxy should show an opposite trend. This pattern should also be true for the corresponding BPI measurements.

These trends are not apparent in Figures 4.11 and 4.12, possibly because of the small number of patients with Rutherford 1, 2, and 3 disease and the fact that the Rutherford scoring system is not entirely ranked. The degree of ischaemia in patients with a Rutherford classification of 5 or 6 and tissue loss is not necessarily worse than that in patients with ischaemic pain at rest but no ulcers (Rutherford 4). In fact, HT-Oxy and HT-Sat, and their corresponding BPIs were lowest in patients with a Rutherford classification of 4, while HT-Deoxy was highest.

When the study population was re-categorised using the SSS into “volunteers”, “claudicants” and those with CLI, the trends for OxyVu readings and BPI were clearer (Figures 4.13 and 4.14).

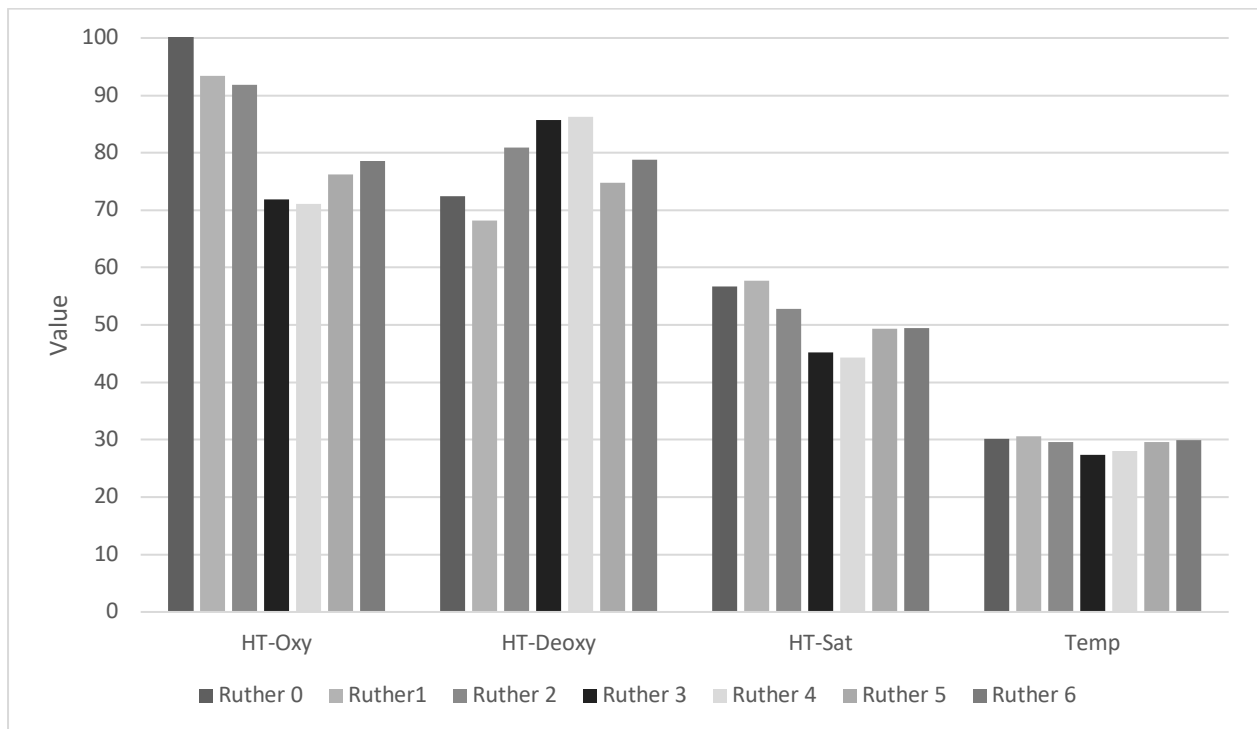


Figure 4. 11. OxyVu™ measurements in the diseased limb according to Rutherford classification.

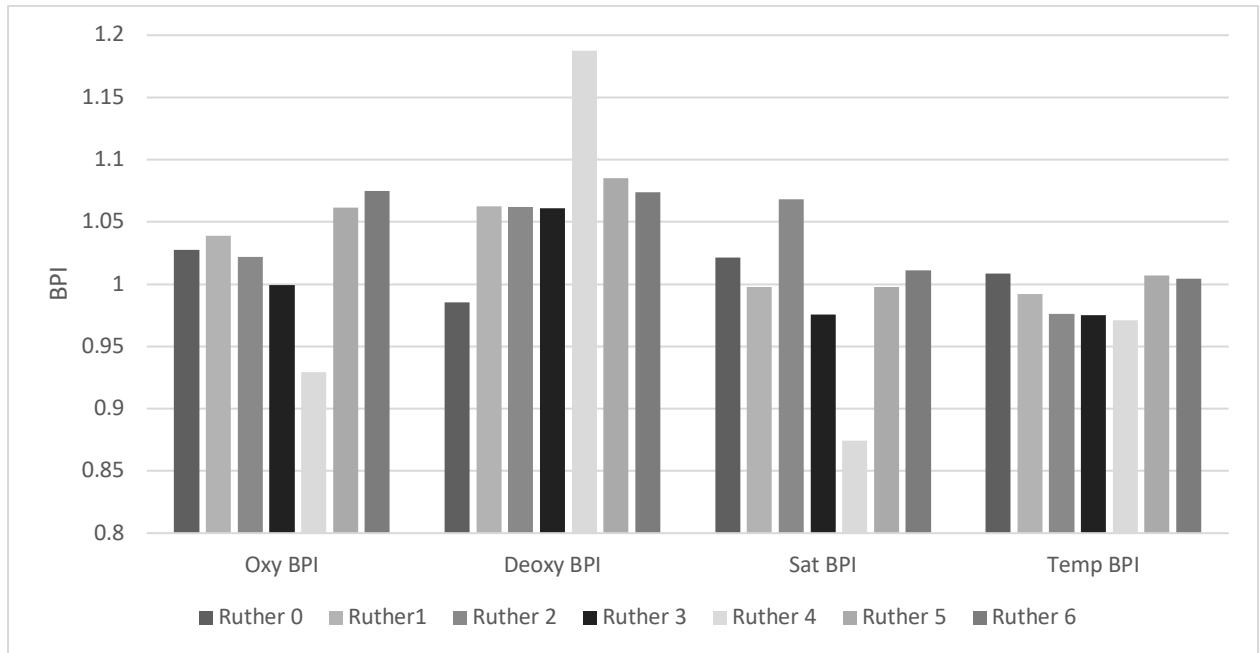


Figure 4. 12. Bilateral perfusion index in the diseased limb according to Rutherford classification.

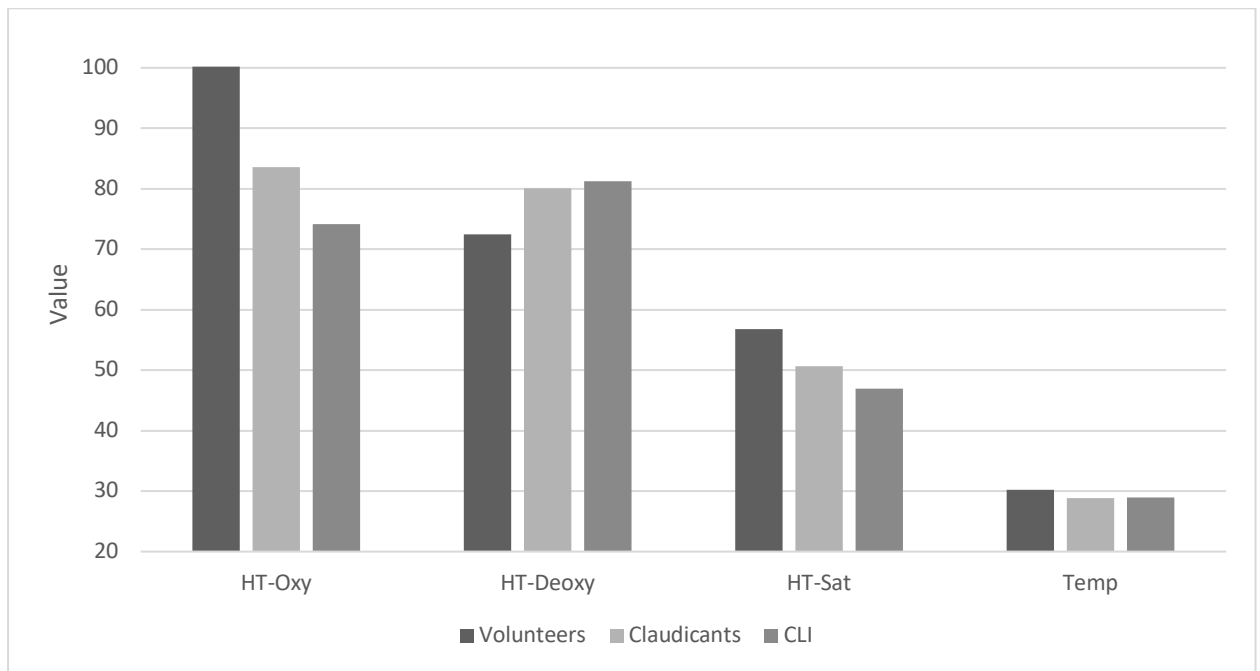


Figure 4. 13. OxyVu™ readings in the diseased limb according to severity of peripheral vascular disease.

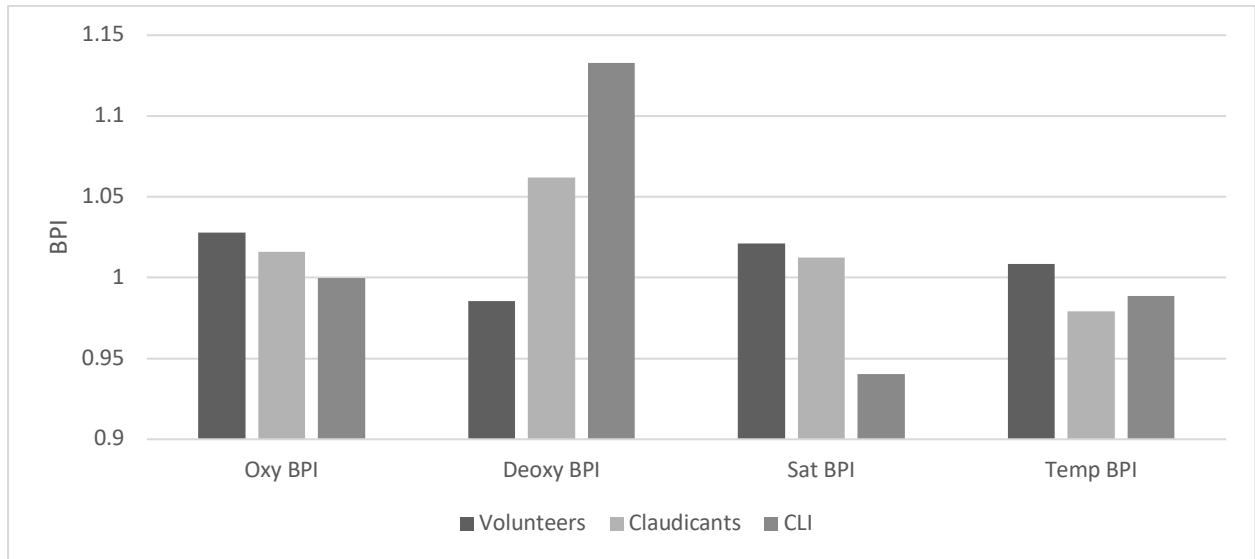


Figure 4. 14. Bilateral perfusion index in diseased limb varied according to severity of peripheral vascular disease.

From this point onwards, the SSS was used as the measure of PVD severity. Hyperspectral readings correlated with SSS, in particular HT-Oxy and HT-Sat (Table 4.14). Absolute HTCOM values correlated better with PVD than with BPI, perhaps due to the presence of PVD in the contralateral limb or compounding of random errors from BPI calculations.

DISEASED LIMB		HT-OXY	HT-DEOXY	HT-SAT	TEMP	OXY BPI	DEOXY BPI	SAT BPI	TEMP BPI
SSS	(R)	-0.29	0.08	-0.29	-0.11	-0.05	0.16	-0.15	-0.09
SSS	(p)	0.0001	0.29	0.0001	0.17	0.56	0.04	0.046	0.25

Table 4. 14. Spearman’s rank correlation coefficients and p-values comparing OxyVu™ readings for the diseased limb with severity of peripheral vascular disease. **Abbreviations:** BPI, bilateral perfusion index; SSS, Simplified Severity Score.

HTCOM was tested in the contralateral limb. Table 4.15 shows that HT-Oxy and HT-Sat were influenced by the severity of PVD, indicating that OxyVu was able to detect the presence of co-existing PVD in the contralateral limb. It was also able to distinguish the “diseased” limb from the “contralateral” limb on the basis that the degree of reduction in HT-Sat was greater in the former than the latter as the severity of PVD increased. Due to the small sample size available for analysis of RPI, the relationship between RPI and severity of PVD was not investigated.

CONTRALATERAL LIMB		HT-OXY	HT-DEOXY	HT-SAT	TEMPERATURE
SSS	(R)	-0.26	-0.07	-0.16	-0.065
SSS	(p)	0.001	0.38	0.04	0.40

Table 4. 15. Spearman’s rank correlation coefficients and p-values comparing OxyVu™ readings for the contralateral limb with severity of peripheral vascular disease. **Abbreviation:** SSS, Simplified Severity Score

Correlation between hyperspectral measurements and skin temperature

The mean skin temperature of the diseased limb was lower than that of the contralateral limb (28.9°C versus 29.4°C; $p=0.036$, Table 4.7). However, neither absolute skin temperature nor Temp-BPI was sensitive to the severity of PVD (Table 4.14). Despite this, skin temperature and Temp-BPI were lower in the diseased limb in patients with PVD than in the left limb of the volunteers, which was assumed to be the “diseased” limb ($p=0.013$ for skin temperature, $p=0.007$ for Temp-BPI; Tables 4.7–4.10). Skin temperature did not differ between the two feet in volunteers ($p=0.32$).

Skin temperature and Temp-BPI correlated with HTCOM and their BPIs (Table 4.16). Absolute values for skin temperature had the strongest correlation with HT-Sat ($R=0.56$).

		HT-OXY	HT-DEOXY	HT-SAT	OXY-BPI	DEOXY-BPI	SAT-BPI
Temp (°C)	(R)	0.41	-0.40	0.56			
	(p)	0.0001	0.0001	0.0001			
Temp BPI	(R)				0.27	-0.52	0.50
	(p)				0.0001	0.0001	0.0001

Table 4. 16. Summary of Pearson’s correlation coefficients and p-values comparing skin temperature with OxyVu™ measurements in the diseased limb. **Abbreviation:** BPI, bilateral perfusion index.

Correlation between hyperspectral measurements and Doppler ABI

The ABIs in the diseased limb and the contralateral limb are described for all 170 study participants in Table 4.17. Figure 4.15 demonstrates that a small proportion of patients had a falsely elevated ABI of >1.3 due to calcified arteries. Using the SSS, there was a downward trend of ABI in the diseased limb as the severity of PVD increased, especially when patients with falsely elevated ABI were excluded ($R= -0.37$, $p=0.0001$, Table 4.18). Similarly, when subjects with incompressible vessels were excluded, the ABI in the contralateral limb also trended with the SSS, indicating co-existing PVD ($R= -0.19$, $p=0.02$).

	DISEASED LIMB			CONTRALATERAL LIMB		
	Volunteers	Claudicants	CLI	Volunteers	Claudicants	CLI
Mean	1.03	0.74	0.68	1.03	0.93	0.93
Range	0.9–1.2	0.00–1.6	0.00–1.9	0.9–1.2	0.4–1.6	0.4–1.9
SD	0.10	0.35	0.44	0.09	0.29	0.33

Table 4. 17. Descriptive summary of ABI in the diseased and contralateral limb according to severity of vascular disease using the Simplified Severity Score. **Abbreviations:** CLI, critical limb ischaemia; SD, standard deviation

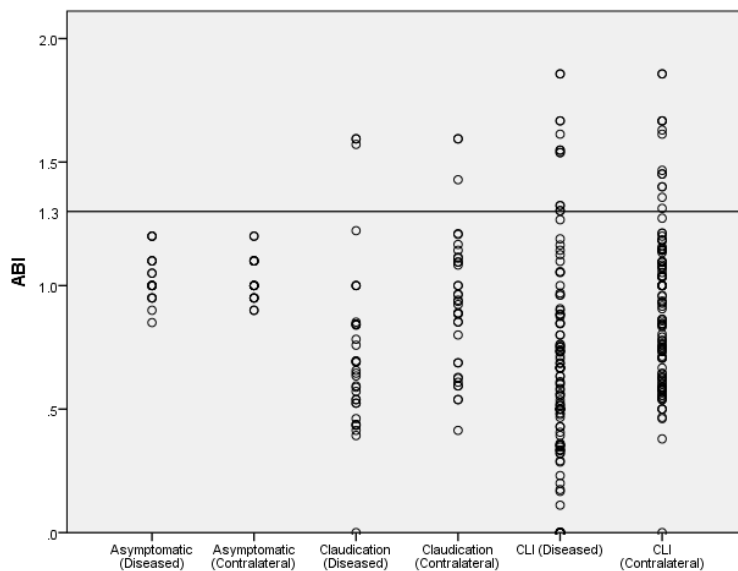


Figure 4. 15. Scatter plot of the ankle-brachial pressure index in the diseased limb and contralateral limb according to the Simplified Severity Score. **Abbreviation:** CLI, critical limb ischaemia.

		ABI (DISEASED LIMB)		ABI (CONTRALATERAL LIMB)	
		All participants	ABI <1.3	All participants	ABI <1.3
		n=170	n=158	n=170	n=154
SSS	(R)	-0.29	-0.37	-0.11	-0.19
SSS	(p)	0.0001	0.0001	0.17	0.02

Table 4. 18. Summary of Spearman’s rank correlation coefficients and p-values when comparing ABI with severity of peripheral vascular disease. **Abbreviations:** ABI, ankle-brachial pressure index; SSS, Simplified Severity Score

ABI correlated with HTCOM in the diseased limb, in particular for HT-Sat and its indices. This relationship was even stronger when the falsely elevated ABI values (i.e. ABI >1.3) were excluded (Table 4.19). ABI was most strongly associated with Sat-RPI ($R=0.45$), perhaps because a reference point on the upper body was chosen for both variables without association with possible PVD in the contralateral limb.

DISEASED LIMB		HT-OXY	HT-DEOXY	HT-SAT	OXY-BPI	DEOXY-BPI	SAT-BPI	OXY-RPI	DEOXY-RPI	SAT-RPI
ABI	(R)	0.12	-0.14	0.19	0.11	-0.26	0.21	0.20	-0.19	0.45
	(p)	0.11	0.07	0.01	0.14	0.001	0.005	0.10	0.10	0.0001
ABI <1.3	(R)	0.30	-0.29	0.42	0.13	-0.31	0.27	0.18	-0.12	0.36
	(p)	0.00	0.0001	0.0001	0.10	0.0001	0.001	0.0001	0.0001	0.00201

Table 4. 19. Pearson’s correlation coefficients and p-values when comparing the ABI of the diseased limb with OxyVu™ readings. **Abbreviations:** ABI, ankle-brachial pressure index; BPI, bilateral perfusion index

Correlation between hyperspectral and TCOM measurements

TcpO₂ and TcpCO₂ were measured for both limbs in all 170 study participants. The patient with abnormally high TcpCO₂ was removed from the statistical analysis in this section. The TcpCO₂ variable is therefore assumed to follow a “normal” distribution.

Chest TcpO₂ and TcpCO₂ were recorded in 68 and 30 patients with PVD, respectively. No chest measurements were collected from the volunteers. Due to the small sample size, there was no analysis of RPI for TCOM.

Table 4.20 lists the means \pm standard deviation for TcPO₂ and TcPCO₂ in the diseased limb and the respective BPI values. These measurements were also categorised according to the severity of PVD. As with HTCOM, it was expected that TcPO₂ and its BPI would decrease as the severity of PVD increased and that TcPCO₂ and its BPI would show the opposite trend. This pattern was more apparent for TcPCO₂ and its BPI. In fact, TcPCO₂ linked more strongly with the severity of PVD than TcPO₂ (Table 4.21).

DISEASED LIMB		TCPO ₂	TCPCO ₂	TCPO ₂ BPI	TCPCO ₂ BPI
Volunteers	Mean	79.3	26.4	1.02	1.06
	SD	13.9	12.8	0.15	0.34
Claudicants	Mean	84.2	28.3	1.04	1.14
	SD	17.9	7.9	0.14	0.34
CLI	Mean	75.8	36.0	0.99	1.29
	SD	22.8	14.5	0.29	0.57

Table 4. 20. TCOM readings of the diseased limb according to severity of peripheral vascular disease using the Simplified Severity Score. **Abbreviations:** CLI, critical limb ischaemia; SD, standard deviation; BPI, bilateral perfusion index; TCOM, transcutaneous oxygenation measurement.

DISEASED LIMB		TCPO ₂	TCPCO ₂	TCPO ₂ BPI	TCPCO ₂ BPI
SSS	(R)	-0.11	0.31	-0.14	0.18
SSS	(p)	0.14	0.0001	0.08	0.02

Table 4. 21. Spearman's rank correlation coefficients and p-values when comparing transcutaneous oxygenation measurement readings for the diseased limb with the severity of peripheral vascular disease using the SSS. **Abbreviations:** BPI, bilateral perfusion index; SSS, Simplified Severity Score

TCOM values for the reference points, (i.e., the contralateral limb and chest) are described in Table 4.22. The TcPCO₂ of the contralateral limb correlated with the SSS, indicating co-existing disease in the contralateral limb and that TcPCO₂ may be more sensitive than TcPO₂ in detecting PVD.

REFERENCE POINTS	CONTRALATERAL LIMB		CHEST	
	TcpO ₂	TcpCO ₂	TcpO ₂	TcpCO ₂
Volunteers	Mean	79.0	24.8	
	SD	13.7	6.9	
Claudicants	Mean	83.5	26.4	66.6 41.0
	SD	23.9	7.9	13.2 10.5
CLI	Mean	79.2	29.2	60.9 39.5
	SD	21.2	6.8	11.0 7.6
SSS	(R)	-0.03	0.18	
	(p)	0.74	0.02	

Table 4. 22. Transcutaneous oxygenation measurements for reference points according to severity of peripheral vascular disease using the SSS. **Abbreviations:** CLI, critical limb ischaemia; SSS, Simplified Severity Score; SD, standard deviation

DISEASED LIMB	HT-OXY	HT-DEOXY	HT-SAT	OXY-BPI	DEOXY-BPI	SAT-BPI
TcpO₂	(R)	0.02	0.19			
	(p)	0.77	0.012			
TcpCO₂	(R)	0.28	-0.26			
	(p)	0.0001	0.001			
TcpO₂-BPI	(R)			-0.04		-0.01
	(p)			0.60		0.95
TcpCO₂-BPI	(R)				0.33	-0.20
	(p)				0.0001	0.01

Table 4. 23. Pearson’s correlation coefficients and p-values when comparing transcutaneous oxygenation measurements in the diseased limb with OxyVu™ readings. Full details of correlation coefficients can be found in Appendix A.6.1. **Abbreviation:** BPI, bilateral perfusion index.

Table 4.23 shows the correlation coefficients (R) and p-values for the comparison of TCOM and HTCOM. TcpCO₂ and its BPI correlated with HT-Deoxy and HT-Sat. No relationships

were found between TcpO₂ and HT-Oxy or their respective BPIs. The TCOM of the contralateral limb was also compared with the hyperspectral readings (Appendix A6.2). Relationships similar to those in the diseased limb would be expected. Only TcpCO₂ and HT-Deoxy in the contralateral limb showed a correlation ($R=0.19$, $p=0.02$).

Correlation between hyperspectral oxygenation and demographics

VARIABLES	LIMB	HTCOM	P-VALUE	NON-STANDARDISED COEFFICIENTS (B)
Skin colour (Coloured, 1) (White, 0)	Diseased	HT-Oxy	0.79	
		HT-Deoxy	0.94	
		HT-Sat	0.83	
	Contralateral	HT-Oxy	0.95	
		HT-Deoxy	0.14	
		HT-Sat	0.58	
Gender (Male, 1) (Female, 0)	Diseased	HT-Oxy	0.94	
		HT-Deoxy	0.003	-9.1
		HT-Sat	0.03	3.8
	Contralateral	HT-Oxy	0.09	
		HT-Deoxy	0.13	
		HT-Sat	0.85	
Age	Diseased	HT-Oxy	0.004	-0.42
		HT-Deoxy	0.02	0.23
		HT-Sat	0.002	-0.18
	Contralateral	HT-Oxy	0.046	-0.25
		HT-Deoxy	0.54	
		HT-Sat	0.15	

Table 4. 24. Summary of p-values from linear regression investigating how race, sex, and age affected OxyVu™ findings.

Hyperspectral technology measures the intensity of colour chromophores. One hundred and forty-one (83%) of the 170 participants were Whites and 29 had “coloured skin”. With adjustment for the severity of PVD, multi-variate analysis using linear regression (analysis of variance) did not show “colour of the skin” to be a factor in HT-Oxy, HT-Deoxy, or HT-Sat of the diseased and contralateral limbs (Table 4.24).

Sex, age, history of diabetes, renal disease, smoking history, and number of pack-years were also tested. Age and sex were confounding factors for HTCOM. The non-standardised coefficient, B, provided a “gradient”, i.e., the degree of variation of HTCOM with, for example, increasing age. For instance, age was a confounding factor in HT-Sat of the diseased limb, with a B= -0.18. This means that HT-Sat decreased by a factor of 0.18 with each increasing year of age despite adjustment for severity of PVD. The HT-Sat of the diseased limb appeared to be 3.8 times higher in men than in women. The p-values for the other factors are presented in Appendix A.6.3.

Correlation between HT-Sat and TcPO₂

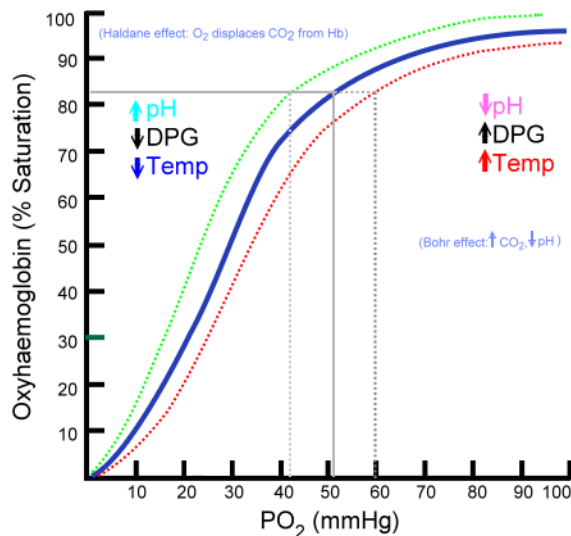


Figure 4. 16. Oxygen-haemoglobin dissociation curve. (Retrieved from https://en.wikipedia.org/wiki/Oxygen%E2%80%93hemoglobin_dissociation_curve)⁴⁰⁷

The oxygen-haemoglobin dissociation curve is a well-known physiological concept that compares oxyhaemoglobin saturation with partial pressure of oxygen in the blood (Figure 4.16). It is an important tool for understanding oxygen transport and delivery, specifically the affinity of oxygen for haemoglobin.

HT-Sat is the saturation of oxyhaemoglobin (%) and TcpO₂ reflects PaO₂. Figure 4.17 compares HT-Sat and TcpO₂ for the diseased limb and the contralateral limb (n=340). Using the regression model for curve estimation, several shapes of curves were tested. The sigmoid-shaped curve linked most strongly to the data when compared with linear, logarithmic, logistic, exponential and quadratic models. Although the R square coefficient was small (R²= 0.036), the fitness of an S-shaped curve did not happen by chance (p=0.001). The R² statistic is a measure of the strength of association between observed and model-predicted values for the dependent variable.

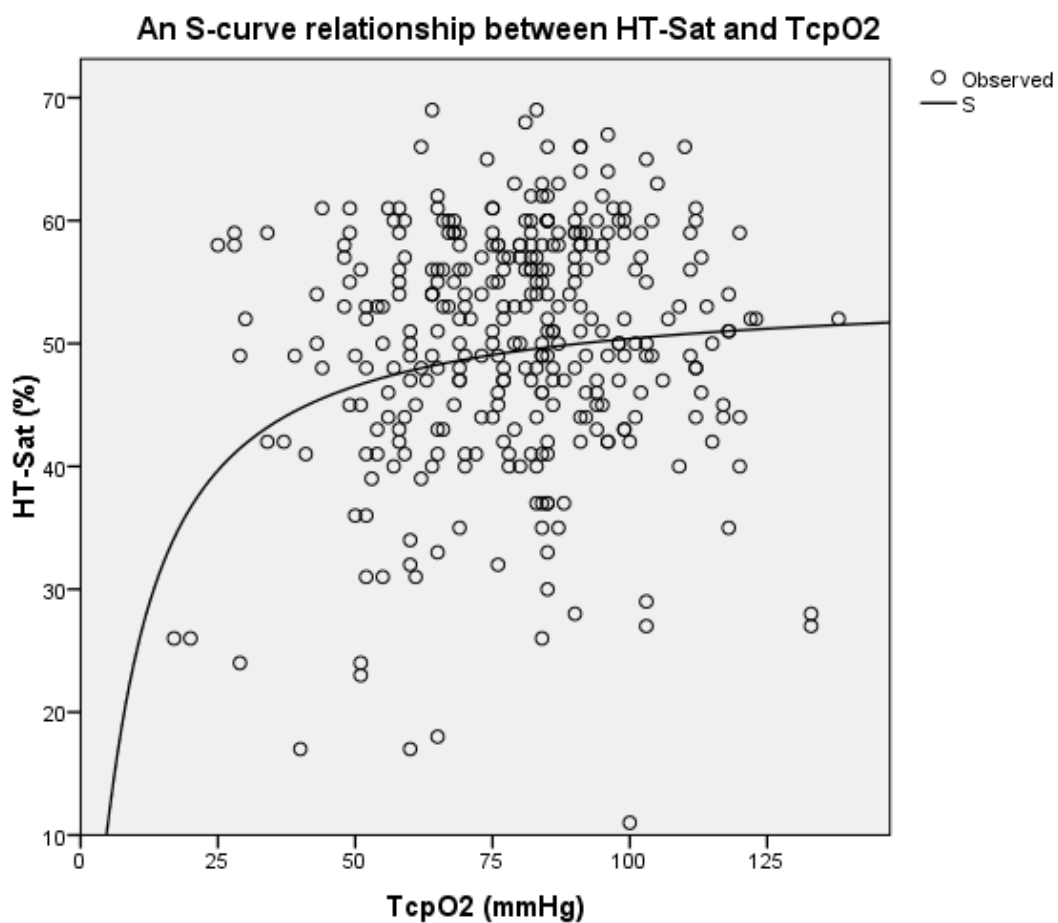


Figure 4. 17. Scatter plot with an S-curve showing the association between HT-Sat and TcpO₂.

The purpose of this exercise was to demonstrate that OxyVu could perform and produce variables in the way it was designed for. HTC_{COM} was also used to detect the presence of anaemia. The results are shown in Appendix A.6.4.

5 Results: WOIOW study

Patient recruitment and demographics

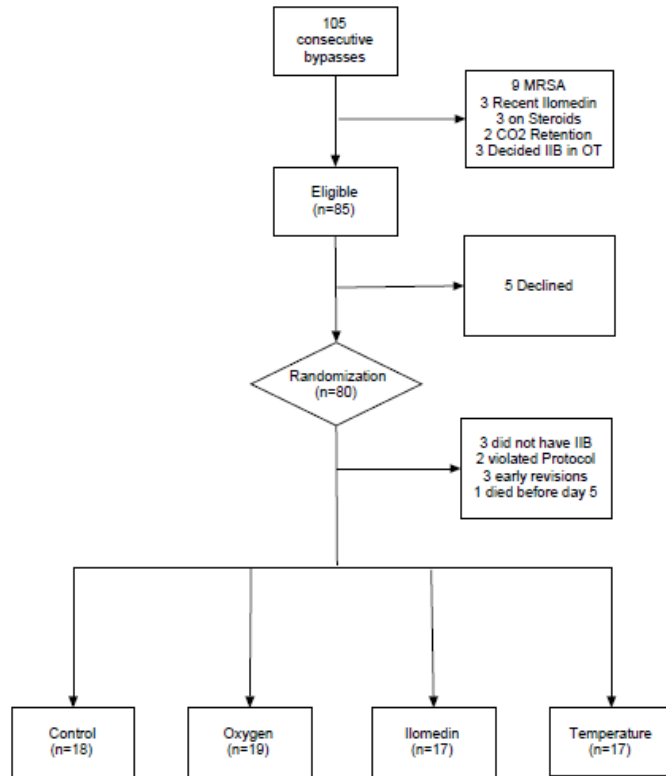


Figure 5. 1. Flow diagram showing patient recruitment.

Patient recruitment commenced in January 2009 and ended in July 2011. One hundred and five consecutive patients underwent infrainguinal bypass (IIB) requiring a knee incision (Figure 5.1). Eighty-five of these patients were invited to participate in this study. Those who failed to meet the inclusion criteria or where the decision to perform bypass surgery was only made intraoperatively were not invited to participate. The most common reason for exclusion was a history of methicillin-resistant *Staphylococcus aureus*. Eighty patients were consented for the study; nine patients were subsequently excluded in the course of the study (three did not have the proposed IIB, three had bypass graft revisions before day 5, and two violated the protocol by having higher FiO_2 than prescribed by the study). One patient allocated to the oxygen group had a cardiac arrest and died on day 1. There were no complications as a direct result of the study. Seventy-one patients completed the study on day 5, when the PTFE implant was removed to evaluate the primary outcome. Recruitment was slower than anticipated.

Tissue Oxygenation and Wound Healing in Vascular Surgery

GROUP	CONTROL	OXYGEN	ILOMEDIN	TEMPERATURE	P-VALUE
Patients	18	19	17	17	0.99
Male	11	14	10	12	0.74
Mean age, years	71	69	67	74	0.19
(range)	(47–86)	(35–83)	(50–87)	(58–85)	
Whites	15	15	15	17	0.32
BMI (SD)	26 (6)	27 (4)	27 (4)	27 (4)	0.96
Acute presentation	8	5	6	3	0.35
Rutherford 2	3	2	1	2	0.77
Rutherford 3	2	4	1	1	
Rutherford 4	4	7	8	5	
Rutherford 5	5	4	2	5	
Rutherford 6	4	2	5	4	
Active smoker	4	2	5	3	0.89
Ex-smoker	12	15	10	12	
Pack-years (SD)	36 (37)	30 (29)	45 (37)	44 (38)	0.62
Diabetes (DM)	8	7	5	4	0.59
DM on insulin	5	4	2	2	0.74
Previous plasty	10	10	6	9	0.62
Previous BPG	6	8	8	6	0.83
Previous BPG	5	3	5	3	0.69
(Ipsilateral)					
Prev AKA/BKA	1	0	0	1	0.55
Previous minor amputation	2	1	1	4	0.29
AAA	1	1	1	2	0.29
Renal impairment	4	4	1	3	0.58
ESRF	0	2	0	1	
Hypertension	13	18	13	15	0.20
Dyslipidaemia	13	16	11	12	0.56

IHD	8	8	6	12	0.18
Previous CABG	2	3	1	2	0.83
TIA/CVA	5	4	2	1	0.32
Previous CEA	1	3	2	2	0.81
COPD	4	2	1	1	0.37
Preoperative warfarin	4	0	3	5	0.11
Preoperative aspirin	14	18	13	14	0.67
Preoperative statins	14	16	13	12	0.91
Postoperative heparin	3	3	1	0	0.28
On antibiotics	2	2	3	5	0.41

Table 5. 1. Basic demographics of study participants. **Abbreviations:** AAA, abdominal aortic aneurysm; AKA, above-knee amputation; BKA, below-knee amputation; CABG, coronary artery bypass grafting; CEA, carotid endarterectomy; COPD, chronic obstructive pulmonary disease; CVA, cerebrovascular accident; ESRF, end-stage renal failure; IIB, infrainguinal bypass; IHD, ischaemic heart disease; TIA, transient ischaemic attack.

There were no differences in patient demographics between the four groups (Table 5.1). Sixty-two of the 71 participants (87%) were Whites, eight were Maori, and one was Fijian Indian. Fifty-five (77%) patients had rest pain or ulcers (Rutherford 4, 5, or 6). Twenty-four patients (34%) had diabetes. Thirty-five patients had undergone previous endovascular interventions in the form of angioplasty and/or stenting, and 28 patients had previous lower limb bypasses, 16 of which were for the diseased limb. The risk factors are defined in Appendix A.1.1.

Operative findings are shown in Table 5.2. There were no differences between the groups. The most common site of proximal anastomosis was the common femoral artery (79%), while the below-knee popliteal artery was the most common outflow vessel (65%). A minority of patients had revisions to the previous bypass graft with interposition grafts where the anastomoses were at the previous saphenous vein graft. The great saphenous vein was the preferred bypass conduit (48%). Twenty-eight (39%) patients received PTFE grafts. In these settings, a Miller cuff with a vein was routinely formed at the distal end. The proportions of patients receiving therapeutic heparin and antibiotics in the recovery phase were similar.

GROUP		CONTROL	OXYGEN	ILOMEDIN	TEMP	P-VALUE
V-POSSUM	PS (SD)	22 (6)	22 (8)	22 (5)	24 (7)	0.83
	OS (SD)	11 (2)	11 (2)	10 (1)	11 (2)	0.76
Run-offs	(SD)	1.6 (0.7)	2.1 (0.9)	1.9 (0.8)	1.9 (0.7)	0.22
Duration of surgery	Min (SD)	235 (62)	214 (56)	224 (79)	243 (89)	0.64
GA		18	17	16	17	0.56
Proximal anastomosis	External Iliac	0	2	1	0	0.40
	CFA	16	13	13	14	
	SFA	2	2	2	2	
	PFA	0	0	1	0	
	GSV BPG	0	2	0	1	
Distal anastomosis	AK pop	2	3	2	2	0.52
	BK pop	13	10	11	12	
	AT	0	2	0	1	
	TPT	0	1	1	0	
	PT	2	0	3	1	
	Peroneal	1	0	0	1	
	GSV BPG	0	2	0	0	
Conduit	GSV	8	10	7	9	0.31
	Cephalic	3	1	0	1	
	Basilic	0	0	0	2	
	Composite	1	0	1	0	
	PTFE + vein cuff	6	8	9	5	
Heparin	After surgery	2	3	1	2	0.83
Antibiotics	After surgery	5	7	4	4	0.78

Table 5. 2. Operative findings in the participants. **Abbreviations:** AK, above knee; AT, anterior tibial artery; BK, below knee; BPG, bypass graft; GA, general anaesthetics; OS, operative score; PS, physiological score.

Systemic effects of perioperative adjuncts

Arterial blood gases were routinely sampled intraoperatively. The arterial partial pressure of oxygen (PaO₂) was significantly higher in the oxygen group than in the other three groups (p=0.0001; Table 5.3).

GROUP		CONTROL	OXYGEN	ILOMEDIN	TEMP	P-VALUE
Arterial pO ₂	mmHg (SD)	115 (32)	249 (64)	120 (29)	103 (22)	0.0001
Mean core temperature °C (SD)	At incision	35.9 (0.4)	36.0 (0.5)	36.2 (0.5)	36.2 (0.4)	0.28
	After surgery	36.7 (0.7)	36.6 (0.5)	36.6 (0.4)	37.1 (0.9)	0.09
	2 hours after surgery	36.4 (0.6)	36.4 (0.7)	36.6 (0.4)	36.6 (0.5)	0.41

Table 5. 3. Influence of supplemental oxygen and active warming on arterial oxygenation and core temperature.

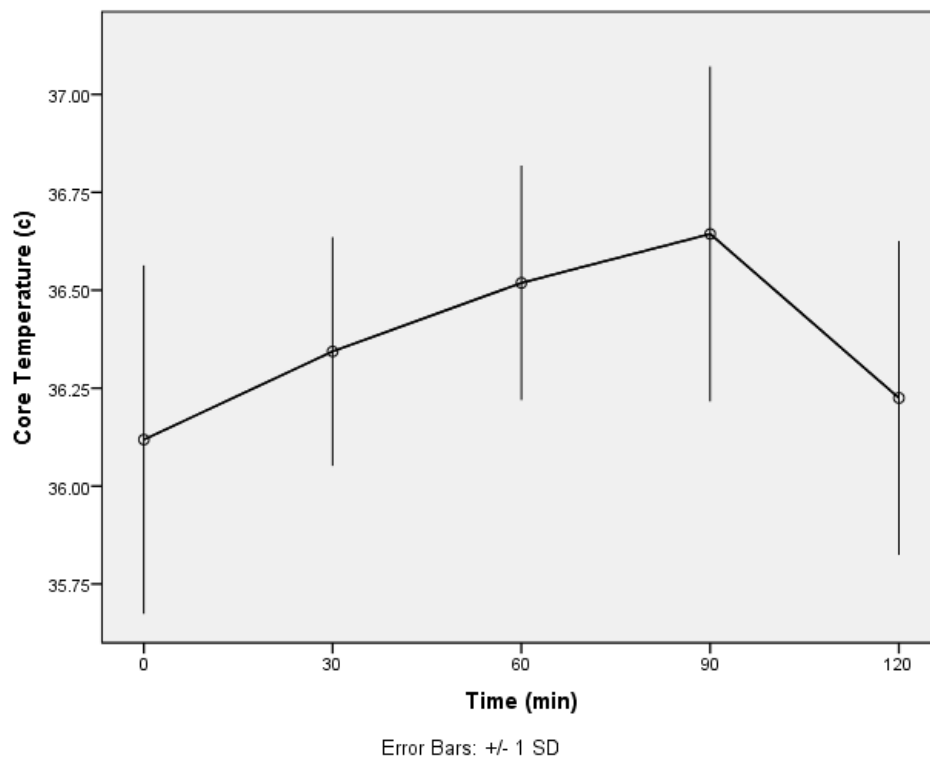


Figure 5. 2. Change in core temperature over time with active warming in the preoperative period. **Abbreviation:** SD, standard deviation.

In the temperature group, active warming with a Bair Hugger® was commenced 2 hours prior to “knife-to-skin”. This could only be an estimate, taking into account the duration of induction of anaesthesia and preparation of the operating theatre and staff. Mean core temperature was recorded at 30-minute intervals during the preoperative phase. All patients had a minimum of 2 hours of preoperative warming that did not exceed 150 minutes. Five patients had to go to the bathroom or for a short break from warming.

Core temperature increased with active warming in the first 90 minutes. This decreased by the time of “knife-to-skin” despite receiving active warming throughout the transit from the ward to the preoperative bay and theatre (Figure 5.2). The gradient of change in core temperature in the first 90 minutes for each patient in the “temperature” group was calculated using logistic regression. All 17 patients had a positive gradient, with a mean increase of 0.4°C per hour and a standard deviation of 0.24 (range 0.06°C–1.2°C). The drop in core temperature between 90 and 120 minutes was perhaps due to an interruption from transferring from a warm bed to a cooler operating table, a change in ambient temperature from the ward to the operating theatre, or the side effects of the anaesthetic agents used. The application of a Bair Hugger® 2 hours prior to surgery had a significant effect on core temperature (36.1°C at baseline 2 hours previously, 36.2°C at “knife-to-skin”; $p \leq 0.0001$).

Pre and post warming did not have an effect on core temperature at the time of skin incision or after surgery, although the patients in the temperature group appeared to have a higher core temperature immediately following surgery ($p=0.09$).

Accumulation of hydroxyproline

The primary outcome was accumulation of hydroxyproline (OHP) on day 5. There were no statistically significant differences between the four groups when each treatment arm was compared with the control group (Student’s *t*-test; Table 5.4). P-values are shown in Appendix A.7.1. There appeared to be more collagen deposition in the control group than in the three treatment arms.

Accumulation of OHP did not correlate with intraoperative PaO₂ (Pearson’s correlation; $p=0.84$), core temperature at the time of skin incision ($p=0.19$), or core temperature at 2 hours postoperatively ($p=0.90$).

GROUP	CONTROL	OXYGEN	ILOMEDIN	TEMPERATURE
OHP $\mu\text{g}/\text{cm}$	2.39 (2.26)	1.73 (0.99)	2.19 (1.62)	1.59 (0.72)
TGF- β ng/mL	0.25 (0.33)	0.29 (0.21)	0.24 (0.16)	0.26 (0.31)
FGF-2 ng/mL	0.70 (1.6)	0.40 (0.45)	0.35 (0.28)	0.31 (0.22)
VEGF ng/mL	2.63 (1.37)	2.43 (2.06)	2.58 (1.45)	2.84 (1.92)
TNF- α pg/mL	30.0 (22.5)	56.3 (80.6)	33.1 (22.3)	45.2 (35.2)
IL-8 ng/mL	22.7 (15.4)	16.4 (7.5)	17.5 (11.4)	32.6 (34.7)

Table 5. 4. Mean (SD) hydroxyproline and growth factor levels in tissue samples from each group. **Abbreviations:** OHP, hydroxyproline; TGF- β , transforming growth factor beta; FGF-2, fibroblast growth factor 2; VEGF, vascular endothelial growth factor; TNF- α , tumor necrosis factor alpha; IL-8, interleukin-8; SD, standard deviation

Balance between growth factors and cytokines

In congruence with the primary outcome, there was no difference in the biochemical marker levels detected in wound fluid from the knee between the treatment arms and the control group on day 5 (Student's *t*-test; Table 5.4 and Appendix A.7.1). The only growth factor that correlated with OHP was FGF-2 (Pearson's $r=0.38$, $p=0.001$). Despite employing different methods of analysis, TGF- β (enzyme-linked immunosorbent assay) correlated with FGF-2 (Milliplex®) with a Pearson's correlation coefficient of 0.49 ($p<0.0001$). The ratios of TGF- β to TNF- α and FGF-2 to TNF- α were not different between the groups (p -values not shown).

Analyses of mRNA

Despite using validated methods to purify the mRNA in a supervised environment, the quality of the tissue samples was suboptimal. Most samples yielded undetectable levels, and there were insufficient samples remaining to repeat the purification process. Nanodrop™ is an RNA quality control system that assesses the purity of RNA in a preparation. Using spectrophotometry, the ratio of absorbance at 260 nm and 280 nm of pure RNA (A_{260}/A_{280}) should be >2.1 . Most protocols would accept values of 1.8–2.0. The average level of proteins extracted from the 71 samples was 266 (51–654) ng/ μL ; however, that of A_{260}/A_{280} was 1.43 (1.19–1.69) ng/ μL , implying significant impurity.

Assessments of tissue oxygenation

Postoperative recordings of ABI, TCOM, and OxyVu were compared with recordings made prior to surgery.

Tissue oxygenation at the surgical wound

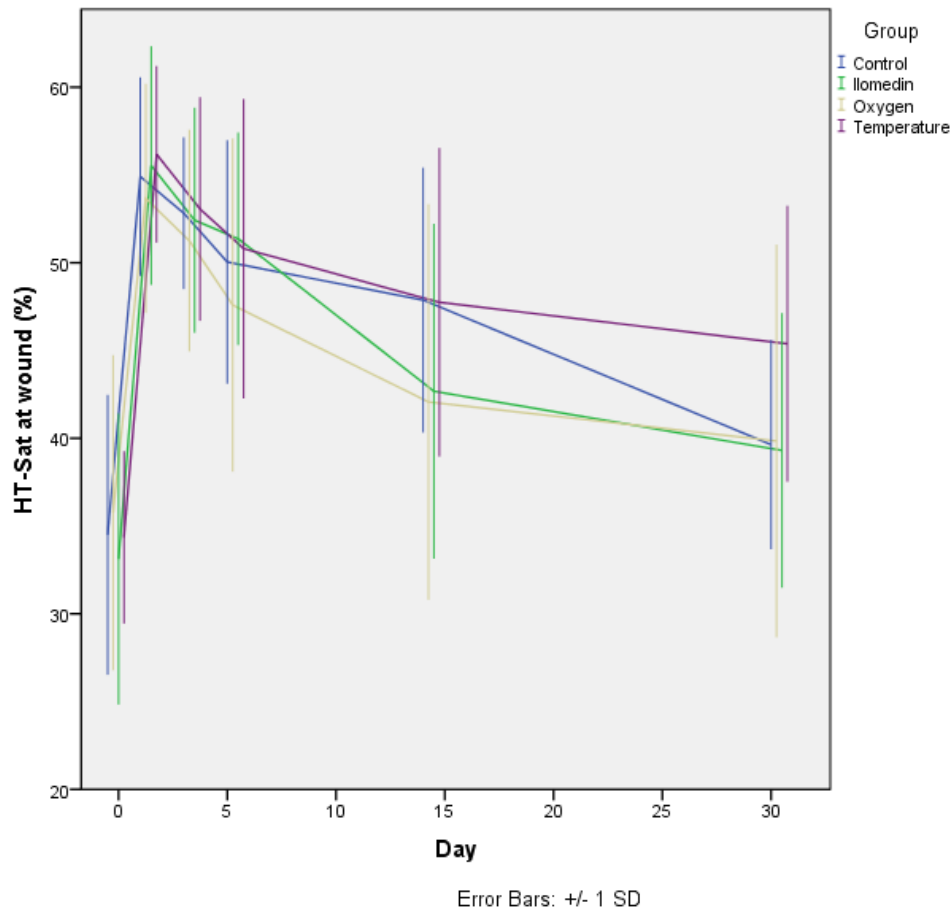


Figure 5. 3. Changes in HT-Sat at the surgical wound over time. **Abbreviation:** SD, standard deviation.

Oxygenation at the surgical wound site was measured by OxyVu to determine if production of OHP was related to peri-wound oxygenation. In all patients, the HT-Sat of the wound at day 5 was compared with the baseline HT-Sat prior to surgery to provide a ratio. The mean of this ratio was 1.51, implying that the saturation of oxyhaemoglobin increased by 51% on day 5 after surgery. In fact, the ratio for HT-Sat was 1.67 on day 1, 1.51 on day 5, and 1.23 on day 30. Similarly, the ratio for HT-Sum was 1.52 on day 3, 1.47 on day 5, and 1.39 at the end of the study. Changes in HT-Sat and HT-Sum amongst the four groups were plotted against time (Figures 5.3 and 5.4).

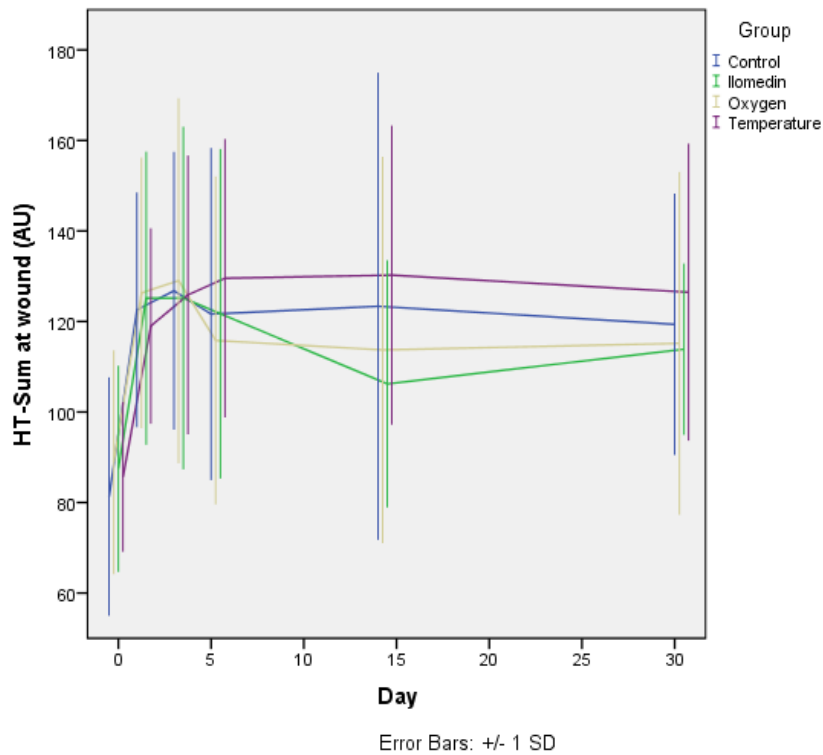


Figure 5. 4. Changes in HT-Sum at the wound over time. **Abbreviation:** SD, standard deviation.

Tissue oxygenation at the foot

Oxygenation at the foot showed similar changes to that at the wound site following surgery. When all patients were included, HT-Sat increased by 4.8% by day 5. The BPI for HT-Sum at the foot increased by 20% on day 3 when compared with before surgery and decreased to 11% on day 5. At day 30, the increase in haemoglobin at the foot was 7% compared with baseline. BPI for HT-Sat showed a similar pattern, with a 25% increase on day 3, but this decreased to 20% on day 5 and 11% on day 30. Figures 5.5 and 5.6 show the changes in BPI for HT-Sum and HT-Sat over time in the four groups.

On average, the ABI of the diseased foot increased by 94% on day 5, and continued to increase slowly by another 35% (to 129%) by day 30. In contrast, minimal variation was observed in the ABI of the contralateral limb, justifying the use of BPI to demonstrate changes in perfusion over time (Figure 5.10). TcpO₂ in the diseased foot showed a similar pattern, where the BPI for TcpO₂ increased by 7.1% on day 5 and continued to be steady at 7.3% on day 30. Conversely, TcpCO₂ decreased postoperatively by 3% at day 5, 7.7% at day 14 and 9.1% at day 30.

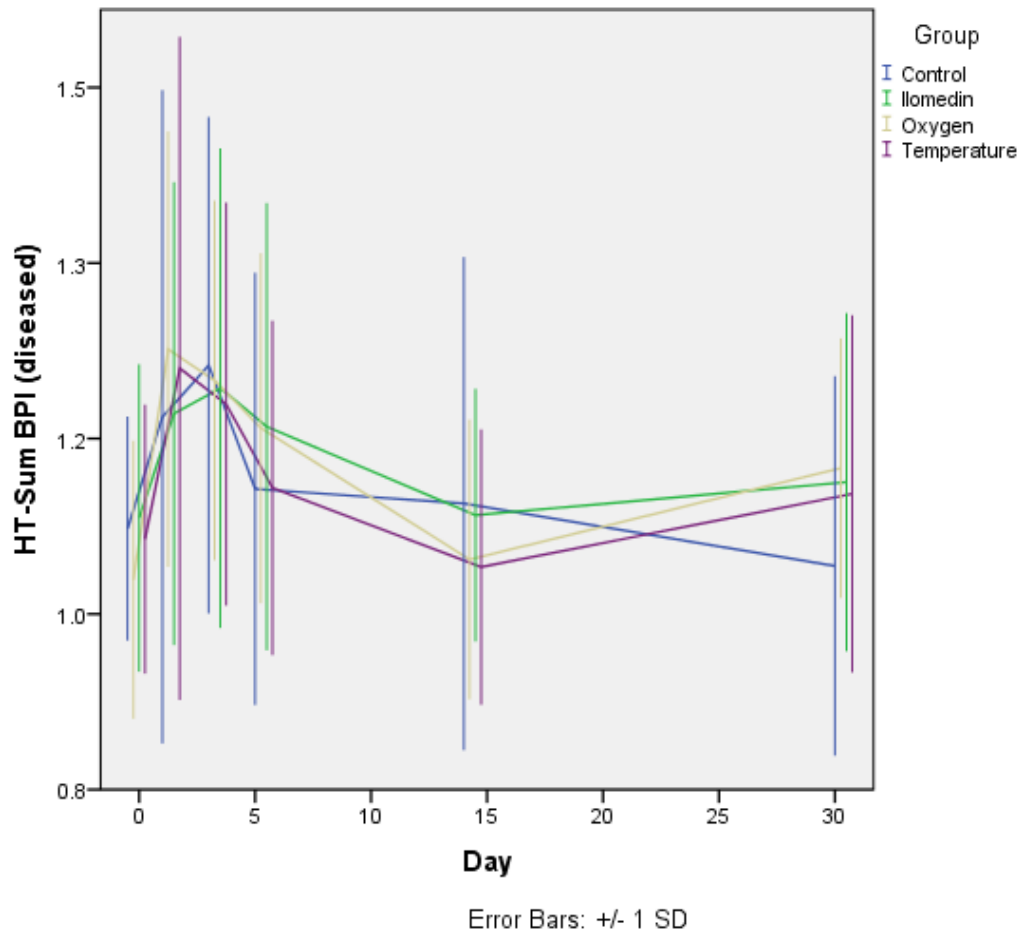


Figure 5. 5. Changes in HT-Sum BPI in the diseased foot over time. **Abbreviations:** BPI, bilateral perfusion index; SD, standard deviation.

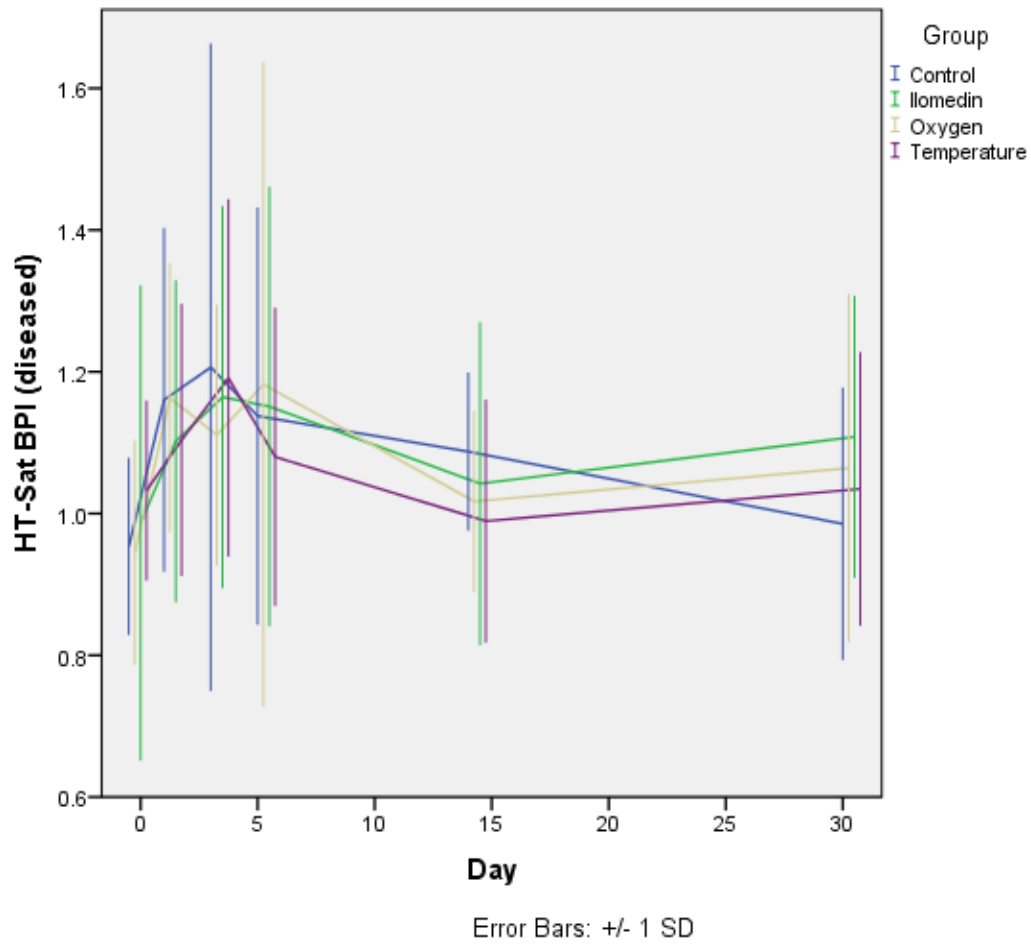


Figure 5. 6. Changes in HT-Sat BPI in the diseased foot over time. **Abbreviations:** BPI, bilateral perfusion index; SD, standard deviation.

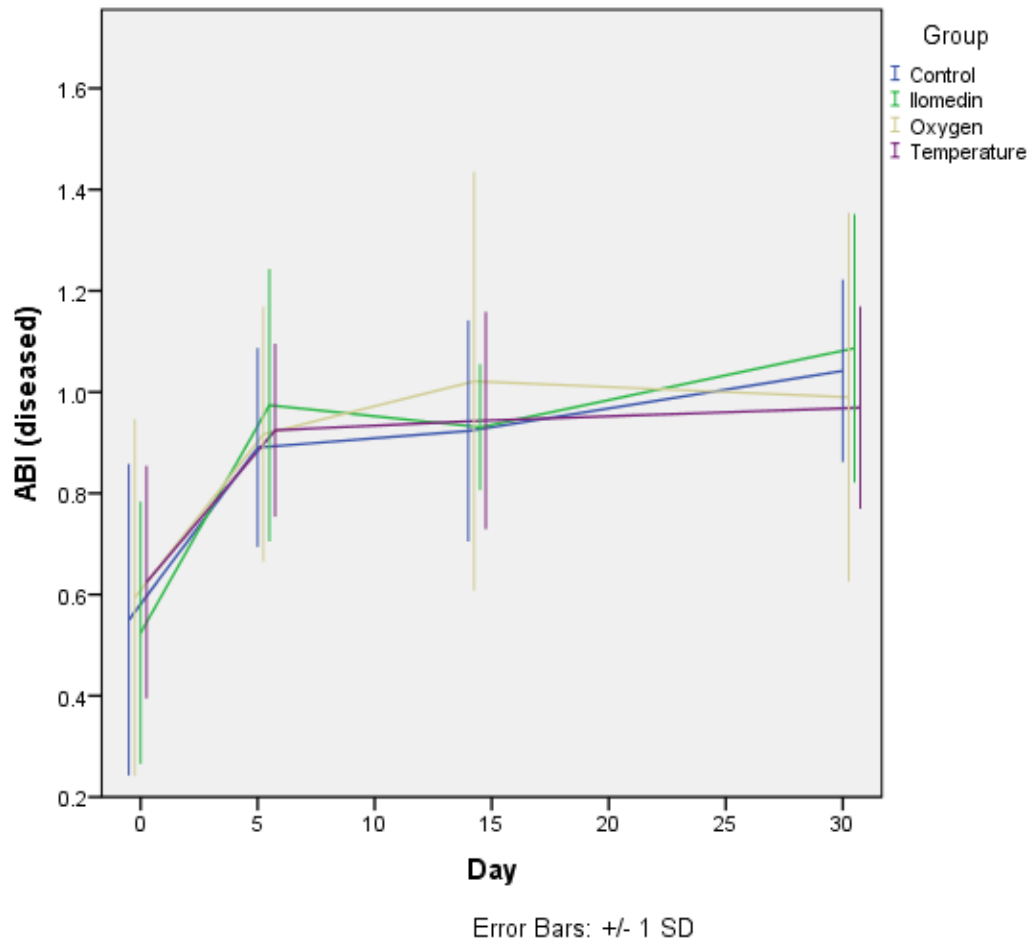


Figure 5. 7. Changes in ABI for the diseased limb over time. **Abbreviations:** ABI, ankle-brachial index; SD, standard deviation.

Tissue Oxygenation and Wound Healing in Vascular Surgery

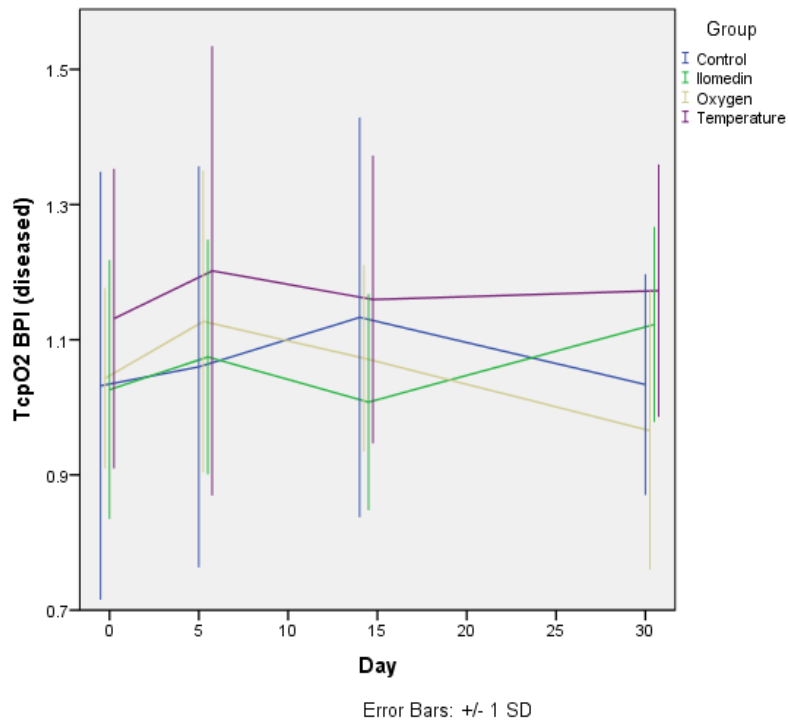


Figure 5. 8. Changes in TcpO₂ BPI for the diseased foot over time. **Abbreviations:** BPI, bilateral perfusion index; SD, standard deviation.

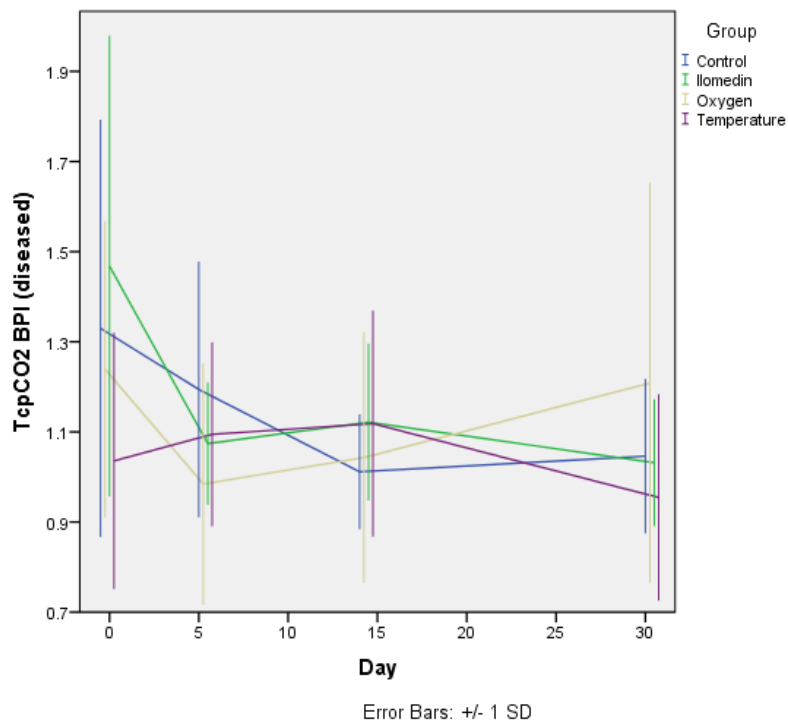


Figure 5. 9. Changes in TcpCO₂ BPI for the diseased foot over time. **Abbreviations:** BPI, bilateral perfusion index; SD, standard deviation.

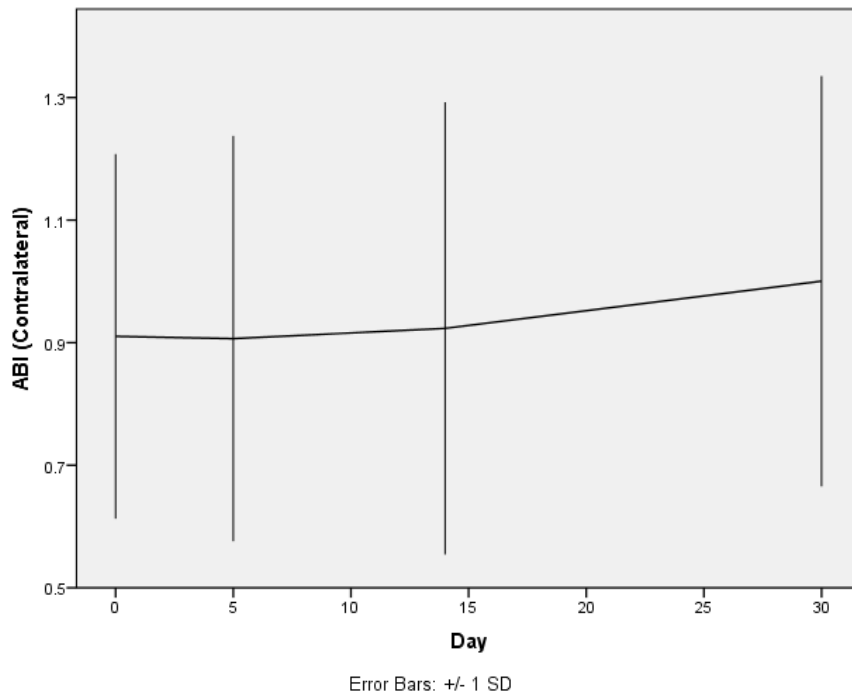


Figure 5. 10. Changes in ABI in the contralateral limb over time. **Abbreviations:** ABI, ankle-brachial index; SD, standard deviation.

Tissue oxygenation at the foot

When changes in skin perfusion at the wound site and foot indicated by TCOM and OxyVu readings (absolute values and BPI) in each treatment group were compared with those in the control group, there were several statistically significant differences (Student's *t*-test; Figures 5.3–5.9). Descriptive statistics and *p*-values for all variables are not described here. Table 5.5 details differences that are statistically significant at $p < 0.05$. Of note, the *p*-values were not corrected for multiple comparisons. Care should be taken when interpreting these *p*-values, given that this study failed to meet the primary outcome measure. Peripheral blood flow to the foot on day 5 appeared to be increased following a course of Ilomedin. Oxygenation at the foot appeared to be better in the control group than in the oxygen and temperature groups. There was a significant reduction in HT-Deoxy on day 5 in the control group when compared with the oxygen and temperature groups. There was also a significant decrease in HT-Sat in the temperature group for up to 14 days.

Accumulation of OHP was not influenced by transcutaneous oxygenation at the surgical incision site (Pearson's correlation; *p*-values not shown).

VARIABLES	GROUP	DAY	TREATMENT ARM (%)	CONTROL (%)	P-VALUE
HT-Deoxy	Oxygen	5	0	-18.1	0.037
HT-Sum	Ilomedin	5	0	-14.6	0.045
HT-Deoxy	Temperature	5	-2.2	-12.2	0.039
HT-Sat	Temperature	1	-1.4	10.0	0.044
		3	-1.9	8.3	0.050
		5	-7.7	5.3	0.04
		14	-12.8	2.2	0.007
HT-Sat BPI	Temperature	14	-3.6	14.9	0.026

Table 5. 5. Summary of statistically significant changes in OxyVu™ readings at the foot in the treatment arms versus the control group.

GROUP	CONTROL	OXYGEN	ILOMEDIN	TEMPERATURE	TOTAL
SSI	7	6	6	8	28
Major SSI	3	0	2	0	5
Dehiscence	2	6	3	5	16
Major dehiscence	0	0	1	1	2
Lymphatic Complications	5	8	4	6	23
ACS	0	3	1	1	5
LRTI	0	1	1	0	2

Table 5. 6. Summary of postoperative complications. **Abbreviations:** SSI, surgical site infection; ACS, acute coronary syndrome; LRTI, lower respiratory tract infection.

Complications

Wound complications (such as surgical site infection and dehiscence) and systemic complications (such as acute coronary syndrome and lower respiratory tract infection) within 30 days following surgery are described in Table 5.6. Surgical site infections were defined as per the criteria set by the Centers for Disease Control and Prevention. Major complications were defined as those requiring hospitalisation for intravenous antibiotics or surgical intervention. One patient in the oxygen group had a PTFE bypass graft explanted within 30 days secondary to infection. There was no difference in prevalence of complications between the treatment arms and the control group (Fisher's Exact test; p-values not shown).

Long-term follow-up

GROUP		CONTROL	OXYGEN	ILOMEDIN	TEMPERATURE
Primary patency rate (%)	1 month	89	84	94	88
	12 months	47	51	40	58
Secondary patency rate (%)	1 month	94	89	100	94
	12 months	58	61	53	81
Limb salvage (%)	12 months	72	95	82	94
Overall survival (%)	12 months	89	95	95	88

Table 5. 7. Patency, limb salvage, and mortality rates in the four groups.

Patients were followed until June 2013, with a mean follow-up period of 1,035 days. Patency rates (primary and secondary), limb salvage rates, and mortality rates were determined using Kaplan-Meier survival analysis and are shown in Table 5.7. Overall primary and secondary patency rates at 12 months were 53% and 67%, respectively, while the limb salvage rate at 12 months was 86%. There was no difference in these rates between the treatment arms and the control group (p-values not shown). While the secondary patency rate at 12 months in the

control group (58%) appeared to be lower than in the temperature group (81%), the difference was not statistically significant ($p=0.22$). Similarly, the limb salvage rate at 12 months in the control group (72%) was not significantly different from that in the oxygen group or the temperature group (95% and 94%; $p=0.78$ and $p=0.23$, respectively).

6 Results: Validation of FastScan™ and Silhouette Mobile™

Patient recruitment

This study included 16 wounds in 11 patients with vascular disease. Nine patients were White and two were Maori. The median age was 77 (range 57–86) years. The majority of wounds were diabetic or pressure ulcers (Figure 6.1), with some open postoperative wounds from amputations and infected surgical wounds (Figures 6.2–6.5). Wound locations included the toe (n=4), foot (n=5), calf (n=3), Achilles tendon region (n=1), heel (n=1), open sites at the knee stump following a major amputation (n=1), and the medial thigh (n=1). The average volume and depth measured by computed tomography (CT) were 4.63 (0–23.5) cm³ and 1.28 (0–4.9) cm, respectively.



Figure 6. 1. Image of several lower limb diabetic ulcers from the Silhouette Mobile™.



Figure 6. 2. Image of an infected surgical wound on a lower limb from the Silhouette Mobile™.

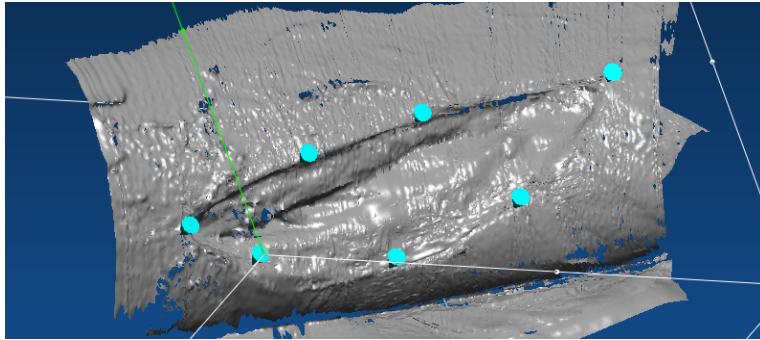


Figure 6. 3. Image of an infected surgical wound on a lower limb from the FastScan™. The blue stylus points give an outline of the wound boundary.



Figure 6. 4. Image of an open foot wound following digital amputation from the Silhouette Mobile™.

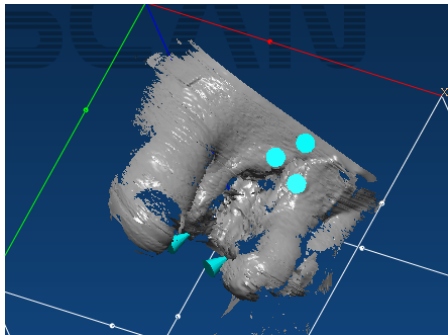


Figure 6. 5. Image of an open foot wound following digital amputation from FastScan™.

Sixteen sets of wound measurements were analysed by Silhouette Mobile™ (SM) and three-dimensional CT reconstruction. Only eleven sets of wound measurements were compared between FastScan™ (FS) and CT because of suboptimal imaging in the remaining five sets. This occurred particularly in small and superficial wounds or when too few stylus laser points (i.e., blue dots in Figure 6.3) were used to outline the wound with the FS. The stylus points impact the ability to carry out the necessary calculations using the Delta software.

Evaluation of intra-operator and inter-operator reliability

SILHOUETTE MOBILE™	INTRA-ICC (AVERAGE)	INTER-ICC (AVERAGE)
Volume	0.97 (0.99)	0.97 (0.99)
Depth	0.97 (0.99)	0.94 (0.98)
Surface area	0.99 (1.00)	0.99 (1.00)

Table 6. 1. Intra-operator and inter-operator reliability of Silhouette Mobile™. **Abbreviation:** ICC, intraclass coefficient

FASTSCAN™	INTRA-ICC (AVERAGE)	INTER-ICC (AVERAGE)
Volume	0.96 (0.99)	0.97 (0.99)
Depth	0.95 (0.98)	0.98 (0.99)
Surface area	0.99 (1.00)	0.99 (1.00)

Table 6. 2. Intra-operator and inter-operator reliability of the FastScan™. **Abbreviation:** ICC, intraclass coefficient

Intraclass correlation coefficients of at least 0.94 indicated excellent intra-operator and inter-operator reliability for the SM and FS in assessing the surface area, depth and volume, as shown in Tables 6.1 and 6.2. The depth varied slightly more than the other measures.

Correlation between SM and FS versus CT reconstruction

The mean values of the three repeated FS and SM readings from the three operators were compared (16 comparisons for SM and eleven for FS). Table 6.3 shows the mean differences and standard deviations for surface area, maximum depth, and volume measurements when comparing the different measurement modalities. Surface area was not able to be measured using the three-dimensional CT reconstruction software.

Ideally, the mean difference in a measurement obtained by two different recording devices (e.g., SM volume and CT volume) should be zero with a standard deviation of zero, and there should not be a statistically significant difference using the Student's *t*-test. There was

statistically significant difference in SM volume when compared with CT volume, and for FS depth and FS volume when compared with CT depth and CT volume. Depth measurements using SM were significantly smaller than those using CT (-0.65 cm; $p=0.04$). SM appeared to be consistently underestimating the wound dimensions produced by CT, whereas FS tended to overestimate them. While surface area measurements obtained by SM and FS were not compared with those obtained by CT, they were compared with each other. Surface areas measured by SM were on average underestimated by 1.6 cm² ($p=0.02$).

COMPARISONS	MEAN DIFFERENCE	SD	P-VALUES
SM volume – CT volume	-0.93	4.0	0.37
SM depth – CT depth	-0.65	1.2	0.040
FS volume – CT volume	14.0	48.7	0.36
FS depth – CT depth	0.77	3.2	0.45
SM volume – FS volume	-16.0	50.9	0.32
SM depth – FS depth	-1.3	3.5	0.26
SM SA – FS SA	-1.64	2.0	0.02

Table 6. 3. Depth and volume measurements using the SM compared with those obtained by CT. **Abbreviations:** SM, Silhouette Mobile™, CT, computed tomography; SA, surface area; SD, standard deviation

Although no differences were detected when comparing the CT volume and the SM volume with the FS volume, the mean differences suggested that the FS volumes were overestimated by 14 cm³ and 16 cm³, respectively, with a large standard deviation. In patient 10, the volumes measured by FS were about 10 times larger than measured by CT. This did not appear to be a technical error, because the FS recordings in this patient were similar to the repeated measurements taken by the three operators. If patient 10 was excluded from the analysis, the

difference in mean volume between FS and CT was -0.66 cm^3 (standard deviation 1.2; $p=0.10$), and that between SM and FS was -0.70 cm^3 (standard deviation 2.0; $p=0.30$).

Bland-Altman plots were used to compare SM and FS with three-dimensional CT reconstruction. The x-axis represents the average measurements for depth or volume produced by CT and the FS or by CT and the SM. The y-axis plots the subtracted difference in values between CT and FS or between CT and SM, and therefore the error.

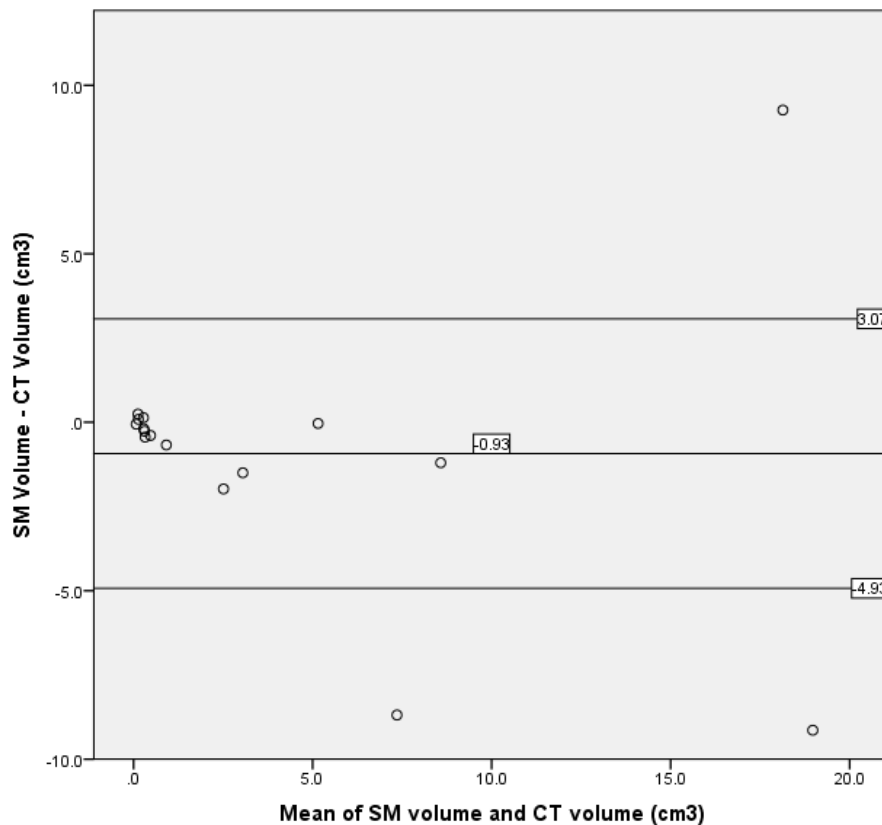


Figure 6. 6. Bland-Altman plot showing the difference in volume measurements between the Silhouette Mobile™ and CT. **Abbreviation:** CT, computed tomography

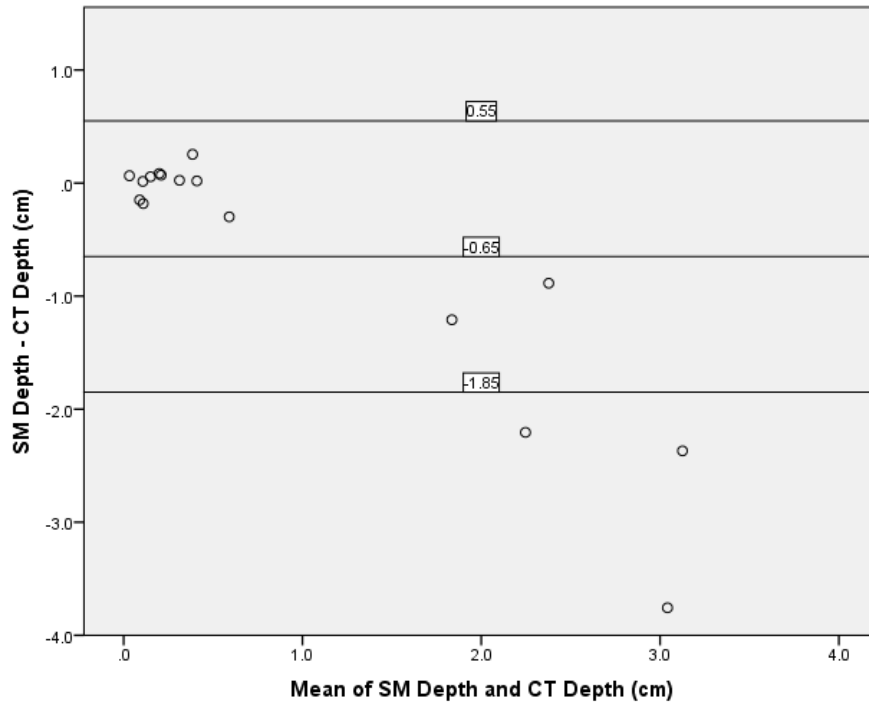


Figure 6. 7. Bland-Altman plot showing the difference in depth measurements between the Silhouette Mobile™ and CT. **Abbreviation:** CT, computed tomography

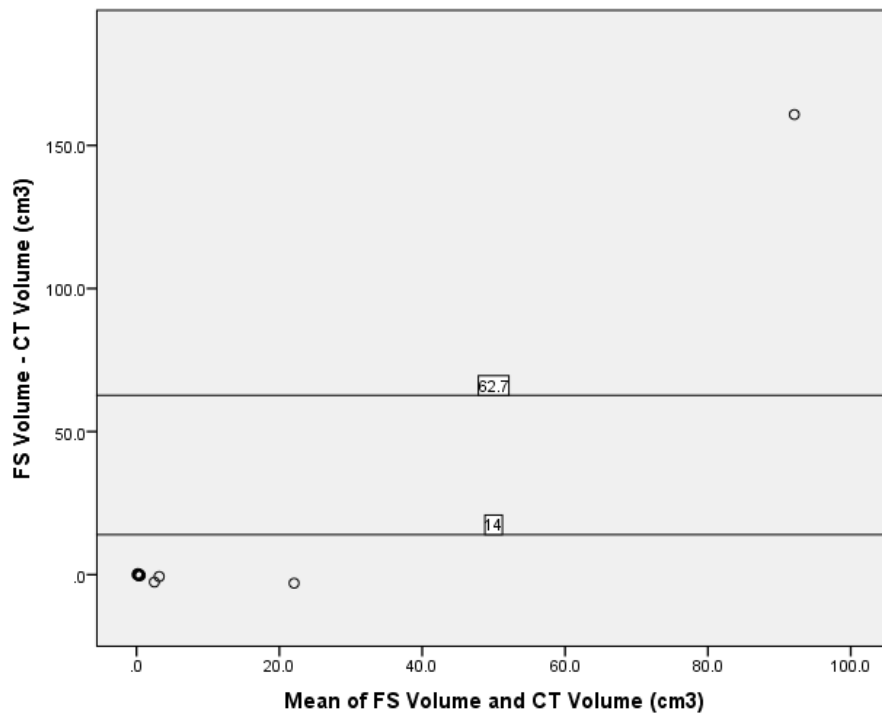


Figure 6. 8. Bland-Altman plot showing the difference in volume measurements between the FastScan™ and CT. **Abbreviation:** CT, computed tomography

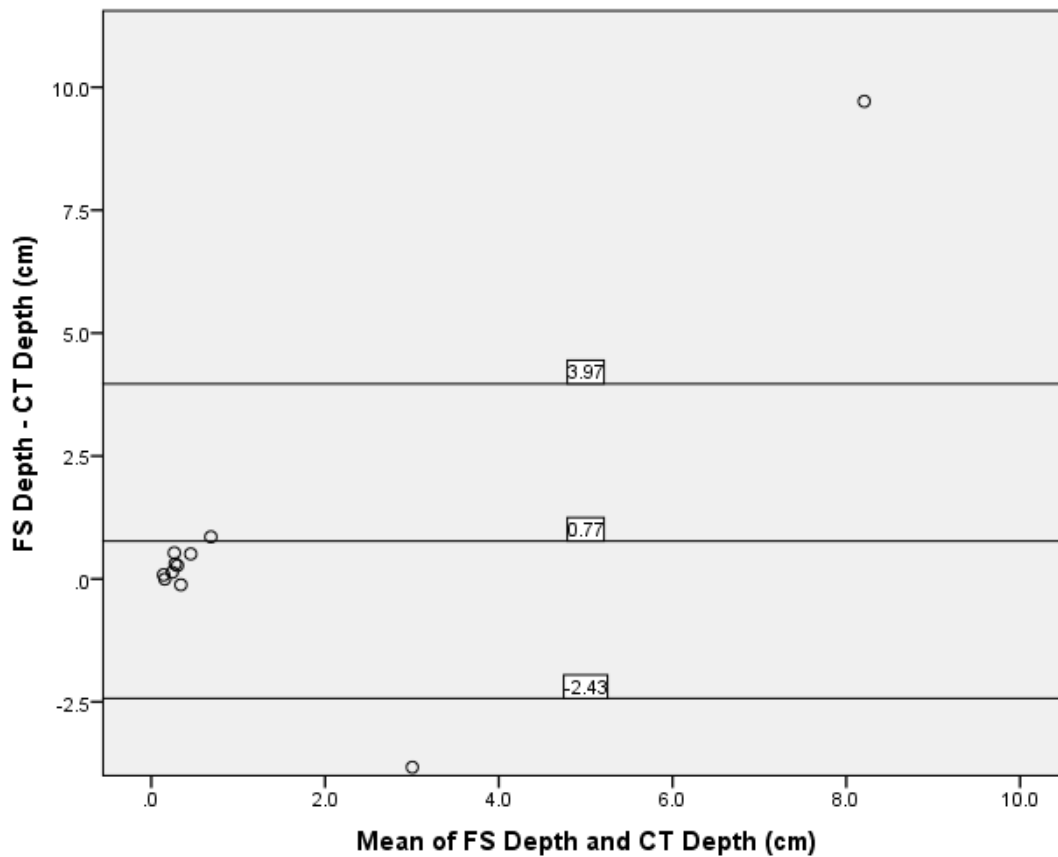


Figure 6. 9. Bland-Altman plot show the difference in depth measurements between the FastScan™ and CT. **Abbreviation:** CT, computed tomography.

The primary observation was that a negative difference in SM volume and depth existed for CT (Figures 6.6 and 6.7). This implies that most CT measurements were higher than those obtained by SM. A systematic bias could be deduced from this pattern of underestimation from SM. For FS, in contrast, a pattern of overestimation was observed, with most points lying above the zero line in the Bland-Altman plots (Figures 6.8 and 6.9).

Ideally, the SM and FS outcomes should be the same as the CT outcomes (Pearson’s correlation coefficient 1). Table 6.4 shows a strong linear correlation for SM depth and SM volume when compared with CT, with Pearson’s correlation coefficients (r) of 0.81 and 0.88, respectively. Neither volumetric nor depth assessments with FS were significantly consistent with CT. However, if the correlation tests for volume were repeated without patient 10, they yielded strong correlations between FS and CT ($r=0.99$; $p\leq 0.0001$) and between FS and SM ($r=0.99$; $p\leq 0.0001$).

SYSTEMS	MEASUREMENTS	CORRELATION COEFFICIENTS (R)	P-VALUE
SM versus CT	Volume	0.81	<0.0001
	Depth	0.88	<0.0001
FS versus CT	Volume	0.45	0.16
	Depth	0.54	0.09
SM versus FS	Volume	0.19	0.58
	Depth	0.65	0.03
	Surface area	1.00	<0.0001
<i>Excluding patient 10</i>			
FS versus CT	Volume	0.99	<0.0001
SM versus FS	Volume	0.99	<0.0001

Table 6. 4. Summary of Pearson's correlation coefficients when comparing measurements for the Silhouette Mobile™, FastScan™, and CT. **Abbreviation:** CT, computed tomography

7 Results: Wound healing and tissue oxygenation in TNP therapy

Patient recruitment and demographics

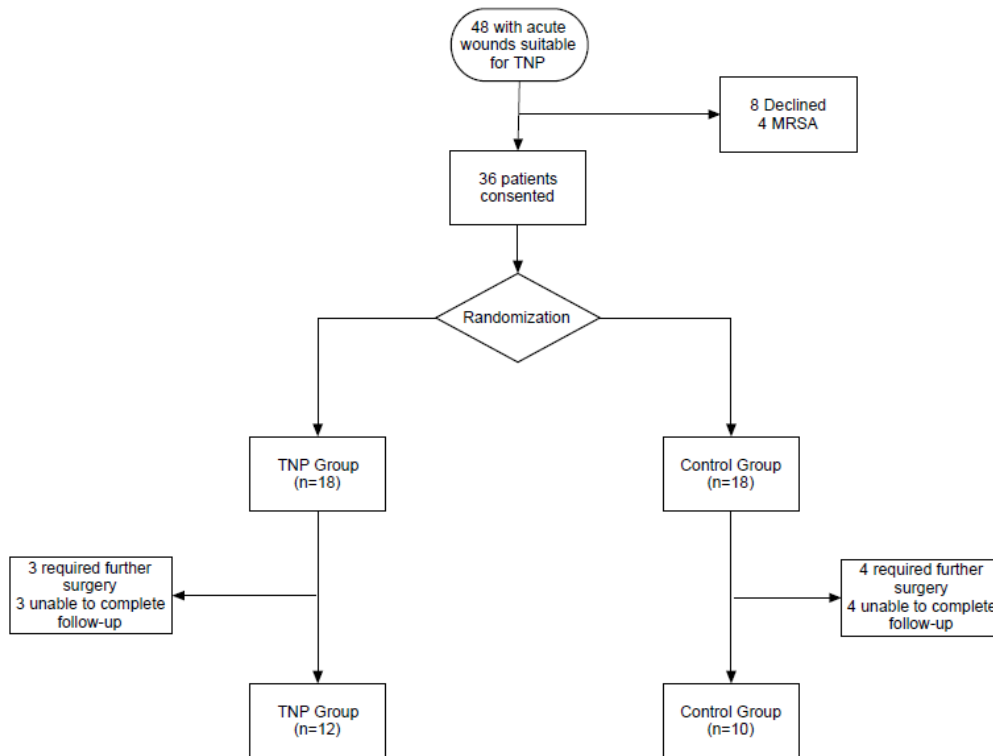


Figure 7. 1. Flow diagram detailing the recruitment process.

Recruitment commenced in March 2010 and ended in June 2011. Twenty-two patients completed the study (12 in the treatment arm and ten in the control arm; Figure 7.1). On average, TNP was used for 10.6 ± 3.7 days in the treatment group. Fourteen patients (63.6%) were men and seven (31.8%) were Maori. The mean patient age was 61.5 ± 13 (range 41–83) years. Twenty patients (86.4%) had diabetes and 14 of these were on insulin. Twelve (54.5%) had renal impairment and nine were dialysis-dependent. The two patients who did not have diabetes had end-stage renal failure. Table 7.1 details the basic demographic and clinical characteristics of the two arms. There were no differences between the two groups for wound location, past history of major and minor amputations, or ankle-brachial pressure index. The erroneously “normal” ankle-brachial pressure index was probably reflective of the stiff calcified vessels that can be found in patients with diabetes and/or renal disease. Definitions of these variables are found in Appendix A.1.1.

	CONTROL GROUP (N=10)	TNP GROUP (N=12)	P-VALUE
Male	6	8	0.75
Maori	3	4	0.87
Age, years	62.0	61.0	0.86
BMI	27.1	27.4	0.93
Smoking history			0.35
Active smoker	4	2	
Ex-smoker	3	7	
Non-smoker	3	3	
Diabetes	10	10	0.24
On insulin	7	7	0.61
Renal impairment	4	8	0.24
ESRF	3	6	0.41
IHD	8	7	0.28
COPD	3	3	0.79
Hypertension	10	12	1.00
Dyslipidaemia	7	10	0.46
Previous amputations	6	7	0.94
Location of wound			0.26
Toe	7	5	
Forefoot	3	5	
Heel	0	2	
ABI	1.21	1.18	0.93
On antibiotics	8	6	0.25

Table 7. 1. Basic patient demographic and clinical characteristics. **Abbreviations:** ABI, ankle-brachial index; BMI, body mass index; COPD chronic obstructive pulmonary disease; ESRF, end-stage renal failure; IHD, ischaemic heart disease; TNP, topical negative pressure

Changes in wound dimensions

	CONTROL GROUP	TNP GROUP	P-VALUE
	MEAN (SD)	MEAN (SD)	
“Body” surface area (cm ²)	32.9 (16.2)	38.8 (16.6)	0.41
“Cap” surface area (cm ²)	27.0 (14.9)	29.5 (13.2)	0.69
Maximum depth (mm)	14.0 (5.1)	13.6 (6.4)	0.89
Mean depth (mm)	2.9 (1.6)	2.7 (2.0)	0.85
Volume (cm ³)	7.1 (4.6)	6.3 (4.3)	0.70

Table 7. 2. Summary of wound dimensions at day 0.

On day 0, there was no difference in wound surface area, depth, or volume between the TNP group and the control group (Student’s *t*-test; Table 7.2). The “body” surface area (surface area of the wound) was often irregular, with variable wound contour and areas of concavity and convexity. Therefore, this was larger than the “cap” surface area (surface area of the wound at the skin surface) that was assumed to have a flat surface by the computer software.

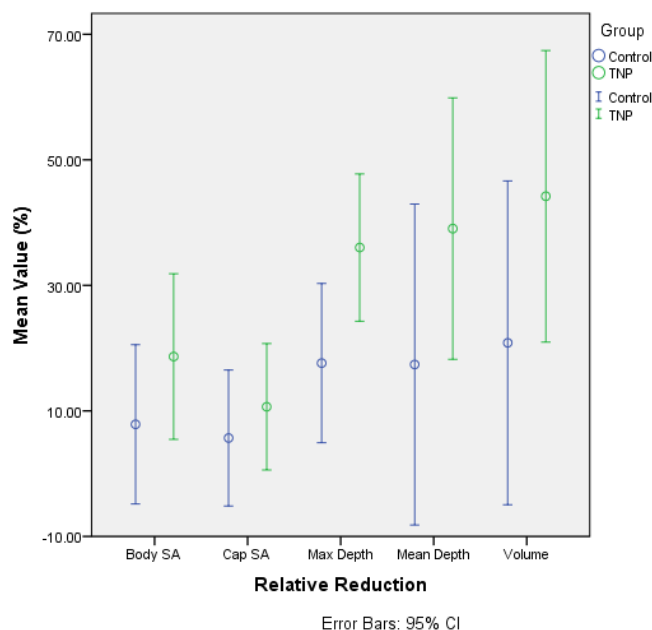


Figure 7. 2. Error bar graph showing the mean ± 95% CI of the relative reduction of various wound dimensions between the two groups. **Abbreviations:** CI, confidence interval; SA, surface area; TNP, topical negative pressure

	CONTROL GROUP (SD)	TNP GROUP (SD)	P-VALUE
<i>Absolute reduction from day 0 to day 14</i>			
“Body” surface area (cm²)	2.7 (7.1)	7.0 (9.7)	0.24
“Cap” surface area (cm²)	1.6 (5.7)	2.2 (3.9)	0.77
Maximum depth (mm)	2.3 (2.6)	4.9 (4.0)	0.09
Mean depth (mm)	0.5 (0.8)	1.2 (1.2)	0.11
Volume (cm³)	1.5 (2.8)	3.2 (3.3)	0.21
<i>Relative reduction from day 0 to day 14</i>			
“Body” surface area (%)	7.9 (17.7)	18.7 (20.8)	0.20
“Cap” surface area (%)	5.7 (15.2)	10.7 (15.9)	0.46
Maximum depth (%)	17.6 (17.7)	36.0 (18.5)	0.03
Mean depth (%)	17.4 (35.7)	39.0 (32.8)	0.16
Volume (%)	20.9 (36.1)	44.2 (36.6)	0.15

Table 7. 3. Summary of absolute and relative reduction in wound dimensions between the two treatment groups.

Abbreviations: SD, standard deviation; TNP, topical negative pressure

Table 7.3 shows the degree of reduction of wound dimensions as a result of the specific wound dressing regimes used and describes the absolute and relative reductions. While the primary outcome of the study in terms of wound volume reduction at day 14 did not yield statistically significant results with regard to either absolute or relative reduction to suggest that TNP therapy would expedite wound healing, there were constant trends indicating that TNP enhanced reduction in wound surface area, depth, and volume when compared with traditional dressings (Student's *t*-test). Wound volume reduction in the TNP group appeared to be twice that in the traditional dressing group (44.2% versus 20.9%; $p=0.15$). The relative maximum reduction in depth in the TNP group was significantly greater than in the control group (39.0% and 17.4%, respectively; $p=0.03$).

While there were no statistically significant differences in wound location between the groups, there appeared to be more wounds in the TNP group at the forefoot and the heel (n=7) than in the control group (n=3). It could be argued that the findings in Table 7.3 represent “false positives” because the healing potential at the two sites might be different. Therefore, wound healing rates at the toes and above the toes (forefoot and heel) were compared.

	TOE (SD)	FOREFOOT/HEEL (SD)	P-VALUE
“Body” surface area (cm ²)	26.8 (14.7)	47.3 (10.1)	0.001
“Cap” surface area (cm ²)	20.9 (13.5)	37.3 (7.2)	0.002
Maximum depth (mm)	13.6 (4.6)	13.9 (7.1)	0.91
Mean depth (mm)	3.3 (1.7)	2.2 (1.9)	0.18
Volume (cm ³)	6.1 (3.4)	7.3 (5.2)	0.55

Table 7. 4. Wound dimensions at day 0 for wounds at the toe and those at forefoot/heel. **Abbreviation:** SD, standard deviation

	TOE (SD)	FOREFOOT /HEEL (SD)	P-VALUE
Absolute reduction from day 0 to 14			
“Body” surface area (cm ²)	5.1 (6.3)	5.0 (11.3)	0.98
“Cap” surface area (cm ²)	2.7 (4.6)	1.0 (4.9)	0.41
Maximum depth (mm)	4.4 (3.9)	2.9 (3.3)	0.32
Mean depth (mm)	1.0 (1.1)	0.7 (1.0)	0.58
Volume (cm ³)	2.4 (2.6)	2.5 (3.8)	0.97
Relative reduction from day 0 to 14			
“Body” surface area (%)	17.7 (19.3)	9.0 (20.2)	0.32
“Cap” surface area (%)	11.7 (15.7)	4.4 (14.8)	0.28
Maximum depth (%)	31.4 (19.4)	23.1 (20.8)	0.35
Mean depth (%)	31.5 (30.8)	26.5 (41.2)	0.76
Volume (%)	37.7 (32.7)	28.7 (43.7)	0.60

Table 7. 5. Absolute and relative reductions in wound dimension between wounds at the toes and those at the forefoot and heel. **Abbreviation:** SD, standard deviation

As expected, the mean surface area of the toe wounds at day 0 was smaller than those of wounds at the forefoot and heel; however, depth and volume measurements were similar between the two groups (Student's *t*-test; Table 7.4). Wound healing rates at the toes were not different from those at the forefoot and heel (Student's *t*-test; Table 7.5). This would suggest that the trends observed in Table 7.3 comparing healing potential between the TNP group and the control group were not influenced by location of the wounds.

Changes in collagen content of granulation tissue

The OHP content in tissue biopsies sampled from the wound beds on days 0 and 14 was analysed and expressed in micrograms of collagen per milligram of granulation tissue. There was no difference in OHP levels between the groups at baseline (Student's *t*-test; Table 7.6). Irrespective of the type of dressing used, the mean increase in OHP over 14 days was 0.62 ± 1.02 $\mu\text{g}/\text{mg}$ and this was statistically significant (Student's *t*-test; $p=0.01$). Relative changes measured from day 0 were calculated as percentages. At variance with the study hypothesis, 63% more OHP was found in the control group than in the TNP group (94.5% versus 58%, respectively; $p=0.32$; Student's *t*-test), although this finding was not statistically significant

	CONTROL GROUP (SD)	TNP GROUP (SD)	P-VALUE
OHP at day 0 ($\mu\text{g}/\text{mg}$)	1.29 (0.51)	1.97 (1.61)	0.21
OHP at day 14 ($\mu\text{g}/\text{mg}$)	2.25 (1.10)	2.32 (0.97)	0.89
Percent increase in OHP	94.5 (86.7)	58 (68)	0.32

Table 7. 6. Summary of mean OHP findings at baseline and percentage increase at 14 days for the TNP group and the control group. **Abbreviations:** OHP, hydroxyproline; SD, standard deviation

Changes in growth factor and cytokine levels

Technical issues were encountered when performing the biochemical analyses for FGF-2, VEGF, IL-8, and TNF- α using Milliplex®. Wound fluids were difficult to extract from the dressings. Alginates and hydrofibres are absorbants designed to trap moisture. Despite aggressive centrifugation, many samples returned insufficient fluid. Similarly, most of the

wound fluid in the foam sponge in the VAC® was drawn into the sealed cylinder and emulsified with the gel inside the container. The wound fluid inside the sponge in contact with the wound bed was often minimal. Fluid trapped in the suction tube was also sampled to test the balance between levels of growth factors in wound fluid that was in direct contact with the wound and wound fluid that was suctioned. However, the fluid volume was again often inadequate. Wound fluid from the hydrogels was often contaminated with gel products that increased fluid viscosity. This, together with the fact that these fluids often contained blood, with infiltration of debris and protein, meant that many samples could not be analysed. Interrogation of the samples that were successfully processed did not yield reliable statistically significant results.

Analysis of TGF-β by enzyme-linked immunosorbent assay was more successful. Baseline levels on day 2 were not significantly different between the groups (Student's *t*-test; Table 7.7). The relative percent increase in TGF-β in the control group was 106% but was 89.5% in the TNP group; again, there was no statistically significant difference between the two groups, and the pattern of change was similar to that for OHP.

	CONTROL GROUP (SD)	TNP GROUP (SD)	P-VALUE
TGF-β at day 0 (ng/mL)	503 (287)	647 (507)	0.45
Percent increase in TGF-β	106 (281)	89.5 (359)	0.92

Table 7. 7. Mean TGF-β findings at baseline and mean percentage increase at 14 days for the TNP group and the control group. **Abbreviations:** SD, standard deviation; TGF-β, transforming growth factor beta

Changes in skin perfusion

Skin perfusion was determined by OxyVu at baseline and on day 14. There were no statistically significant differences between the groups at these two time points, although it appeared that wound oxygenation in the TNP group decreased to a lesser degree (Student's *t*-test; Table 7.8). When all patients in both groups were considered together, HT-Oxy, HT-Sat, and HT-Sum had decreased significantly by the end of the study when compared with baseline (Student's *t*-test; Table 7.9). This indicates that oxygen saturation and blood flow around the wound decreased as the wound healed.

	CONTROL GROUP (SD)	TNP GROUP (SD)	P-VALUE
At baseline			
HT-Oxy (AU)	83.5 (23.0)	82.3 (22.4)	0.92
HT-Deoxy (AU)	62.3 (15.8)	60.7 (19.1)	0.86
HT-Sat (%)	56.1 (2.9)	56.9 (6.5)	0.71
HT-Sum (AU)	146 (38.3)	143 (35.4)	0.89
Percent change at day 14			
HT-Oxy	-28.4 (31.0)	-22.4 (33.4)	0.79
HT-Deoxy	-25.0 (20.4)	-4.2 (19.4)	0.21
HT-Sat	-19.4 (28.3)	-12.0 (20.0)	0.70
HT-Sum	-27.3 (25.0)	-15.3 (24.9)	0.52

Table 7. 8. OxyVu™ findings at baseline and mean percentage increase at 14 days in the TNP group and the control group. **Abbreviations:** SD, standard deviation; TNP, topical negative pressure

	MEAN DIFFERENCE (SD)	P-VALUE
Day 14 – day 0		
HT-Oxy	-22.1 (29.4)	0.02
HT-Deoxy	-7.2 (13.7)	0.10
HT-Sat	-8.2 (12.3)	0.04
HT-Sum	-29.3 (38.2)	0.02

Table 7. 9. Comparison of OxyVu™ findings at baseline and day 14, showing mean differences and their p-values. **Abbreviation:** SD, standard deviation

Clinical outcome

Wound failure-free, major amputation-free survival, and overall survival rates were examined using Kaplan-Meier survival analysis. Wound failure was defined as requirement for further

surgical debridement or distal or major amputations after day 14. The overall wound failure-free rate was 95.5% at one month and 45.7% at 12 months; limb salvage rates were 95.5% at one month and 60.3% at one year; and overall survival at one month was 95.5% and that at 12 months was 72.7%. Survival analyses comparing the three outcomes between the two groups did not show significant differences (Table 7.10 and Figure 7.2).

	CONTROL GROUP		TNP GROUP		P-VALUE
	At 1 month	At 12 months	At 1 month	At 12 months	
Wound failure-free (%)	80	40	91.7	50.9	0.70
Amputation-free (%)	100	70	91.7	50.9	0.29
Survival (%)	100	70	91.7	75.0	0.95

Table 7. 10. Comparison of survival analysis outcome between TNP group and control group. **Abbreviation:** TNP, topical negative pressure.

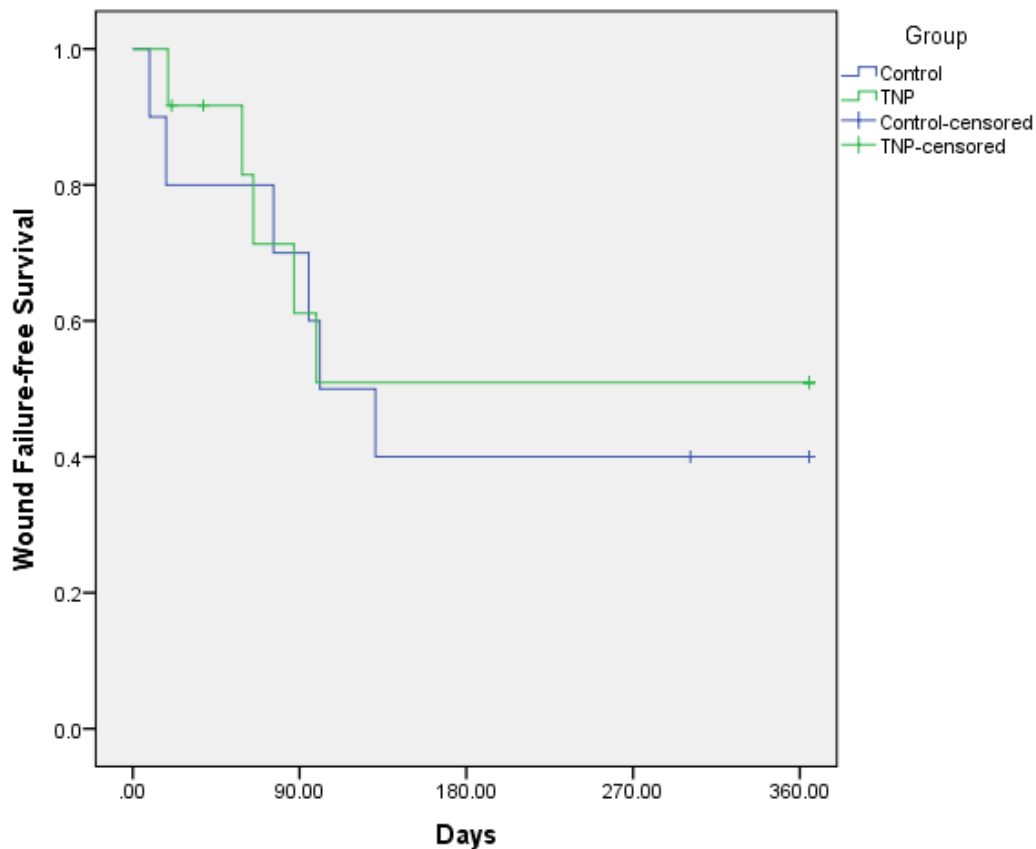


Figure 7. 3. Kaplan-Meier curve showing wound failure-free survival between the two groups.

8. Discussion

8.1 Key findings

Validation of OxyVu™

Inter-operator reliability ranged from 86% to 94% across the four OxyVu™ outputs, whilst intra-operator reliability ranged from 92% to 94%. HT-Oxy, HT-Sat, TcpCO₂ and ABI in the diseased limb correlated significantly with the severity of PVD. HT-Sat significantly correlated with TcpO₂ (R=0.19), TcpCO₂ (R= -0.26), ABI (R=0.19), and skin temperature (R=0.56). HT-Deoxy also correlated with TcpCO₂ (R=0.27). Using reference points such as the contralateral limb (i.e., BPI) did not appear to offer better correlations than absolute values. Hyperspectral oxygenation correlated with other modalities, and may be a superior method for assessment of tissue oxygenation in appropriate clinical settings, given that it was easy to operate and provided immediate non-invasive measurements. The results of the validation study justified use of the OxyVu to assess tissue oxygenation in the subsequent studies.

WOIOW study

Whilst the intra-operative arterial partial pressure of oxygen was higher in the oxygen group and the core temperature immediately after surgery appeared to be higher in the temperature group than in the control group (37.1°C versus 36.7°C, respectively; p=0.09), no differences were demonstrated when the treatment arms were compared with the control group in terms of the primary outcome of hydroxyproline (OHP), growth factor and cytokine levels, or change in tissue oxygenation at the site of the surgical incision on the knee and foot. The OHP level correlated with the amount of FGF-2 at the site of the surgical wound (Pearson's $r=0.38$, p=0.001). There were no differences in primary and secondary patency, limb salvage, SSI, or mortality rates between the treatment groups. The perioperative adjunctive treatments examined did not dramatically improve wound healing or tissue oxygenation.

Validation of FastScan™ and Silhouette Mobile™

Volumetric measurements using the FS and SM were not significantly different from those using CT. However, due to systematic bias, the SM consistently underestimated wound volume and depth compared with CT scanning. A pattern of overestimation was observed for the FS. Volume measurements in one patient were anomalous, being ten times larger than

those measured by CT. When the measurements for that patient were excluded, there was a much stronger correlation in wound volume for SM and CT ($r=0.81$; $p\leq 0.0001$), for FS and CT ($r=0.99$; $p\leq 0.001$), and for SM and FS ($r=0.99$; $p\leq 0.0001$). The intra-operator and inter-operator reliability values for volume recordings were 0.97 and 0.97, respectively, for the SM, and 0.96 and 0.97 for the FS.

Wound healing and tissue oxygenation in TNP therapy

All 22 patients had a past medical history of either diabetes mellitus or dialysis-dependent renal failure. No statistically significant difference in wound volume reduction was found between the two groups on day 14 (44.2% for TNP versus 20.9% for the control; $p=0.15$). Nevertheless, there was a trend towards a better healing rate in the TNP group in terms of surface area, depth, and volume. The relative reduction in maximum wound depth was statistically significant (36.0% for TNP versus 17.6% for the control; $p=0.03$). No differences were found with regard to changes in OHP levels, growth factors or cytokines, or in tissue oxygenation at day 14. There was no significant difference in wound failure-free rate, amputation-free rate, or survival rate at 12 months. Applying TNP to acute vascular foot wounds improved the wound healing rate, and in particular decreased the relative wound depth. Tissue oxygenation and OHP levels were not improved, suggesting the difference in healing rate might have been a result of macro-strain effects from contracting wound edges and decreasing tissue oedema.

8.2 Validation of OxyVu™

To date, this study is the largest and most extensive series validating hyperspectral oxygenation in patients with PVD. Various modalities were used for comparisons, including severity of PVD, skin temperature, ABI, and TCOM measurements. Hyperspectral oxygenation correlated with each one of these to some extent, indicating that the OxyVu was fulfilling the role that it was designed for, i.e., quantifying oxygenation. Unfortunately, even though TCOM has been considered to be most sensitive technique in the clinical setting for the last three decades because its $TcpO_2$ and $TcpCO_2$ measurements take into account both the macrocirculation and the microcirculation, it is not the gold standard and the OxyVu cannot be tested for superiority over other modalities. However, with the advantages described earlier, from a practical perspective it may be time now for a paradigm shift in support of the use of OxyVu in the clinical setting for diagnosis of PVD and assessment of its severity, prediction of wound healing, detecting a change in oxygenation following revascularisation, evaluation of the potential for hyperbaric oxygen therapy, and differentiation between ischaemic and neurogenic claudication, as well as in the many other settings where TCOM is currently used.

As hypothesised, HT-Sat was the most sensitive of the HTCOT measurements used, because it takes into account both the concentration of oxyhaemoglobin (oxygen delivery) and deoxyhaemoglobin (oxygen consumption) in a region of interest. HT-Sat was the only marker that correlated significantly with SSS ($R = -0.29$), ABI ($R = 0.19$), skin temperature ($R = 0.56$), $TcpO_2$ ($R = 0.19$), and $TcpCO_2$ ($R = -0.26$). Other findings of interest included HT-Deoxy correlating with $TcpCO_2$ ($R = 0.27$), HT-Oxy with SSS ($R = -0.29$), Sat-BPI with ABI ($R = 0.21$), skin temperature with HT-Oxy ($R = 0.41$), and skin temperature with HT-Deoxy ($R = -0.40$).

While there were associations between BPI from HTCOT and other oxygenation measurement methods, the correlation coefficients overall did not appear to be significantly higher than when comparing actual values. Theoretically, BPI would be useful when examining oxygenation at different time points, assuming there would be no relative change in oxygenation in the contralateral limb. Relative measurements such as BPI and RPI are prone to inaccuracies due to doubling of the operator variability, which was quantified in this study. Inter-operator reliability ranged from 86% to 94%, whereas intra-operator reliability ranged from 92% to 94%.

To some extent, the findings of this study are in contrast with those of the study by Chin *et al* discussed in Section 1.11.³¹⁴ HT-Oxy and HT-Sat correlated with the severity of PVD and HT-Deoxy did not. The ABI had no relationship with HT-Deoxy or HT-Oxy but did correlate with HT-Sat; the latter variable was not described by Chin *et al*.

While TcpO₂ can predict wound healing,²⁹⁰ this study did not show an interaction between TcpO₂, HT-Oxy, and/or the severity of PVD. Figure 8.1 shows TcpO₂ values according to the severity of PVD. Mean TcpO₂ was higher in the claudicant group than in the control group; despite the mean TcpO₂ being lowest in patients with CLI, the range and variance in the claudicant and CLI groups were larger than in the control group. This finding might be explained by the reactive hyperaemia that occurs in patients with PVD.

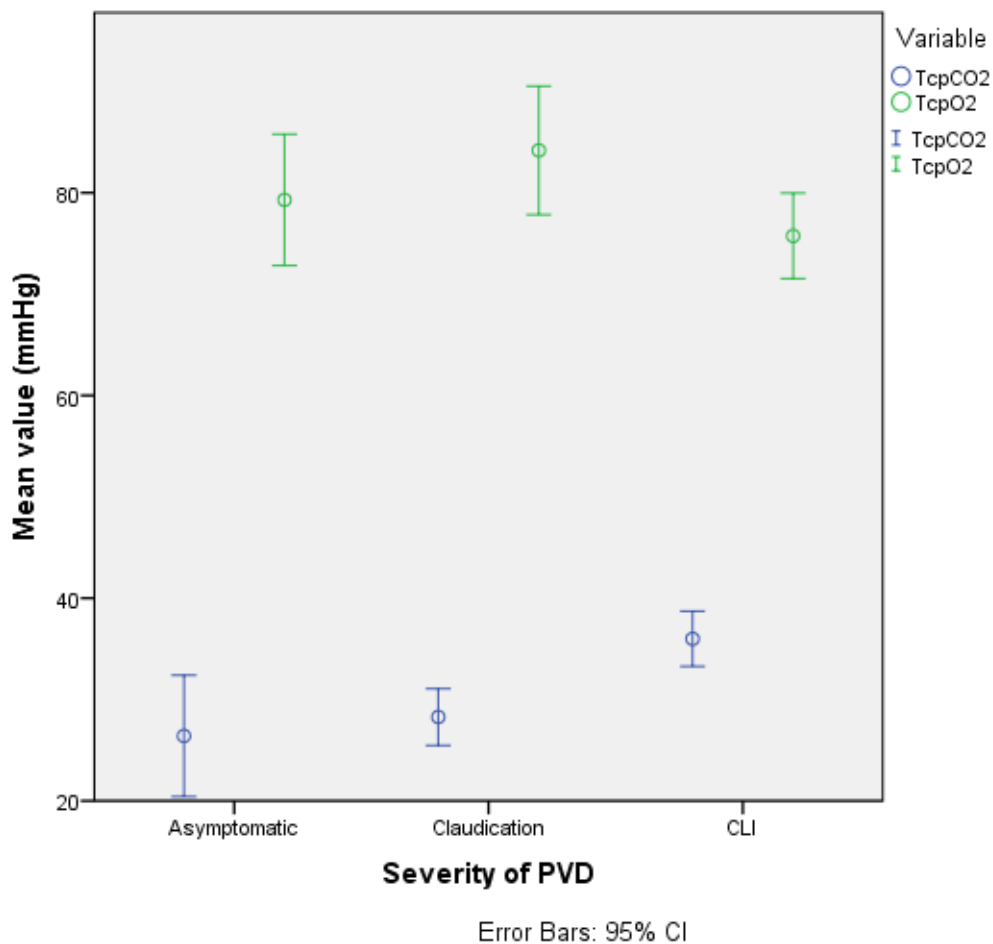


Figure 8. 1. Error bar graph showing the mean \pm 95% CI of TcpO₂ and TcpCO₂ in the diseased limb categorised according to severity of PVD. **Abbreviations:** CI, confidence interval; CLI, critical limb ischaemia; PVD, peripheral vascular disease; TCOM, transcutaneous oxygenation measurement.

In contrast, there was a relationship between $TcpCO_2$ and SSS ($R=0.34$; Figure 8.1). This was an unexpected finding, but not implausible. It was not only the quantity of oxygen delivered or available that was associated with tissue ischaemia, but also the accumulation of carbon dioxide in the tissue at the molecular level. This might be explained by the Bohr effect. The demand for oxygen is increased in ischaemic tissue, perhaps because of increased metabolism in non-healing ulcer tissue, which would produce more carbon dioxide. If there was an increase in $TcpCO_2$ in the ischaemic tissue, there would be a right shift in the oxygen-haemoglobin dissociation curve, promoting dissociation of oxygen from haemoglobin and maximising delivery of oxygen to the peripheral tissues. Simultaneously, the decrease in pH resulting from increased carbon dioxide and lactic acidosis, together with impairment of the peripheral sympathetic autonomic vasoregulation mechanism in the venoarterioles as a result of ischaemia or neuropathy, could cause reactive hyperaemia in an attempt to maximise blood flow from the microcirculation to the tissue and decrease capillary resistance.⁴⁰⁸ Despite this, the flow velocity might be low. This factor and perhaps increased production of carbon dioxide as a result of increased metabolism might affect the diffusion gradient transporting carbon dioxide out of the tissue. Previous studies in patients with vascular disease had mainly used $TcpO_2$ to evaluate wound healing. However, although information on its role in wound healing is limited, $TcpCO_2$ might be a more sensitive marker for determining the severity of PVD and predicting the outcome. It would be interesting to test the hypothesis that measuring $TcpCO_2$ in vascular patients during exercise testing can detect underlying PVD.

The only link yet to be explained here was why $TcpCO_2$ correlated with HT-Deoxy when HT-Deoxy did not correlate with the severity of PVD. In addition, HT-Oxy correlated with severity but did not correlate with $TcpO_2$. The latter could be explained by potential false-negative findings, or perhaps HT-Oxy was better than $TcpO_2$ for detection of PVD. Physiologically, HT-Deoxy and $TcpCO_2$ are two separate entities. HT-Deoxy reflects the amount of deoxyhaemoglobin in the tissue and $TcpCO_2$ quantifies the carbon dioxide concentration. An increase in the carbon dioxide level would not directly increase the deoxyhaemoglobin level. Perhaps HT-Deoxy is an indicator of tissue metabolism and, indirectly, blood outflow with prolonged capillary blood transit time for diffusion, where oxyhaemoglobin delivers oxygen for respiration and becomes deoxyhaemoglobin, and then exits via the venules into the veins. This study showed that, unlike HT-Oxy and HT-Sat, HT-Deoxy was not affected by PVD. This could mean that there is no relationship between tissue metabolism and the degree of tissue

ischaemia. As a result of all these findings, HT-Sat remained the only consistent marker for tissue oxygenation.

The SSS was introduced for the purposes of this study. One of the reasons for this was the relatively small patient numbers in Rutherford classifications 1, 2, and 3. Another reason was that the Rutherford classification is not a genuine rank-able score. The Rutherford 1, 2, and 3 classifications are subjective to some extent, and the Rutherford 5 and 6 classifications in patients with ulcers may not necessarily imply worse tissue oxygen tension than the Rutherford 4 classification in patients with rest pain. The findings of this study are consistent with that observation, with tissue perfusion in patients who have a Rutherford classification of 5 and 6 appearing to be better than in those with a Rutherford 4 classification (Tables 4.11 and 4.12). Fifty-two patients had diabetes, and 36 (69%) of these had ulcers (Rutherford classification 5 and 6). This number was proportionately higher than for Rutherford 0, 1, 2, 3, and 4 patients ($p \leq 0.0001$, Fisher's Exact test). Patients with diabetes often have neuropathy, which impairs the sympathetic tone to the arterial vessels, causing impaired vasoconstriction and relative hyperaemia from arteriovenous shunting, and this could be a further reason for the higher oxygenation in patients classified as Rutherford 5 or 6.

Several limitations were identified in this study:

- The sample population was skewed towards patients with CLI. This might have affected the sensitivity of oxygenation measurements to the severity of PVD. Only two target points were chosen, one at the plantar aspect of the head of the first metatarsophalangeal joint of the diseased foot and the other on the contralateral limb. Each target covered a fixed area of 204 mm² 1 cm around a "target" in a doughnut contour. The average TcpO₂ values from two or more adjacent sites of an area are better predictors of healing potential than single site values.²⁹⁰ Sheffield *et al* typically assessed tissue oxygenation at six different sites simultaneously.²⁷³ One of the advantages of the OxyVu is that even when oxygenation is measured at a target point in a region of interest, the OxyVu software has the capability to quantify hyperspectral oxygenation beyond this point for an area of any size visible on the photograph by selecting the boundary on the computer touchscreen to detect potential ischaemic areas. The standardised method used in this study, even though it assessed a relatively small area, eliminated systematic bias attributable to the operator.

- The plantar angiosome chosen at the first metatarsophalangeal joint is covered by glabrous skin that is rich in arteriovenous anastomoses. This skin tissue has more oxygenation and is more reactive to changes in oxygenation than skin on other parts of the body. It is also a point that is easier to identify than, for example, the plantar arch or between the second and third metatarsophalangeal joints. However, the skin in this area can be particularly thick. In some individuals, this skin can be pathologically hypertrophic, taking the form of calluses or corns. Calluses are common in patients with diabetic neuropathy because of continuous friction and are associated with less tissue oxygenation and a predisposition to formation of ulcers. OxyVu typically assesses skin 1–2 mm in depth, and how this might have affected the findings of the validation study is unknown.
- Although many of the correlation analyses were significant at $p < 0.05$, their clinical significance is unclear, given the relatively low correlation coefficient values.
- Patients with leg oedema were not excluded from the study. A skin surface with underlying leg oedema typically has less tissue oxygenation, precipitating the development of ulcers. There were few, if any, study participants with significant leg oedema. Therefore, leg oedema can be assumed not to be a confounding factor when comparing oxygenation values in this study.
- Hyperspectral oxygenation was not compared with laser angiography or laser Doppler flowmetry.

8.3 WOLOW study

This is the first study to investigate the effects of perioperative adjuncts in vascular surgery on tissue oxygenation and wound healing at a molecular level by analysis of OHP incorporation, growth factors, and transcutaneous oxygenation.

Despite evidence of the beneficial effects of high-dose oxygen and extended active warming on wound healing in abdominal surgery, no such evidence was found in this study. Was this due to a difference in microcirculation between vascular and non-vascular patients influencing wound healing potential and oxygen transport? Patients with vascular disease are prone to endothelial injury, which produces an imbalance in the release of thromboxane and leukotrienes. This imbalance, in turn, disrupts the local vasculature and impairs vasoregulation, causing capillaries to vasoconstrict irreversibly and become coagulopathic, resulting in “plugging”. In addition, patients with CLI often have peripheral neuropathy from ischaemia or diabetes. This might produce autonomic nerve dysfunction, where the capillaries fail to be vasoactive in response to tissue ischaemia, changes in temperature, and hostile conditions. The diseased capillaries remain “maximally dilated” as a compensatory response to the severity of ischaemia. Perhaps there is relative hypoxia secondary to increased oxygen demands and cell metabolism in patients with CLI? Or perhaps there is a difference in oxygen levels and redistribution of heat between the central and peripheral compartments?

Bair Hugger® devices were placed on all patients intraoperatively over the central compartment from the shoulders down the torso to the umbilicus, leaving the groins and lower limbs exposed. Heat loss is more significant in the peripheral compartments, including the lower limbs. The effects of such adjuncts may not enhance perfusion of the skin in the lower extremities in the intraoperative phase, which is considered to be the most important time in wound healing. Studying skin perfusion intraoperatively as part of this research would not have been possible for practical and sterility reasons.

Two major setbacks were encountered. First was the inability to complete the mRNA analyses for statistical analysis. In retrospect, it was an oversight that the methodology was not validated in the study design prior to patient recruitment, Purifying DNA from tissue samples was considered to be a well-established process and one that was carried out with appropriate supervision. Second, the study was underpowered, such that the target sample size of 100 patients with 25 patients in each arm was not achieved. This may have been due to a shift in

management of PVD at the unit where the research was carried out, whereby endovascular interventions were becoming the first-line treatment, even for technically challenging lesions. This was probably related to advances in technology, where products such as balloons and stents are yielding increasingly promising results in terms of patency. Only 5 of the 85 patients eligible for randomisation declined to participate in the study.

The sample size was calculated to detect a 25% absolute increase in OHP with 90% power at a 5% level. The study did in fact achieve 80% power due to the small standard deviation in the original study by Goodson and Hunt, where 12 patients would have been required in each group.⁴⁰⁹ Aiming to detect a 25% absolute increase in OHP by day 5 in these treatment arms could have been overly ambitious, and it may have been better to have focussed on one treatment arm, ie, using one of the adjuncts alone or in combination. This would have provided a better powered study, with more patients in each arm to reduce the risk of type 2 error. It was believed that an absolute increase in OHP of 25% would have been a clinically realistic endpoint to conclude improved wound healing as a result of the adjuncts used in this study.

There were some reasons why the adjuncts were ineffective. For example, even with a higher circulating PaO₂ in the oxygen group during surgery, intraoperative arterial clamping may have prevented the increased oxygen levels reaching the surgical wound site, which could result in a prolonged period of ischaemia. Additionally, the warmed blood and intravenous fluid may not have reached the lower limb during clamping. Perhaps the hypothesis of this study might have been proven if the study population had included patients undergoing other vascular procedures, such as major and distal amputations, which are also associated with a significant incidence of wound complications but where the surgery does not involve arterial clamping. Nonetheless, high-dose oxygen was applied throughout surgery and for 2 hours in recovery. There was extended active warming 2 hours before and after surgery. Despite Ilomedin having a short half-life of 30 minutes and haemodynamic effects of a similar duration, an infusion was applied for 6 hours postoperatively.²⁰⁵ Considering the critical phase of wound healing is in the immediate postoperative period, where accumulation of growth factors and cell proliferation determine the potential for wound healing, the theoretical benefits of these adjuncts were not invalid and, as mentioned previously, have benefited patients undergoing other types of surgery.

While Goodson and Hunt demonstrated the presence of OHP on day 5, comparing OHP levels in this early period focussed on one single snapshot of the wound healing process, namely the inflammatory phase. The effects of these adjuncts might not have been significant until the proliferative phase, when there may be a higher type I to type III collagen ratio. However, implanting a prosthetic tube for a prolonged period of time would be ethically challenging in human clinical research because of the increased risk of wound and graft infections.

There appeared to be more OHP accumulation in the control group than in the treatment groups, although the difference was not statistically significant. This is not implausible, given that hypoxia induces angiogenesis and release of growth factors stimulating collagen synthesis, as well as release of reactive oxygen species during respiratory burst.¹⁴⁹ An optimally balanced level of oxygen is then required to maintain this release, and a high level of oxygenation, such as in the setting of HBOT, enhances production of OHP.⁴⁰ Future study of hypoxia-inducible factor 1 (HIF-1), a key growth factor in the regulation of oxygen homeostasis and cell metabolism in wound tissue, would provide insight into this.^{143 150 156 161}

Production of OHP was not influenced by transcutaneous oxygenation at the surgical incision site. This might have been because oxygenation measurements were made in the “peri-wound” area rather than inside the wound where granulation occurred. However, even though caution is needed when interpreting subanalyses of a secondary outcome, it was interesting to note that a pattern emerged with regard to change in tissue oxygenation in the foot and production of OHP. HTCOM at the foot (not the surgical wound) at day 5 appeared relatively more enhanced in the control group than in the oxygen and temperature groups, with a significant reduction in HT-Deoxy in the control group and in HT-Sat in the temperature group. This appeared to be consistent with the higher OHP and FGF-2 levels observed in the control group. The trends suggest that these adjuncts could in fact be harmful, at least in some patients.

Potential factors influencing production of OHP that were not standardised in this study include the patient’s hydration status, physical and mental stress levels, degree of wound inflammation (where there might be focal hyperaemia and vasodilation), degree of lymphatic injury causing tissue oedema, and the vasomotor response. Oxygen delivery can be affected by the vasomotor response. The length of the skin incision, the presence of “skin bridges”, and the placement of the conduit (subfascial or subcutaneous) should also have been compared.

OxyVu and TCOM were used to assess changes in transcutaneous oxygenation in the early postoperative phase. Oxygen saturation and blood flow in the lower limb increased after surgery, peaking around day 3; this was probably related to post-ischaemic hyperaemia and settled over time. The two systems measured two separate entities, i.e., OxyVu quantified oxyhaemoglobin and deoxyhaemoglobin, while TCOM measured TcpO₂ and carbon dioxide. It is important to note that technically these systems do not measure the wound oxygen tension but rather the oxygen tension in the skin surrounding the wound. This is a potential limitation, given that wound oxygenation is likely to be lower than that in the skin adjacent to the wound.

OxyVu was again shown to be an effective tool for assessing changes in skin perfusion and blood flow at the wound and foot in terms of post-revascularisation and comparison with TCOM and ABI. Despite this, the adjuncts do not appear to have provided added effects. Perhaps these adjuncts administered on day 0 should not be expected to have an effect on oxygenation at day 30.

Measuring changes in TcpO₂ before and after revascularisation can predict wound healing.²⁸⁵ A retrospective analysis was performed on the study data to determine the feasibility of utilising tissue oxygenation measurements following IIB surgery to predict vessel patency and limb loss. This can aid the decision as to whether revascularisation is adequate. Using receiver operating characteristic curve analyses, an HT-Deoxy level below 69.5 AU measured on day 5 could predict limb salvage with a sensitivity and specificity of 85.7% and 56.9%, respectively ($p=0.02$), while at the same level, it could predict secondary patency with a sensitivity of 70% and specificity of 59.5% ($p=0.03$). HT-Sum of more than 143.5 AU on day 5 could predict secondary patency with a sensitivity and specificity of 73.3% and 51.4%, respectively ($p=0.049$). These predictive abilities lacked specificity in this pilot study, and the model needs to be tested prospectively.

Wound complications following IIB remain a significant issue and a major cause of failed surgery. While the most influential period in terms of wound healing potential is the immediate perioperative phase, the three adjuncts used had neither beneficial nor detrimental effects on wound healing, tissue oxygenation, or clinical outcome. Perioperative high-dose oxygen and warming should still be used because of their benefits in terms of anaesthesia, maintaining normothermia, and coagulation, and to reduce the risks of SSI and cardiac events.^{160 358 359}

8.4 Validation of FastScan™ and Silhouette Mobile™

Wound depth is an important factor in wound healing, such that a wound with a large surface area often has a better prognosis than a deep, small wound.⁴¹⁰ This is why wound volume and depth measurements are considered to have merit. Current clinical methods for assessment of wound size, particularly depth, are often inadequate and inaccurate. Most clinicians prefer to use observational estimations or wound diameter measurements via tracing tools. FS and SM have been shown to be reliable in volumetric assessments.

Three-dimensional CT reconstruction has been considered the gold standard, partly due to the advantages of CT for visualisation of a wound in the sagittal plane, defining the air-wound interface, revealing bone erosion, and identifying the presence of undermined wound or inflammatory tissue below the peripheral border. The major limitations of CT relate to the quality of the reconstruction software and include the inability to obtain wound surface area measurements, inadequate capture of small and superficial wounds (Figures 8.2 and 8.3), and inaccuracies in assessment of wounds where the dimensions are affected by pressure or dependency. An example of this in the present study was patient 10, who had a large open wound on the stump following an above-knee amputation, where the wound was “squashed” when the patient was lying supine in the CT scanner (Figure 8.4). Scanning with the SM and FS was more flexible in that the patient could lie prone or in a lateral decubitus position, or the leg could be elevated by an assistant so the wound could lie freely.

While systematic bias appeared to exist for FS and SM measurements when compared to CT, the relevance of this is questionable. Systematic bias exists with all imaging modalities used in clinical practice, including CT, magnetic resonance imaging, and ultrasound. A consistent methodology in terms of the imaging modality used, steps in imaging acquisition, and patient positioning is critical when monitoring wound progression. The advantages and disadvantages of each system should be considered. Further validation studies should include measurement of cavities of known volumetric dimensions to reassess the accuracy of each device and the degree of systematic bias.



Figure 8. 2. Image from the Silhouette Mobile™ showing a small ulcer on the dorsal surface of the toe.



Figure 8. 3. Image from the Silhouette Mobile™ showing a small ulcer on the lateral dorsal surface of the foot.



Figure 8. 4. Image from the Silhouette Mobile™ showing an open wound on an above-knee amputation stump.

The individual scanning times were fastest for CT and slowest for the FS. However, the data processing time was longest for CT and shortest for the SM. CT image measurements taken by more than one operator would have improved the quality control in this study.

This is the first study to validate use of the FS and SM in human subjects, and the first time that these devices have been used for research purposes. Some technical difficulties have been discussed already. A further difficulty was keeping patients still during the scanning procedure. Any patient movement would interfere with the final images, and therefore affect the measurements obtained.

The FS and SM were only useful for wounds that were not undermined, as deep wounds with small orifices could be underestimated using these devices. Further, the volume and depth measurements of the SM depended on the angles assumed by each operator, which varied according to the location of the wound. Wounds embedded in highly curved areas, e.g., a toe amputation stump or at the heel (Figure 8.4), were difficult to capture. The laser lines from the SM were often disrupted if there was no flat surface bordering the wound.

Several other factors might have affected the quality of the FS imaging:

1. The SM was more efficient than the FS for wound assessment because it produced surface area, volume, and depth measurements without the need for another programme or use of an external device (e.g., a computer), whereas the FS images had to be processed with the Delta software programme. This step itself added a new dimension of operator and/or software variability. Since the study was performed, ARANZ has made improved software available to the principal investigator for analysis of wound dimensions, so that images can be independently analysed in future studies.
2. The operators found it challenging to outline the wound boundary accurately using the optical stylus in the FS. This depended on the operator's ability to maintain a steady hand and precisely click stylus points outlining the wound, which were visualised on the computer screen. The SM was more convenient because the wound boundary was outlined on the PDA screen. In the TNP study, the advice was to outline the wound completely with optical stylus points when using the FS, rather than using 6–8 landmarks. Because of inadequate stylus placements in the early scans, there were fewer FS images to analyse than those taken with the SM. This might also explain the difference in surface area measurements between the SM and FS. There was a definite learning curve for the operators. However, placing an excessive number of styluses around wounds could produce erroneous results, with the Delta software failing to accurately represent the wound edges.
3. Wounds containing blood and necrotic tissue appeared dark red, blue, or black in colour. The FS laser did not register black objects, resulting in “patches” and incomplete scans. Blood pooling within the wound would also lead to underestimation of wound depth and volume.
4. Metal interference from the electromagnetic transmitter-receiver field disrupted the final FS scans. All efforts were made to adjust for metal objects, mainly by using a wooden trolley to transport the FS unit. However, metal is found everywhere in a hospital environment, including in beds, trays, heaters, and various medical equipment. Despite this, the final images were not greatly affected, but ideally metal interference should be minimised to obtain the most accurate and consistent results.
5. Quality FS images required placement of the FS receiver for laser signals at a fixed point. Fastening the FS receiver in close proximity to the patient's wound and finding a method to keep the receiver fixed onto the patient's limb was difficult due to the delicate nature of the skin surrounding a wound. Scan quality also depended on the

lighting, the patient's skin colour, and the laser speed, contributing to longer times being required to complete the scans.

The concepts behind FS appear to be technologically more advanced and accurate in assessing wound dimensions than CT or the SM. The entire wound bed was mirror-imaged in details of pixels from the wound boundary with the surrounding skin to the deepest crevices of the wound. The accompanying software could then assess the locations of each coordinate of the pixel, and from that, the dimensions of the cavity deficit could be extrapolated. This would appear superior to the SM, for which volumes were calculated from up to three "slices" of depth measurements across a wound, and the cavity was assumed to be of a conical shape. This might explain the consistent underestimation observed with the SM when compared with CT. Three-dimensional CT reconstruction is considered the "gold standard", but its accuracy in assessing depth and volume depends on the thickness of the imaging slices, which was 1 mm in this study. FS imaging would appear to be more comprehensive. Perhaps FS assessments were more indicative of "true" volume than CT.

The ideal wound assessment device should provide quantitative, reproducible, and completely objective measurements. Both SM and FS provided quantitative recordings and proved to be reproducible with near-excellent operator reliability. Their measurements correlated strongly with those of CT if patient 10 was excluded from the analyses for FS. In the opinion of the operators, the discrepancy in depth measurement between FS and CT was an issue with CT rather than with FS.

CT, FS, and SM were all prone to subjective bias in their measurements. They are essentially three-dimensional imaging devices, and the operators had to actively outline the wound boundary over the computerised image. As discussed earlier, the quality of the measurements was software-dependent. All three modalities encountered a common problem that affected their accuracy, i.e., they all assumed that the skin surface of a healed wound would have a flat surface. This was commonly not the case, for example, at the heel, which has a semi-spherical surface, or the calf, which has a curved surface. However, this should not affect monitoring of the progress of wound healing.

Compared with the FS, the SM is possibly more cost-effective and time-efficient. The SM is also more portable than the FS, and the PDA can generate a report immediately without the need for further computer analysis. All data from the SM could be connected to the hospital

and/or Internet database, improving communication between clinicians. SM lasers were unaffected by metal objects, and the SM was slightly more precise and consistent than the FS when compared with CT. The relative values and digital images produced by the SM could indicate whether wounds were improving with treatment by generating graphical reports (Figure 8.5), whereas the FS could not. It is envisaged that the SM would be a helpful tool in podiatric clinics and hospital wards for wound monitoring and comparing wound intervention outcomes.

Use of CT as the gold standard for assessment of wound dimensions should be questioned. The FS and SM offered benefits as non-contact and effective portable devices for measuring wound dimensions without radiation risk, and convenience as a bedside technology. The SM is potentially more clinically valuable than the FS due to its lower cost. This study provides a basis for further research comparing the outcomes of interventions for wound healing. Since completion of the study, ARANZ has upgraded their SM model and named it Silhouette Star®.

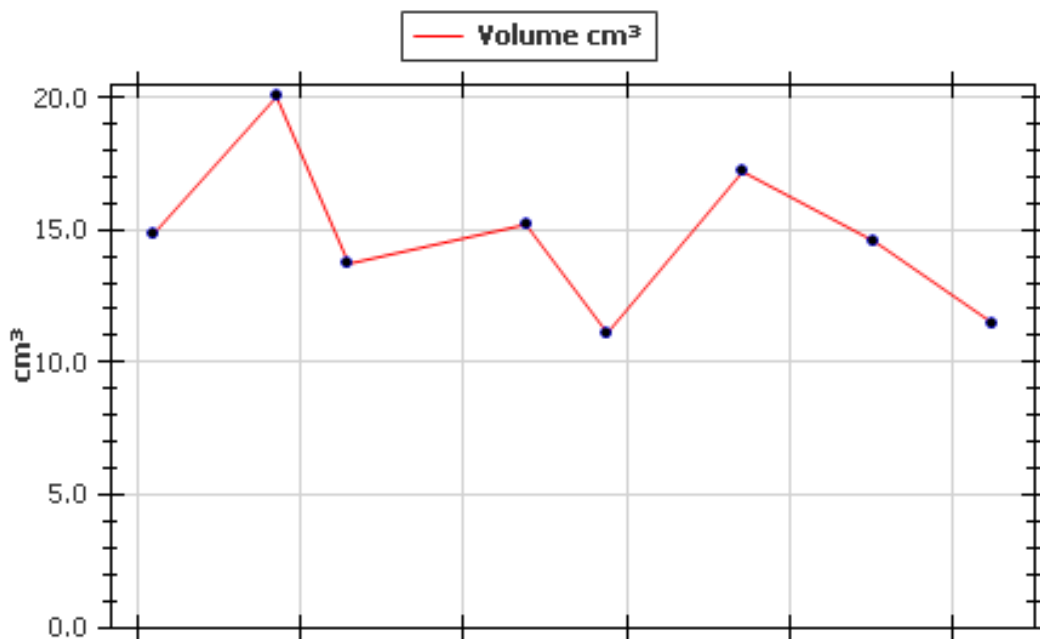


Figure 8. 5. Wound report using SM from one of the participants showing variation in volume over time.

8.5 Wound healing and tissue oxygenation in TNP therapy

Following the validation study of FS and SM, FS was chosen to assess the effects of TNP on wound healing rates. Technical issues using FS in the previous study were addressed to improve accuracy, and included placing multiple stylus points around the wound edges at the time of imaging. While the findings in the previous study suggested that the SM would be more practical at the bedside, the accuracy and reliability of the FS and SM were similar. In addition, the technology behind the FS was more advanced and more suited for this study.

This research became a pilot study rather than a powered randomised controlled trial as initially designed. Nevertheless, it represents the largest series of its type. Recruitment only lasted 12 months due to the time restraint on this project, and was slower than anticipated. Due to the relatively strict inclusion/exclusion criteria, there were significant numbers of dropouts and refusals to participate in the study.

However, this is the first clinical study in humans to investigate changes in wound volume following TNP therapy in vascular wounds over time using accurate and objective wound measurement devices like the FS. Compared with other volumetric studies of TNP therapy, this study compared TNP with modern traditional dressings such as hydrogels and hydrofibres rather than saline-soaked gauze dressings. It was not the intention of the study design to target diabetic foot wounds. All but two patients had a history of diabetes, while the remaining two had end-stage renal failure, which is associated with wound healing problems similar to those encountered in diabetes.

TNP therapy appeared to achieve a greater reduction in wound volume when compared with traditional dressings, although the difference was not statistically significant. TNP also achieved a greater relative reduction in maximum depth wound of 36% by day 14 compared with an 18% reduction using traditional dressings. As suggested in previous wound healing studies, “wounds heal from the bottom up”. Wound depth recovered at a faster rate than surface area. Volumetric findings in our study were similar to those of the four other studies described in Section 1.14.

Several patients had negative values for reduction in wound dimensions, implying an increase in wound size over time. In retrospect, the wound in one control patient was in fact “dying back” despite adequate proximal revascularisation, and the wound were surgically debrided

on day 17. Another patient in the TNP group had a forefoot wound that was over-granulating, rendering it difficult to interpret the wound dimensions when the skin surface extrapolated by the Delta software was constantly changing.

Biochemical analyses of granulation tissue and wound fluid provided an insight into the mechanisms behind TNP therapy at a molecular level. It appeared that more collagen and TGF- β were deposited in the wound bed on day 14 when compared with baseline in patients who had traditional dressings rather than TNP therapy. This might have important implications, and could suggest that while TNP therapy reduces the wound size at a greater rate, the reduction might not be a direct result of increased collagen deposition. Instead, it might be related to the macro-strain effects of TNP therapy, i.e., contracting wound edges and decreasing tissue oedema.

There were limitations to the biochemical analyses. Some of the technical issues encountered during the analyses of growth factors and cytokines were mentioned earlier. Even though assessment of accumulation of OHP as a surrogate marker of wound healing is a well-documented and validated technique, the method employed in this study was different, in that OHP levels were compared between day 0 and day 14. Implanting an ePTFE tube in a toe or forefoot wound over bony structures would have been impractical, especially when dressings were changed regularly.

It was hypothesised that optimal wound healing would rely on the balance between promoting growth factors and inhibitory cytokines based on previous animal studies. It was disappointing that biochemical analyses of VEGF, FGF-2, TNF- α , and IL-8 were not successful.

One of the shortcomings of the study design was that collection of wound fluid commenced on day 2 rather than on day 0. This was for quality control purposes. When designing the study, prior to encountering the issues with Milliplex®, the consensus was that the wound dressings on day 0 would usually be the dressings put on in theatre 24–48 hours earlier, typically an alginate dressing to complete haemostasis. This dressing might become saturated with clotted blood, contaminated with local anaesthetic agents or antiseptic solution, or infiltrated with tissue debris. Processing these dressings would not have provided a standardised sampling method for wound fluid to accurately assess wound healing dynamics at a molecular level.

Skin perfusion around the wound was not different between the two groups. However, skin perfusion in all patients decreased significantly by day 14. This is possibly a reflection of resolution of inflammation around the wound with less vasodilation. Again, this is another testament to the ability of OxyVu to detect changes in tissue oxygenation.

TNP therapy could be used for many wound types outside the field of vascular surgery. It is commonly used in plastics and burns surgery, as well as in abdominal surgery to facilitate wound closure and production of granulation tissue. It should be emphasised that this study focussed on patients who had compromised wound healing ability, including those with tissue ischaemia, those with diabetes, smokers, and patients with renal impairment.

This study provides some evidence that TNP therapy could enhance healing rates in diabetic foot wounds. While the study population might appear to have been heterogeneous in terms of comorbidities and location of the foot wound, it represented a realistic cohort of vascular patients, where evidence of added benefits in any part of the wound healing process would have a significant impact on morbidity, mortality, and cost to the health care system.

8.6 The future

This project has laid the foundations for larger studies that should be conducted in the future. Although quality human clinical studies were conducted, patient recruitment in both randomised studies was slower than expected, resulting in underpowered findings for the primary outcomes. While animal studies would have been a viable alternative, they would have been more costly to perform and their effects in animals could not be directly translated to humans.

It was difficult to obtain accurate estimates of the expected treatment effects from the previous published studies, and the patient groups were relatively heterogeneous. Because the treatments were quite labour-intensive, unless there was a large treatment effect (e.g., a 25% absolute increase in wound healing effects), the treatments would be unlikely to be of strong clinical interest, so these preliminary studies were powered accordingly. The practicalities of conducting research of this nature in a single centre were such that these studies should be viewed as novel pilot studies that can provide valuable information if further multicentre large-scale studies were to be planned to look for smaller treatment effects.

Although the WOLOW study was underpowered, the outcome demonstrated neither clinical nor non-clinical (e.g., biochemical) benefits from the interventions in terms of wound healing and tissue oxygenation. Thus, there seems little incentive to conduct a larger clinical trial of these quite costly and intensive treatments for only small benefit. Instead, further research should target a better understanding of the pathophysiology of wound healing, especially given that there was a trend of a better outcome in the control group.

If the two clinical studies in this thesis were to progress to adequately powered trials, sample size calculations should be revised. Again, power calculation would be difficult without adequate published work, but this could be achieved using data from this research. If one of the perioperative adjuncts were to be re-tested during IIB, or in combination, 224 patients would be required in each arm to test an absolute increase of 25% in OHP level at 80% power and a 5% significance level. Similarly, 106 patients would be required in each arm to test if TNP could reduce wound volume at 2 weeks by an additional 25% when compared with traditional dressings.

In the WOLOW study, although it was not significant, more collagen deposition was noted in the Ilomedin group than in the other treatment arms, suggesting that targeted intervention using Ilomedin could be investigated further. Given its multiple proposed roles in vasodilation, it is plausible that Ilomedin could improve perfusion, mediators of inflammation, and growth factors related to wound healing. The effects of extended active warming may also warrant further investigation, given the finding of a trend towards a higher graft patency rate at 12 months in comparison with the control group (81% vs 58%). While maintenance of graft patency involves many factors, some of which are related to postoperative care, there may be as yet unexplained effects related to perioperative active warming, such as reducing neointimal hyperplasia or a “low reflow” phenomenon.

One of the successes of this research is that it demonstrates the reliability of OxyVu in assessment of skin perfusion. In the absence of a gold standard and the technical challenges of other modalities, the OxyVu system could be developed further as a complementary diagnostic tool in the clinical setting. Larger-scale validation studies are needed to create a predictive model using ROC curve analysis. ABI is useful in patients with mild to moderate PVD, for differentiating between ischaemic and neurogenic claudication, and for assessment of changes in skin perfusion following revascularisation. However, it only provides information on the macrocirculation and may be unreliable in patients with calcified vessels. Toe pressure and TCOM can determine the potential for wound healing and whether hyperbaric oxygen therapy may be useful. However, these two methods (TCOM in particular) only afford a glimpse of the microcirculation, whereas the OxyVu has the advantage of being more flexible and practical in the way it gleanes the critical information required. Toe pressure measures skin perfusion of the toe as a surrogate marker of healing in the rest of the lower limb, while TCOM provides readings in an area the size of a ring. In contrast, the OxyVu produces instant quantitative readings and indicates specific regions of hypoperfusion in imaged areas of any size. Hypermed Inc., the manufacturer of the OxyVu, has now received FDA marketing approval for the HyperView™, which is the same system as the OxyVu but is designed to be more portable and user-friendly.

This research targeted arterial aspects of vascular surgery, such as infra-inguinal arterial bypass and management of arterial ulcers. However, there would be potential benefit in investigating tissue oxygenation and wound healing in venous disease. A recent summer studentship project supervised by the author investigated the effects of varicose vein surgery

(open surgery and laser therapy) and long-term compression therapy on tissue oxygenation in patients with chronic venous insufficiency, which was measured using the OxyVu. The findings were presented at the 2013 New Zealand Vascular Society meeting held in Auckland. The study showed an increased oxyhaemoglobin saturation (HT-Sat) following 28 days of compression stockings; this increase in HT-Sat in those who had compression alone was greater than those who had surgery alone. The benefits of varicose vein surgery and compression therapy for healing of venous ulcers can also be investigated using the FS and SM.

8.7 Conclusions

This thesis furthers our knowledge on tissue oxygenation and wound healing in vascular surgery. OxyVu is an innovative device that was used to measure a different component of tissue oxygenation. Its advantages were clear, i.e., its non-invasiveness, its flexibility in being able to image any area of the body, and its ability to provide instant real-time measurements within 15 seconds. Whilst the device has appeared promising since its release in 2006, there are limited studies on its use and reliability. This project purchased the first machine ever to be used outside the USA and validated its reliability, with promising results in determining tissue oxygenation in clinical settings.

Three perioperative adjuncts were studied during IIB surgery. The benefits of these adjuncts on wound healing and tissue oxygenation were not demonstrated.

The focus of this research was then shifted to studying wound volume, another marker of wound healing. Excellent inter-operator and intra-operator reliability was demonstrated for the FS and SM, with a strong correlation between these devices and CT.

Next, the effects of TNP therapy on tissue oxygenation and healing of diabetic foot wounds were investigated. While no differences were shown with regard to changes in OHP levels, growth factors, or tissue oxygenation, there was a significant reduction in maximum wound depth in patients who received TNP when compared with those who received traditional dressings at day 14, as well as a trend towards decreased wound volume and reduction in wound surface area. The impact of TNP in clinical practice would be significant. The findings of this research also support the concept of “wounds healing from the bottom up”, and therefore wound volume and depth should be a more important dimension for assessment than surface area. Although TNP is already widely used clinically for diabetic foot wounds, systematic reviews in the literature have concluded that there is insufficient scientific evidence of benefit and decisions to use TNP therapy by clinicians are often based on clinical equipoise.

9. Appendices

A.1 Definitions

A.1.1 Risk factors

RISK FACTORS	DEFINITION
Body mass index (BMI)	Weight (kg)/Height ^{1.2} (m ²)
Acute presentation	Presented in emergency or semi-urgent settings (via emergency department or as an arranged admission (in contrast to an elective admission).
Active smoker	Someone who smoked >100 cigarettes in their lifetime and currently smokes at least monthly (as defined by the Ministry of Health, NZ) ²⁴¹
Ex-smoker	Someone who has smoked >100 cigarettes in their lifetime and does not currently smoke. (as defined by the Ministry of Health, NZ) ²⁴¹
Non-smoker	Someone who has smoked <100 cigarettes in their lifetime and does not currently smoke. (as defined by the Ministry of Health, NZ) ²⁴¹
Pack-years	One pack-year is the equivalent of 365.24 packs of cigarettes or 7,305 cigarettes. It is calculated by multiplying the number of packs of cigarettes smoked per day by the number of years the person has smoked.
Diabetes	Diabetes mellitus is diagnosed by demonstrating any one of the following as per the WHO diagnostic criteria: ⁴¹¹ <ul style="list-style-type: none"> • Fasting plasma glucose level ≥ 7.0 mmol/l (126 mg/dl) • Plasma glucose ≥ 11.1 mmol/l (200 mg/dl) two hours after a 75 g oral glucose load • Symptoms of high blood sugar and casual plasma glucose ≥ 11.1 mmol/l (200 mg/dl) • HbA_{1c} ≥ 48 mmol/mol (≥ 6.5 DCCT %)
Renal impairment	eGFR<60ml/min/1.73m ²
ESRF	Patients with chronic kidney disease requiring renal replacement therapy (e.g. transplant or dialysis)
Hypertension	History of BP > 140/90mmHg on two occasions, or lower if on medication.
Dyslipidaemia	History of abnormal fasting lipid profile.
Previous plasty	Previous history of endovascular angioplasty +/- stenting

Op length	Duration of surgery recorded in minutes
GA	General anaesthesia
ACS	Diagnosis of ST elevation myocardial infarction (STEMI), non-STEMI and unstable angina
LRTI	Lower respiratory tract infection.

A.1.2 Rutherford and Fontaine classifications

Fontaine		Rutherford		
Stage	Clinical	Grade	Category	Clinical
I	Asymptomatic	0	0	Asymptomatic
IIa	Mild claudication	I	1	Mild claudication
IIb	Moderate to severe claudication	I	2	Moderate claudication
		I	3	Severe claudication
III	Ischemic rest pain	II	4	Ischemic rest pain
IV	Ulceration or gangrene	III	5	Minor tissue loss
		III	6	Major tissue loss

Figure 9. 1. Rutherford and Fontaine classifications for peripheral vascular disease.²¹³

A.1.3 V-POSSUM


Variable	One	Two	Four	Eight
Age (years)	<60	61–70	>71	—
Cardiac status	Normal	Cardiac drugs or steroids	Oedema, warfarin, borderline cardiomegaly	Increased JVP, cardiomegaly
Respiratory status	Normal	Dyspnoea on exertion; mild COPD	Limiting dyspnoea (one flight); moderate COPD	Dyspnoea at rest (RR > 30/min)
Systolic BP (mmHg)	110–130	131–170	>170	<90
Pulse (b.p.m)	50–80	81–100 40–49	90–99 101–120	>120 <40
Glasgow coma score	15	12–14	9–11	<9
Haemoglobin (g/100 mL)	13–16	11.5–12.9 16.1–17.0	10.0–11.4 17.1–18.0	<10.0 >18.0
White cell count ($\times 10^{12}$)	4–10	10.1–20.0 3.1–3.9	>20.0 <3.1	—
Urea (mmol/L)	<7.5	7.5–10.0	10.1–15.0	>15.0
Sodium (mmol/L)	>136	131–135	126–130	<126
Potassium (mmol/L)	3.5–5.0	3.2–3.4 5.1–5.3	2.9–3.1 5.4–5.9	<2.9 >5.9
Electrocardiogram	Normal	—	Atrial fibrillation (rate 60–90)	Any other abnormality

Figure 9. 2. Physiological score for V-POSSUM.⁴¹²

Variable	One	Two	Four	Eight
Operative severity	Minor	Intermediate	Major	Major+
Multiple procedures	1	—	2	>2
Total blood loss (mL)	<100	101–500	501–999	>1000
Peritoneal soiling	None	Minor (serous fluid)	Local pus	Free bowel content, pus or blood
Presence of malignancy	None	Primary only	Nodal metastases	Distant metastases
Mode of surgery	Elective	—	Emergency resuscitation of >2 h possible; operation < 24 h after admission	Emergency (immediate surgery <2 h needed)

Figure 9. 3. Operative score for V-POSSUM⁴¹²

A.5 Post-operative Ilomedin® protocol



AUCKLAND
HEALTH BOARD
Te Toka Taumatū

**Nursing Care Plan for
ILOPROST Infusion Chart**

SURNAME: _____ NHC: _____

FIRST NAMES: _____

DATE OF BIRTH: ____ / ____ / ____ SEX: _____

Please attach patient label here

Weight.....

Recommended Dose Range:
0.5-2.0 nanograms /Kg/min

DATE	MEDICATION	ROUTE	FREQUENCY	SIGNATURE & BLOCK PRINT	LOCATOR NUMBER	STOPPED DATE & INITIALS
	iloprost 50 micrograms in 250ml NaCl or Glucose 5% infusion (0.2 microgram/mL)	iv	Once daily infusion (should not run > 6 hrs)			

• Commence next day's infusion rate at previous day's last tolerated rate

Administration record (for dosage titration refer to algorithm overleaf)

Maximum infusion rates (titrated to patient weight)

< 33kg: 10 mL/hr	<50kg: 20	< 65kg: 30 mL/hr	<75kg: 40 mL/hr	>75kg: 50mL/hr
------------------	-----------	------------------	-----------------	----------------

Other: Titrated for Hepatic Clearance

Co-morbidities (prescribing doctor to tick) :

Renal impairment Dialysis Hepatic Impairment

DAY	DATE	START TIME	TITRATION mL/hr (see algorithm overleaf)						ADVERSE EFFECTS <i>*See below and overleaf</i>	STOP TIME	SIGNATURE
			5	10	20	30	40	50			

***Stop infusion, and contact medical staff if:**

- BP falls by 50mmHg or
- Systolic <90mmHg
- Diastolic <50mmHg
- Pulse >120bpm or irregular or <.....

OR

- with excessive adverse effects
- if infusion solution runs out prior to expected time frame

Adverse Effects Include:

FF Facial flushing	N&V Nausea and Vomiting
AC Abdominal cramps	CP Chest pain
B Bradycardia	T Tachycardia
H Headache	BP Hypotension
I Itching	BL Bleeding

NURSING CARE PLAN FOR ILOPROST INFUSION CHART

CR4514

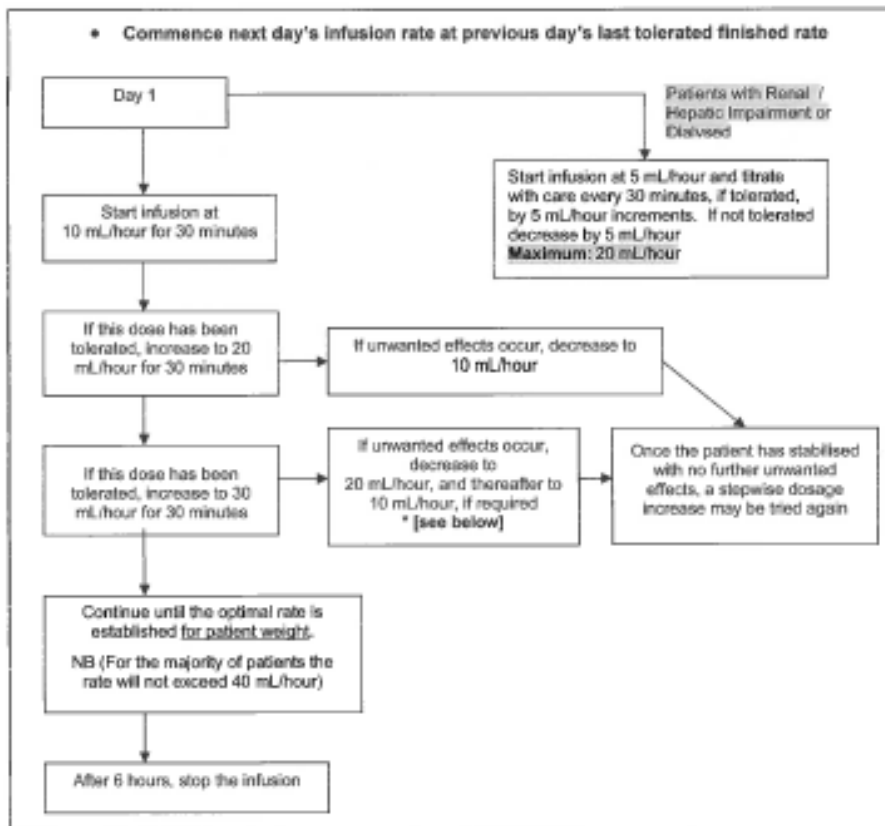
09/12



Nursing Care Plan for ILOPROST Infusion Chart

SURNAME: _____ NHI: _____
 FIRST NAMES: _____
 DATE OF BIRTH: ____ / ____ / ____ SEX: _____
Please attach patient label here

Guidelines for the Administration of ILOPROST
 Recommended administration guidelines for Iloprost 50 micrograms in 250mL of NaCl or Glucose 5% Injection via an infusion pump



N.B. Monitor patients' BP & pulse before and after every rate increase then hourly once stable

- STOP infusion and Contact medical staff if:
 - BP falls by 50 mmHg or
 - Systolic <90 mmHg
 - Diastolic <50 mmHg
 - Pulse >120 bpm or irregular
- excessive adverse effects
- if infusion solution runs out prior to expected time frame

NURSING CARE PLAN FOR ILOPROST INFUSION CHART

CR4514



A.6 Additional tables from results: Validation of OxyVu™

A.6.1 Correlation between OxyVu and TCOM of the diseased limb

PEARSON'S		HT- OXY	HT- DEOXY	HT-SAT	OXY- BPI	DEOXY -BPI	SAT- BPI	OXY- RPI	DEOXY- RPI	SAT- RPI
TcpO₂	(r)	0.02	-0.26	0.19	0.04	-0.13	0.14	-0.05	-0.04	0.04
	(p)	0.77	0.001	0.012	0.59	0.11	0.08	0.68	0.74	0.76
TcpCO₂	(r)	-0.17	0.27	-0.35	-0.10	0.36	-0.33	-0.13	0.08	-0.16
	(p)	0.03	0.0001	0.0001	0.20	0.0001	0.0001	0.29	0.51	0.21
TcpO₂-BPI	(r)	0.05	-0.10	0.10	-0.04	-0.03	-0.01	0.02	0.001	0.04
	(p)	0.49	0.21	0.20	0.60	0.74	0.95	0.89	1.00	0.76
TcpCO₂-BPI	(r)	-0.15	0.17	-0.27	-0.10	0.36	-0.28	-0.05	-0.06	0.04
	(p)	0.06	0.03	0.0001	0.21	0.0001	0.0001	0.70	0.62	0.74
TcpO₂-RPI	(r)	0.13	-0.271	0.26	0.04	-0.13	0.06	0.03	-0.06	0.15
	(p)	0.29	0.03	0.03	0.75	0.30	0.65	0.83	0.66	0.24
TcpCO₂-RPI	(r)	0.02	-0.36	0.20	0.09	0.06	0.21	0.08	0.12	0.12
	(p)	0.93	0.05	0.28	0.64	0.74	0.27	0.67	0.54	0.52

A.6.2 Correlation between OxyVu and TCOM of the contralateral limb and chest

		Pearson's	CONTRALATERAL LIMB			CHEST		
			HT-Oxy	HT-Deoxy	HT-Sat	HT-Oxy	HT-Deoxy	HT-Sat
Contralateral	TcpO₂	(r)	-0.06	-0.06	-0.01	0.03	-0.12	0.09
		(p)	0.44	0.42	0.89	0.78	0.31	0.49
	TcpCO₂	(r)	-0.02	0.19	-0.10	-0.06	-0.05	0.03
		(p)	0.84	0.02	0.21	0.63	0.71	0.82
Chest	TcpO₂	(r)	-0.12	0.06	-0.31	0.09	0.07	0.05
		(p)	0.31	0.62	0.01	0.46	0.59	0.67
	TcpCO₂	(r)	-0.04	0.57	-0.10	-0.13	0.14	-0.41
		(p)	0.85	0.001	0.60	0.50	0.45	0.03

A.6.3 ANOVA to determine confounding factors that affect OxyVu™.

VARIABLES	LIMB	HT-READINGS	P-VALUE
Smokers (0, non) (1, ex) (2, active)	Diseased	HT-Oxy	0.82
		HT-Deoxy	0.85
		HT-Sat	0.84
	Contralateral	HT-Oxy	0.91
		HT-Deoxy	0.36
		HT-Sat	0.29
Pack-years	Diseased	HT-Oxy	0.26
		HT-Deoxy	0.57
		HT-Sat	0.69
	Contralateral	HT-Oxy	0.19
		HT-Deoxy	0.37
		HT-Sat	0.66
Diabetes (0=No) (1=Yes)	Diseased	HT-Oxy	0.18
		HT-Deoxy	0.10
		HT-Sat	0.90
	Contralateral	HT-Oxy	0.10
		HT-Deoxy	0.07
		HT-Sat	0.77
Renal disease (0=No) (1=Yes)	Diseased	HT-Oxy	0.19
		HT-Deoxy	0.64
		HT-Sat	0.53
	Contralateral	HT-Oxy	0.79
		HT-Deoxy	0.40
		HT-Sat	0.39

A.6.4 Correlation between hyperspectral oxygenation and haemoglobin

HT-Sum (arbitrary units) is the sum of oxyhaemoglobin and deoxyhaemoglobin and is assumed to be total haemoglobin. It is designed to indicate haemoglobin concentration and the microvascular volume of capillary density.

In the 150 patients with peripheral vascular disease (PVD), haemoglobin (g/L) was recorded within 12 hours before or after OxyVu™ readings. (Table 9.1) Haemoglobin correlated with the severity of PVD according to the Simplified Severity Score (SSS; Spearman's $R = -0.24$, $p = 0.003$; Figure 9.4).

	MEAN (RANGE)	SD	SKEWNESS	KURTOSIS
HT-Sum diseased (AU)	159 (87–248)	32.8	0.41	-0.07
HT-Sum contralateral (AU)	154 (64–235)	30.3	0.19	0.05
Haemoglobin (g/L)	127 (74–170)	18.7	-0.11	-0.37

Table 9. 1. Descriptive summary for HT-Sum and haemoglobin. **Abbreviations:** AU, arbitrary units; SD, standard deviation

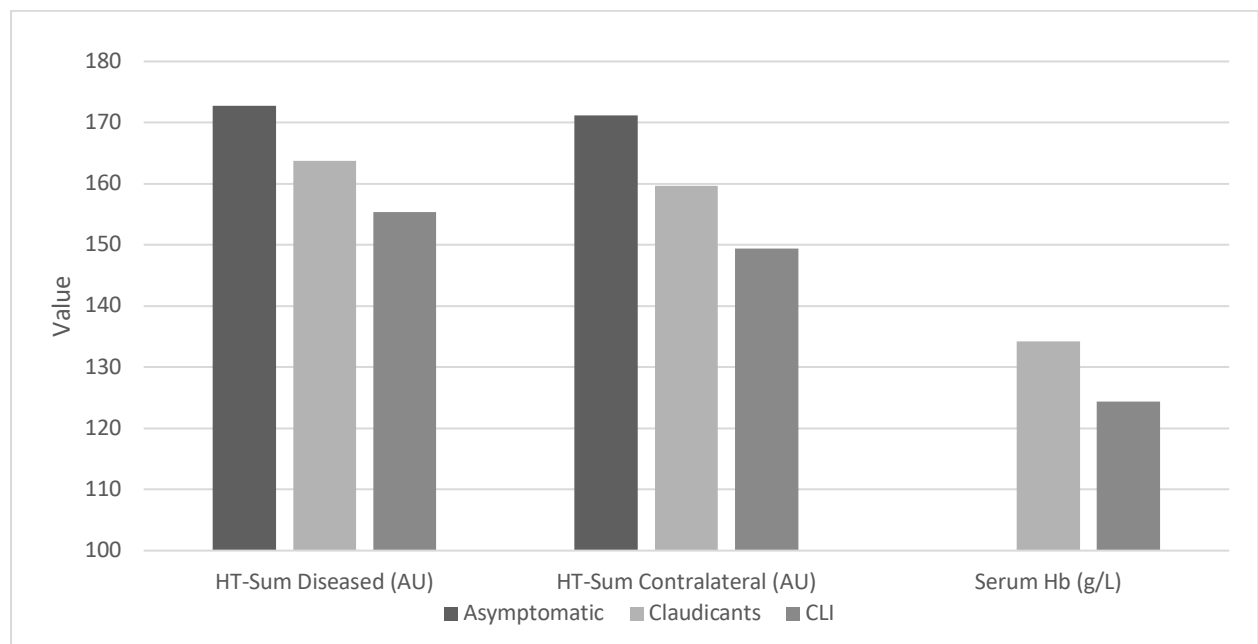


Figure 9. 4. Bar chart showing the variation in HT-Sum and haemoglobin according to severity of peripheral vascular disease using the Simplified Severity Score. **Abbreviations:** AU, arbitrary units; CLI, critical limb ischaemia; Hb, haemoglobin

With adjustment for the SSS, potential confounding factors that could affect haemoglobin, such as age, gender, race, diabetes, smoking, and cardiac history, were tested using logistic regression analysis. Table 9.2 shows only the relevant findings. Gender and age were confounding factors, whereby men had higher haemoglobin and haemoglobin decreased with increasing age.

VARIABLES	CONFOUNDING FACTORS	COEFFICIENT, B	P-VALUE
Haemoglobin (g/L)	Male sex	11.4	0.001
	Age	-0.35	0.02
	Smoking history	7.8	0.51
HT-Sum (diseased)	Haemoglobin	0.35	0.03
	Male sex	-12.2	0.053
HT-Sum (contralateral)	Haemoglobin	0.39	0.005
	Diabetes	-14.4	0.008
	Male sex	-14.5	0.01

Table 9. 2. Summary of unstandardised coefficients and p-values using linear regression to identify confounding factors for haemoglobin and HT-Sum.

There was a downward trend of HT-Sum in both limbs as the SSS increased (Spearman's $R = -0.19$, $p = 0.01$ for the diseased limb; $R = -0.24$, $p = 0.001$ for the contralateral limb). HT-Sum for the diseased limb was strongly associated with that for the contralateral limb (Pearson's $R = 0.73$, $p = 0.0001$) with no statistically significant difference between HT-Sum of both limbs ($p = 0.14$).

Haemoglobin was the only factor influencing the HT-Sum of the diseased limb when SSS was adjusted (Table 9.2). Haemoglobin, as well as diabetes and sex, were confounding factors for HT-Sum of the contralateral limb. In contrast with haemoglobin, HT-Sum was lower in men than in women, indicating haemoglobin in the peripheries was lower in men while "serum" haemoglobin was higher. Age and skin temperature had no influence on HT-Sum.

Overall, HT-Sum at the peripheries decreased bilaterally with haemoglobin as the severity of PVD increased. There might have been a "central" cause, such as anaemia or anaemia of

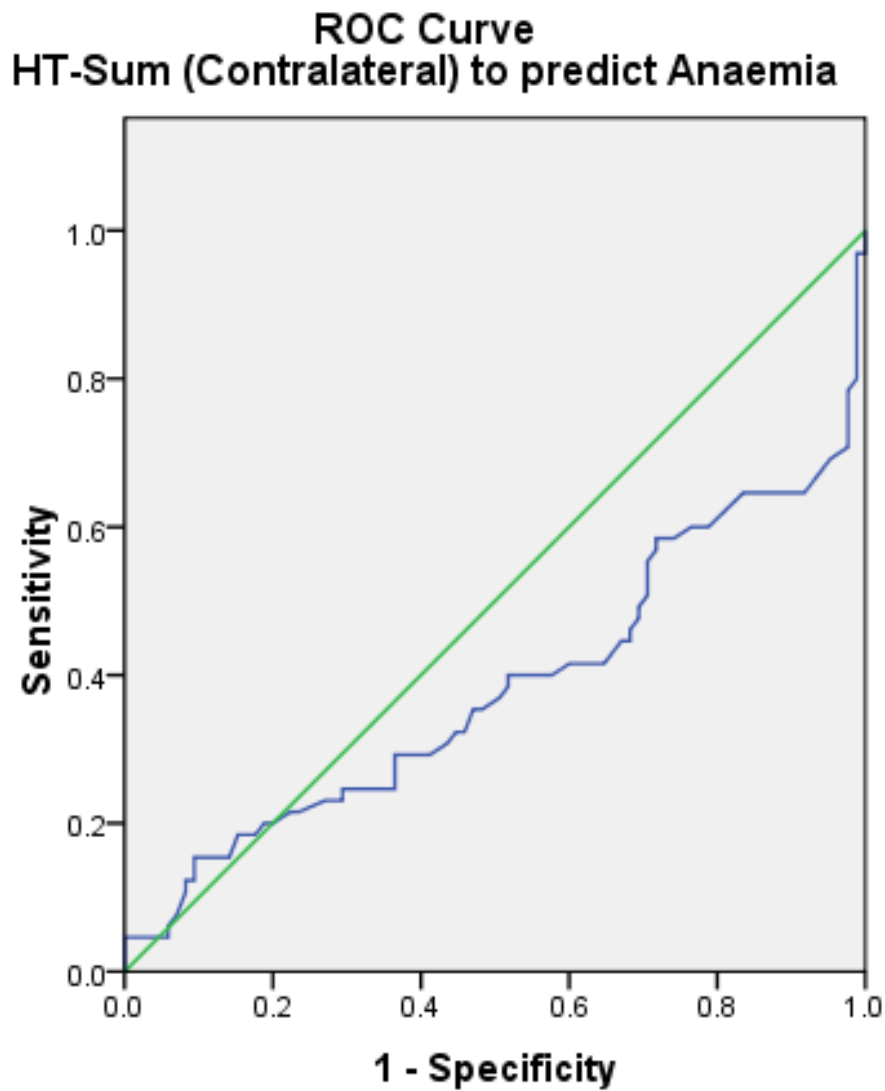
chronic disease. Haemoglobin did not correlate with HT-Sum for the diseased limb (Pearson's $R=0.15$, $p=0.07$), but was associated with that of the contralateral limb ($R=0.22$, $p=0.007$).

HTCOM measurements to estimate haemoglobin level?

According to the World Health Organization, the haemoglobin threshold defining anaemia is 130 g/L in men and 120 g/L in non-pregnant women. Anaemia was defined as haemoglobin ≤ 125 g/L for this study.

A receiver operating characteristic (ROC) curve was used to determine if HT-Sum for the contralateral limb was an effective tool for diagnosing anaemia (Figure 9.5). The area under the ROC curve (AUC, 0.38) represented the probability that the HT-Sum value for a randomly chosen patient with anaemia (haemoglobin ≤ 125 g/L) would exceed the HT-Sum value for a randomly chosen negative case. The p-value was 0.01, indicating that interpreting the HT-Sum to diagnose anaemia was better than guessing. However, the ROC curve lay below the diagonal line. Therefore, HT-Sum was not an accurate tool for predicting anaemia.

Using linear regression to adjust for SSS, $\text{HT-Sum (contralateral)} = 0.342 \times \text{haemoglobin} + 108.4$. At a haemoglobin of 125 g/L, the HT-Sum was 151. An HT-Sum of 151 had a sensitivity of 40%, a specificity of 47%, a positive predictive value of 43%, and a negative predictive value of 44%. This was a pilot study, but if this hypothesis was to be tested further, inclusion of normal individuals without PVD and a larger sample size would be recommended.



Diagonal segments are produced by ties.

Figure 9. 5. ROC curve to determine if HT-Sum of the contralateral limb would be an accurate tool to diagnose haemoglobin. **Abbreviation:** ROC, receiver operating characteristic

A.7 Additional results from the WOLOW study

A.7.1. P-values for hydroxyproline and growth factors in treatment arms versus the control group

GROUP	OXYGEN	ILOMEDIN®	TEMPERATURE
OHP	0.27	0.77	0.16
TGF- β	0.71	0.91	0.98
FGF-2	0.46	0.39	0.33
VEGF	0.74	0.93	0.72
TNF- α	0.21	0.67	0.15
IL-8	0.13	0.26	0.31

Abbreviations: OHP, hydroxyproline; TGF- β , transforming growth factor beta; FGF-2, fibroblast growth factor 2; VEGF, vascular endothelial growth factor; TNF- α , tumor necrosis factor alpha; IL-8, interleukin-8

A.8 Additional results: Wound healing and tissue oxygenation in TNP therapy

A.8.1. Summary of kurtosis and skewness values on variables

	SKEWNESS	KURTOSIS
“Body” surface area	1.35	4.01
“Cap” surface area	0.34	1.12
Maximum depth	1.09	0.76
Mean depth	0.60	−.44
Volume	0.62	−0.10
Pre OHP	1.43	0.93
Post OHP	0.72	0.26
Pre TGF- β	1.18	1.77
Post TGF- β	1.41	1.77
Pre HT-Oxy	0.15	−0.63
Pre HT-Deoxy	0.39	−0.04
Pre HT-Sat	0.17	−1.21
Pre HT-Sum	−0.11	−0.16
Post HT-Oxy	0.41	−0.62
Post HT-Deoxy	−0.36	−1.32
Post HT-Sat	−0.56	−0.67
Post HT-Sum	0.64	−0.74

10 Determining time duration for TCOM electrodes to reach equilibrium.

Background

TCOM measurements are applied in wound healing research to determine wound hypoxia; however, the methods are not standardised and clear descriptions are not readily available. Guidelines for the duration for the electrodes to reach equilibrium for measurements were difficult to find from the literature.

From our experience with TCOM3, measurements do not completely reach equilibrium, with a constant variation by a small percentage over the latter period of recording. This may be due to technical issues related to ongoing tissue demand from the capillary hyperperfusion caused by the heated electrode consuming oxygen and producing carbon dioxide within a closed chamber; or the contact fluid failing to provide the optimal diffusion barrier over time because it is dried up by the heat.

Aim

To determine a suitable duration for the TCOM electrode to reach equilibrium for reliable measurements to minimise errors and to standardise protocols for the other studies in this thesis.

Methods

Fifty patients were recruited by responding to an advertisement placed in the vascular ward between December 2008 and February 2009. Eighty-two sets of minute-by-minute TCOM readings for T_{cp}O₂ and T_{cp}CO₂ of the foot over the first metatarsal head at the plantar aspect were recorded over a 15-minute period. Of these, 25 sets of recordings were from hospitalised vascular patients with known PVD of the lower limb, 30 were from patients hospitalised within vascular or cardiothoracic subspecialties with no known PVD of the lower limb; and 27 were from healthy volunteers (i.e. medical and nursing staffs or students). Details on the application of the TCOM3 system are described in the manufacturer's operating manual and in the literature.^{273 400} These are summarised in Section 3.7.2. Ethical approval was secured from the local ethics committee (NTY/08/08/082).

Results

Demographics

Sixteen participants were vascular patients with known PVD, 18 were patients hospitalised with no known PVD; and 16 were from healthy volunteers. Background information were described in Table 10.1.

	KNOWN PVD	NO KNOWN PVD	VOLUNTEERS
Number of participants	16	18	16
Age (SD)	70 (14)	52 (11)	36 (9)
Male (%)	13 (81)	10 (56)	6 (38)
White (%)	13 (81)	17 (94)	9 (56)
Active smoker	3	4	4
Diabetes mellitus	4	4	0

Table 10. 1. Basic demographics of the three groups of patients

Quality of data

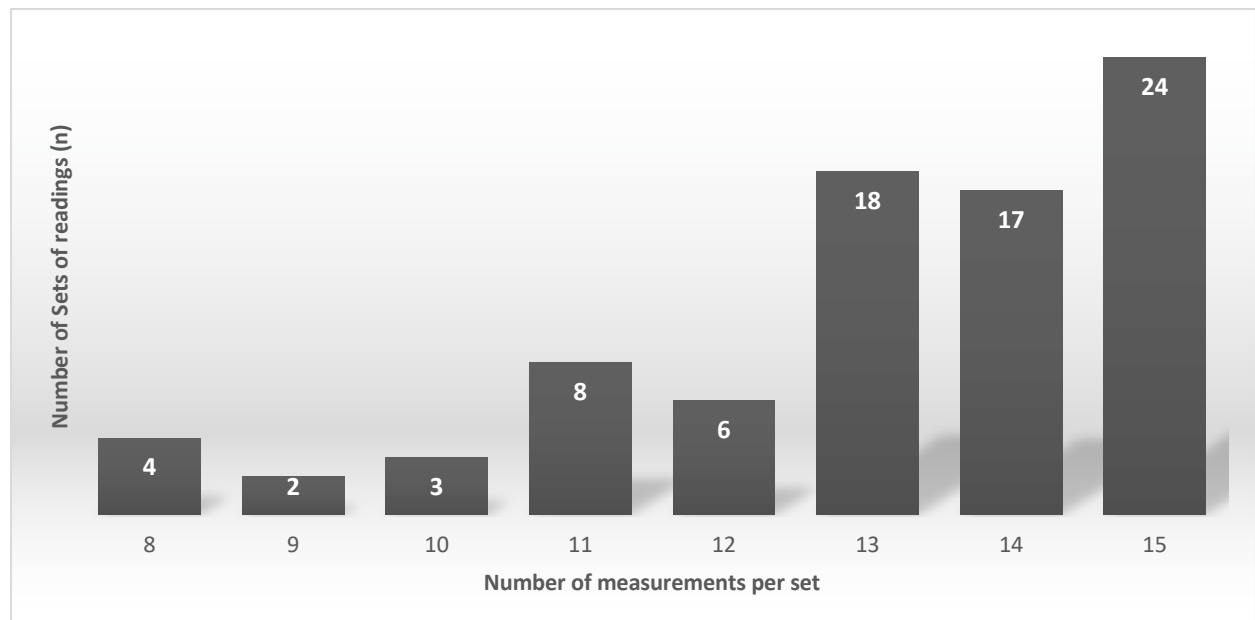


Figure 10. 1. Bar chart showing the total number of measurements per set of readings.

Eighty-two sets of readings were analysed. Missing data were present due to operator error. Figure 10.1 shows the range of the total number of measurements per set of readings. All sets had measurements at minutes 1 to 15. No sets of recordings were missing a measurement for intervals of longer than 2 minutes. Fifty-nine recordings (72%) had at least 13 of the 15 measurements.

Changes in measurements over time

The means of the absolute values were plotted of $TcpO_2$ and $TcpCO_2$ over the 15-minute period of 82 sets of readings against time (Figure 10.2). There were two curves showing a trend of the measurements reaching a plateau during the latter phase. Note the mean $TcpO_2$ at minute 15 is around 80mmHg and that for $TcpCO_2$ is around 25mmHg.

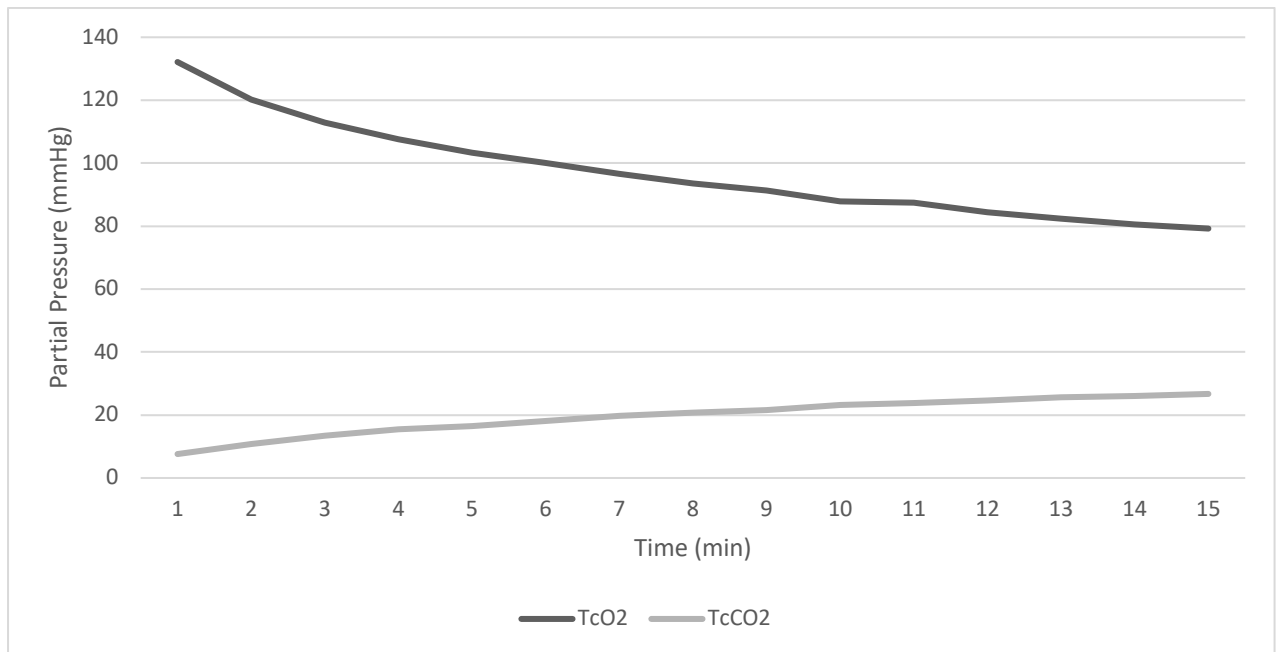


Figure 10. 2. Line graph showing mean variation in $TcpO_2$ and $TcpCO_2$ over time.

The proportional change in percentages for $TcpO_2$ and $TcpCO_2$ over time are demonstrated in Figures 10.3 and 10.4, respectively. The curves showed reducing decrements in the latter period of recording of less than 3% change between minutes 14 and 15 for both measurements. The degree of change was less in the $TcpO_2$ measurements at 0.8% between minutes 14 and 15 and less than 5% between minutes 11 and 15. However, the mean $TcpCO_2$ value at minute 15 was around 25mmHg, and 3% of 25mmHg would be insignificant.

Tissue Oxygenation and Wound Healing in Vascular Surgery

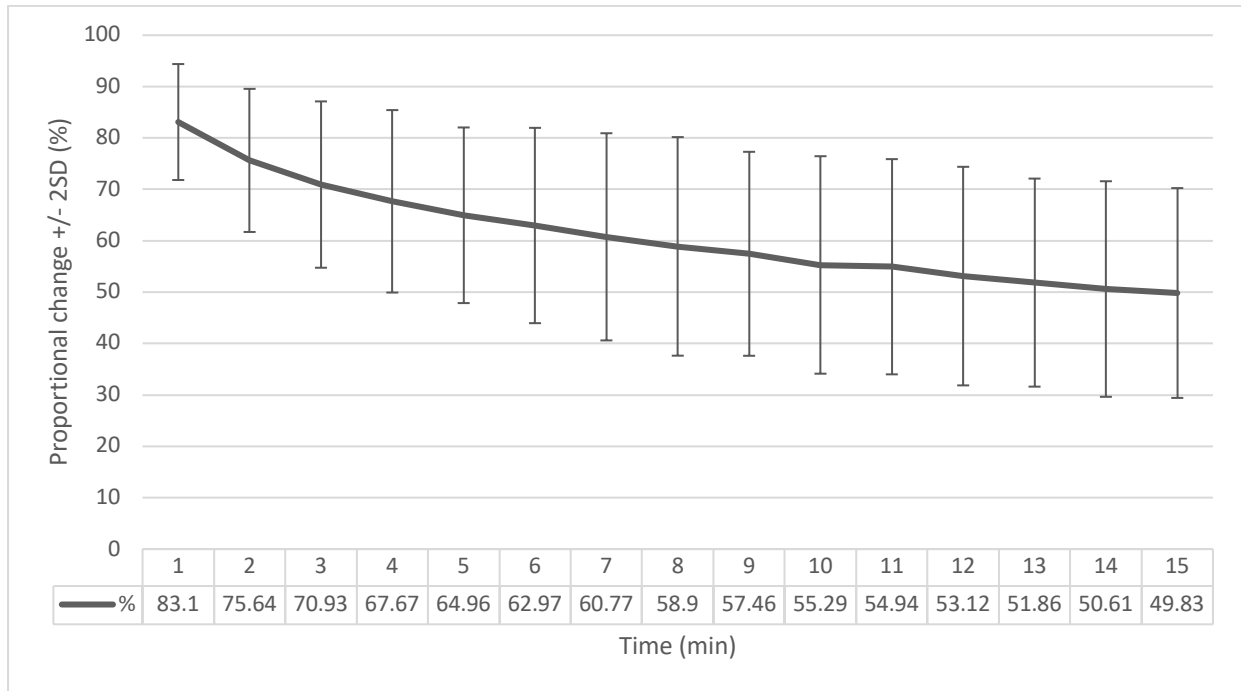


Figure 10. 3. Line graph showing proportional change in $TcpO_2$ over time.

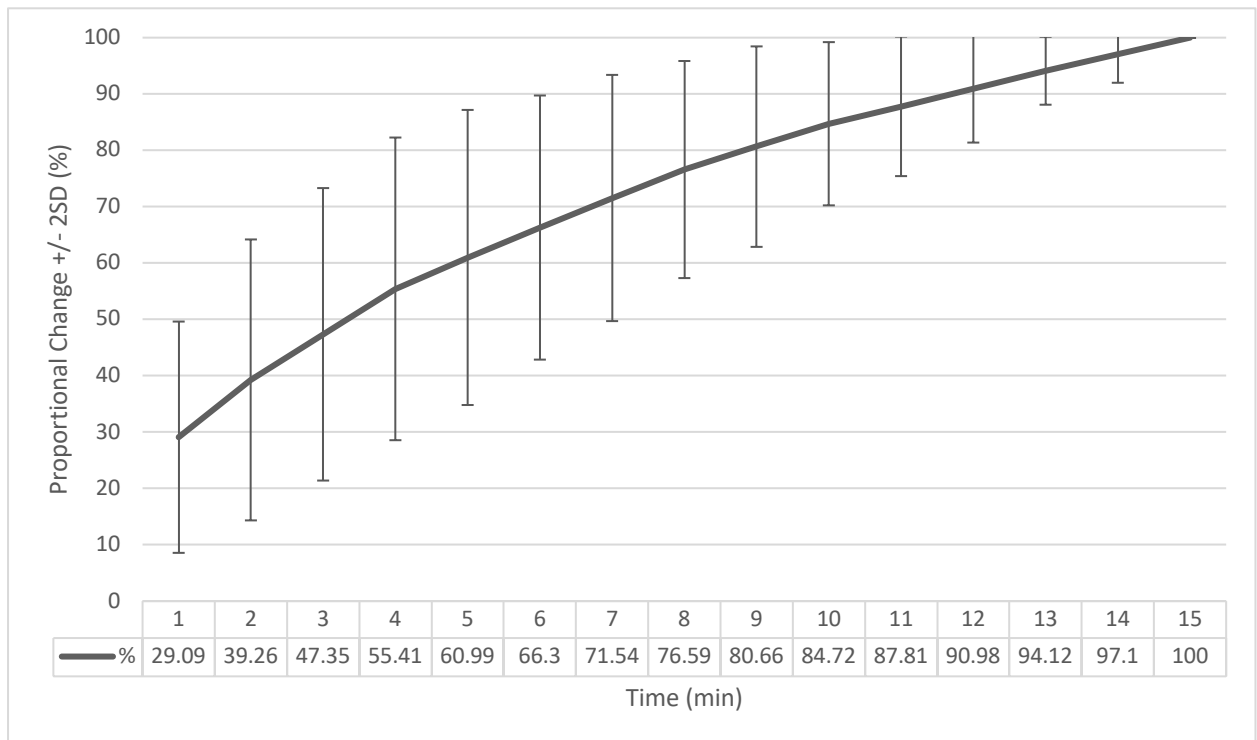


Figure 10. 4. Line graph showing proportional change in $TcpCO_2$ over time.

The sets of recordings were subdivided for the three groups of study participants, i.e., those with PVD of the lower limb (PVD group), hospitalised patients without documented PVD of the lower limb (non-PVD group), and healthy volunteers (volunteer group). The trend of Tc_pO₂ and Tc_pCO₂ reaching equilibrium at around 15 minutes was still present and similar in pattern, with a less than 4% proportional change between minutes 14 and 15 (Figures 10.5 and 10.6).

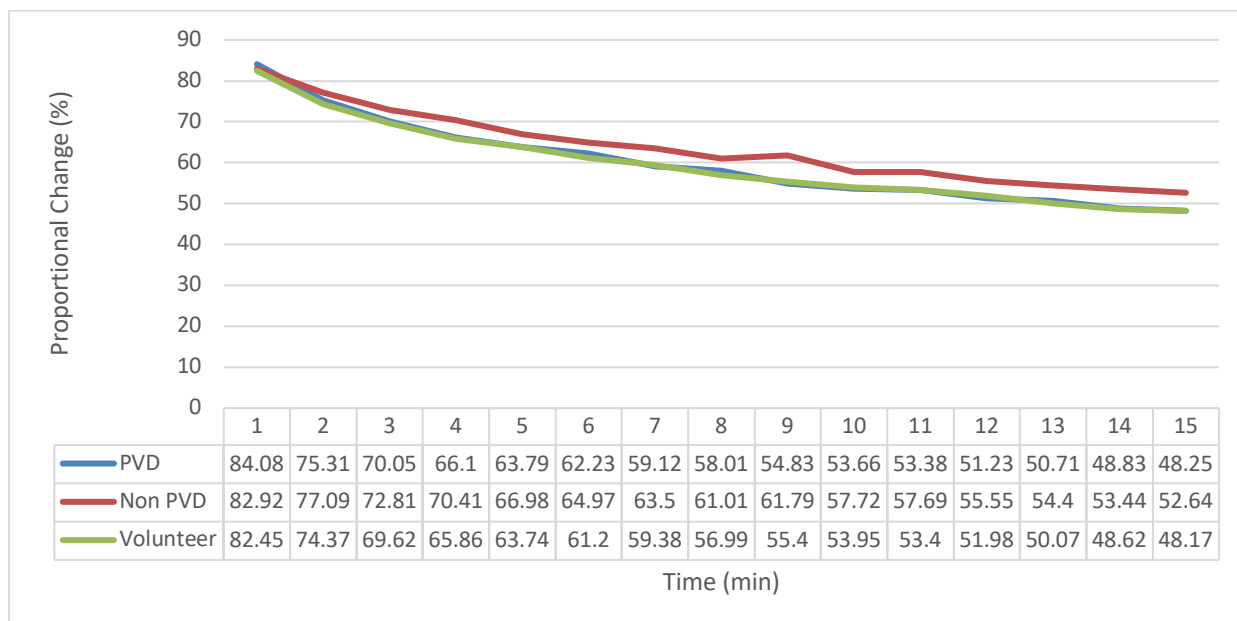


Figure 10. 5. Line graph showing the proportional change in Tc_pO₂ in subgroups over time.

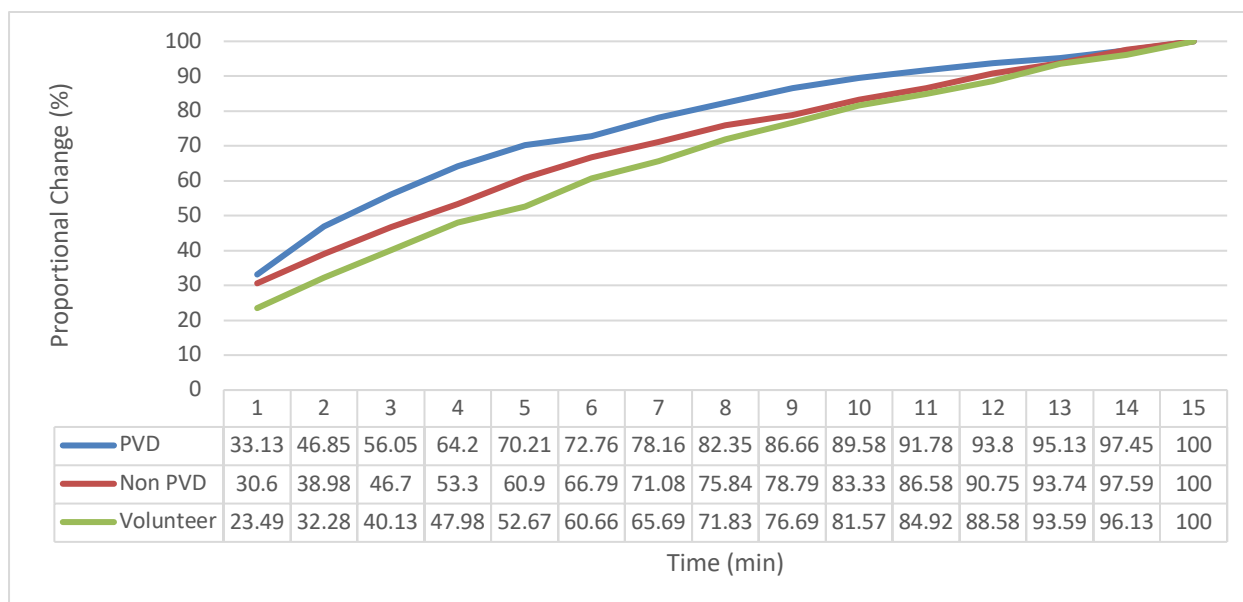


Figure 10. 6. Line graph showing the proportional change in Tc_pCO₂ in subgroups over time.

Even if the “diseased” limbs in the 16 patients with PVD were investigated separately, similar trends were shown in Figure 10.7.

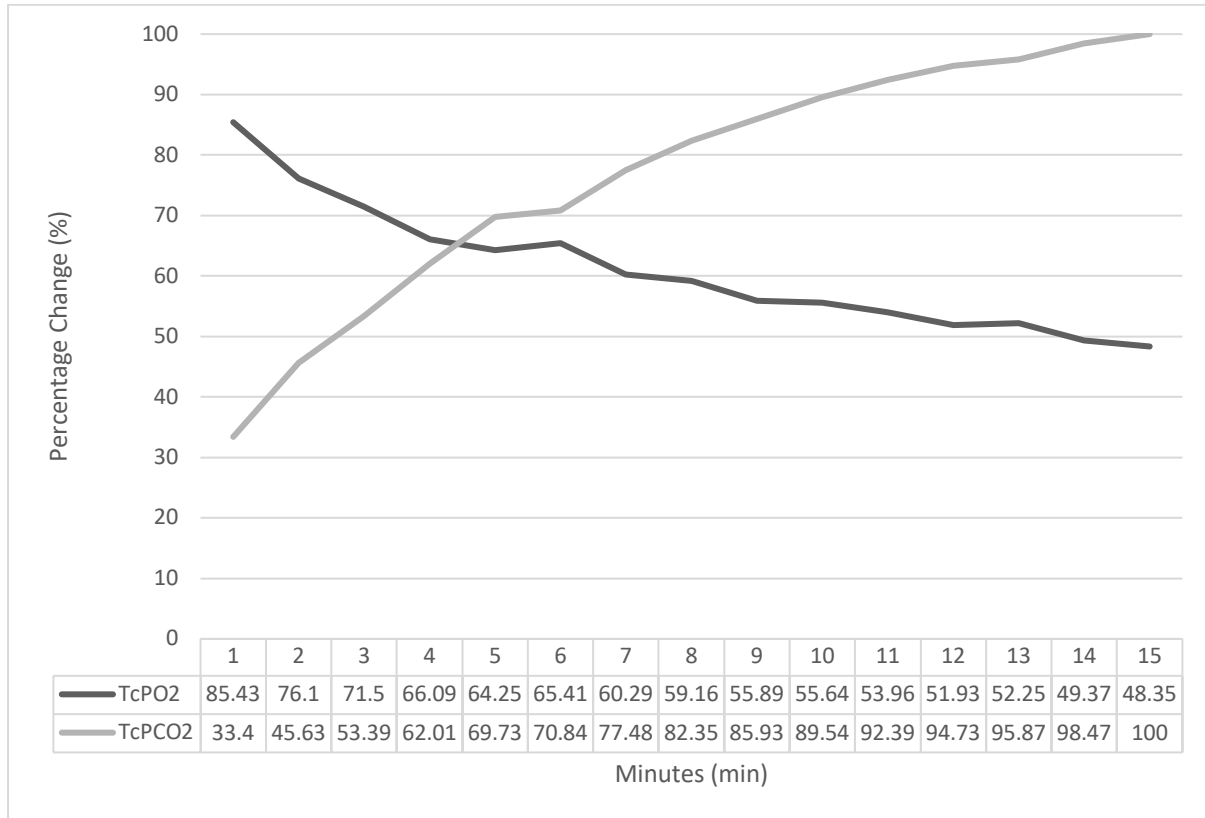


Figure 10. 7. Line graph showing the proportional change in TcPO₂ and TcPCO₂ over time in the 16 diseased limbs of patients with PVD.

Discussion

This study was the first series that targeted minute-to-minute variation in TcPO₂ and TcPCO₂ measurements obtained using the TINA TCOM3 device. Previous research studies used the recommendations of Sheffield *et al* regarding duration needed for the electrodes to reach equilibrium. However, these recommendations are based on beliefs rather than evidence. This study provided evidence that it is reliable to record TcPO₂ and TcPCO₂ readings at 15 minutes of monitoring when there is less than 3% variation between minutes 14 and 15 irrespective of the presence of PVD. Such findings can provide a more standardised and robust protocol, eliminating operator bias and avoiding waste of valuable time and resources. Interpreting these values prematurely can result in up to 10% variation. Based on the mean values of

TcpO₂ and TcpCO₂ at 15 minutes, this could lead to significant deviation of 80 +/- 8mmHg and 25 +/- 3mmHg respectively.

In this study, recordings in patients with PVD sometimes included the contralateral limb “without PVD”; similarly, participants in the non-PVD group or volunteer group might have had undiagnosed PVD. This heterogeneity was irrelevant to the aim of the study. Comparative studies of TcpO₂ and TcpCO₂ measurements in various subgroups have been described, for example, in normal individuals, claudicants, those with critical limb ischaemia, smokers, and diabetes. This study confirmed the reliability of recording TCOM measurements at 15 minutes, irrespective of whether the individual has PVD or is healthy.

As discussed in Section 1.14, Vesterager *et al* described the relationship between TcpO₂ and time taken to reach equilibrium of the electrode. A typical dip in measurements at around 8 minutes was described, where TcpO₂ reached the lowest value and subsequently rebounded to equilibrium at around 15 minutes (Figure 1.14). This study failed to demonstrate such a pattern, despite consisting of a relative large sample size in the TCOM literature.

Conclusion

This study shows that the 15 minutes would be a reliable cut-off point when recording TcpO₂ and TcpCO₂. This benchmark was set in the other studies in terms of TCOM measurements. Setting such a benchmark would maintain quality assurance in research studies and in clinical practice.

References

1. Niinikoski J. Current concepts of the role of oxygen in wound healing. *Ann Chir Gynaecol Suppl* 2001(215):9-11.
2. Niinikoski J. Effect of oxygen supply on wound healing and formation of experimental granulation tissue. *Acta Physiol Scand Suppl* 1969;334:1-72.
3. Enoch SL, Leaper DJ. Basic science of wound healing. *Surgery* 2007;26(2):31-7.
4. Kirsner RS, Eaglstein WH. The wound healing process. *Dermatol Clin* 1993;11(4):629-40.
5. Clark RA. Biology of dermal wound repair. *Dermatol Clin* 1993;11(4):647-66.
6. Kurkinen M, Vaheri A, Roberts PJ, et al. Sequential appearance of fibronectin and collagen in experimental granulation tissue. *Lab Invest* 1980;43(1):47-51.
7. Sprugel KH, McPherson JM, Clowes AW, et al. Effects of growth factors in vivo. I. Cell ingrowth into porous subcutaneous chambers. *Am J Pathol* 1987;129(3):601-13.
8. Broughton G, 2nd, Janis JE, Attinger CE. The basic science of wound healing. *Plast Reconstr Surg* 2006;117(7 Suppl):12S-34S.
9. Werner S, Grose R. Regulation of wound healing by growth factors and cytokines. *Physiol Rev* 2003;83(3):835-70.
10. Dormandy JA, Charbonnel B, Eckland DJ, et al. Secondary prevention of macrovascular events in patients with type 2 diabetes in the PROactive Study (PROspective pioglitAzone Clinical Trial In macroVascular Events): a randomised controlled trial. *Lancet* 2005;366(9493):1279-89.
11. Viljanto JA. Assessment of wound healing speed in man. *Prog Clin Biol Res* 1991;365:279-90.
12. Dvonch VM, Murphey RJ, Matsuoka J, et al. Changes in growth factor levels in human wound fluid. *Surgery* 1992;112(1):18-23.
13. Viljanto J, Kulonen E. Correlation of tensile strength and chemical composition in experimental granuloma. *Acta Pathol Microbiol Scand* 1962;56:120-6.
14. Jorgensen LN. Collagen deposition in the subcutaneous tissue during wound healing in humans: a model evaluation. *APMIS Suppl* 2003(115):1-56.
15. Slavin J. The role of cytokines in wound healing. *J Pathol* 1996;178(1):5-10.
16. Rizk M, Witte MB, Barbul A. Nitric oxide and wound healing. *World J Surg* 2004;28(3):301-6.

17. Abraham DJ, Shiwen X, Black CM, et al. Tumor necrosis factor alpha suppresses the induction of connective tissue growth factor by transforming growth factor-beta in normal and scleroderma fibroblasts. *J Biol Chem* 2000;275(20):15220-5.
18. Yager DR, Nwomeh BC. The proteolytic environment of chronic wounds. *Wound Repair Regen* 1999;7(6):433-41.
19. Goldman R. Growth factors and chronic wound healing: past, present, and future. *Adv Skin Wound Care* 2004;17(1):24-35.
20. Serhan CN, Chiang N. Novel endogenous small molecules as the checkpoint controllers in inflammation and resolution: entree for resoleomics. *Rheum Dis Clin North Am* 2004;30(1):69-95.
21. Grotendorst GR, Soma Y, Takehara K, et al. EGF and TGF-alpha are potent chemoattractants for endothelial cells and EGF-like peptides are present at sites of tissue regeneration. *J Cell Physiol* 1989;139(3):617-23.
22. Lawrence WT, Diegelmann RF. Growth factors in wound healing. *Clin Dermatol* 1994;12(1):157-69.
23. Xia YP, Zhao Y, Marcus J, et al. Effects of keratinocyte growth factor-2 (KGF-2) on wound healing in an ischaemia-impaired rabbit ear model and on scar formation. *J Pathol* 1999;188(4):431-8.
24. Smola H, Thiekotter G, Fusenig NE. Mutual induction of growth factor gene expression by epidermal-dermal cell interaction. *J Cell Biol* 1993;122(2):417-29.
25. Pierce GF, Mustoe TA, Altmann BW, et al. Role of platelet-derived growth factor in wound healing. *J Cell Biochem* 1991;45(4):319-26.
26. Vanttinen E, Viljanto J. Tensile strength of new connective tissue formed in pretreated viscose cellulose implants. *Ann Med Exp Biol Fenn* 1965;43(4):257-9.
27. Tonnesen MG, Feng X, Clark RA. Angiogenesis in wound healing. *J Investig Dermatol Symp Proc* 2000;5(1):40-6.
28. Steinbrech DS, Longaker MT, Mehrara BJ, et al. Fibroblast response to hypoxia: the relationship between angiogenesis and matrix regulation. *J Surg Res* 1999;84(2):127-33.
29. Witte MB, Kiyama T, Barbul A. Nitric oxide enhances experimental wound healing in diabetes. *Br J Surg* 2002;89(12):1594-601.
30. Henry G, Garner WL. Inflammatory mediators in wound healing. *Surg Clin North Am* 2003;83(3):483-507.

31. Ehrlich HP, Krummel TM. Regulation of wound healing from a connective tissue perspective. *Wound Repair Regen* 1996;4(2):203-10.
32. Kanzler MH, Gorsulowsky DC, Swanson NA. Basic mechanisms in the healing cutaneous wound. *J Dermatol Surg Oncol* 1986;12(11):1156-64.
33. Gottrup F. Healing of incisional wounds in stomach and duodenum. A biomechanical study. *Am J Surg* 1980;140(2):296-301.
34. Nelson DL, Lehninger AL, Cox MM. *Lehninger Principles of Biochemistry*. 5th ed, 2008.
35. Tymoczko JL, Stryer L, Berg J. *Biochemistry*. 6th ed, 2006.
36. Gross J, Piez KA. *Calcification in Biological Systems*. R.F. Sognaes ed. Washington DC, 1960.
37. Viljanto J. Biochemical basis of tensile strength in wound healing: an experimental study with viscose cellulose sponges in rats. *Acta Chir Scand (Suppl)* 1964;333(1).
38. Woessner JF. Determination of hydroxyproline in connective tissues. The methodology of connective tissues research. Oxford, UK: Johnson-Bruvvers Ltd, 1976:235-45.
39. Goodson WH 3rd, Hunt TK. Development of a new miniature method for the study of wound healing in human subjects. *J Surg Res* 1982;33(5):394-401.
40. Jorgensen LN. Collagen deposition in the subcutaneous tissue during wound healing in humans: a model evaluation. *APMIS Suppl* 2003;115:1-56.
41. Beer HD, Fassler R, Werner S. Glucocorticoid-regulated gene expression during cutaneous wound repair. *Vitam Horm* 2000;59:217-39.
42. Beer HD, Longaker MT, Werner S. Reduced expression of PDGF and PDGF receptors during impaired wound healing. *J Invest Dermatol* 1997;109(2):132-8.
43. Massague J. The transforming growth factor-beta family. *Annu Rev Cell Biol* 1990;6:597-641.
44. Desmouliere A, Geinoz A, Gabbiani F, et al. Transforming growth factor-beta 1 induces alpha-smooth muscle actin expression in granulation tissue myofibroblasts and in quiescent and growing cultured fibroblasts. *J Cell Biol* 1993;122(1):103-11.
45. Roberts AB, Sporn MB. *Transforming Growth Factor- β* . 2nd ed. New York: Plenum, 1996.
46. Roberts AB, Sporn MB, Assoian RK, et al. Transforming growth factor type beta: rapid induction of fibrosis and angiogenesis in vivo and stimulation of collagen formation in vitro. *Proc Natl Acad Sci U S A* 1986;83(12):4167-71.

47. Zambruno G, Marchisio PC, Marconi A, et al. Transforming growth factor-beta 1 modulates beta 1 and beta 5 integrin receptors and induces the de novo expression of the alpha v beta 6 heterodimer in normal human keratinocytes: implications for wound healing. *J Cell Biol* 1995;129(3):853-65.
48. Gailit J, Welch MP, Clark RA. TGF-beta 1 stimulates expression of keratinocyte integrins during re-epithelialization of cutaneous wounds. *J Invest Dermatol* 1994;103(2):221-7.
49. Assoian RK, Komoriya A, Meyers CA, et al. Transforming growth factor-beta in human platelets. Identification of a major storage site, purification, and characterization. *J Biol Chem* 1983;258(11):7155-60.
50. Shah M, Foreman DM, Ferguson MW. Neutralisation of TGF-beta 1 and TGF-beta 2 or exogenous addition of TGF-beta 3 to cutaneous rat wounds reduces scarring. *J Cell Sci* 1995;108(Pt 3):985-1002.
51. Chan T, Ghahary A, Demare J, et al. Development, characterization, and wound healing of the keratin 14 promoted transforming growth factor-beta1 transgenic mouse. *Wound Repair Regen* 2002;10(3):177-87.
52. Lee TY, Chin GS, Kim WJ, et al. Expression of transforming growth factor beta 1, 2, and 3 proteins in keloids. *Ann Plast Surg* 1999;43(2):179-84.
53. Peltonen J, Hsiao LL, Jaakkola S, et al. Activation of collagen gene expression in keloids: co-localization of type I and VI collagen and transforming growth factor-beta 1 mRNA. *J Invest Dermatol* 1991;97(2):240-8.
54. Basilico C, Moscatelli D. The FGF family of growth factors and oncogenes. *Adv Cancer Res* 1992;59:115-65.
55. Miller DL, Ortega S, Bashayan O, et al. Compensation by fibroblast growth factor 1 (FGF1) does not account for the mild phenotypic defects observed in FGF2 null mice. *Mol Cell Biol* 2000;20(6):2260-8.
56. Gale NW, Yancopoulos GD. Growth factors acting via endothelial cell-specific receptor tyrosine kinases: VEGFs, angiopoietins, and ephrins in vascular development. *Genes Dev* 1999;13(9):1055-66.
57. Brown LF, Yeo KT, Berse B, et al. Expression of vascular permeability factor (vascular endothelial growth factor) by epidermal keratinocytes during wound healing. *J Exp Med* 1992;176(5):1375-9.

58. Frank S, Hubner G, Breier G, et al. Regulation of vascular endothelial growth factor expression in cultured keratinocytes. Implications for normal and impaired wound healing. *J Biol Chem* 1995;270(21):12607-13.
59. Lauer G, Sollberg S, Cole M, et al. Expression and proteolysis of vascular endothelial growth factor is increased in chronic wounds. *J Invest Dermatol* 2000;115(1):12-8.
60. Peters KG, De Vries C, Williams LT. Vascular endothelial growth factor receptor expression during embryogenesis and tissue repair suggests a role in endothelial differentiation and blood vessel growth. *Proc Natl Acad Sci U S A* 1993;90(19):8915-9.
61. Howdieshell TR, Callaway D, Webb WL, et al. Antibody neutralization of vascular endothelial growth factor inhibits wound granulation tissue formation. *J Surg Res* 2001;96(2):173-82.
62. Swift ME, Kleinman HK, DiPietro LA. Impaired wound repair and delayed angiogenesis in aged mice. *Lab Invest* 1999;79(12):1479-87.
63. Breitbart AS, Grande DA, Laser J, et al. Treatment of ischemic wounds using cultured dermal fibroblasts transduced retrovirally with PDGF-B and VEGF121 genes. *Ann Plast Surg* 2001;46(5):555-61; discussion 61-2.
64. Corral CJ, Siddiqui A, Wu L, et al. Vascular endothelial growth factor is more important than basic fibroblastic growth factor during ischemic wound healing. *Arch Surg* 1999;134(2):200-5.
65. Karkkainen MJ, Makinen T, Alitalo K. Lymphatic endothelium: a new frontier of metastasis research. *Nat Cell Biol* 2002;4(1):E2-5.
66. Failla CM, Odorisio T, Cianfarani F, et al. Placenta growth factor is induced in human keratinocytes during wound healing. *J Invest Dermatol* 2000;115(3):388-95.
67. Hubner G, Brauchle M, Smola H, et al. Differential regulation of pro-inflammatory cytokines during wound healing in normal and glucocorticoid-treated mice. *Cytokine* 1996;8(7):548-56.
68. Feiken E, Romer J, Eriksen J, et al. Neutrophils express tumor necrosis factor-alpha during mouse skin wound healing. *J Invest Dermatol* 1995;105(1):120-3.
69. Mori R, Kondo T, Ohshima T, et al. Accelerated wound healing in tumor necrosis factor receptor p55-deficient mice with reduced leukocyte infiltration. *FASEB J* 2002;16(9):963-74.

70. Engelhardt E, Toksoy A, Goebeler M, et al. Chemokines IL-8, GRO α , MCP-1, IP-10, and Mig are sequentially and differentially expressed during phase-specific infiltration of leukocyte subsets in human wound healing. *Am J Pathol* 1998;153(6):1849-60.
71. Rennekampff HO, Hansbrough JF, Kiessig V, et al. Bioactive interleukin-8 is expressed in wounds and enhances wound healing. *J Surg Res* 2000;93(1):41-54.
72. Iocono JA, Colleran KR, Remick DG, et al. Interleukin-8 levels and activity in delayed-healing human thermal wounds. *Wound Repair Regen* 2000;8(3):216-25.
73. Liechty KW, Crombleholme TM, Cass DL, et al. Diminished interleukin-8 (IL-8) production in the fetal wound healing response. *J Surg Res* 1998;77(1):80-4.
74. Hartmann M, Jonsson K, Zederfeldt B. Importance of dehydration in anastomotic and subcutaneous wound healing: an experimental study in rats. *Eur J Surg* 1992;158(2):79-82.
75. Holt DR, Kirk SJ, Regan MC, et al. Effect of age on wound healing in healthy human beings. *Surgery* 1992;112(2):293-7; discussion 97-8.
76. Trueblood HW, Nelsen TS, Oberhelman HA, Jr. The effect of acute anemia and iron deficiency anemia on wound healing. *Arch Surg* 1969;99(1):113-6.
77. Goodson WH, 3rd, Hunt TK. Wound healing and the diabetic patient. *Surg Gynecol Obstet* 1979;149(4):600-8.
78. Black E, Vibe-Petersen J, Jorgensen LN, et al. Decrease of collagen deposition in wound repair in type 1 diabetes independent of glycemic control. *Arch Surg* 2003;138(1):34-40.
79. Carrico TJ, Mehrhof AI, Jr., Cohen IK. Biology of wound healing. *Surg Clin North Am* 1984;64(4):721-33.
80. Carnevali S, Nakamura Y, Mio T, et al. Cigarette smoke extract inhibits fibroblast-mediated collagen gel contraction. *Am J Physiol* 1998;274(4 Pt 1):L591-8.
81. Yue DK, Swanson B, McLennan S, et al. Abnormalities of granulation tissue and collagen formation in experimental diabetes, uraemia and malnutrition. *Diabet Med* 1986;3(3):221-5.
82. Ashcroft GS, Horan MA, Ferguson MW. The effects of ageing on wound healing: immunolocalisation of growth factors and their receptors in a murine incisional model. *J Anat* 1997;190 (Pt 3):351-65.

83. Adzick NS, Harrison MR, Glick PL, et al. Comparison of fetal, newborn, and adult wound healing by histologic, enzyme-histochemical, and hydroxyproline determinations. *J Pediatr Surg* 1985;20(4):315-9.
84. Goodson WH, 3rd, Lopez-Sarmiento A, Jensen JA, et al. The influence of a brief preoperative illness on postoperative healing. *Ann Surg* 1987;205(3):250-5.
85. Tadros T, Wobbles T, Hendriks T. Blood transfusion impairs the healing of experimental intestinal anastomoses. *Ann Surg* 1992;215(3):276-81.
86. Robson MC. Wound infection. A failure of wound healing caused by an imbalance of bacteria. *Surg Clin North Am* 1997;77(3):637-50.
87. Robson MC, Stenberg BD, Heggens JP. Wound healing alterations caused by infection. *Clin Plast Surg* 1990;17(3):485-92.
88. Robson MC, Mannari RJ, Smith PD, et al. Maintenance of wound bacterial balance. *Am J Surg* 1999;178(5):399-402.
89. Krizek TJ, Robson MC. Evolution of quantitative bacteriology in wound management. *Am J Surg* 1975;130(5):579-84.
90. Robson MC, Heggens JP. Delayed wound closure based on bacterial counts. *J Surg Oncol* 1970;2(4):379-83.
91. Lindstedt E, Sandblom P. Wound healing in man: tensile strength of healing wounds in some patient groups. *Ann Surg* 1975;181(6):842-6.
92. Fullana F, Grande L, Fernandez-Llamazares J, et al. Skin prolylhydroxylase activity and wound healing. *Eur Surg Res* 1993;25(6):370-5.
93. Haydock DA, Hill GL. Improved wound healing response in surgical patients receiving intravenous nutrition. *Br J Surg* 1987;74(4):320-3.
94. Gniadecki R, Gniadecka M, Serup J. Inhibition of glucocorticoid-induced epidermal and dermal atrophy with KH 1060--a potent 20-epi analogue of 1,25-dihydroxyvitamin D3. *Br J Pharmacol* 1994;113(2):439-44.
95. Gniadecki R, Serup J. Enhancement of the granulation tissue formation in hairless mice by a potent vitamin D receptor agonist--KH 1060. *J Endocrinol* 1994;141(3):411-5.
96. Palka J, Galewska Z. The effect of some antiinflammatory drugs on collagen of rat skin. *Pol J Pharmacol Pharm* 1990;42(1):39-42.
97. Schulze S, Andersen J, Overgaard H, et al. Effect of prednisolone on the systemic response and wound healing after colonic surgery. *Arch Surg* 1997;132(2):129-35.
98. Hunt TK, Zederfeldt B, Goldstick TK. Oxygen and healing. *Am J Surg* 1969;118(4):521-5.

99. Stephens FO, Hunt TK. Effect of changes in inspired oxygen and carbon dioxide tensions on wound tensile strength: an experimental study. *Ann Surg* 1971;173(4):515-9.
100. Sen CK, Khanna S, Babior BM, et al. Oxidant-induced vascular endothelial growth factor expression in human keratinocytes and cutaneous wound healing. *J Biol Chem* 2002;277(36):33284-90.
101. Falabella AF, Falanga V. Wound healing. In: Freinkel RK, Woodley DT, eds. *The Biology of the Skin*. New York, NY: The Pathenon Publishing Group; 2001:281-97.
102. Gottrup F. Oxygen in wound healing and infection. *World J Surg* 2004;28(3):312-5.
103. Rodriguez PG, Felix FN, Woodley DT, et al. The role of oxygen in wound healing: a review of the literature. *Dermatol Surg* 2008;34(9):1159-69.
104. Knighton DR, Silver IA, Hunt TK. Regulation of wound-healing angiogenesis-effect of oxygen gradients and inspired oxygen concentration. *Surgery* 1981;90(2):262-70.
105. Schultz S, Diegelmann RF, Chegini N. *Biochemistry of Wound Healing in Wound Care Practice*: Flagstaff, AZ: Best Publishing, 2004.
106. Hunt TK, Hussain Z. Wound microenvironment. In: Cohen IK, Diegelmann RF, Linblad WJ, eds. *Wound Healing: Biochemical And Clinical Aspects*. Philadelphia, PA: WB Saunders, 1992:274-81.
107. Allen DB, Maguire JJ, Mahdavian M, et al. Wound hypoxia and acidosis limit neutrophil bacterial killing mechanisms. *Arch Surg* 1997;132(9):991-6.
108. Tandara AA, Mustoe TA. Oxygen in wound healing--more than a nutrient. *World J Surg* 2004;28(3):294-300.
109. Sarsour EH, Kumar MG, Chaudhuri L, et al. Redox control of the cell cycle in health and disease. *Antioxid Redox Signal* 2009;11(12):2985-3011.
110. Hart J. Inflammation. 1: Its role in the healing of acute wounds. *J Wound Care* 2002;11(6):205-9.
111. Juranek I, Bezek S. Controversy of free radical hypothesis: reactive oxygen species--cause or consequence of tissue injury? *Gen Physiol Biophys* 2005;24(3):263-78.
112. Bishop A. Role of oxygen in wound healing. *J Wound Care* 2008;17(9):399-402.
113. Alleva R, Nasole E, Di Donato F, et al. alpha-Lipoic acid supplementation inhibits oxidative damage, accelerating chronic wound healing in patients undergoing hyperbaric oxygen therapy. *Biochem Biophys Res Commun* 2005;333(2):404-10.

114. Pryor KO, Fahey TJ, 3rd, Lien CA, et al. Surgical site infection and the routine use of perioperative hyperoxia in a general surgical population: a randomized controlled trial. *JAMA* 2004;291(1):79-87.
115. Pryor KO, Lien CA, Fahey TJ, 3rd, et al. Supplemental oxygen and risk of surgical wound infection. *JAMA* 2006;295(14):1642; author reply 42-3.
116. LaVan FB, Hunt TK. Oxygen and wound healing. *Clin Plast Surg* 1990;17(3):463-72.
117. Belda FJ, Aguilera L, Garcia de la Asuncion J, et al. Supplemental perioperative oxygen and the risk of surgical wound infection: a randomized controlled trial. *JAMA* 2005;294(16):2035-42.
118. Greif R, Akca O, Horn EP, et al. Supplemental perioperative oxygen to reduce the incidence of surgical-wound infection. *N Engl J Med* 2000;342(3):161-7.
119. Schmidt E. Supplemental perioperative oxygen at 80% FIO₂ reduced surgical site infections in elective colorectal surgery. *Evid Based Nurs* 2006;9(2):52.
120. Hopf HW, Hunt TK, West JM, et al. Wound tissue oxygen tension predicts the risk of wound infection in surgical patients. *Arch Surg* 1997;132(9):997-1004; discussion 05.
121. Al-Niaimi A, Safdar N. Supplemental perioperative oxygen for reducing surgical site infection: a meta-analysis. *J Eval Clin Pract* 2009;15(2):360-5.
122. Chura JC, Boyd A, Argenta PA. Surgical site infections and supplemental perioperative oxygen in colorectal surgery patients: a systematic review. *Surg Infect (Larchmt)* 2007;8(4):455-61.
123. Qadan M, Akca O, Mahid SS, et al. Perioperative supplemental oxygen therapy and surgical site infection: a meta-analysis of randomized controlled trials. *Arch Surg* 2009;144(4):359-66; discussion 66-7.
124. Whitney JD. Supplemental perioperative oxygen and fluids to improve surgical wound outcomes: Translating evidence into practice. *Wound Repair Regen* 2003;11(6):462-7.
125. Turtiainen J, Saimanen EI, Partio TJ, et al. Supplemental postoperative oxygen in the prevention of surgical wound infection after lower limb vascular surgery: a randomized controlled trial. *World J Surg* 2011;35(6):1387-95.
126. Verklin RM, Jr., Mandell GL. Alteration of effectiveness of antibiotics by anaerobiosis. *J Lab Clin Med* 1977;89(1):65-71.
127. Kulikovsky M, Gil T, Mettanes I, et al. Hyperbaric oxygen therapy for non-healing wounds. *Isr Med Assoc J* 2009;11(8):480-5.

128. Goldman RJ. Hyperbaric oxygen therapy for wound healing and limb salvage: a systematic review. *PM R* 2009;1(5):471-89.
129. Huang ET, Mansouri J, Murad MH, et al. A clinical practice guideline for the use of hyperbaric oxygen therapy in the treatment of diabetic foot ulcers. *Undersea Hyperb Med* 2015;42(3):205-47.
130. Bishop AJ, Mudge E. Diabetic foot ulcers treated with hyperbaric oxygen therapy: a review of the literature. *Int Wound J* 2014;11(1):28-34.
131. Londahl M. Hyperbaric oxygen therapy as adjunctive treatment of diabetic foot ulcers. *Med Clin North Am* 2013;97(5):957-80.
132. Margolis DJ, Gupta J, Hoffstad O, et al. Lack of effectiveness of hyperbaric oxygen therapy for the treatment of diabetic foot ulcer and the prevention of amputation: a cohort study. *Diabetes Care* 2013;36(7):1961-6.
133. Forsythe JA, Jiang BH, Iyer NV, et al. Activation of vascular endothelial growth factor gene transcription by hypoxia-inducible factor 1. *Mol Cell Biol* 1996;16(9):4604-13.
134. Knighton DR, Hunt TK, Scheuenstuhl H, et al. Oxygen tension regulates the expression of angiogenesis factor by macrophages. *Science* 1983;221(4617):1283-5.
135. Trabold O, Wagner S, Wicke C, et al. Lactate and oxygen constitute a fundamental regulatory mechanism in wound healing. *Wound Repair Regen* 2003;11(6):504-9.
136. Hopf HW, Gibson JJ, Angeles AP, et al. Hyperoxia and angiogenesis. *Wound Repair Regen* 2005;13(6):558-64.
137. Semenza GL. HIF-1 and human disease: one highly involved factor. *Genes Dev* 2000;14(16):1983-91.
138. Gerber HP, Condorelli F, Park J, et al. Differential transcriptional regulation of the two vascular endothelial growth factor receptor genes. Flt-1, but not Flk-1/KDR, is up-regulated by hypoxia. *J Biol Chem* 1997;272(38):23659-67.
139. Kranke P, Bennett M, Roeckl-Wiedmann I, et al. Hyperbaric oxygen therapy for chronic wounds. *Cochrane Database Syst Rev* 2004;2:CD004123.
140. Patel V, Chivukula IV, Roy S, et al. Oxygen: from the benefits of inducing VEGF expression to managing the risk of hyperbaric stress. *Antioxid Redox Signal* 2005;7(9-10):1377-87.
141. Ragheb J, Buggy DJ. Editorial III: Tissue oxygen tension (PTO₂) in anaesthesia and perioperative medicine. *Br J Anaesth* 2004;92(4):464-8.

142. Gordillo GM, Sen CK. Revisiting the essential role of oxygen in wound healing. *Am J Surg* 2003;186(3):259-63.
143. Semenza GL. Hydroxylation of HIF-1: oxygen sensing at the molecular level. *Physiology (Bethesda)* 2004;19:176-82.
144. Wiesener MS, Maxwell PH. HIF and oxygen sensing; as important to life as the air we breathe? *Ann Med* 2003;35(3):183-90.
145. Gajendrareddy PK, Sen CK, Horan MP, et al. Hyperbaric oxygen therapy ameliorates stress-impaired dermal wound healing. *Brain Behav Immun* 2005;19(3):217-22.
146. Sander AL, Henrich D, Muth CM, et al. In vivo effect of hyperbaric oxygen on wound angiogenesis and epithelialization. *Wound Repair Regen* 2009;17(2):179-84.
147. Alleva R, Tomasetti M, Sartini D, et al. alpha-Lipoic acid modulates extracellular matrix and angiogenesis gene expression in non-healing wounds treated with hyperbaric oxygen therapy. *Mol Med* 2008;14(3-4):175-83.
148. Sheikh AY, Gibson JJ, Rollins MD, et al. Effect of hyperoxia on vascular endothelial growth factor levels in a wound model. *Arch Surg* 2000;135(11):1293-7.
149. Falanga V, Qian SW, Danielpour D, et al. Hypoxia upregulates the synthesis of TGF-beta 1 by human dermal fibroblasts. *J Invest Dermatol* 1991;97(4):634-7.
150. Falanga V, Zhou L, Yufit T. Low oxygen tension stimulates collagen synthesis and COL1A1 transcription through the action of TGF-beta1. *J Cell Physiol* 2002;191(1):42-50.
151. Siddiqui A, Galiano RD, Connors D, et al. Differential effects of oxygen on human dermal fibroblasts: acute versus chronic hypoxia. *Wound Repair Regen* 1996;4(2):211-8.
152. Wada M, Gelfman CM, Matsunaga H, et al. Density-dependent expression of FGF-2 in response to oxidative stress in RPE cells in vitro. *Curr Eye Res* 2001;23(3):226-31.
153. Sen CK. The general case for redox control of wound repair. *Wound Repair Regen* 2003;11(6):431-8.
154. Salo T, Makela M, Kylmaniemi M, et al. Expression of matrix metalloproteinase-2 and -9 during early human wound healing. *Lab Invest* 1994;70(2):176-82.
155. Mauviel A, Chung KY, Agarwal A, et al. Cell-specific induction of distinct oncogenes of the Jun family is responsible for differential regulation of collagenase gene expression by transforming growth factor-beta in fibroblasts and keratinocytes. *J Biol Chem* 1996;271(18):10917-23.

156. O'Toole EA, Marinkovich MP, Peavey CL, et al. Hypoxia increases human keratinocyte motility on connective tissue. *J Clin Invest* 1997;100(11):2881-91.
157. Xia YP, Zhao Y, Tyrone JW, et al. Differential activation of migration by hypoxia in keratinocytes isolated from donors of increasing age: implication for chronic wounds in the elderly. *J Invest Dermatol* 2001;116(1):50-6.
158. Prockop DJ, Kivirikko KI, Tuderman L, et al. The biosynthesis of collagen and its disorders (first of two parts). *N Engl J Med* 1979;301(1):13-23.
159. Roy S, Khanna S, Wallace WA, et al. Characterization of perceived hyperoxia in isolated primary cardiac fibroblasts and in the reoxygenated heart. *J Biol Chem* 2003;278(47):47129-35.
160. Mehm WJ, Pimsler M, Becker RL, Lissner CR. Effect of oxygen on in vitro fibroblast cell proliferation and collagen biosynthesis. *Journal of Hyperbaric Medicine* 1988;3(4):227-34.
161. Kan C, Abe M, Yamanaka M, et al. Hypoxia-induced increase of matrix metalloproteinase-1 synthesis is not restored by reoxygenation in a three-dimensional culture of human dermal fibroblasts. *J Dermatol Sci* 2003;32(1):75-82.
162. Hunt TK, Pai MP. The effect of varying ambient oxygen tensions on wound metabolism and collagen synthesis. *Surg Gynecol Obstet* 1972;135(4):561-7.
163. Jonsson K, Jensen JA, Goodson WH 3rd, et al. Tissue oxygenation, anemia, and perfusion in relation to wound healing in surgical patients. *Ann Surg* 1991;214(5):605-13.
164. Dinar S, Agir H, Sen C, et al. Effects of hyperbaric oxygen therapy on fibrovascular ingrowth in porous polyethylene blocks implanted under burn scar tissue: an experimental study. *Burns* 2008;34(4):467-73.
165. Nakada T, Saito Y, Chikenji M, et al. Therapeutic outcome of hyperbaric oxygen and basic fibroblast growth factor on intractable skin ulcer in legs: preliminary report. *Plast Reconstr Surg* 2006;117(2):646-51; discussion 52-3.
166. Puckridge PJ, Saleem HA, Vasudevan TM, et al. Perioperative high-dose oxygen therapy in vascular surgery. *ANZ J Surg* 2007;77(6):433-6.
167. Meyhoff CS, Wetterslev J, Jorgensen LN, et al. Effect of high perioperative oxygen fraction on surgical site infection and pulmonary complications after abdominal surgery: the PROXI randomized clinical trial. *JAMA* 2009;302(14):1543-50.

168. Meyhoff CS, Jorgensen LN, Wetterslev J, et al. Increased long-term mortality after a high perioperative inspiratory oxygen fraction during abdominal surgery: follow-up of a randomized clinical trial. *Anesth Analg* 2012;115(4):849-54.
169. Frank SM, Higgins MS, Breslow MJ, et al. The catecholamine, cortisol, and hemodynamic responses to mild perioperative hypothermia. A randomized clinical trial. *Anesthesiology* 1995;82(1):83-93.
170. Leaper D. Effects of local and systemic warming on postoperative infections. *Surg Infect (Larchmt)* 2006;7 Suppl 2:S101-3.
171. Sajid MS, Shakir AJ, Khatri K, et al. The role of perioperative warming in surgery: a systematic review. *Sao Paulo Med J* 2009;127(4):231-7.
172. Wong PF, Kumar S, Bohra A, et al. Randomized clinical trial of perioperative systemic warming in major elective abdominal surgery. *Br J Surg* 2007;94(4):421-6.
173. Kurz A, Sessler DI, Lenhardt R. Perioperative normothermia to reduce the incidence of surgical-wound infection and shorten hospitalization. Study of Wound Infection and Temperature Group. *N Engl J Med* 1996;334(19):1209-15.
174. Ikeda T, Tayefeh F, Sessler DI, et al. Local radiant heating increases subcutaneous oxygen tension. *Am J Surg* 1998;175(1):33-7.
175. Thiernemann C. Biosynthesis and interaction of endothelium-derived vasoactive mediators. *Eicosanoids* 1991;4(4):187-202.
176. Bertele V, Cerletti C, de Gaetano G. Pathophysiology of critical leg ischaemia and mode of action of prostaglandins. *Agents Actions Suppl* 1992;37:18-26.
177. *Intravenous Administration of Iloprost*. Berlin: Bayer Schering Pharma AG, 2009.
178. Schror K. Antiplatelet effect of iloprost. *Am J Med* 1992;92(2):231.
179. Gorman RR, Bunting S, Miller OV. Modulation of human platelet adenylate cyclase by prostacyclin (PGX). *Prostaglandins* 1977;13(3):377-88.
180. Tateson JE, Moncada S, Vane JR. Effects of prostacyclin (PGX) on cyclic AMP concentrations in human platelets. *Prostaglandins* 1977;13(3):389-97.
181. Shah P, Murray AK, Moore TL, et al. Effects of iloprost on microvascular structure assessed by nailfold videocapillaroscopy: a pilot study. *J Rheumatol* 2011;38(9):2079-80.
182. Adaikan PG, Kottegoda SR. Prostacyclin analogs. *Drugs of the Future*. 1985:765-74.
183. Andreozzi GM, Di Pino L, Li Pira M, et al. Iloprost, stable analogue of the prostacyclin, is able to improve the tissue resistance to ischaemia. *Int Angiol* 1994;13(1):68-9.

184. Pehlivan Y, Turkbeyler IH, Balakan O, et al. Possible anti-metastatic effect of Iloprost in a patient with systemic sclerosis with lung cancer: a case study. *Rheumatol Int* 2012;32(5):1437-41.
185. Vesper A, Schror K. The cardioprotective actions of iloprost in myocardial ischemia of the rabbit can be separated from its vasodilatory effects mediated by KATP(+)-channel opening. *Agents Actions Suppl* 1995;45:93-9.
186. Clapp LH, Turcato S, Hall S, et al. Evidence that Ca²⁺-activated K⁺ channels play a major role in mediating the vascular effects of iloprost and cicaprost. *Eur J Pharmacol* 1998;356(2-3):215-24.
187. Dumas M, Dumas JP, Rochette L, et al. Role of potassium channels and nitric oxide in the effects of iloprost and prostaglandin E1 on hypoxic vasoconstriction in the isolated perfused lung of the rat. *Br J Pharmacol* 1997;120(3):405-10.
188. Schulz BG, Muller B. Iloprost antagonizes endothelin-induced vasoconstriction in macro- and microcirculation. *Eicosanoids* 1990;3(3):135-8.
189. Rubanyi GM. Endothelium-derived relaxing and contracting factors. *J Cell Biochem* 1991;46(1):27-36.
190. Tooke JE. European Consensus Document on Critical Limb Ischaemia: implications for diabetes. *Diabet Med* 1990;7(6):544-6.
191. Nomura N, Niiya K, Shinbo M, et al. Inhibitory effect of a synthetic prostacyclin analogue, beraprost, on urokinase-type plasminogen activator expression in RC-K8 human lymphoma cells. *Thromb Haemost* 1996;75(6):928-32.
192. Chomard D, Habault P, Ledemenev M, et al. Prognostic aspects of TcPO₂ in iloprost treatment as an alternative to amputation. *Angiology* 1999;50(4):283-8.
193. Watson HR, Belcher G, Horrocks M. Adjuvant medical therapy in peripheral bypass surgery. *Br J Surg* 1999;86(8):981-91.
194. Grant SM, Goa KL. Iloprost. A review of its pharmacodynamic and pharmacokinetic properties, and therapeutic potential in peripheral vascular disease, myocardial ischaemia and extracorporeal circulation procedures. *Drugs* 1992;43(6):889-924.
195. Piaggese A, Vallini V, Iacopi E, et al. Iloprost in the management of peripheral arterial disease in patients with diabetes mellitus. *Minerva Cardioangiol* 2011;59(1):101-8.
196. Loosemore TM, Chalmers TC, Dormandy JA. A meta-analysis of randomized placebo control trials in Fontaine stages III and IV peripheral occlusive arterial disease. *Int Angiol* 1994;13(2):133-42.

197. [No authors listed]. Treatment of limb threatening ischaemia with intravenous ilomedin: a randomised double-blind placebo controlled study. U.K. Severe Limb Ischaemia Study Group. *Eur J Vasc Surg* 1991;5(5):551-6.
198. [No authors listed]. Prostanoids for chronic critical leg ischemia. A randomized, controlled, open-label trial with prostaglandin E1. The ICAI Study Group. *Ischemia Cronica degli Arti Inferiori. Ann Intern Med* 1999;130(5):412-21.
199. Belcaro G, Nicolaidis AN, Cipollone G, et al. Nomograms used to define the short-term treatment with PGE(1) in patients with intermittent claudication and critical ischemia. The ORACLE (Occlusion Revascularization in the Atherosclerotic Critical Limb) Study Group. The European Study. *Angiology* 2000;51(8 Pt 2):S3-13; discussion S14.
200. Smith FC, Thomson IA, Hickey NC, et al. Adjuvant prostanoid treatment during femorodistal reconstruction. *Ann Vasc Surg* 1993;7(1):88-94.
201. Hickey NC, Shearman CP, Crowson MC, et al. Iloprost improves femoro-distal graft flow after a single bolus injection. *Eur J Vasc Surg* 1991;5(1):19-22.
202. Shearman CP, Hickey NC, Simms MH. Femoro-distal graft flow augmentation with the prostacyclin analogue iloprost. *Eur J Vasc Surg* 1990;4(5):455-7.
203. de Donato G, Gussoni G, Andreozzi GM, et al. The ILAILL study: iloprost as adjuvant to surgery for acute ischemia of lower limbs: a randomized, placebo-controlled, double-blind study by the italian society for vascular and endovascular surgery. *Ann Surg* 2006;244(2):185-93.
204. Watson HR, Schroeder TV, Simms MH, et al. Relationship of femorodistal bypass patency to clinical outcome. Iloprost Bypass International Study Group. *Eur J Vasc Endovasc Surg* 1999;17(1):77-83.
205. Watson HR, Smith FC, Shearman CP, et al. Pharmacokinetics and pharmacodynamics of intra-graft iloprost in femorodistal bypass surgery. *Prostaglandins Leukot Essent Fatty Acids* 1997;56(5):389-93.
206. Effects of perioperative iloprost on patency of femorodistal bypass grafts. The Iloprost Bypass International Study Group. *Eur J Vasc Endovasc Surg* 1996;12(3):363-71.
207. Scott HM, Scott WG. Critical leg ischaemia in New Zealand: economic cost of amputation versus intravenous iloprost. *Pharmacoeconomics* 1994;6(2):149-54.

208. Kent KC, Bartek S, Kuntz KM, et al. Prospective study of wound complications in continuous infrainguinal incisions after lower limb arterial reconstruction: incidence, risk factors, and cost. *Surgery* 1996;119(4):378-83.
209. Nam JH, Gahtan V, Roberts AB, et al. Influence of incisional complications on infrainguinal vein bypass graft outcome. *Ann Vasc Surg* 1999;13(1):77-83.
210. Wengrovitz M, Atnip RG, Gifford RR, et al. Wound complications of autogenous subcutaneous infrainguinal arterial bypass surgery: predisposing factors and management. *J Vasc Surg* 1990;11(1):156-61; discussion 61-3.
211. Chung J, Bartelson BB, Hiatt WR, et al. Wound healing and functional outcomes after infrainguinal bypass with reversed saphenous vein for critical limb ischemia. *J Vasc Surg* 2006;43(6):1183-90.
212. Criqui MH, Fronek A, Barrett-Connor E, et al. The prevalence of peripheral arterial disease in a defined population. *Circulation* 1985;71(3):510-5.
213. Norgren L, Hiatt WR, Dormandy JA, et al. Inter-Society Consensus for the Management of Peripheral Arterial Disease (TASC II). *J Vasc Surg* 2007;45 Suppl S:S5-67.
214. De Vivo S, Palmer-Kazen U, Kalin B, et al. Risk factors for poor collateral development in claudication. *Vasc Endovascular Surg* 2005;39(6):519-24.
215. Tunis SR, Bass EB, Steinberg EP. The use of angioplasty, bypass surgery, and amputation in the management of peripheral vascular disease. *N Engl J Med* 1991;22;325(8):556-62.
216. Hagberg E, Berlin OK, Renstrom P. Function after through-knee compared with below-knee and above-knee amputation. *Prosthet Orthot Int* 1992;16(3):168-73.
217. Houghton AD, Taylor PR, Thurlow S, et al. Success rates for rehabilitation of vascular amputees: implications for preoperative assessment and amputation level. *Br J Surg* 1992;79(8):753-5.
218. McWhinnie DL, Gordon AC, Collin J, et al. Rehabilitation outcome 5 years after 100 lower-limb amputations. *Br J Surg* 1994;81(11):1596-9.
219. Nehler MR, Coll JR, Hiatt WR, et al. Functional outcome in a contemporary series of major lower extremity amputations. *J Vasc Surg* 2003;38(1):7-14.
220. Ruckley CV, Stonebridge PA, Prescott RJ. Skewflap versus long posterior flap in below-knee amputations: multicenter trial. *J Vasc Surg* 1991;13(3):423-7.
221. Siriwardena GJ, Bertrand PV. Factors influencing rehabilitation of arteriosclerotic lower limb amputees. *J Rehabil Res Dev* 1991;28(3):35-44.

222. Stirnemann P, Walpoth B, Wursten HU, et al. Influence of failed arterial reconstruction on the outcome of major limb amputation. *Surgery* 1992;111(4):363-8.
223. Lavery LA, Van Houtum WH, Armstrong DG. Institutionalization following diabetes-related lower extremity amputation. *Am J Med* 1997;103(5):383-8.
224. Muradin GS, Bosch JL, Stijnen T, et al. Balloon dilation and stent implantation for treatment of femoropopliteal arterial disease: meta-analysis. *Radiology* 2001;221(1):137-45.
225. Cejna M, Thurnher S, Illiasch H, et al. PTA versus Palmaz stent placement in femoropopliteal artery obstructions: a multicenter prospective randomized study. *J Vasc Interv Radiol* 2001;12(1):23-31.
226. Grimm J, Muller-Hulsbeck S, Jahnke T, et al. Randomized study to compare PTA alone versus PTA with Palmaz stent placement for femoropopliteal lesions. *J Vasc Interv Radiol* 2001;12(8):935-42.
227. Vroegindeweij D, Vos LD, Tielbeek AV, et al. Balloon angioplasty combined with primary stenting versus balloon angioplasty alone in femoropopliteal obstructions: A comparative randomized study. *Cardiovasc Intervent Radiol* 1997;20(6):420-5.
228. Wolf GL, Wilson SE, Cross AP, et al. Surgery or balloon angioplasty for peripheral vascular disease: a randomized clinical trial. Principal investigators and their Associates of Veterans Administration Cooperative Study Number 199. *J Vasc Interv Radiol* 1993;4(5):639-48.
229. Bradbury AW, Adam DJ, Bell J, et al. Bypass versus Angioplasty in Severe Ischaemia of the Leg (BASIL) trial: An intention-to-treat analysis of amputation-free and overall survival in patients randomized to a bypass surgery-first or a balloon angioplasty-first revascularization strategy. *J Vasc Surg* 2010;51(5 Suppl):5S-17S.
230. Fowkes F, Leng GC. Bypass surgery for chronic lower limb ischaemia. *Cochrane Database Syst Rev* 2008;2:CD002000.
231. Adam DJ, Beard JD, Cleveland T, et al. Bypass versus angioplasty in severe ischaemia of the leg (BASIL): multicentre, randomised controlled trial. *Lancet* 2005;366(9501):1925-34.
232. Albers M, Battistella VM, Romiti M, et al. Meta-analysis of polytetrafluoroethylene bypass grafts to infrapopliteal arteries. *J Vasc Surg* 2003;37(6):1263-9.

233. Griffiths GD, Nagy J, Black D, et al. Randomized clinical trial of distal anastomotic interposition vein cuff in infrainguinal polytetrafluoroethylene bypass grafting. *Br J Surg* 2004;91(5):560-2.
234. Twine CP, McLain AD. Graft type for femoro-popliteal bypass surgery. *Cochrane Database Syst Rev* 2010;5:CD001487.
235. Jackson MR, Belott TP, Dickason T, et al. The consequences of a failed femoropopliteal bypass grafting: comparison of saphenous vein and PTFE grafts. *J Vasc Surg* 2000;32(3):498-504; 04-5.
236. Nicoloff AD, Taylor LM, Jr., McLafferty RB, et al. Patient recovery after infrainguinal bypass grafting for limb salvage. *J Vasc Surg* 1998;27(2):256-63; discussion 64-6.
237. Baldwin ZK, Pearce BJ, Curi MA, et al. Limb salvage after infrainguinal bypass graft failure. *J Vasc Surg* 2004;39(5):951-7.
238. Obesity - social report 2008. Secondary Obesity - social report 2008. <http://www.socialreport.msd.govt.nz/health/obesity.html>.
239. Coppel KJ, Mann JI, Williams SM, et al. Prevalence of diagnosed and undiagnosed diabetes and prediabetes in New Zealand: findings from the 2008/09 Adult Nutrition Survey. *N Z Med J* 2013;126(1370):23-42.
240. Ministry of Health. Totou Kahukuro: Maori Health Chart Book 2010. 2nd ed: Ministry of Health, NZ, 2010.
241. Ministry of Health. Monitoring Tobacco Use in New Zealand: A technical report on defining smoking status and estimates of smoking prevalence. Wellington: Ministry of Health, New Zealand; 2008.
242. New Zealand Census. Secondary New Zealand Census. <http://www.stats.co.nz>.
243. Ellison TL, Elliott R, Moyes SA. HbA1c screening for undiagnosed diabetes in New Zealand. *Diabetes Metab Res Rev* 2005;21(1):65-70.
244. Joshy G, Simmons D. Epidemiology of diabetes in New Zealand: revisit to a changing landscape. *N Z Med J* 2006;119(1235):U1999.
245. Joshy G, Colonne CK, Dunn P, et al. Ethnic disparities in causes of death among diabetes patients in the Waikato region of New Zealand. *N Z Med J* 2010;123(1310):19-29.
246. Simmons D, Rush E, Crook N. Prevalence of undiagnosed diabetes, impaired glucose tolerance, and impaired fasting glucose among Maori in Te Wai o Rona: Diabetes Prevention Strategy. *N Z Med J* 2009;122(1288):30-8.

247. Simmons D, Fleming C. Prevalence and characteristics of diabetic patients with no ongoing care in South Auckland. *Diabetes Care* 2000;23(12):1791-3.
248. Robinson T, Simmons D, Scott D, et al. Ethnic differences in Type 2 diabetes care and outcomes in Auckland: a multiethnic community in New Zealand. *N Z Med J* 2006;119(1235):U1997.
249. Ihaka B, Bayley A, Rome K. Foot problems in Maori with diabetes. *N Z Med J* 2012;125(1360):48-56.
250. Management of Type 2 Diabetes. Wellington: The New Zealand Guidelines Group; 2003.
251. Thompson C, McWilliams T, Scott D, et al. Importance of diabetic foot admissions at Middlemore Hospital. *N Z Med J* 1993;106(955):178-80.
252. Simmons D, Scott D, Kenealy T, et al. Foot care among diabetic patients in south Auckland. *N Z Med J* 1995;108(996):106-8.
253. Simmons D, Harry T, Gatland B. Prevalence of known diabetes in different ethnic groups in inner urban South Auckland. *N Z Med J* 1999;112(1094):316-9.
254. Simmons D, Schaumkel J, Cecil A, et al. High impact of nephropathy on five-year mortality rates among patients with Type 2 diabetes mellitus from a multi-ethnic population in New Zealand. *Diabet Med* 1999;16(11):926-31.
255. Payne CB, Scott RS. Hospital discharges for diabetic foot disease in New Zealand: 1980-1993. *Diabetes Res Clin Pract* 1998;39(1):69-74.
256. Kumar V, Abbas AK, Fausto N, Aster JC. *Robbins and Cotran Pathologic Basis of Disease*. 8th ed, 2010.
257. Hall JE. *Guyton and Hall Textbook of Medical Physiology*. 13th ed: Elsevier, 2015.
258. Barrett KE, Barman SM, Boitano S, Brooks H. *Ganong's Review of Medical Physiology*. 24th ed: McGraw-Hill; 2012.
259. Franzeck UK, Talke P, Bernstein EF, et al. Transcutaneous PO₂ measurements in health and peripheral arterial occlusive disease. *Surgery* 1982;91(2):156-63.
260. Apelqvist J, Castenfors J, Larsson J, et al. Prognostic value of systolic ankle and toe blood pressure levels in outcome of diabetic foot ulcer. *Diabetes Care* 1989;12(6):373-8.
261. Waszczykowska A, Gos R, Waszczykowska E, et al. Assessment of skin microcirculation by laser Doppler flowmetry in systemic sclerosis patients. *Postepy Dermatol Alergol*. 2014;31(1):6-11.

262. Stern MD. Laser Doppler velocimetry in blood and multiply scattering fluids: theory. *Appl Opt* 1985;24(13):1968.
263. Gurtner GC, Jones GE, Neligan PC, et al. Intraoperative laser angiography using the SPY system: review of the literature and recommendations for use. *Ann Surg Innov Res* 2013;7(1):1.
264. Perry D, Bharara M, Armstrong DG, et al. Intraoperative fluorescence vascular angiography: during tibial bypass. *J Diabetes Sci Technol* 2012;6(1):204-8.
265. Braun JD, Trinidad-Hernandez M, Perry D, et al. Early quantitative evaluation of indocyanine green angiography in patients with critical limb ischemia. *J Vasc Surg* 2013;57(5):1213-8.
266. Huch R, Huch A. Fetal and maternal PtcO₂ monitoring. *Crit Care Med* 1981;9(10):694-7.
267. Silver IA. Some observations on the cerebral cortex with an ultramicro, membrane-covered, oxygen electrode. *Med Electron Biol Eng* 1965;3(4):377-87.
268. Clark LC, Jr., Wolf R, Granger D, et al. Continuous recording of blood oxygen tensions by polarography. *J Appl Physiol* 1953;6(3):189-93.
269. Hunt TK. A new method of determining tissue oxygen tension. *Lancet* 1964;2(7374):1370-1.
270. Huch R, Lubbers DW, Huch A. Quantitative continuous measurement of partial oxygen pressure on the skin of adults and new-born babies. *Pflugers Arch* 1972;337(3):185-98.
271. Niinikoski J. Hyperbaric oxygen therapy of diabetic foot ulcers, transcutaneous oxymetry in clinical decision making. *Wound Repair Regen* 2003;11(6):458-61.
272. Melis P, Noorlander ML, van der Kleij AJ, et al. Oxygenation and microcirculation during skin stretching in undermined and nonundermined skin. *Plast Reconstr Surg* 2003;112(5):1295-301.
273. Sheffield PJ. Measuring tissue oxygen tension: a review. *Undersea Hyperb Med* 1998;25(3):179-88.
274. Holdich TA, Reddy PJ, Walker RT, et al. Transcutaneous oxygen tension during exercise in patients with claudication. *Br Med J* 1986;292(6536):1625-8.
275. Wattel F, Mathieu D, Coget JM, et al. Hyperbaric oxygen therapy in chronic vascular wound management. *Angiology* 1990;41(1):59-65.

276. Dooley J, King G, Slade B. Establishment of reference pressure of transcutaneous oxygen for the comparative evaluation of problem wounds. *Undersea Hyperb Med* 1997;24(4):235-44.
277. Hauser CJ, Klein SR, Mehringer CM, et al. Superiority of transcutaneous oximetry in noninvasive vascular diagnosis in patients with diabetes. *Arch Surg* 1984;119(6):690-4.
278. Mayrovitz HN, Larsen PB. Functional microcirculatory impairment: a possible source of reduced skin oxygen tension in human diabetes mellitus. *Microvasc Res* 1996;52(2):115-26.
279. Hauser CJ, Klein SR, Mehringer CM, et al. Assessment of perfusion in the diabetic foot by regional transcutaneous oximetry. *Diabetes* 1984;33(6):527-31.
280. Bacharach JM, Rooke TW, Osmundson PJ, et al. Predictive value of transcutaneous oxygen pressure and amputation success by use of supine and elevation measurements. *J Vasc Surg* 1992;15(3):558-63.
281. Christensen KS, Klarke M. Transcutaneous oxygen measurement in peripheral occlusive disease. An indicator of wound healing in leg amputation. *J Bone Joint Surg Br* 1986;68(3):423-6.
282. Kalani M, Brismar K, Fagrell B, et al. Transcutaneous oxygen tension and toe blood pressure as predictors for outcome of diabetic foot ulcers. *Diabetes Care* 1999;22(1):147-51.
283. Wyss CR, Matsen FA, 3rd, Simmons CW, et al. Transcutaneous oxygen tension measurements on limbs of diabetic and nondiabetic patients with peripheral vascular disease. *Surgery* 1984;95(3):339-46.
284. Padberg FT, Back TL, Thompson PN, et al. Transcutaneous oxygen (TcPO₂) estimates probability of healing in the ischemic extremity. *J Surg Res* 1996;60(2):365-9.
285. Smart DR, Bennett MH, Mitchell SJ. Transcutaneous oximetry, problem wounds and hyperbaric oxygen therapy. *Diving and Hyperbaric Medicine* 2006;36(2):72-86.
286. Dowd GS. Predicting stump healing following amputation for peripheral vascular disease using the transcutaneous oxygen monitor. *Ann R Coll Surg Engl* 1987;69(1):31-5.
287. Wimberley PD, Gronlund Pedersen K, Olsson J, et al. Transcutaneous carbon dioxide and oxygen tension measured at different temperatures in healthy adults. *Clin Chem* 1985;31(10):1611-5.

288. Coleman LS, Dowd GS, Bentley G. Reproducibility of tcPO₂ measurements in normal volunteers. *Clin Phys Physiol Meas* 1986;7(3):259-63.
289. Restrepo RD, Hirst KR, Wittnebel L, et al. AARC clinical practice guideline: transcutaneous monitoring of carbon dioxide and oxygen: 2012. *Respir Care* 2012;57(11):1955-62.
290. Fife CE, Smart DR, Sheffield PJ, et al. Transcutaneous oximetry in clinical practice: consensus statements from an expert panel based on evidence. *Undersea Hyperb Med* 2009;36(1):43-53.
291. Wimberley PD, Burnett RW, Covington AK, et al. Guidelines for transcutaneous p O₂ and p CO₂ measurement. *J Int Fed Clin Chem* 1990;2(3):128-35.
292. Hauser CJ, Appel P, Shoemaker WC. Pathophysiologic classification of peripheral vascular disease by positional changes in regional transcutaneous oxygen tension. *Surgery* 1984;95(6):689-93.
293. Wahr JA, Tremper KK. Noninvasive oxygen monitoring techniques. *Crit Care Clin* 1995;11(1):199-217.
294. Tobias JD. Transcutaneous carbon dioxide monitoring in infants and children. *Paediatr Anaesth* 2009;19(5):434-44.
295. Yudovsky D, Nouvong A, Schomacker K, et al. Assessing diabetic foot ulcer development risk with hyperspectral tissue oximetry. *J Biomed Opt* 2011;16(2):026009.
296. Sassaroli A, Fantini S. Comment on the modified Beer-Lambert law for scattering media. *Phys Med Biol* 2004;49(14):N255-7.
297. van Gemert MJ, Jacques SL, Sterenborg HJ, et al. Skin optics. *IEEE Trans Biomed Eng* 1989;36(12):1146-54.
298. Anderson RR, Parrish JA. The optics of human skin. *J Invest Dermatol* 1981;77(1):13-9.
299. Turchin VV. *Tissue optics: Light Scattering Methods And Instruments for Medical Diagnosis*. 2nd ed. San Diego, CA: SPIE Press, 2007.
300. Jacques SL, Ramella-Roman JC, Lee K. Imaging skin pathology with polarized light. *J Biomed Opt* 2002;7(3):329-40.
301. Yudovsky D, Nouvong A, Pilon L. Hyperspectral imaging in diabetic foot wound care. *J Diabetes Sci Technol* 2010;4(5):1099-113.

302. Marquardt DW. An algorithm for least-squares estimation of nonlinear parameters. *J Soc Indust Appl Math* 1963;11(2):431-41.
303. Yudovsky D, Pilon L. Rapid and accurate estimation of blood saturation, melanin content, and epidermis thickness from spectral diffuse reflectance. *Appl Opt* 2010;49(10):1707-19.
304. Prahl S. Optical absorption of hemoglobin. Secondary optical absorption of hemoglobin. 2002. <http://omlc.ogi.edu/spectra/hemoglobin/>.
305. Yudovsky D, Pilon L. Retrieving skin properties from in vivo spectral reflectance measurements. *J Biophotonics* 2011;4(5):305-14.
306. Yudovsky D, Nouvong A, Schomacker K, et al. Monitoring temporal development and healing of diabetic foot ulceration using hyperspectral imaging. *J Biophotonics* 2011;4(7-8):565-76.
307. Jafari-Saraf L, Wilson SE, Gordon IL. Hyperspectral image measurements of skin hemoglobin compared with transcutaneous PO₂ measurements. *Ann Vasc Surg* 2012;26(4):537-48.
308. Dwyer PJ, DiMarzio CA. Hyperspectral imaging for dermal hemoglobin spectroscopy. *Conf Proc IEEE - Subsurface Sensors and Applications* 1999;3752:72-82.
309. Greenman RL, Panasyuk S, Wang X, et al. Early changes in the skin microcirculation and muscle metabolism of the diabetic foot. *Lancet* 2005;366(9498):1711-7.
310. Khaodhiar L, Dinh T, Schomacker KT, et al. The use of medical hyperspectral technology to evaluate microcirculatory changes in diabetic foot ulcers and to predict clinical outcomes. *Diabetes Care* 2007;30(4):903-10.
311. Neville RG, Gupta S. Establishment of normative perfusion values using hyperspectral tissue oxygenation mapping technology. *Vasc Dis Manag* 2009;6(6):156-61.
312. Nagaoka T, Eikje NS, Nakamura A, et al. Inspection of skin hemodynamics with hyperspectral camera. *Conf Proc IEEE Eng Med Biol Soc* 2007;2007:3357-61.
313. Jafari-Saraf L, Gordon IL. Hyperspectral imaging and ankle: brachial indices in peripheral arterial disease. *Ann Vasc Surg* 2010;24(6):741-6.
314. Chin JA, Wang EC, Kibbe MR. Evaluation of hyperspectral technology for assessing the presence and severity of peripheral artery disease. *J Vasc Surg* 2011;54(6):1679-88.
315. Galiano R. Lower extremity ulcers. *ACS Surgery: Principles and Practice*. Philadelphia, PA: Decker Publishing Inc., 2010.

316. Raju S, Sanford P, Herman S, et al. Postural and ambulatory changes in regional flow and skin perfusion. *Eur J Vasc Endovasc Surg* 2012;43(5):567-72.
317. Wild S, Roglic G, Green A, et al. Global prevalence of diabetes: estimates for the year 2000 and projections for 2030. *Diabetes Care* 2004;27(5):1047-53.
318. Assal JP, Mehnert H, Tritschler HJ, et al. On your feet! Workshop on the diabetic foot. *J Diabetes Complications* 2002;16(2):183-94.
319. Apelqvist J, Bakker K, van Houtum WH, et al. Practical guidelines on the management and prevention of the diabetic foot: based upon the International Consensus on the Diabetic Foot (2007) Prepared by the International Working Group on the Diabetic Foot. *Diabetes Metab Res Rev* 2008;24 Suppl 1:S181-7.
320. Ahmad J. The Diabetic Foot. *Diabetes & Metabolic Syndrome: Clinical Research & Reviews* 2016;10(1):48-60.
321. Boulton AJ. The diabetic foot: from art to science. The 18th Camillo Golgi lecture. *Diabetologia* 2004;47(8):1343-53.
322. Singh N, Armstrong DG, Lipsky BA. Preventing foot ulcers in patients with diabetes. *JAMA* 2005;293(2):217-28.
323. Reiber GEL, W.R. Epidemiology of diabetic foot ulcers and amputations: evidence for prevention. In: Williams B, Herman WH, Kinmonth AL, Wareham NJ, ed. *The Evidence-base for Diabetes Care*. Chichester, UK: John Wiley, 2002:641–65
324. Selvin E, Marinopoulos S, Berkenblit G, et al. Meta-analysis: glycosylated hemoglobin and cardiovascular disease in diabetes mellitus. *Ann Intern Med* 2004;141(6):421-31.
325. Muntner P, Wildman RP, Reynolds K, et al. Relationship between HbA1c level and peripheral arterial disease. *Diabetes Care* 2005;28(8):1981-7.
326. Reiber GE, Vileikyte L, Boyko EJ, et al. Causal pathways for incident lower-extremity ulcers in patients with diabetes from two settings. *Diabetes Care* 1999;22(1):157-62.
327. Ebskov B, Josephsen P. Incidence of reamputation and death after gangrene of the lower extremity. *Prosthet Orthot Int* 1980;4(2):77-80.
328. Pecoraro RE, Reiber GE, Burgess EM. Pathways to diabetic limb amputation. Basis for prevention. *Diabetes Care* 1990;13(5):513-21.
329. Tentolouris N, Al-Sabbagh S, Walker MG, et al. Mortality in diabetic and nondiabetic patients after amputations performed from 1990 to 1995: a 5-year follow-up study. *Diabetes Care* 2004;27(7):1598-604.

330. Papazafiropoulou A, Tentolouris N, Soldatos RP, et al. Mortality in diabetic and nondiabetic patients after amputations performed from 1996 to 2005 in a tertiary hospital population: a 3-year follow-up study. *J Diabetes Complications* 2009;23(1):7-11.
331. Armstrong DG, Lavery LA. Diabetic foot ulcers: prevention, diagnosis and classification. *Am Fam Physician* 1998;57(6):1325-32, 37-8.
332. Khanolkar MP, Bain SC, Stephens JW. The diabetic foot. *QJM* 2008;101(9):685-95.
333. Lateef H, Stevens MJ, Varani J. All-trans-retinoic acid suppresses matrix metalloproteinase activity and increases collagen synthesis in diabetic human skin in organ culture. *Am J Pathol* 2004;165(1):167-74.
334. Varani J, Warner RL, Gharaee-Kermani M, et al. Vitamin A antagonizes decreased cell growth and elevated collagen-degrading matrix metalloproteinases and stimulates collagen accumulation in naturally aged human skin. *J Invest Dermatol* 2000;114(3):480-6.
335. Noor S, Zubair M, Ahmad J. Diabetic foot ulcer--A review on pathophysiology, classification and microbial etiology. *Diabetes Metabol Syndr* 2015;9(3):192-9.
336. McNeely MJ, Boyko EJ, Ahroni JH, et al. The independent contributions of diabetic neuropathy and vasculopathy in foot ulceration. How great are the risks? *Diabetes Care* 1995;18(2):216-9.
337. Armstrong DG, Lavery LA, Kimbriel HR, et al. Activity patterns of patients with diabetic foot ulceration: patients with active ulceration may not adhere to a standard pressure off-loading regimen. *Diabetes Care* 2003;26(9):2595-7.
338. Armstrong DG, Nguyen HC, Lavery LA, et al. Off-loading the diabetic foot wound: a randomized clinical trial. *Diabetes Care* 2001;24(6):1019-22.
339. Smiell JM, Wieman TJ, Steed DL, et al. Efficacy and safety of becaplermin (recombinant human platelet-derived growth factor-BB) in patients with nonhealing, lower extremity diabetic ulcers: a combined analysis of four randomized studies. *Wound Repair Regen* 1999;7(5):335-46.
340. Newman GR, Walker M, Hobot JA, et al. Visualisation of bacterial sequestration and bactericidal activity within hydrating Hydrofiber wound dressings. *Biomaterials* 2006;27(7):1129-39.

341. Vermeulen H, Ubbink DT, Goossens A, et al. Systematic review of dressings and topical agents for surgical wounds healing by secondary intention. *Br J Surg* 2005;92(6):665-72.
342. Ryan M. The issues surrounding the continued use of saline soaked gauze dressings. *Wound Pract Res* 2008;16(2):16-21.
343. Ubbink DT, Westerbos SJ, Nelson EA, et al. A systematic review of topical negative pressure therapy for acute and chronic wounds. *Br J Surg* 2008;95(6):685-92.
344. Vig S. A systematic review of topical negative pressure therapy for acute and chronic wounds (*Br J Surg* 2008; 95: 685-692). *Br J Surg* 2008;95(9):1185-6; author reply 86.
345. Noble-Bell G, Forbes A. A systematic review of the effectiveness of negative pressure wound therapy in the management of diabetes foot ulcers. *Int Wound J* 2008;5(2):233-42.
346. Banwell PE, Teot L. Topical negative pressure (TNP): the evolution of a novel wound therapy. *J Wound Care* 2003;12(1):22-8.
347. Fleischmann W, Strecker W, Bombelli M, et al. [Vacuum sealing as treatment of soft tissue damage in open fractures]. *Unfallchirurg* 1993;96(9):488-92. German.
348. Bovill E, Banwell PE, Teot L, et al. Topical negative pressure wound therapy: a review of its role and guidelines for its use in the management of acute wounds. *Int Wound J* 2008;5(4):511-29.
349. Argenta LC, Morykwas MJ. Vacuum-assisted closure: a new method for wound control and treatment: clinical experience. *Ann Plast Surg* 1997;38(6):563-76; discussion 77.
350. Chen CS, Mrksich M, Huang S, et al. Geometric control of cell life and death. *Science* 1997;276(5317):1425-8.
351. Banwell PE, Musgrave M. Topical negative pressure therapy: mechanisms and indications. *Int Wound J* 2004;1(2):95-106.
352. Venturi ML, Attinger CE, Mesbahi AN, et al. Mechanisms and clinical applications of the vacuum-assisted closure (VAC) device: a review. *Am J Clin Dermatol* 2005;6(3):185-94.
353. Morykwas MJ, Faler BJ, Pearce DJ, et al. Effects of varying levels of subatmospheric pressure on the rate of granulation tissue formation in experimental wounds in swine. *Ann Plast Surg* 2001;47(5):547-51.

354. Timmers MS, Le Cessie S, Banwell P, et al. The effects of varying degrees of pressure delivered by negative-pressure wound therapy on skin perfusion. *Ann Plast Surg* 2005;55(6):665-71.
355. Anesater E, Borgquist O, Hedstrom E, et al. The influence of different sizes and types of wound fillers on wound contraction and tissue pressure during negative pressure wound therapy. *Int Wound J* 2011;8(4):336-42.
356. Borgquist O, Anesater E, Hedstrom E, et al. Measurements of wound edge microvascular blood flow during negative pressure wound therapy using thermodiffusion and transcutaneous and invasive laser Doppler velocimetry. *Wound Repair Regen* 2011;19(6):727-33.
357. Borgquist O, Ingemansson R, Malmso M. The effect of intermittent and variable negative pressure wound therapy on wound edge microvascular blood flow. *Ostomy Wound Manage* 2010;56(3):60-7.
358. Borgquist O, Ingemansson R, Malmso M. Wound edge microvascular blood flow during negative-pressure wound therapy: examining the effects of pressures from -10 to -175 mmHg. *Plast Reconstr Surg* 2010;125(2):502-9.
359. Malmso M, Ingemansson R, Martin R, et al. Wound edge microvascular blood flow: effects of negative pressure wound therapy using gauze or polyurethane foam. *Ann Plast Surg* 2009;63(6):676-81.
360. Malmso M, Ingemansson R, Lindstedt S, et al. Comparison of bacteria and fungus-binding mesh, foam and gauze as fillers in negative pressure wound therapy--pressure transduction, wound edge contraction, microvascular blood flow and fluid retention. *Int Wound J* 2013;10(5):597-605.
361. Saxena V, Hwang CW, Huang S, et al. Vacuum-assisted closure: microdeformations of wounds and cell proliferation. *Plast Reconstr Surg* 2004;114(5):1086-96; discussion 97-8.
362. Erba P, Ogawa R, Ackermann M, et al. Angiogenesis in wounds treated by microdeformational wound therapy. *Ann Surg* 2011;253(2):402-9.
363. Greene AK, Puder M, Roy R, et al. Microdeformational wound therapy: effects on angiogenesis and matrix metalloproteinases in chronic wounds of 3 debilitated patients. *Ann Plast Surg* 2006;56(4):418-22.

364. Fabian TS, Kaufman HJ, Lett ED, et al. The evaluation of subatmospheric pressure and hyperbaric oxygen in ischemic full-thickness wound healing. *Am Surg* 2000;66(12):1136-43.
365. Stechmiller JK, Kilpadi DV, Childress B, et al. Effect of Vacuum-Assisted Closure Therapy on the expression of cytokines and proteases in wound fluid of adults with pressure ulcers. *Wound Repair Regen* 2006;14(3):371-4.
366. Gustafsson R, Johnsson P, Algotsson L, et al. Vacuum-assisted closure therapy guided by C-reactive protein level in patients with deep sternal wound infection. *J Thorac Cardiovasc Surg* 2002;123(5):895-900.
367. Hunter JE, Teot L, Horch R, et al. Evidence-based medicine: vacuum-assisted closure in wound care management. *Int Wound J* 2007;4(3):256-69.
368. Derrick KL, Norbury K, Kieswetter K, et al. Comparative analysis of global gene expression profiles between diabetic rat wounds treated with vacuum-assisted closure therapy, moist wound healing or gauze under suction. *Int Wound J* 2008;5(5):615-24.
369. Jacobs S, Simhaee DA, Marsano A, et al. Efficacy and mechanisms of vacuum-assisted closure (VAC) therapy in promoting wound healing: a rodent model. *J Plast Reconstr Aesthet Surg* 2009;62(10):1331-8.
370. Labler L, Rancan M, Mica L, et al. Vacuum-assisted closure therapy increases local interleukin-8 and vascular endothelial growth factor levels in traumatic wounds. *J Trauma* 2009;66(3):749-57.
371. Yang SL, Han R, Liu Y, et al. Negative pressure wound therapy is associated with up-regulation of bFGF and ERK1/2 in human diabetic foot wounds. *Wound Repair Regen* 2014;22(4):548-54.
372. McCallon SK, Knight CA, Valiulus JP, et al. Vacuum-assisted closure versus saline-moistened gauze in the healing of postoperative diabetic foot wounds. *Ostomy Wound Manage* 2000;46(8):28-32, 34.
373. Etöz A; Özgenel Y, Özcan M. The use of negative pressure wound therapy on diabetic foot ulcers: A preliminary controlled trial. *Wounds* 2004;16:264-69.
374. Eginton MT, Brown KR, Seabrook GR, et al. A prospective randomized evaluation of negative-pressure wound dressings for diabetic foot wounds. *Ann Vasc Surg* 2003;17(6):645-9.

375. Joseph E, Hamori CA, Bergman S, Roaf E, Swann NF, Anastasi GW A prospective randomized trial of vacuum-assisted closure versus standard therapy of chronic non-healing wounds. *Wounds* 2000;12(3):60-7.
376. Ford CN, Reinhard ER, Yeh D, et al. Interim analysis of a prospective, randomized trial of vacuum-assisted closure versus the healthpoint system in the management of pressure ulcers. *Ann Plast Surg* 2002;49(1):55-61; discussion 61.
377. Vikatmaa P, Juutilainen V, Kuukasjarvi P, et al. Negative pressure wound therapy: a systematic review on effectiveness and safety. *Eur J Vasc Endovasc Surg* 2008;36(4):438-48.
378. Armstrong DG, Lavery LA. Negative pressure wound therapy after partial diabetic foot amputation: a multicentre, randomised controlled trial. *Lancet* 2005;366(9498):1704-10.
379. Dalla Paola L, Carone A, Ricci S, Russo A, Ceccacci T, Ninkovic S. Use of vacuum assisted closure therapy in the treatment of diabetic foot wounds. *The Journal of Diabetic Foot Complications* 2010;2(2):33-44.
380. Dumville JC, Hinchliffe RJ, Cullum N, et al. Negative pressure wound therapy for treating foot wounds in people with diabetes mellitus. *Cochrane Database Syst Rev* 2013;10:CD010318.
381. Ubbink DT, Westerbos SJ, Evans D, et al. Topical negative pressure for treating chronic wounds. *Cochrane Database Syst Rev* 2008;3:CD001898.
382. Wanner MB, Schwarzl F, Strub B, et al. Vacuum-assisted wound closure for cheaper and more comfortable healing of pressure sores: a prospective study. *Scand J Plast Reconstr Surg Hand Surg* 2003;37(1):28-33.
383. Vuerstaek JD, Vainas T, Wuite J, et al. State-of-the-art treatment of chronic leg ulcers: A randomized controlled trial comparing vacuum-assisted closure (V.A.C.) with modern wound dressings. *J Vasc Surg* 2006;44(5):1029-37; discussion 38.
384. Driver VR, Blume PA. Evaluation of wound care and health-care use costs in patients with diabetic foot ulcers treated with negative pressure wound therapy versus advanced moist wound therapy. *J Am Podiatr Med Assoc* 2014;104(2):147-53.
385. Langemo DK, Melland H, Olson B, et al. Comparison of 2 wound volume measurement methods. *Adv Skin Wound Care* 2001;14(4):190-6.
386. Ahn C, Salcido RS. Advances in wound photography and assessment methods. *Adv Skin Wound Care* 2008;21(2):85-93; quiz 94-5.

387. Liu X, Kim W, Schmidt R, et al. Wound measurement by curvature maps: a feasibility study. *Physiol Meas* 2006;27(11):1107-23.
388. Edgar D, Day R, Briffa NK, et al. Volume measurement using the Polhemus FastSCAN 3D laser scanning: a novel application for burns clinical research. *J Burn Care Res* 2008;29(6):994-1000.
389. ARANZ Medical. Secondary ARANZ Medical. <http://www.aranz.org.nz/>.
390. Kirkwood BR, Sterne JAC. *Essential Medical Statistics*. 2nd ed: Blackwell Science, 2005.
391. Bland M. How should I calculate a within-subject coefficient of variation? Secondary How should I calculate a within-subject coefficient of variation? 2006. <http://www-users.york.ac.uk/~mb55/meas/cv.htm>.
392. Rutherford RB, Baker JD, Ernst C, et al. Recommended standards for reports dealing with lower extremity ischemia: revised version. *J Vasc Surg* 1997;26(3):517-38.
393. Benumof JL. Respiratory physiology and respiratory function during anaesthesia. In: Miller RD, ed. *Anaesthesia*. 5th ed: Churchill Livingstone 2000:612-13.
394. Scarpa M, Bortolami M, Morgan SL, et al. TGF-beta1 and IGF-1 production and recurrence of Crohn's disease after ileo-colonic resection. *J Surg Res* 2009;152(1):26-34.
395. Vogt PM, Lehnhardt M, Wagner D, et al. Determination of endogenous growth factors in human wound fluid: temporal presence and profiles of secretion. *Plast Reconstr Surg* 1998;102(1):117-23.
396. Brazdzionyte J, Macas A.. Bland-Altman analysis as an alternative approach for statistical evaluation of agreement between two methods for measuring hemodynamics during acute myocardial infarction. *Medicina (Kaunas)* 2007;43(3):208-14.
397. Chiariello M, Ambrosio G, Cappelli-Bigazzi M, et al. A biochemical method for the quantitation of myocardial scarring after experimental coronary artery occlusion. *J Mol Cell Cardiol* 1986;18(3):283-90.
398. Broadbent E, Kahokehr A, Booth RJ, et al. A brief relaxation intervention reduces stress and improves surgical wound healing response: A randomised trial. *Brain Behav Immun* 2012;26(2):212-7.

399. Jorgensen LN, Sorensen LT, Kallehave F, et al. Increased collagen deposition in an uncomplicated surgical wound compared to a minimal subcutaneous test wound. *Wound Repair Regen* 2001;9(3):194-9.
400. Wimberly PD, Burnett RW, Covington AK, et al. International Federation of Clinical Chemistry (IFCC). Scientific Division. Committee on pH, Blood Gases and Electrolytes. Guidelines for transcutaneous pO₂ and pCO₂ measurement. *Clin Chim Acta* 1990;190(1-2):S41-S50.
401. Khan TH, Farooqui FA, Niazi K. Critical review of the ankle brachial index. *Curr Cardiol Rev* 2008;4(2):101-6.
402. Dormandy JA, Murray GD. Reprinted article "The fate of the claudicant--a prospective study of 1969 claudicants". *Eur J Vasc Endovasc Surg* 2011;42 Suppl 1:S4-6.
403. Fowkes FG, Housley E, Cawood EH, et al. Edinburgh Artery Study: prevalence of asymptomatic and symptomatic peripheral arterial disease in the general population. *Int J Epidemiol* 1991;20(2):384-92.
404. Ankle Brachial Index Collaboration: Fowkes FG, Murray GD, Butcher I, et al. Ankle brachial index combined with Framingham Risk Score to predict cardiovascular events and mortality: a meta-analysis. *JAMA* 2008;300(2):197-208.
405. Mehler PS, Coll JR, Estacio R, et al. Intensive blood pressure control reduces the risk of cardiovascular events in patients with peripheral arterial disease and type 2 diabetes. *Circulation* 2003;107(5):753-6.
406. Norman PE, Eikelboom JW, Hankey GJ. Peripheral arterial disease: prognostic significance and prevention of atherothrombotic complications. *Med J Aust* 2004;181(3):150-4.
407. Wikipedia. Oxygen-haemoglobin dissociation curve. Secondary Oxygen-haemoglobin dissociation curve. http://en.wikipedia.org/wiki/Oxygen-haemoglobin_dissociation_curve.
408. Husmann M, Willenberg T, Keo HH, et al. Integrity of venoarteriolar reflex determines level of microvascular skin flow enhancement with intermittent pneumatic compression. *J Vasc Surg* 2008;48(6):1509-13.
409. Goodson WH, 3rd, Hunt TK. Development of a new miniature method for the study of wound healing in human subjects. *J Surg Res* 1982;33(5):394-401.

410. Lavery LA, Barnes SA, Keith MS, et al. Prediction of healing for postoperative diabetic foot wounds based on early wound area progression. *Diabetes Care* 2008;31(1):26-9.
411. Vijan S. In the clinic. Type 2 diabetes. *Ann Intern Med* 2010;152(5):ITC31-15; quiz ITC316.
412. Mosquera D, Chiang N, Gibberd R. Evaluation of surgical performance using V-POSSUM risk-adjusted mortality rates. *ANZ J Surg* 2008;78(7):535-9.